GEOLOGY, STRUCTURE AND MICROFABRIC OF GRENVILLE ROCKS, CARDIFF AREA, ONTARIO

A thesis

presented to the

Department of Geology

University of Ottawa

In partial fulfillment

of the requirements for the degree

DOCTOR OF PHILOSOPHY

in Geology

by

Nicholas Culshaw

March, 1983

UNIVERSITÉ D'OTTAWA
UNIVERSITY OF OTTAWA

Abstract

The study area is underlain by supracrustal rocks (marble, amphibolite and both calcsilicate and quartzofeldspathic gneiss) and voluminous orthogneiss, metamorphosed in the amphibolite facies. It is part of an extensive northeasterly trending tract of gneissic rocks characterized by a pervasive lineation plunging moderately SE and zones of high strain. The tract straddles the northern border of the Grenville Central Metasedimentary Belt with basement(?) rocks which are represented by stratiform slabs of grey migmatitic tonalitic gneiss within the supracrustal rocks. The slabs could be thrust slices.

Gabbro, anorthosite and pyroxenite form a complex of sheet-like bodies in which primary textures and coronas are locally preserved. These rocks, after differentiating at depth, were probably emplaced during ductile thrusting.

Syenitic gneiss also forms extensive sheets whereas granites are concentrated in two subcircular complexes at the northern end of a NNE-SSW trending plutonic-structural arch. The granite bodies are inclined NW parallel to the regional lineation. Elliptical outcrop patterns within them suggest originally more circular bodies, probably syntectonic diapirs, were deformed by ductile shear.

The regional lineation (L1), which with its associated foliation forms an LS1 fabric, includes stretched mineral aggregates, deformed granitoid vein arrays, mica edge lineations and the intersection of new foliations on older. The shape of these fabrics indicates that plane strain was widespread with prolate strains concentrated in zones of folds, which are coaxial with the L1 regional lineation. In most cases the fold zones lie between the granitic bodies assumed to be

syntectonic and the folding appears to be coeval with L1. Although all of the rocks are LS tectonites, strain appears to be particularly high in the granitoids and supracrustal rocks overlying the tonalitic gneiss.

Microstructures contain information of both kinematic and mechanical significance. For example, quartz microstructures and c-axis microfabrics that formed synkinematically with L1 vary with rock type. In quartzites exaggerated grain growth is associated with c-axis microfabrics which lack a simple relationship with the mesoscopic fabric. In contrast, c-axes of polycrystalline quartz ribbons in granite gneiss display consistent, kinematically meaningful patterns of preferred orientation, evidently recording, in part, dynamic recrystallization. It is suggested that complete destruction of the dynamic c-axis microfabric by grain growth, such as in the quartzites, was hindered in the granite by the high percentage of feldspar. In the granites there are also differences between c-axis microfabrics of grains which form proportionally more of a ribbon from those which form less. The longer grains tend to form YZ girdles with maxima near Y or Z (patterns found in samples measured in YZ plane); the shorter, more numerous grains tend to form cross girdles (patterns found in samples measured in XZ plane). This variation of c-axis microfabrics with grain length suggests that the longer grains (YZ girdles) have grown at the expense of the shorter grains (cross girdles) - an example of metadynamic oriented grain growth. Asymmetry of c-axis microfabrics in the granites is consistent with NW ductile thrusting, parallel to the lineation.

LS2 tectonites are present in narrow high strain zones concordant with the LS1 fabric. Finely recrystallized quartz forms an asymmetric fabric in which L2 lies in the XZ plane of LS1. The c-axis microfabrics appear to reflect a geometry of initial kinking (accomplished by basal slip) of coarse early quartz, the orientation of which was determined by the LS1 c-axis microfabric, such that LS1 microfabrics with Y maxima may be followed by LS2 YZ girdles with 2 maxima around Y. LS2 microfabrics and microstructures indicate a shear-sense precisely reversed from that of LS1. Perhaps this local reversal is related to the NW ductile thrusting much as the antithetic shear which occurs between volumes in a sheared row of books. Alternatively, the zones could express late back-sliding of an overthickened pile.

The formation of foliation in the gabbroic rocks was accompanied by processes that differed from those in quartz-rich rocks. Such features as growth and shrinkage of hornblende grains surrounded by plagioclase crystals, which takes place with increasing whole rock strain, indicates the dominance of intra- and intercrystalline diffusional processes dependent on the presence of introduced water. The relative slowness of such processes explains both the preservation of primary fabrics in the gabbros and the relative hardness of these bodies during regional deformation.

TABLE OF CONTENTS PAGE

List of Figures

Page

List of Plates

List of Tables

1. INTRODUCTION

1.1 Location and Rock Outcrop

The study area (Figs. 1.1 and 1.2) is within the mapsheets 31 E/I and 31 D/6 of the Canadian National Topographic 1:50,000 series. It contains most of Cardiff, Harcourt and Dudley Townships and parts of Herschel, Faraday, Monmouth and Dysart Townships in Hastings and Haliburton Counties, Southeastern Ontario. Good access is provided by Highways 28, 121 and 648 and by township, logging and cottage roads.

The area is about 400 metres above sea level with a local relief varying between 50 and 100 metres. Outcrops are typically small to very small, depending on the bedrock present. Glacial deposits and swamp cover the bedrock. All of the area is thickly forested. Many areas are recently logged.

1.2 Previous Work

The area is covered by two regional compilations, Map 70-2 of the Department of Geology, Carleton University and Map 1957b, "Haliburton and Bancroft Area," of the Ontario Department of Mines (Hewitt 1957b). It falls within Map 708 of the Geological Survey of Canada, the pioneering work of Adams and Barlow (1910), which covers the Haliburton and

Bancroft area. The eastern margin of the area is covered by Fig. 7 of Lumbers (1967), the southern part by preliminary map P. 2205 "Eels Lake Area" by the Ontario Geological Survey (Bright 1980). More detailed maps which overlap with the study area include, maps by the Ontario Department of Mines, 1957-1 "Cardiff and Faraday Township" (Hewitt 1957c), accompanied by a report (Hewitt 1957a), and 2174 "Monmouth Township" accompanied by Open File Report 5021 (Armstrong and Gittins 1968). The Drag Lake area is covered by Ontario Geological Survey Preliminary Map P. 2404 (Culshaw 1981).

Several studies have been completed on various topics within and adjacent to the map area. The most notable recent petrological studies are those of Lal and Moorhouse (1969) on the gedrite-cordierite rocks of Fishtail Lake, Chesworth (1967) on the petrogenesis of the Glamorgan Gneiss Complex, Breaks and Shaw (1973) on the petrogenesis of the Silent Lake pluton, Grieve and Gittins (1975) who studied aspects of corona formation in the Glamorgan Gabbro and there are several studies on the alkaline (nepheline bearing) rocks (Gittins & Miller 1978 for references). Structurally oriented studies have been carried out in area to the south and west of the map by Francoeur (1975) and in adjacent areas 10 kilometres to the east by Best (1966) and Divi (1972).

The area is on the western boundary of the Bancroft Uranium camp and has been extensively explored during several waves of activity. There are three abandoned mines within the area and numerous properties.

1.3 Geological Setting

The study area is in the border zone of the Helikian Central Metasedimentary Belt of the Grenville Province of southern Ontario and the Aphebian basement complex (Fig. 1.2).

The geology of the basement is poorly known although recent efforts have been made to upgrade this knowledge (Davidson et.al. 1982). Ages somewhat greater than 1400 Ma have been recorded at some localities (Krogh and Davis 1969, Bell and Blenkinsop 1980). This complex has long been regarded as a sea of monotonous grey gneiss (Wynne-Edwards 1972).

The Central Metasedimentary Belt has been divided into the older Hermon Group, predominantly metavolcanics which are, in the region of the Elzevir pluton, tholeiitic and calc-alkalic (Brown et.al. 1975) grading away upwards and laterally into the Mayo Group, which is predominantly metasedimentary with an abundance of marbles (Lumbers 1967). The basal member of the Tudor metavolcanics has been dated at 1286 ±15 Ma (Silver and Lumbers 1965). In the area east of the Elzevir and Weslemkoon-Abinger massifs the Tudor metavolcanics are overlain unconformably by the Flinton group of clastic and carbonate metasediments (Moore and

Thompson 1980). This unconformity is marked by an intervening period of plutonism, metamorphism and deformation.

Plutonism plays an important role in the Central Metasedimentary Belt (Fig. 1.2). Lumbers (1967) considered that a biotite-diorite series (albite granite, syenite, diorite, trondhjemite and sodic granite) preceded, at 1250 ±25 Ma, gabbros and diorites, which were succeeded by nepheline syenite, and later potassic syenite, monzonite and quartz monzonite at 1125 ±25 Ma, the latter coinciding with the peak of high grade metamorphism. Moore and Thompson (1980) point out that there are wide uncertainties in Rb/Sr dates for many of these plutons resulting from long term open system behaviour. Nevertheless they recognize a long period of plutonism spanning 1225-1100 Ma which preceded the deposition of the Flinton group in the east of the region. Within this period sodic plutonism (1226-1180) preceded potassic (1104-1072).

In the region of Chandos Township (north and east of Apsley, Fig. 1.1) Heaman (1982) identified three periods of plutonism falling within the broad time span recognized by Moore and Thompson. The gabbroic Tallan Lake Sill is early (1246 ±24 Ma) succeeded by the emplacement of the potassic Silent Lake pluton (1118 ±12 Ma) which coincided with the metamorphic peak followed by the Loon Lake pluton (1065 ±13 Ma).

In the Haliburton-Bancroft belt of alkalic rocks Miller and Gittins (1982) recognize a long history of emplacement of magmatic nepheline bearing rocks which essentially coincides with this time span (1225-1040 Ma). The youngest nepheline bearing pegmatites (1040-1075 Ma) are considered to slightly postdate the metamorphic peak. Considerably younger (970 Ma) are the granitic uraniferous pegmatites adjacent to the Cheddar and Centre Lake and Faraday granites (Fowler and Doig 1979).

Moore (1982) has suggested a useful subdivision of the Central Metasedimentary Belt based on spatial association of type of plutonism and supracrustal rocks. Undersaturated plutonics and carbonates are associated in the Bancroft terrain on the northwest side which encompasses the purported basement-cover contact. This terrain interfingers with, to the southeast, the Elzevir terrain in which tholeitic and calc-alkaline volcanics and carbonates are associated with pre-Flinton trondhjemitic plutonism then unconformably overlain by the Flinton clastics.

Most of the west Grenville province is in the upper amphibolite facies. However the map area is on the flank of the only regional progression from high to low grade rocks (Fig. 1.2). The metamorphism is considered to belong to a facies series of intermediate pressure, with a P, T path close to the alumino-silicate triple point (Chesworth 1971, Chesworth et.al. 1975, Dostal 1975). It appears to be intermediate between the classic Barrovian and Abukuma facies series.

Lumbers (1967) stated that there were two metamorphic culminations. An early greenschist facies event in the central Hastings basin followed a high grade amphibolite facies event at the margins. Moore and Thompson (1980) also have evidence for two metamorphic events, before and after the deposition of the Flinton group. However, the early metamorphism is not thought to be equivalent to the early event of Lumbers, which is considered to be part of a prograde sequence of the second event (Moore; personal communication 1982).

Regionally, there is a broad two-fold structural division first noted by Hewitt (1962). In the high grade rocks close to the boundary with the basement there is a penetrative moderately southeast plunging lineation (Fig. 1.2). Southeast of a line roughly coinciding with the boundary of high-grade metamorphism the lineation has more variable but predominantly northeast trends. The zone of southeast plunging LS fabric appears to be one of several present in the west Grenville province, where they are considered to mark zones of displacement (Davidson et. al. 1982). It is noteworthy also that the Grenville Front tectonic zone is marked by a similar fabric (Lumbers 1975).

Southeast of the zone of southeast plunging lineation northeast trending fold axial traces are common. Two major fold phases are recognized (Rivers 1976, Divi 1972, Thompson 1972, Carmichael 1968). A third phase is of lesser importance. The major folds are generally isoclinal and often of large scale (Fig. 1.2). They may have been initially recumbent. At the boundary of the zone of southeast plunging lineation Divi and Fyson (1973) have shown that the axes of F_2 folds are swung into parallelism with this lineation and the folds are tightened. In the zone of southeast plunging lineation several workers consider the most important mesoscopic folds to be F_2. They are reclined with axes parallel to the lineation (Appleyard 1974, Francoeur 1975).

In the Grenville province of Eastern Ontario, based on studies primarily east of the Elzevir Batholith, Moore and Thompson (1980) have presented a comprehensive tectonic history. This encompasses two orogenic cycles: the Elzeviran (ca. 1300-1100 Ma) and the Ottawan (ca. 1000-1050 Ma). In the Elzeviran a Helikian sedimentary and volcanic succession was deposited. Its central portion was an island-arc complex resting on oceanic crust, while its margins lay on continental crust. Major plutonism, deformation and metamorphism was followed by crustal stabilization, uplift and deposition of the Flinton group in an extensional environment. This second orogeny culminated in polyphase deformation and regional metamorphism, possibly the result of continental collision.

In the basement of the west Grenville crustal imbrication in Tibetan type collision tectonics has been suggested (Davidson et.al. 1982). It seems likely that the zone of southeast plunging lineation at the boundary of the Central Metasedimentary Belt plays some role in this tectonic regime since this fabric is also very important in the basement.

There is no extant correlation of events in this zone with the better known events to the southeast. It is reasonable to assume that orogenic culminations in both areas are identical, that is the Ottawan orogeny, especially since the metamorphic climax in the Haliburton-Bancroft area is generally dated at ca. 1000 Ma (Heaman 1982, Miller and Gittins 1982).

1.4 Present Work

The thesis consists of three sections: General Geology; Major and Minor Structures; Microstructures.

The first section synthesizes the geology as it was known with the knowledge gained during the project. Considerable additions to knowledge of the geology of the north and west parts of the map area were made (see also Culshaw 1981). In particular the following items were elucidated: (i) the nature and extent of the Drag Lake Gneiss Complex (Fig. 1.1, 1.2b) and its stratigraphic and structural relationships with the enveloping rocks of the Central Metasedimentary Belt; (ii) the extent and stratigraphic and structural relationships of the Farquhar Lake Mafic Complex; (iii) the nature and extent of the Straggle Lake Grey Gneiss Complex; (iv) and complementary to the delineation of the grey gneiss complexes (possible basement) is the elucidating of the nature of their enveloping rocks both metaplutonic and supracrustal, the most important of which is the delineation of the large syenite body south of Drag Lake. Although lithological boundaries in the southern and eastern part of Fig. 1.2 are adopted with little modification from Hewitt (1957c) and Armstrong and Gittins (1970) the composition and structure of the Cheddar batholith was poorly known previously and was mapped by the author. All rock units and their relationships are described in the text.

In the second section the results of structural mapping are described. This was conducted with a view to understanding the origin of the SE plunging regional lineation. It is clear that several features were associated with the imposition of the lineation: (i) most obviously, a synmetamorphic stretching of all the rocks; (ii) the emplacement and deformation of large granitoid bodies; (iii) that gravity probably played a role both in the emplacement of the granitoids and in forming structures around the Farquhar Lake Mafic Complex; (iv) the probable thrust emplacement of basement gneiss; (v) the formation of NW trending fold structures which are coaxial with the regional lineation.

In the third section, the results of the investigation of some microstructures are presented. Several features of relevance to the overall tectonic picture were discovered: (i) the presence in quartz ribbons from granite gneiss of evidence for dynamic and metadynamic oriented grain-growth; (ii) that as a result of the cessation of this growth early in the metadynamic phase a memory of the dynamic recrystallisation is retained by the C-axis microfabrics in the quartz ribbons which can therefore be used for kinematic analysis, in contrast to those of the quartzites, in which static grain growth is much further advanced; (iii) the subsequent kinematic analysis generally agrees with that gained from large scale structures, upper layers were sheared to the NW parallel the lineation; (iv) an asymmetric quartz microfabric which destroys the earlier microstrucures can be used as a kinematic indicator; the sense of shear which it implies is the opposite to that deduced from earlier structures, but due to the local nature of the fabric can be reconciled with an overall model of NW directed ductile shearing; (v) the deformation of gabbro relies on inter- and intracrystalline diffusion processes which rely on the access of water and relatively long range diffusion of components. Thus a gabbro which was emplaced early can appear anomalously young and fresh and behave as a hard resistant mass during the regional deformation.

1.5 Acknowledgements

The writer is indebted to Dr. W.K. Fyson for his supervision and constructive criticism of this work. Discussion with other members of the staff at the University of Ottawa, particularly with Drs. R. Kretz, C. Pride and A.J. Baer have been most useful. I am especially indebted to Dr. C. Mawer, presently at the University of New Brunswick, to Dr. J. Starkey, of the University of Western Ontario, to Dr. S. Hanmer of the Geological Survey of Canada, and to J. Wood, Chief Geologist of the Ontario Geological Survey for encouragement, advice and catalytic discussion. I acknowledge the warm support of fellow graduate students, Toby Rivers, Bob Thivierge, John Van der Leeden and Leo Nadeau. It has been my privilege to work with and learn from Dr. A. Davidson of the Geological Survey of Canada for much of the past two years; to him I express my gratitude for fostering and deepening my interest in the geology of the Grenville Province and continued support during the latter stage of writing this thesis.

Mapping of the western part of the area was accomplished under contract to the Ontario Geological Survey, to whom I am also indebted for some geochemical analytical services. Other analyses were performed by Ron Hartree at the University of Ottawa. Dr. S. Reed provided microprobe analyses performed at the University of Carleton. Andre Lalonde at McGill University enthusiastically performed X-ray determinations of structural state in some feldspars. Abdul Choudry provided excellent geological assistance in mapping the western part of the area. Edward Hearn of the University of Ottawa was a consistent source of aid and advice concerning draughting and photography. Mrs. Anne Buie heroically typed and retyped the thesis.

This work was also supported by a research grant from the National Research Council to Dr. W. K. Fyson, the writer would like to acknowledge this and thank the students and permanent staff of the University of Ottawa for providing a friendly work environment.

Finally, I must express my gratitude to my wife, Julie, without whom this work would not have been accomplished and to my children, Rebecca and Elena, for affording me a first hand knowledge of diapirism.

2. GENERAL GEOLOGY

2.1 Introduction

In this chapter the distribution, field appearance and petrography of the major rock units are described. The basic geochemistry of some of the plutonic gneisses is also presented. The problem of the time relations of the plutonic orthogneisses is discussed with respect to deformation and metamorphism. An attempt is made to relate these relations to those known outside the map area.

There are five major lithostratigraphic units: (1) the tonalitic grey gneiss (Unit 3) forms a large mass around Drag Lake (Fig. 1.1) and, with associated rocks, is distributed across the north of the map area. The origin of this unit is problematic. It may represent the basement complex of the supracrustal rocks or one of the oldest plutonic gneisses intruding them. (2) Supracrustal rocks, which are predominantly calcareous, include marbles (Unit 1A), amphibolites (Unit 2A) and a variety of paragneisses (Units 2A and B). (3) Mafic intrusive rocks (Unit 4) are now predominantly gneissic but include some with primary igneous textures in various states of preservation. (4) Granitic gneisses (Unit 6) are concentrated in large bodies e.g. the Cheddar, Monck Lake and Centre Lake granites. Locally these cross-cut the enclosing supracrustal rocks although on the large scale they form concordant bodies. (5) Syenitic gneisses (Unit 5) are mostly of plutonic origin. These are related to the nepheline syenites for which the Bancroft area is famous. In many places supracrustal rocks, granitic and syenitic gneisses are interlayered forming a characteristic terrain of rapidly changing mixed lithologies in which the precise definition of lithological boundaries is difficult.

The estimated proportions of the various rock types present in the area is given in Table 1 (Appendix I). A noteworthy feature is the large amount of gneiss present which is interpreted as having a plutonic origin (~ 66%). It is evident that the history of the plutonism is a key factor in understanding this area and correlating events in it with those elsewhere.

There is some disagreement between previous workers' accounts of the relative time of emplacement of the rocks interpreted as plutonic orthogneiss in areas overlapping with and surrounding the map region (Table 2, Appendix I). The most notable discrepancies regard the age of gneiss forming the core of the Glamorgan Gneiss Complex. This gneiss is correlated with the grey tonalitic gneiss of this study. Previous workers have considered it as basement to the supracrustals (Bright 1980), probably basement to the supracrustals (Culshaw 1981), as predating the syenites and gabbros (Armstrong and Gittins 1968, Chesworth et.al. 1975), and as succeeding the mafic plutonics (Chesworth 1967). There is a similar disagreement about the age of the granitoids of the Cheddar batholith. However, it is recognized that the major bodies of plutonic orthogneiss predate or were emplaced at the same time as the metamorphism and deformation.

There are indeed practical problems of assigning relative ages to the orthogneiss bodies (Table 3, Appendix I). The major plutonic bodies form conformable bodies with rare mutual contacts, which are often ambiguous. The relative age of the gabbros, syenite and granites can be determined on the basis of the cross-cutting of a major body of one by a minor body of another, and, in the case of the gabbros and syenites, by the inclusion of a xenolith of one in another. However, it may be somewhat presumptuous to correlate a thin vein of foliated granite which cuts a metagabbro with, for example, the Monck Lake Granite Sheet. The main feature of a postulated sequence of plutonic events is that emplacement of the gabbroic rocks is interpreted as preceding the syenites and the granites. The age of the grey tonalitic gneiss is problematic. There are two acceptable hypotheses:

1) that all of the bodies of grey gneiss are basement rocks;
2) that all are early plutons which intrude the supracrustals. These possibilities will be considered further in the relevant section.

The supracrustal rocks have long been known to be similar to rocks elswhere in the Central Metasedimentary Belt and have been termed Grenville Type Metasediments (Hewitt 1957a). Lumbers (1967) subdivided the rocks of the central and western parts of his Ottawa River Remnant into the Hermon Group, dominated by metavolcanics, and the Mayo Group, dominated by carbonate metasediments. The south-eastern part of the map area lies in the western part of his Ottawa Part of his Ottawa River Remnant. Bright (1977) extended this stratigraphy and assigned lithologies to the west of the Anstruther and Cheddar Complexes of the Cardiff-Harvey Arch to the Mayo and Hermon Groups according to the dominance of marble or of rocks interpreted as being meta-volcanic. The western part of the map area lies partly within and partly to the north of the area treated by Bright. It contains units which are continuous into this area. This general stratigraphic framework may be accepted tentatively. However detailed stratigraphic correlation must be questioned since in such a structurally complex area the role of such processes as, for example, transposition may considerably obscure the true stratigraphic relations (Hobbs et. al. 1976).

2.2 Supracrustal Rocks

On the map (Fig. 1.2) the supracrustal rocks are subdivided into two major units. These consist of marbles and associated rocks (Units 1A and B) and non-carbonate rocks (Units 2A and B). The latter are divided into calcarous (Amphibole-rich) (Unit 2A) and non-calcareous rocks (Unit 2B), following Lumbers (1967). Mineralogy is summarized in Table 4 (Appendix I).

There is both a broad regional variation in the composition of these units and their relative abundance. This is described below.

2.2.1 Unit 1a; Marble and Associated Rocks

Southwest of the Cheddar and Cardiff Complexes a thick belt of marble strikes northeast across Paudash Lake. This marble is reported to have some interbeds of paragneiss and amphibolite but not to be associated with quartzite (Hewitt 1957a). The thinner belt which almost completely encircles the Cheddar Complex is similar in this respect.

In marble to the west and north of the Cheddar and Cardiff Complexes marble, rusty paragneiss and quarztite are intimately associated and in places are thick enough to map as separate units. This association of marble, rusty paragneiss and quartzite is also found south of Drag Lake and north and south of Farquhar Lake where it forms the primary supracrustal component of the heterogeneous syenite gneiss. This unit north and west of the Cheddar and Cardiff Complexes forms one interconnected body. It continues out of the map area on the west, southwest and northern margins where it is of unknown extent.

The outcrop appearance of the marble is characteristic.

It is usually massive and coarse-grained with a weathered aspect in which the cleavage and the grain-boundaries of the carbonate are prominent and the silicate minerals stand out in sharp relief. There is much evidence for flowage and great ductility contrast between marble and silicate layers (Lumbers 1967) which are often broken, folded, rotated or boudinaged (Plate 1a). Such marbles with chaotic fabrics of silicate fragments termed tectonic-breccias by Hewitt (1957a), are treated in greater detail in Section 3.2.5. Fine grained marble is rare. It is often associated with a high percentage of graphite in a rock with mylonitic aspect.

Metamorphic pyroxenite is associated with marbles and quartzite in the Marble Unit north and west of the Harvey-Cardiff Arch. In the Drag Lake area it is recorded at between 10 and 15 per cent of all outcrops of this unit. It is a massive, green, equigranular fine to medium grained rock interbedded with or occurring as large pods in the marble. The massive pyroxenite commonly has fractures filled with coarse actinolite and other silicates. The largest bodies are found northwest of Allen Lake and north of Farquhar Lake. These can be traced for over 300 metres along the strike. The rock is sometimes found as drop-shaped pods in syenitic gneiss, which are criss-crossed by straight walled cracks filled with undeformed syenite. It is also found with an agmatitic relationship to syenite and granite. Deformation of this variety results in a gneiss with feldspathic layering which anastamoses around pyroxenite lenses.

The most common silicates present throughout the area are phlogopite and diopside. Graphite often accompanies these. Serpentine is less common but ubiquitous. Armstrong and Gittins (1968) and Hewitt (1957a) do not report assemblages with dolomite present. In the Drag Lake area, however, calcite and calcite-dolomite marbles are juxtaposed everywhere. Calcite and dolomite may be associated with any of the silicates except diopside. Armstrong and Gittins (1968) report rare occurrences of serpentine replacing forsterite. In a marble from the northern border of the map area in the unit overlying the Grey Gneiss Complex of Drag Lake tremolite replaces forsterite. Phlogopite, calcite and dolomite are present in this rock. In marble from the south of Miskwabi Lake tremolite and tremolite with quartz rim diopside which is accompanied by phlogopite and calcite. Throughout the area rosettes of coarse tremolite which appear to be totally unstrained, are quite common. In a sample of this texture from Highway 121 at the extreme western edge of the map sheet the coarse tremolite overgrows calcite and diopside.

Marbles rich in silicates have been referred to as silicate(d) marble (Hewitt 1957a, Armstrong and Gittins 1968). An increase in silicate content is related to increasing proximity to granitic or syenitic bodies. The end product may be an exotic rock with up to 50 per cent of a variety of ferromagnesian minerals with carbonate, apatite, feldspar, quartz and sphene.

In thin section the microstructure of the carbonate belies the evident strain which the rock has suffered. Grain size is coarse, from 1 to 10 millimetres with an average around 3 or 4 millimetres. The coarsest grains are in rocks which are free of silicates. The grains have little or no undulatory-extinction. The only signs of strain are the twin lamellae. The grains vary in shape from equant to moderately elongate. The grain boundaries are irregular and embayed. Silicates may lie on the carbonate grain boundaries or within the grains (Plate 1c). The silicate inclusions very often have a rounded drop-like form. Occasionally silicate inclusions show signs of great crystalline strain which contrasts with that of the surrounding carbonate (Plate 1d).

The metamorphic pyroxenite is formed of equiaxed diopside with regular grain boundaries. Microcline, phlogopite, calcite and quartz may be present in accessory amount. It is very similar to the diopside rich layers sometimes found in quartzite. It may be distinguished from a coarser pyroxenite formed of dark green elongate clinopyroxene intimately associated with coarse calcite, scapolite and sphene.

2.2.2. Unit 1B, Quartzite

Quartzite is commonly closely associated with marble, especially west and north of the Harvey-Cardiff Arch. In the Drag Lake area there are between seven and eight times as many marble as quartzite outcrops. At Esson Lake it forms a thick layer which continues for over ten kilometres southeast past Tory Hill. More commonly it is present as isolated outcrops among the marbles, evidently forming elongate pods.

The quartzite may be massive or layered due to variations in proportion of non-quartz minerals. Rarely a layered rock is formed of alternating quartz and diopside horizons. The layered appearance is accentuated where it is penetrated by recrystallised syenitic and granitic sheets. Especially northwest of the Cardiff complex the quartzite has a highly foliated flaggy aspect. It is usually medium or coarse grained. Elongate minerals such as diopside form a regular linear fabric. Biotite, when present, forms a very planar foliation.

There are two varieties of quartz microstructure. The most common is formed of medium to very coarse irregularly shaped grains in which accessory minerals lie within the quartz grains or on the grain boundaries. The second type is locally developed and is a fine grained recrystallisation product of the coarse microstructure. The nature and significance of these microstructures is more fully discussed in Section 4.2.8.

Among the accessory minerals diopside, biotite, actinolite and feldspar are the most common, sometimes accompanied by sphene, pyrite, calcite and zircon.

Glaucophane accompanying green clinopyroxene has been reported by Armstrong and Gittins (1968) from quartzite in Monmouth Township which shows signs of LS2 recrystallisation.

2.2.3. Units 2A and B, Non-Carbonate Supracrustal Rocks

There is a variety of supracrustal rocks in which hornblende, pyroxene or biotite are the major constituents besides plagioclase or quartz and plagioclase. The small group of supracrustal rocks spatially associated with the tonalitic grey gneisses are described in Section 2.3.5.

The thickest development of non-carbonate supracrustal rocks flanks the Cheddar and Cardiff complexes. Within this mass on the southeast sides of the plutonic complexes a biotite-plagioclase-quartz gneiss is dominant over amphibolite and calc-silicate gneiss. Locally true pelitic gneiss is found, for example on the east flank of the Cardiff antiform and as isolated outcrops within the east part of the Cheddar complex. In the supracrustal layer underlying the Centre Lake granite of the Cardiff complex there appears to be a change along strike from biotite-plagioclase-quartz gneiss to amphibole bearing assemblanges (Hewitt 1957c). On the west and northern sides of the Cheddar and Cardiff complexes amphibolites and calc-silicate gneisses dominate over calc-silicate-free assemblages, no pelitic rocks are known. This unit is continuous out of the map area across the southern margin on the west side of the Harvey-Cardiff Arch.

Two other isolated masses, predominantly amphibolitic, are found south of Miskwabi Lake and to the west of this lake associated with the Farquhar Lake Mafic Complex. A thin continuous layer surrounds the grey tonalite gneiss complex of Drag Lake. Other bodies are found throughout the northern part of the map area intimately associated with marble or the heterogenous syenite gneiss but are not big enough to map.

In all the rocks primary features are lacking. However, layering and mineral foliation are parallel, intrafolial folds are fairly common as well as boudinage of competent layers, and, in certain cases, internal boudinage. A mineral lineation is found in all appropriate compositions. Sometimes a compositional layering is present which may correspond to an original layering even though it is much modified.

Amphibolites and clinopyroxene rich rocks are medium grained and equigranular. Both types may be massive or layered. The pyroxene rich types especially tend to be layered. Some amphibolites have a mesoscopic fabric formed of ellipsoidal aggregates of feldspar in an amphibole matrix. This may correspond to a deformed plagioclase-phyric texture. It is found in parts of the large mass of amphibolite which cuts Highway 121 east of Dudmon Lake and in the thin discontinuous amphibolite overlying the grey gneiss north of Farquhar Lake.

Biotite-quartz-plagioclase rocks vary from medium-grained equigranular with or without a layering through fine grained, delicately laminated rusty varieties common in the west to rare schistose pelitic varieties.

All of these rocks contain some granitic or syenitic material either as discrete layers or pods or an increased content of disseminated pink alkali feldspar. This is common in the vicinity of the major syenitic bodies and especially in the northern areas where granite, syenite and supracrustal rocks are intermixed intimately.

Details of mineralogy are given in Table 4 (Appendix I), which is compiled from petrography by the author and from the reports of Hewitt (1957a) and Armstrong and Gittins (1968). A relatively small number of major minerals are present, e.g. hornblende, biotite, plagioclase.

In the amphibole rich rocks (Unit 2A), plagioclase composition is restricted to the oligoclase-andesine range. It is often replaced by scapolite. More calcic compositions (greater than An_{45}), sometimes display fine, parallel bright-lamellae lying at 18 to 20° to (010). These are identical to Boggild intergrowths, a high grade unmixing intergrowth found in intermediate plagioclase (Smith 1974). Sphene and apatite are the most characteristic accessory phases. Clinopyroxene is sporadic but widespread. In some samples from the amphibolite body east of Dudmon Lake nepheline has been reported (Pride, personal communication 1981).

In the rocks in which clinopyroxene is important a wider variety of minerals are present, which are often present in different amounts forming layers. Again sphene is the dominant accessory.

In the rocks dominated by biotite-plagioclase-quartz assemblages (Unit 2B), plagioclase compositions are restricted to the oligoclase-andesine range. More calcic plagioclase is found in the rusty biotite gneiss assocated with marble in the west. As in the amphibolites these plagioclase often display Boggild intergrowth. The most common accessory mineral throughout the area is tourmaline. In the rusty biotite gneiss graphite is also common. The high grade assemblage comprising microcline-sillimanite-garnet-biotite-plagioclase and quartz is found in the rusty biotite gneiss south of Miskwabi Lake. Hewitt (1957a) reports a very small amount of kyanite in one sample from a drill hole in the sillimanite bearing paragneiss on the east side of the Cardiff antiform. With few exceptions these rocks show textures typical of high grade regional metamorphism. The dominant variety is the decussate texture (Spry 1969, Vernon 1976) present in biotite, amphibole or biotite-amphibole aggregates. In this microstructure the interface between neighbouring grains tends to be parallel to a low index plane of one of the grains. Plagioclase forms equant grains with simple boundaries. Twins are few, most commonly on the albite law.

2.2.4. Origin of the Supracrustal Rocks

There can be little doubt that most of the supracrustal rocks are metasediments comparable to similar rocks elsewhere in the Central Metasedimentary Belt (e.g. Lumbers 1967). All features are compatible with this, such as the close spatial association of marble, calcareous gneisses, quartzite and biotite gneiss. The latter with its common content of tourmaline and/or graphite is clearly a paragneiss. Armstrong and Gittins (1968) have pointed out the dominance of calcareous compositions and the lack of abundant pelites. Noting the relative abundance of quartzites in Glamorgan and Monmouth Townships in comparison to the surrounding areas they speculated that the quartzites represented sediments which had been reworked in a coastal environment.

Bright (1977, 1979, 1980) has gone into great detail assigning specific sedimentary designations to specific metamorphic rocks. His scheme is an elaboration on the general notion of a pile of calcareous sediments. While in some cases the interpretation of specific metamorphic rock types is credible others are much less certain. For example, calc-silicate marble is fairly interpreted as a metamorphosed siliceous dolostone. On the other hand there are many pink feldspathic layers which are not meta-arkoses but deformed granitic layers of igneous origin.

Bright (1977) considers some of the larger amphibolite bodies to be meta-volcanic rocks, for example, that on the west side of the Cheddar Complex. For bodies with fabrics interpreted as deformed and recrystallised plagiophyric textures this is an acceptable hypothesis. The body east of Dudmon Lake is the best example. In light of its known alkaline character (Pride, personal communication, 1981), the possibility that it is a metamorphosed alkaline lava should be investigated farther (see also Bright 1979).

2.3 Unit 3:The Grey Gneiss Complexes

2.3.1. Introduction

There are three grey gneiss complexes (Fig. 1.2b): The Drag Lake Complex, in the northwest and extending westward out of the map area,, the Straggle Lake Complex in the northeast and extending northward out of the map area, and the Farquhar Lake Sheet, a small folded discontinuous sheet associated with gabbroic rocks in the north of the map area. The boundaries of all three bodies as shown in Fig.1.2 are quite different from those shown in previous maps. The complexes are formed dominantly of grey tonalitic gneiss (Map unit 3a), the "Grey Granite" of Adams and Barlow (1910). The majority of the complexes are very large in comparison with other bodies of orthogneiss and continuous out of the map area. In the Drag Lake and Straggle Lake complexes a subordinate but significant garnet gneiss (Map unit 3c) includes cordierite-gedrite rocks of Fishtail Lake and new gedrite and cordierite-gedrite localities (Lal and Moorhouse 1969), that lie along a discontinuous horizon mostly near the contact of the grey tonalitic gneiss with its enveloping rocks.

An important question is whether the grey tonalitic gneiss and the "grey granite" of the Glamorgan Gneiss Complex (Chesworth 1967) to the south of the study area represent remobilized basement of the supracrustal rocks or whether they are orthogneiss which intruded the supracrustal rocks, and are correlatable with the early sodic granites described by Lumbers (1967). A second consideration is whether the grey gneiss of the Farquhar Lake Sheet (which lies within the supracrustal rocks) is correlatable with the other larger masses. If it is and if these larger masses are basement gneiss then it is a thrust sheet. A related question concerns the status of the garnet gneiss, whether it is the structurally lowest member of the Grenville Supergroup metasediments or part of an older basement assemblage.

These questions are not definitively answered here. The weight of petrological and structural evidence is in favour of the grey gneiss being a member of a basement assemblage and the garnet gneiss unit representing the lowermost units of the overlying metasedimentary sequence.

The Drag Lake Complex dominates the northwest corner of the mapsheet. It is part of a larger mass which extends more than 15 kilometres to the west and southwest which has been named the Dysart Granite Gneiss (Hewitt 1957b). It is a stratified body mainly dipping shallowly to the south east. A more complete structural treatment is given in Sections 3.2.5. and 3.3.6.

The Farquhar Lake Sheet is a relatively thin discontinuous stratified sheet (Fig. 1.2). The outcrop pattern is complex owing to upright folding on a variety of axial surfaces and axes which plunge very gently southeast. The sheet is closely associated with the Farquhar Lake Mafic Complex (Unit 4). It separates the Mafic Complex into two levels.

The Straggle Lake Complex is part of a larger gneiss complex which extends north beyond the bounds of the map area (Hewitt 1957b). The eastern boundary from the eastern side of Elephant Lake to Baptiste Lake is known only from reconnaissance by the author. The nature of the interior of the complex in this part is unknown.

No cross cutting relations of other rocks by the grey tonalitic gneiss are known. Within the tonalitic gneiss no xenoliths of Grenville Supergroup rocks or other plutonic rocks have been found.

The grey gneiss complexes, with the exception of the Farquhar Lake Sheet, lie at the structural base of the supracrustal rocks of the Central Metasedimentary Belt. This contrasts with the position of the syenitic, granitic and gabbroic orthogneisses which occur throughout the supracrustal rocks in large and small bodies.

At the western boundary of the Farquhar Lake Sheet, northwest of Yankton Lake, there are several narrow, discontinuous conformable bodies of the gneiss within the underlying supracrustal rocks. Whether or not these bodies were tectonically emplaced cannot be ascertained.

Within unfoliated gabbro (Unit 4a) at the southwest tip of Farquhar Lake there is a thin (15 cm) layer of grey gneiss of unknown (> 1 m) lateral extent with foliation parallel to its margins. The presence of a foliation in the gneiss and its absence in the gabbro host has two possible interpretations: i) that the gneiss is a xenolith and the foliation is earlier than the intrusion of the gabbro; or ii) that the gneiss is a sill in which shear has been concentrated. Since there is locally a complete absence of foliation in the host the first interpretation is favoured.

2.3.2. Unit 3A and B; Grey Gneiss and Pink Granite

Characteristically the gneiss complex has three components: the tonalitic gneiss, amphibolite layers or pods and foliated pink granitic sheets and dykes (Plate 2c). It may be described as migmatitic.

The tonalitic gneiss forms greater than 85 percent of the complexes. It is generally fine to medium grained and uniform in composition. The mafic content (biotite and hornblende) varies from 5 to 20 percent with most varieties having an estimated 5 to 10 percent. The most common variety is even grained and lacks a shape fabric. In the Drag Lake Complex a planar-linear shape fabric formed by clustering of light and dark minerals and by elongate quartz is present particularly in the centre. This type of fabric is interpreted as a deformed megacrystic igneous texture although no gradations to undeformed igneous textures have been found.

Amphibolite pods and layers, long known to be characteristic of the grey gneiss (Adams and Barlow 1910), form approximately 10 percent of the complexes. The layers vary in length from metric to decametric and in width, from centimetric slivers to layers greater than 3 metres thick. Most commonly the average width is in the 30 to 50 centimetre range and the length to width ratio is between 5 and 10 to 1. The amphibolites are fine grained and lineated and always conformable with fabric in the host rock. In some varieties of the gneiss the amphibolite forms more than 40 percent of the rock interlayered with tonalitic or trondjhemitic and granitic material. This layered gneiss is present on the boundaries of the Drag Lake Complex and sporadically in the other bodies. It is in this kind of gneiss that the mafic layers may be broken into square-ended boudins with the interstices filled by matrix trondjhemite. In such gneiss NE of Drag Lake clinopyroxene in mafic layers and matrix is partially replaced by amphibole (Plate 2a). Since the boudinage here precedes amphibolization it suggests that a high ductility contrast deformation predated the regional amphibolite facies event and the formation of the lineation.

The pink granitic fraction (Unit 3B) forms approximately 5 percent of the unit. Locally it forms up to 80 percent, for example in the southwest corner of Drag Lake. The granite occurs in thin stringers, sills and dykes which are tens of centimetres or, less often, one or two metres wide and cross cut all fabrics of the grey gneiss. Rarely, as for example on the northeast shore of Drag Lake, the granite forms mappable bodies. It is medium to coarse grained and only rarely is it strongly deformed with a corresponding reduction in grain size. The granite has a planar-linear fabric of quartz corresponding to the regional lineation. The veins often have a larger-scale fabric in which a near concordance between vein margins and fabrics is present in all sections except those at a high angle to the lineation (Section 3.2.5.). Because the granite both cross-cuts structures and yet displays an internal fabric it may be regarded as syntectonic.

Very coarse pegmatites are found sporadically within the southern part of the Drag Lake Complex. These are unfoliated and the country rock foliation is distorted around them. They are clearly the latest element of the complex.

The host gneiss has a mineralogy which is everywhere simple. The main minerals are hornblende, biotite, quartz and oligoclase (Table 5, Appendix I). Microcline is usually present in accessory amounts such that the modal composition of the rock falls within the tonalite field (Table 6, Appendix I). Zircon, magnetite, apatite and sphene are common accessories. Garnet is rare. The oligoclase varies from An_{13-30} with most in the range An_{25-30}. Most of the rocks have subequal hornblende and biotite, rare more mafic compositions are hornblende rich. Approximately one sixth of the Drag Lake Complex is underlain by gneiss in which biotite is the only mafic mineral present.

Textures are all metamorphic, there is little textural trace of primary igneous parentage, such as relict unrecrystallised feldspar. This contrasts with all the other orthogneisses.

The grain size in all varieties is uniformly fine average approximately 0.75 mm). In equigranular varieties quartz is dispersed uniformly in equant grains. In the lineated varieties, which are more common, the quartz grains form ribbons with aspect ratios in excess of 5 to 1. These ribbons are identical to those found in all the other granitic rocks of the area. They are formed of relatively few quartz grains, have a weakly developed undulatory extinction, regular quartz-quartz grain boundaries which lie near perpendicular to the ribbon length and have elongate, aligned feldspathic inclusions.[1]

Plagioclase forms equant grains with irregular grain-boundaries. Twinning is relatively sparsely developed, only on the albite and pericline laws. Undulatory extinction and

---

[1] They are comparable to the "True Granulite" texture of Spry (1969, Plate XXXI (a)).

kinking are very rare in the plagioclase. Microcline, when present, forms fine interstitial grains. No trace of perthite or antiperthite has been observed.

Biotite and hornblende, when present together, are always intergrown forming a decussate texture.

A rare exception to these equilibrium metamorphic textures is found in a sample from the extreme northwest corner of the Drag Lake Complex. The gneiss is a layered variety formed of 30-40 percent of thin mafic layers with a medium grained trondhjemitic matrix. Both in the trondhjemitic and the mafic layers clinopyroxene is partially replaced by amphibole (Plate 2a).

In the amphibolite layers the main minerals present are hornblende and plagioclase (An_{27-48}). Biotite and clinopyroxene may be present, garnet is rare. Magnetite, apatite and sphene are accessories. Microscopic bright lamellae, at a low angle to (010), are present in more calcic plagioclase. These are interpreted as Boggild intergrowths (Smith 1974). Hornblende forms more than 60 percent of the rock and has the characteristic decussate texture.

In a typical pink granite from the northwest shore of Drag Lake, medium grained (1-2 mm) albite (An_{10-11}), microcline and quartz are subequal. Minor muscovite and biotite and accessory magnetite, zircon and sphene are present. The plagioclase has sodic (An_{0-5}) rims and narrow rectangular domains lying parallel to the albite twin trace. It is also flecked by very fine white micas. However there

FIGURE
2.1

Chemical variation in the Drag Lake grey gneiss complex and comparable Grenville and Precambrian gneisses. Symbols: Drag Lake, 1. Hornblende-biotite gneiss; 1a. biotite gneiss; 1b. hornblende gneiss; 1c. mafic gneiss. 2. hornblende-biotite gneiss, Farquhar Lake sheet. 3. hornblende-biotite gneiss, Straggle Lake complex. 4. average grey granite (Hewitt and James 1956). 6a. Weslemkoon Trondjhemite; 6b. Weslemkoon granodiorite (Lumbers 1967). 7. average hornblende-biotite gneiss from East Greenland (Sheraton et al. 1973). 8. average Laxfordian hornblende-biotite gneiss, Harris and Lewis (Sheraton et al. 1973). 9a. garnet-gedrite-biotite cordierite gneiss, Drag Lake. 9b. garnet-biotite gneiss, Drag Lake.

1(a)

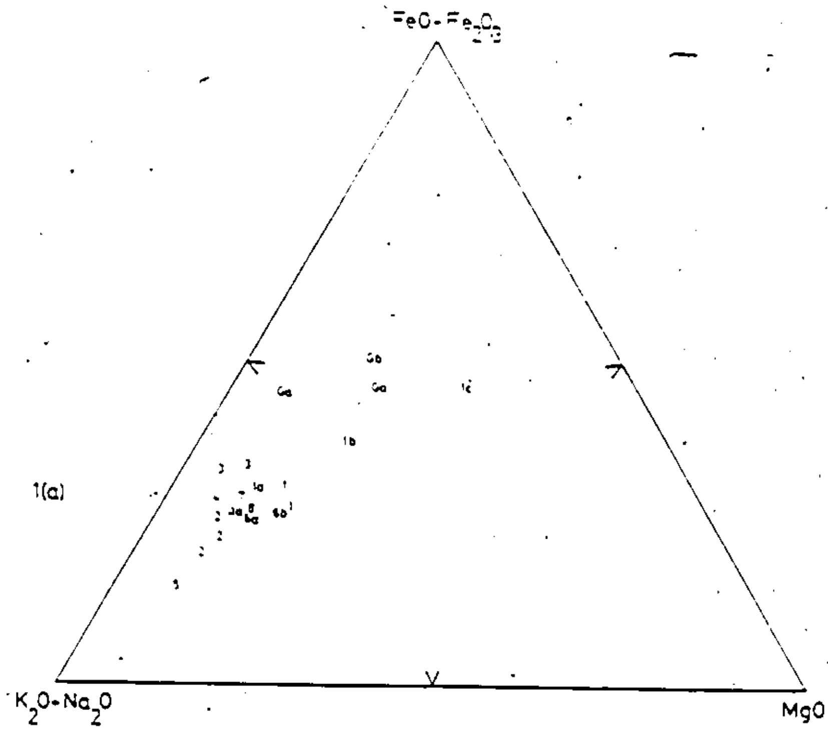

1(b).

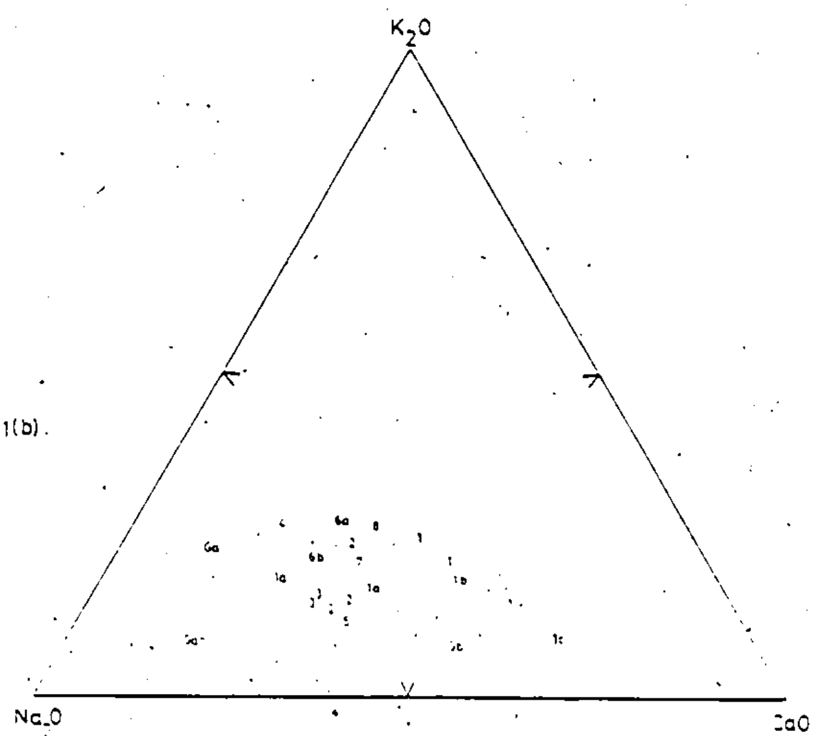

is no sign of kinking or grain size reduction which might be attributed to recrystallisation. Microcline is free from perthitic intergrowths. Quartz has a similar microstructure to that of the grey gneiss.

The geochemical data for the grey tonalite gneiss is summarized in Table 7 (Appendix I). In general, similar looking rocks from the various grey gneiss complexes are similar in major elements and ratios of minor elements. The similarity of the grey gneiss to the grey granite of the Glamorgan Gneiss Complex SW of the study area (see Fig. 1.1) (Chesworth 1967) is not unexpected on account of the similarity and proximity of this complex to the Drag Lake Complex. Major element chemistry is not greatly different from that of the Boulter Pluton which occupies a similar structural position near the base of the Supergroup some 30 km east of the map area (see Fig. 1.1) which is purportedly a representative of the sodic granite suite which has been deformed and metamorphosed (Lumbers 1967). There is also a marked similarity between these rocks and other typical Precambrian grey gneisses.

The similarity of the rocks to members of the sodic-granite suite and other typical Precambrian grey gneisses is also brought out by the CKN and AFM plots (Figure 2.1). The more mafic members of the suite make a clear trend on both plots with the clustered more leucocratic members. There is a strong correlation between certain of the major elements and SiO_2, CaO and total FeO (Table 8, Appendix I), as expected in a suite of igneous rocks.

Rb/Sr ratios tend to conform to rock type. Thus rocks which are biotite rich have the highest ratios, reflecting the high proportion of Rb relative to Sr in biotite. Lower ratios reflect the diminishing importance of biotite and the greater influence of plagioclase, in which Sr is more abundant than Rb. The ratios are comparable to both gneisses from near the base of the Supergroup and representatives of the sodic-granite suite (Bell and Blenkinsop 1980) and typical 'grey gneisses' from the Precambrian of East Greenland (Table 7, Appendix I). K/Rb ratios do not differ greatly from those of the average igneous rock of Shaw (1968). (Table 7, Appendix I).

The pink granite fraction is only represented by a single sample (Table 9, Appendix I). It has a high K_2O/Na_2O (> 1) ratio, comparable to that of similiar two-feldspar-medium grained granites from the Harvey-Cardiff Arch (Table 9, Appendix I), the pink granite of the Glamorgan Gneiss Complex, and the granitic phases of the heterogeneous syenite gneiss unit.

2.3.3. Summary

There are several salient features of the grey gneiss: i) the masses all form stratiform sheet-like bodies with a planar linear fabric; ii) there are no conclusive cross-cutting relations with other rocks; iii) they have a characteristic three-fold association of grey gneiss, amphibolite pods and layers and a pink granitic or pegmatitic fraction; iv) they have a simple and uniform mineralogy, comprising hornblende, biotite, quartz and oligoclase; v) they are, in contrast to all the orthogneisses which intrude the supracrustals, completely recrystallised, with no trace of relict perthite; vi) there is one exceptional case of a partly hydrated assemblage (Plate 2a) which hints at an earlier dry assemblage; vii) although they are rather uniform in composition, they show chemical variation compatible with that of an igneous suite; viii) in major elements they are similar to (a) the mesoscopically comparable gneiss of the nearby Glamorgan Gneiss Complex; (b) to some early sodic granites of southeast Ontario; and (c) to other Precambrian 'grey gneiss' terrains, to which they also favourably compare in terms of minor elements; ix) the Farquhar Lake Sheet is associated with mafic plutonism; x) the major bodies lie at the structural base of the supracrustal rocks contrasting in position with the other orthogneisses, which occur throughout the supracrustal rocks; xi) they form very large bodies, compared to other orthogneiss bodies.

2.3.4. Origin

There are two hypotheses for the origin of the grey tonalitic gneiss: (1) That all of the bodies, including the equivalent rocks in the Glamorgan Gneiss Complex, are members of the early sodic granite suite as defined by Lumbers (1967); (2) That they are the remobilized basement of the Grenville Supergroup.

If the second hypothesis is true then small sheets like that at Farquhar Lake which lie within the supracrustal rocks must be thrust-emplaced.

The geochemical evidence is compatible with either hypothesis. It is possible that a more sophisticated approach involving analysis for the rare earth elements will be more fruitful. Likewise many of the metamorphic features such as the almost complete lack of possible primary minerals, the complete recrystallisation and many of the structural features can be explained on both hypotheses. It is to be expected that an early pluton and a basement complex of similar composition both deformed in a high grade metamorphic event will converge in appearance.

The single feature favouring the first hypothesis is the spatial association of the Farquhar Lake Sheet with gabbroic rocks. Comparable association is observed for rocks of the sodic-granite suite (Lumbers 1967).

There are several features which favour the second hypothesis. The first is the lack of cross-cutting relations between the grey-gneiss and other rocks and the lack of xenoliths of compositions approaching those of the Grenville Supergroup and the presence of an apparent xenolith of foliated grey gneiss in unfoliated metagabbro. The second is the similarity between this grey gneiss and others considered elsewhere to be basement to the Supergroup. The most important similarity is the association of grey gneiss (with oligoclase) amphibolite pods and layers and the pink granitic fraction which was considered by Wynne-Edwards (1972) to be typical of basement gneisses of parts of the Ontario Gneiss segment. Indeed the association of migmatitic grey-gneiss with amphibolite pods and layers seems to be common in crystalline Precambrian basements in many parts of the world (e.g. Wright et.al. 1973). In Section 3.2.5. evidence is presented which indicates that there is a metamorphism and fabric in the grey gneiss older than the regional metamorphic lineation. This is compatible with the reactivated basement hypothesis. Perhaps the most compelling evidence that the grey gneiss is a basement complex is the location of the very large masses, the Drag Lake and Straggle Lake complexes at or near the regional structural base of the supracrustal rocks. Both their position and size contrasts with that of the syenites, gabbros and granites (Fig.1.2). A complete solution of this problem will probably follow more extensive regional mapping coupled with geochemical and geochronological studies. In this regard it is relevant to note the ca. 1400 Ma. date for a granulite facies orthogneiss situated some 60 km northeast of the study area in gneisses, underlying the Central Metasedimentary Belt (Bell and Blenkinsop 1980).

The conclusion based on field evidence, that the emplacement of the granite veins was syntectonic, is in agreement with that of Pride (1982), concerning similar rocks in the Glamorgan Complex (Fig. 1.1a). He stated, moreover, that they were generated by a small degree of partial melting at sites not far removed from that at which they are now.

2.3.5. Unit 3C; Garnet Gneiss

The garnet gneiss unit (Unit 3C) comprises a variety of spatially related rocks most of which contain relatively abundant garnet (Table 5, Appendix I). Varieties containing garnet and orthoamphibole are common, with or without cordierite. Pelitic and semipelitic assemblages are associated in subordinate amounts. The petrography and metamorphism of a cordierite-gedrite occurrence at Fishtail Lake at the extreme north of the map sheet has been studied in detail by Lal and Moorhouse (1969). According to these authors this was the location of the first discovery of cordierite in Canada and of gedrite in North America (Evans and Bancroft 1908). These rocks are currently the object of a geobarometric and thermometric study by S. Reed at the University of Ottawa.

In the Drag Lake area garnetiferous rocks are present along the southern boundary of the grey gneiss (Fig. 1.2). They form narrow pods or strips, nowhere more than a few decametres wide. At the southeast end of Drag Lake they are not clearly separable from the overlying Grenville Supergroup. However, on and near the southern shore of Drag Lake, they are clearly lenses within the grey gneiss near the boundary with rocks of the overlying Supergroup. In this region there are examples of garnet-biotite gneiss which contain the amphibolite pods characteristic of the grey tonalite gneiss. The more schistose garnet biotite rocks as well as the rare pelitic rocks (with sillimanite) and the orthoamphibole bearing rocks of unit 3C do not have these pods and layers.

North of Drag Lake garnetiferous rocks of unit 3C are concentrated in a large mass on the east and southern side of the salient of marble which structurally underlies the grey gneiss (ie. Fig. 1.2). This mass is dominantly a layered garnet-biotite-orthoamphibole gneiss similar to that of southern Drag Lake but much more thickly developed. Marbles fill a small synformal keel in this mass. Pelite form small interlayers. The marble which adjoins this mass along its western margin is notably rich in serpentine. Reconnaissance shows that this unit is present 5 kilometres to the north near the southern shore of Haliburton Lake. Some of these rocks resemble in their outcrop appearance the gedrite rich rocks of Fishtail Lake. The latter lie within the grey gneiss 1.75 kilometres north of its southern boundary. Lal and Moorhouse (1969) record a very small amount of calc-silicate gneiss at Fishtail Lake, and a variety of pelitic and semi-pelitic rocks which enclose the gedrite rich rocks. There are no known occurrences within the Farquhar Lake Sheet.

The most common variety (excluding Fishtail Lake) has a prominent layering of medium grained plagioclase and quartz, 2-3 centimetres thick, peppered with medium to coarse garnets. Somewhat thinner layers are finer grained and charged with biotite, gedrite and minor garnet. Pelitic and semipelitic varieties are schistose while those with less biotite resemble the grey gneiss. At the southwest of Drag Lake there is one occurrence of a thin (20 cm) cordierite-biotite schist layer within garnet-biotite gneiss. This schist has augen of garnet and feldspar and is interpreted as a tectonic schist. A description of the Fishtail Lake rocks is found in Lal and Moorhouse (1969).

The assemblages present are summarized in Table 5, Appendix I. The plagioclase is oligoclase (An_{26-28}). In the layered variety biotite, gedrite and garnet are the most common dark minerals. Cordierite and, rarely, sillimanite occur in some layers and not in others. Cordierite is often not identifiable in hand specimen. Magnetite and apatite are accessories. Gedrite and biotite are intergrown (Plate 2b), in a fashion similar to biotite and hornblende in the grey gneiss.

In the tectonic schist from the south shore of Drag Lake the augen-like garnet porphyroblasts are rimmed by cordierite. In the matrix cordierite, quartz and biotite are subequal.

In pelitic rocks from north and south of Drag Lake plagioclase-quartz-biotite-garnet-sillimanite appear to be a rare stable assemblage. No K-feldspar is present.

Three garnet gneisses have been analysed (Table 10, Appendix I), these comprise two garnet-gedrite-biotite layered gneisses and one garnet poor biotite gneiss. On the AFM plots they they are quite distinct from the grey gneisses being relatively poor in Na and K and correspondingly enriched in total Fe. On the CKN diagram the gedrite bearing rocks are poor in Ca compared to the grey gneisses whereas the garnet-biotite gneiss falls in the main trend of grey gneisses (Figure 2.1). The gedrite bearing gneisses have similar Na and Rb/Sr content as grey gneiss with a similar quartz content. However K, Ca and Al are lower whereas total Fe, Mg and Ti are higher.

It is apparent that gedrite rather than hornblende is formed in these rocks since they are poor in Ca, Na and K and correspondingly rich in total Fe and Mg.

2.3.6. Origin

The principal features of the garnet gneiss are: i) it appears to form discrete pods at or near the contact of the grey gneiss and the Grenville Supergroup; ii) it is found overlying and underlying the grey gneiss at Drag Lake; iii) pelitic as well as gneisses very low in K and Ca and correspondingly high in Mg and Fe are found; iv) these compositions are unlike those found elsewhere in the Grenville Supergroup. The field association of the gedrite rocks with interlayered pelites and marble or calc-silicate rock suggests that the whole assemblage is entirely metasedimentary. The main question is twofold: why are the gedrite bearing rocks so K and Ca poor and correspondingly Mg and Fe rich and what is the age of these rocks?

Lal and Moorhouse (1969) argued against a metasomatic origin for the rocks with extreme compositions at Fishtail Lake on the grounds that there is no source of Mg and Fe and that the rocks have precisely the Mg/Fe ratios of shales. There remain at least two hypotheses: 1) that the Mg and Fe enrichment and its depletion is due to partial melting of an argillaceous protolith; 2) that these compositions represent unique and somewhat rare metasedimentary protoliths. In this case the observed enrichments and depletions may be explained by subaerial weathering in a humid tropical environment of a variety of protoliths (R.K. Herd, personal communication, 1981, Warren 1979).

The principal objections to the first hypothesis is that in the gedrite-garnet rocks of Drag Lake a potassic product of partial melting is not observed interlayered with these rocks. The coarse leucocratic layers of the gneiss, which may be interpreted as melt products, all have a trondhjemitic composition. Furthermore, as Lal and Moorhouse point out, even if partially melting has taken place and was responsible for the almost complete removal of K the parent must still have an unusual composition (Al, Ca, K poorer than the average shale) in order to generate the postulated residue.

The second hypothesis accounts well for the rarity of the gedrite bearing rocks and their occurrence in a discontinuous horizon near the contact of the grey-gneiss with the Grenville Supergroup. The tectonic implications of the grey-gneiss having been exposed subaerially are great. Clearly definitive geochemical studies of these unusual rocks are required as well as further regional mapping to delineate their extent and confirm or deny their stratigraphically unique position.

2.4. Unit 4: Mafic Igneous Rocks, the Farquhar Lake Complex

2.4.1 Introduction

Mafic igneous rocks (Unit 4) are concentrated in two masses: the Farquhar Lake Complex and the Dudmon Lake Diorite. Mapping during this project shows the Farquhar Lake Complex to be more extensive than previously known. There are also scattered within the supracrustal rocks small pods some of which are shown on the map, but most of which are not. The biggest concentration is the Farquhar Lake Complex, which lies at the mid-point of the north margin of the map sheet (Fig. 1.2b). This complex is considered here.

The Farquhar Lake Complex has not been described before as a separate entity, although parts of it have been referred to as individual bodies. Adams and Barlow (1910) described the anorthositic rocks of Kennibik Lake which they considered to be derived from the marbles. The pyroxenite has long been known, since it is the site of a profound negative magnetic anomaly. It has been referred to as the Wilberforce Pyroxenite (Mason 1959, Irwin 1963, Palmer and Carmichael 1973). Bright (1979) noted in Harcourt Township mafic and ultramafic sills which he considered to have been emplaced during and after the culmination of the regional metamorphism. The present author mapped the western part of the Complex (Culshaw 1981) and delineated the eastern part in enough detail to show the general distribution of rock types.

The Complex has three components, pyroxenite, gabbro and anorthosite (gabbroic). An extended magmatic and syntectonic metamorphic history is displayed by these rocks which is outlined in this chapter. It is contended that the rocks were emplaced early in the tectonic history but that since they are originally dry rocks they behave as hard and, in part, dense non-bouyant masses which influence the structural patterns of their ductile matrix (see Sections 3.3.3. and 4.4.). Their metamorphic history may be thought of as one of progressive softening, which happened most quickly in the anorthosite and least quickly in the pyroxenite. This clearly is the result of the softness of labradorite relative to that of pyroxene. Thus primary textures are very rarely found in anorthositic rocks, while the pyroxenites are rarely foliated. The gabbros, composed of equal amounts of both minerals, have a variety of primary, partly recrystallised and completely recrystallised textures. An important result of the material properties of these mafic rocks is that although they are probably the oldest plutonic rocks intruding the Grenville Supergroup, parts of them appear very fresh and "young".

In this chapter the rocks are described mainly from the point of view of structural petrology. In Section 4.4. there are described some of details of the microstructural and mineralogical changes which take place during the development of a foliation in the gabbro. In Section 3.3.5. it is shown how the tendency for heterogeneous deformation in the gabbroic rocks may be turned to an advantage to give kinematic information of regional relevance.

There are many locations where the Complex is cut by both foliated syenitic and granitic sheets. Metagabbroic xenoliths occur sparsely within syenitic gneiss east and west of the pyroxenite body. In Section 2.3.1 an occurrence of foliated grey gneiss (similar to rocks of Unit 3) within unfoliated metagabbro was described. There are, however, no xenoliths of supracrustal rocks in any of the bodies.

The Complex is made of seven distinct sill-like bodies. It is divided into two levels separated one from another by the Farquhar Lake Grey Gneiss Sheet and a thin envelope of supracrustal rocks. It extends 16 kilometres from north-east to southwest and 8 kilometres from north to south.

The north side of the upper level is dominated by a pyroxenite body that lies in a north-northwest trending boat-shaped synform. The pyroxenite has a semi-complete margin of gabbro which is for the most part gneissic, except at the north and south ends of the body.

The southern part of the upper level comprises two sill-like sheets which strike northeast from near Miskwabi Lake to near Elephant Lake. These are mostly metagabbroic with lesser amounts of anorthositic gabbro to gabbroic anorthosite. Partly recrystallised primary textures are preserved especially in the southwest of Farquhar Lake and the western sheet. The eastern sheet is more gneissic and deformed than the western.

There are four bodies in the lower level. In these the largest amount of anorthosite and gabbroic anorthosite is exposed. The relatively large outcrop areas occupied by the western bodies compared to the one east of the pyroxenite is probably due to the shallow and variable dips in the west.

2.4.2 Unit 4A; Gabbroic Rocks

Two main compositional varieties present, gabbro and olivine gabbro, may be divided into three types according to the textures visible in hand specimen: primary, partly recrystallised and gneissic. Small patches of extremely coarse gabbro and metagabbro are present throughout the complex. They have a gradational relation to the main type. They are interpreted as mafic pegmatites.

Rocks with the best preserved primary textures are found near the north and south end of the pyroxenite body, for example, there is a small area of heterogeneously deformed gabbro at the south end of Allen Lake. Primary textures are also present in the sheet south of Yankton Lake. These rocks are dark grey to black on account of the large (1-2 cm) plagioclase laths. In olivine gabbros coronas are readily visible. A subophitic texture is common. A foliation of primary plagioclase crystals has been observed near Yankton Lake parallel to the regional foliation. Where primary textures are preserved olivine gabbro and gabbro are equally abundant. In the early stages of partial recrystallisation the olivine gabbro may still be recognized by their brightly coloured weathered corona structures. However with further recrystallisation coronaed olivine and clinopyroxene are converted to amphibole and are no longer distinguishable in hand specimen. It is not possible, therefore, to estimate the proportions of gabbro and olivine gabbro that contributed to the gneissic metagabbro.

Textures indicating partial recrystallisation are abundant in the gabbro sheet south of Yankton Lake, at southwest Farquhar Lake and in zones of heterogeneous deformation at the north and south ends of the pyroxenite's gabbroic collar. In rocks with this texture the plagioclase is white and the mafics, mostly amphibole, are green and, less often, black. Subophitic texture is still easily discernible, although in more deformed examples only in sections near perpendicular to the lineation. Plagioclase is partially replaced by fine equant grains. Shape and mineral fabrics are absent or moderately developed.

Gneissic metagrabbro is present in all localities where primary textures are preserved but is particularly well developed in the gabbroic margin of the pyroxenite and the sheets to the east of the pyroxenite, where strain appears to be higher. This rock type has a shape fabric of blade-like aggregates of fine white equant plagioclase set in a network of fine to medium grained amphibole. The tectonite fabric may vary in strength. The most strongly deformed are very planar and fine-grained. In gneissic mafic pegmatites spectacular clinopyroxene augen (up to 3 centimetres long) dominate the fabric.

Gneissic metagabbro is present in all locations near rocks preserving primary textures.

In olivine gabbro displaying primary texture, olivine has well developed coronas. The innermost shell is hypersthene succeeded by very pale green amphibole interfingering with spinel. Plagioclase abutting the corona is peppered with extremely fine amphibole and rare spinel. Olivine is partially altered to serpentine and magnetite. Large irregularly shaped primary clinopyroxene (augite) has a very fine exsolution of opaque material forming parallel trails. A thin corona of hornblende (brownish green to olive green) jackets the pyroxene but the abutting plagioclase is free from amphibole inclusions. Large labradorite grains are multiply twinned on the Carlsbad, albite and pericline laws. The twins may be moderately curved and wedge shaped. A small number of equant very fine new plagioclase grains are present. Magnetite is an accessory.

Primary textured gabbro is very similar to the olivine gabbro. Clinopyroxene forms very irregular shapes, filling spaces between plagioclase laths, in a classic subophitic texture (Plate 3a). Labradorite forms elongate laths up to 2 centimetres long and with aspect ratios of 4 to 1. Details of plagioclase twinning, hornblende corona and pyroxene exsolution are same as the olivine gabbro.

In gabbro that is partly recrystallised with little or no tectonic fabric two microstructural types coexist within one thin section. In the first microstructure the sub-ophitic texture is clearly visible (Plate 3b), there are no hornblende inclusions within the plagioclase which, for the most part, are equant laths. Clinopyroxene is now very finely intergrown with equal amounts of hornblende. In the second microstructure the subophitic texture is obscured (Plate 3b). Clinopyroxene is no longer present, in its place is a granoblastic aggregate of fine hornblende. Primary labradorite (An_{66}) is zoned to a more calcic composition near the contact with hornblende aggregates. The zoned areas have fine bright lamellae, interpreted as hutten-locher intergrowths (see Section 2.8.2), are filled with inclusions of amphibole and abut with fine hornblende-plagioclase mosaics (Plates 5a-c). Fine equant plagioclase is also present on boundaries between the primary plagioclase grains and along kinks within them (Plate 4c,d). The plagioclase is dusted with extremely fine scapolite. The amphibole is a deeper green than in the olivine coronas, but does not have the faint brown tinge of the early clinopyroxene coronas.

Partly recrystallised olivine gabbro with a weak fabric differs from the primary textured olivine gabbro in that the corona reactions have all been completed. Former olivine is now marked by a hypersthene-magnetite mosaic surrounded by a relatively wide (4-5 mm) rim of amphibole and spinel. This amphibole is a deeper green than in the olivine cored coronas. The labradorite grains have ragged margins.

A mosaic of fine equant plagioclase (0.2 mm) and amphibole separates large grains of labradorite from the mafic aggregates along part of the margins and occupies a significant volume of the rock. These fine plagioclase grains have fine bright lamellae, interpreted as huttenlocher intergrowths (see Section 2.8.2). Large labradorite grains are crowded with amphibole (but no spinel) inclusions where they abut the mafic or the amphibole-plagioclase mosaic. These inclusions are considerably larger than the equivalent inclusions in the primary textured olivine gabbro. The plagioclase surrounding them is more calcic than that free of them.

In olivine gabbro that is partially recrystallised and displays a moderately strong fabric subophitic texture is visible in hand specimen in sections perpendicular to the lineation but it is not readily discernible in thin section. The microstructure is identical to the type described above where the ophitic texture is obscured by recrystallisation.

There is a correspondingly strong development of granoblastic amphibole and fine amphibole-plagioclase mosaics. The former presence of olivine is indicated by minor serpentine-magnetite concentrations. The amphibole is transitional in its shade of green between that of the very weakly foliated gabbro and that of the partly recrystallised olivine gabbro with a weak fabric.

Plagioclase in gneissic metagabbro forms a fine equant mosaic which is significantly coarser than the fine plagioclase in the partially recrystallised textures. Plagioclase is always more sodic (An_{55-62}) than the primary grains (An_{66}). In some cases relict primary plagioclase persists, displaying undulatory extinction and kinking. The grains surrounding these relict primary grains may be zoned and show huttenlocher intergrowth (Plate 5d). In sections where relict grains are absent, the zoning and intergrowths are not present. Twin morphologies are varied, some sections only growth twins have been observed, in others only deformation twins and in others both. In many sections much of the plagioclase is completely replaced by scapolite, in some individual grains are only partly replaced.

Hornblende in gneissic rock forms decussate elongate clusters (Plate 3d). In some cases, it coexists with fine granular clinopyroxene. Occasionally large clinopyroxene augen are present in these gneisses. The augen are seamed with a delicate intergrowth of amphibole which resembles mesoperthite.

Two examples of diorite have been found. These are of very minor volumetric importance. A gneissic and a partly recrystallised variety have been found near the southern and northern shores of Farquhar Lake respectively. In both a relatively sodic plagioclase is found (An_{38-44}). The gneissic variety resembles the metagabbroic gneiss and will not be described further.

In the partly recrystallised diorite plagioclase very dark green amphibole, biotite, plagioclase and scapolite are the main minerals. Magnetite-ilmenite has a rim of sphene. Coarse primary plagioclase is included within a medium grained equant mosaic of plagioclase and scapolite. All the mafic minerals are relatively coarse.

2.4.3. Unit 4B; Anorthosite and Anorthositic Gabbro

Anorthosite and anorthositic gabbro occur in subordinate amount throughout the gabbro bodies. They form a major proportion, however, of the bodies in the lower level of the Farquhar Lake Complex. Continuous masses of gneissic anorthosite are present along the shores of Kennibik Lake, Grace Lake and the northwest corner of Farquhar Lake. The only known occurrence of primary textured gabbroic anorthosite occurs as a small patch within partly recrystallised olivine gabbro one kilometre to the northwest of Grace Lake.

These plagioclase rich rocks are almost universally gneissic with the one known aforementioned exception. They are formed of a fine to medium grained equant white plagiocase aggregate occasionally containing an augen of grey primary plagioclase or green clinopyroxene. Wispy trails of amphibole and biotite define the tectonic fabric. The anorthosite may include small patches of metagabbro (oikocrystic texture) which become hornblendic schlieren with increasing deformation.

The primary textured anorthositic gabbro has a cumulate texture of large euhedral plagioclase laths (4-5 cm long) and small stellate concentrations of mafic minerals.

In primary textured anorthositic-gabbro the plagioclase is similar in composition (An_{64}) and microstructure to the primary textured gabbro (Plate 4a). Interstitial clinopyroxene is almost completely replaced by hornblende.

The microstructure in gneissic anorthosite is dominated by fine (< 1 mm) equant polygonal plagioclase grains and occasional augen of plagioclase with extremely ragged grain boundaries (Plate 4b). The matrix plagioclase is more sodic (An_{56-60}). The matrix grains have twins with morphologies typical of both growth and deformation twins. Some of the grains, especially those abutting hornblende have reversed zoning with huttenlocher intergrowth. Plagioclase augen have undulatory extinction, huttonlocher intergrowths and enclosed twins. Hornblende and biotite are present in accessory amounts. Scapolite forms up to one quarter of the fine grained matrix, in some cases one grain of scapolite replaces two of plagioclase.

2.4.4. Unit 4C; Pyroxenite and Hornblendite

Pyroxenite is restricted to the body forming the large central synform. It is a fine grained, equigranular green rock mostly devoid of tectonic fabric. Frequently it is studded with randomly oriented, coarse grains of amphibole. In places it is entirely made over to coarse-grained amphibolite, for example, along the northeast margin of the body. This amphibolite is rarely foliated.

Near the boundary of the pyroxenite at the southern tip of Allen Lake, small pods of pyroxenite lie within unfoliated partly recrystallised gabbro. The boundaries of the pyroxenite pods with the metagabbro are not clean-cut. Pyroxene projects from the pod into the metagabbro, where it forms subophitic texture.

The pyroxenite is an aggregate of fine grained (0.33 mm) equant augite. As in the gabbroic rocks the clinopyroxene has trails of very fine opaques lying parallel to the cleavage. These exsolved pods and lamellae are responsible for the reverse magnetism of the body (Palmer and Carmichael 1973). Serpentine forms up to 20 percent of the rock. Amphibole replaces clinopyroxene, forming complex intergrowths.

2.4.5. Geochemistry

All the three main rock types of the complex are nepheline normative (Table 11, Appendix I). The alkaline nature of the suite is also displayed by the extremely flat trend on the AFM diagram (Figure 2.2a). The variation in major and minor elements, is simple (Figure 2.2b, Table 11 Appendix I). The decrease in Al_2O_3, Na_2O, K_2O, Rb, Sr and Ba accompanies the decrease in plagioclase content from anorthosite, through gabbro to pyroxenite. This trend is matched by an increase in MgO, CaO, total Fe, Cr, Ni, TiO_2 and MnO. These two element groups are those common in, respectively, plagioclase and clinopyroxene (and olivine).

2.5.6 Conclusions

Petrogenetic unity of the complex: Considering their close spatial relationship it is highly likely that the gabbroic, anorthositic and pyroxenite bodies are petrogenetically related. Moreover there is a simple pattern of chemical variation related to the major mineral phases and pyroxenite pods occur in metagabbro. The simplest way of generating the anorthosite is to accumulate the plagioclase crystals in a crystallising gabbroic melt and separate the plagioclase rich fraction. Good evidence that this could have happened is offered by the subophitic cumulate textures of unrecrystallised primary textured gabbro, olivine gabbro and gabbroic anorthosite. However the mode of generation of the pyroxenite remains obscure. It is also noteworthy that the gabbros are very similar chemically to the Glamorgan Gabbro which is also nepheline normative (Armstrong and Gittins 1968). The Glamorgan Gabbro is sheet-like, has a large volume of gneissic rocks and has similar coronitic textures (Grieve and Gittins 1975). Moreover it is situated close to the Glamorgan Gneiss Complex, lithologically similar to the grey tonalitic gneiss complexes. It is thus probably part of a regional suite of gabbroic rocks. Note, however, that many rocks of the diorite-gabbro suite of the Hasting Lowlands are not nepheline normative (Lumbers 1967).

Coronas: The occurrence of both coronas and gneissic metagabbro (amphibolite) indicate an involved solid state history for the bodies.

The coronas, which contain successive shells of orthopyroxene and amphibole plus spinel, are distinctive. Besides being found in the nearby gabbro bodies of Glamorgan Township (Armstrong and Gittins 1968, Grieve and Gittins 1975) coronas of this composition are of world-wide occurrence in ancient gneissic terrains. Well known examples are from Greece (Sapountzis 1975), Norway (Starmer 1969, Frodesen 1968) and India (Murthy 1958).

Many coronas found elsewhere in the Western Grenville Province (Ontario, Davidson et.al. 1981; Adirondacks, Whitney and McClelland 1973), appear to be slightly more complex, having two pyroxenes, besides amphibole and garnet.

Further work may show if there is a regional zonation in corona type.

All corona types are found in ancient high-grade gneissic terrains, and are absent from lower grade schistose terrains. They are considered to have been formed at relatively elevated hydrostatic pressures (> 6 kb) where the temperature is high enough to ensure reasonable reaction rates during cooling of the pluton to the local temperature (Griffin and Heier 1973).

Amphibolized margins of coronites are common. The coronites themselves have weak fabrics or none at all. In the single pyroxene-amphibole plus spinel coronites, H_2O necessary for forming the amphibole may be derived from the gabbro itself, which is a closed system (Murthy 1958). The same author pointed out that although amphibolized margins and coronite may have formed at different temperatures or pressures, this is not necessarily so. The main difference may be one of PH_2O, the amphibolization taking place in a system open to H_2O. As described previously amphibolization appears to be microstructurally part of a process continuous with the corona formation. For example, amphibole already present as tiny inclusions in primary plagioclase involved in corona reactions simply grows and becomes deeper green with continuous syntectonic recrystallisation.

Time and place of emplacement: These considerations are compatible with the gabbro being emplaced at fairly deep levels. It appears that corona-formation and subsequent syntectonic amphibolization were uninterrupted by a journey to and from a higher level, which would have surely left some metamorphic record. The fully recrystallised amphibolites belong to the same metamorphic facies as the rocks they intrude and probably thus were formed not far distant from where found now.

There is furthermore evidence of their syntectonic emplacement: the very rare occurrence of primary plagioclase in an unrecrystallised subophitic texture lying parallel to the regional foliation. A similar preferred orientation of primary plagioclase in the Glamorgan gabbro was demonstrated by Armstrong and Gittins (1968) to indicate syntectonic magmatic crystallisation. Also compatible with the hypothesis of syntectonic emplacement is the probable earlier sheet-like nature of the bodies implied by the lack of flattening fabrics with a component of stretching parallel to the strike (lineations are mostly down dip).

It is tempting to speculate that if the crystallisation, recrystallisation and emplacement were syntectonic then the mechanical removal of pyroxenitic liquid from crystalline plagioclase may have been induced also by this tectonism, continued displacement resulting in the emplacement of pyroxenite together with a slice of basement (the Farquhar Lake Grey Gneiss Sheet) on top of anorthosite and gabbro.

2.4.7. Unit 4D; Dudmon Lake Diorite

The Dudmon Lake Diorite is a somewhat elongate homogeneous body lying at the margin of the northeast end of the Glamorgan Gneiss Complex and the underlying supracrustal gneisses. It has not been extensively sampled in this study. Chesworth (1966) presents one analysis of it. Dunlop et. al. (1980) sampled it in a paeleomagnetic study.

The diorite is heterogeneously deformed. It is a grey to black rock in which mesoscopic textures vary from gneissic to partly recrystallised. In the latter primary feldspar laths are still preserved.

Minerals present include plagioclase, clinopyroxene, biotite, hornblende, with accessory magnetite, apatite and calcite. Primary plagioclase is andesine (An_{35-38}) which is extensively recrystallised. Clinopyroxene is replaced by hornblende. Biotite occurs as a member of symplectite with hornblende, magnetite and plagioclase, indicating its metamorphic origin.

2.5. Syenitic Rocks

2.5.1. Introduction

The map area includes several varieties of syenitic gneiss. These include some of the nepheline bearing rocks (Unit 5D) for which the Haliburton-Bancroft area is famous (Tilley and Gittins 1961, Gittins 1961). These well known rocks will not be discussed further. These syenites form the western extremity of a linear belt of alkaline igneous rocks which lie near the contact of the Grenville Supergroup and its basement and are considered synorogenic (Appleyard 1974 and Fig. 1.1). The body south of Farqhuar Lake was previously unmapped and since most of the map units are composites of several rock types and specific rock types may occur in two or more map units the distribution of map units and rock types is treated separately.

2.5.2. Definition and Distribution of Units 5A, B and C.

Unit 5A Buff syenite is composed of the only syenitic rock type that forms large, relatively homogeneous masses. It forms the bodies which lie to the south of Drag Lake and encircle Deer Lake. Table 12, Appendix I shows that buff syenite forms the major part of almost 90 percent of all outcrops within the Drag Lake Syenite. Other syenitic types present in the these bodies tend to be concentrated at their margins, where they cross cut the buff syenite. Locally, the former are unfoliated.

Unit 5B, Heterogeneous Syenite Gneiss is composed of conformable sheets or planar dykes deformed into planarity of a wide variety of syenitic, granitic and supracrustal rock types. Lithological heterogeneity and layered, sheet-like aspect are the key features, although some strongly cross-cutting relations are present. The main concentrations are north of Farquhar Lake, south of the Drag Lake Syenite, and along the north and western margins of the Cardiff complex (Fig. 1.2). The inclusion of the latter body as part of this unit is based on the information available on Hewitt's map (Hewitt 1957c) and limited inspection in the field.

Table 13, Appendix I show the following features of this unit: (i) It contains a large number of rock types (11-15); (ii) syenitic rock types dominate over granitic and supracrustal; (iii) pink syenites dominate over buff syenites; (iv) enclaves of supracrustal rocks, large enough to be mapped at intermediate scale (1:31,680), are common.

This heterogeneity is evident at the outcrop scale. Individual outcrops are very often layered mixtures of igneous or igneous and supracrustal gneisses. The planarity of this layering is very often accentuated by deformation which also imparts to the rock at all scales a powerful tectonite fabric. There is also a lack of continuity of lithologies parallel to the strike.

Unit 5C, Unsubdivided Syenites includes syenitic masses of which the author has little personal knowledge, many of which are small bodies peripheral to the map (Fig. 1.2). Cursory field inspection shows that, as is to be expected, rock types present do not differ greatly from those comprising the other map units. The belt to the west of the Cheddar Complex, for example, may well be similar to the belts of heterogeneous syenite gneiss (Table 13, Appendix I), although it contains a relatively large volume of nepheline bearing gneisses.

2.5.3 Rock Types

Buff Syenite: Buff syenite is present in all map units. It forms the major part of the Drag Lake and Deer Lake Syenites (Buff Syenite Map Unit). In the western part of the map sheet small bodies are present. Those in the extreme west are continuous out of the map area and may well be part of much larger bodies.

The rocks weather buff to creamy white. On fresh surfaces they are olive green and locally grade to pink. They resemble in colour quartzo-feldspathic rocks of the granulite facies.

Grain size is varied from uniformly fine to medium grained. Often the rock has a bimodal grain size of sparse feldspathic augen set in a fine equigranular matrix. Layers of bimodal and uniform grain size may grade one into another and be associated with slight changes in mineral content. All the rocks have a well developed tectonite fabric composed of augen or aggregated mafic minerals, quartz ribbons or feldspathic augen and occasional streaks of magnetite or calcite. Outcrop scale tectonite fabrics, formed by cross-cutting but deformed veins of later pink phases are present. This type of fabric gives the rock, in places, a very planar, layered aspect.

The minerals present in the buff syenite are summarized in Table 14, Appendix I. The major minerals are microcline, plagioclase (An_{6-11}), microcline perthite, augite and hornblende. Magnetite, apatite, sphene, biotite, quartz, calcite and garnet are present in accessory amounts. The relatively high proportion of magnetite present in the Drag Lake syenite accounts for a strong aeromagnetic signature for this body. Hewitt reported aegerine in the Deer Lake Syenite (Hewitt 1957a). It is noteworthy that these rocks contain a relatively high proportion of plagioclase and may be called monzonites with some justification (Culshaw 1981). However it is likely that much of the plagioclase derives from recrystallised perthite. The rock should therefore properly be termed an alkali-feldspar syenite (Streckeisen 1976).

The feldspathic fraction is composed primarily of an aggregate of equant, fine grained (3-.75 mm) microcline and plagioclase which are free of intergrowths. Discontinuous albite rims occur at plagioclase-microcline boundaries. Microscopically visible persisterite lamellae are present in some plagioclase. Only albite and pericline twins occur in the plagioclase. Large feldspathic augen (2-6 mm) are dominantly microcline string and thread perthites (Deer et. al. 1966). Rare plagioclase augen display strong undulatory extinction, indicating recovery, which is lacking in the matrix plagioclase. These large feldspars are the unrecrystallised precursors of the fine matrix feldspars.

Augite is the primary mafic mineral. Hornblende is a metamorphic mineral. The evidence for this is the common occurrence of hornblende-quartz rims of clinopyroxene or of complex spongelike synplectic intergrowths of combinations of hornblende, quartz, magnetite and biotite. The hornblende lies parallel to the lineation although there are examples of hornblende growth postdating deformation.

Apart from magnetite a characteristic accessory in the Drag Lake Syenite is calcite. This may be present as dispersed grains or as elongate millimetric aggregates. It is not known in the Deer Lake Syenite.

A rare mafic variety has a colour index in excess of 40. It forms layers in the buff syenite. The dominant mineral is a green clinopyroxene which is partially replaced by amphibole.

<u>Pink Syenites and Quartz Syenites</u>: These types form a major portion of the heterogeneous syenite gneiss unit (Unit 5B). Within the buff syenites (Unit 5A) they occur as concordant or cross-cutting but deformed layers. They are concentrated with pegmatitic types, near the margins of these bodies.

In the north, where the largest proportion of the heterogeneous syenite gneiss unit is found, the appearance is characteristic. The rocks range from medium grained equigranular to very fine grained and sugary. If quartz is present it is smeared out into delicate ribbons. In many varieties there are augen of feldspar. In some of these rocks extremely large augen (15 cm long) sit in a fine grained matrix, suggesting that the rocks were derived from pegmatites by grain size reduction during dynamic recrystallisation. The gneisses often contain streaks, layers blocks or pods of non-feldspathic rock such as diopside rock, quartzite, amphibolite, biotite gneiss and metagabbro. Pink syenites, quartz syenites, pegmatites, buff syenite and the whole range of supracrustal rocks may be interlayered together. Such a migmatite has often a distinctive planar, flaggy aspect characteristic of high strain.

Locally unfoliated to moderately unfoliated pink syenite intruded strongly foliated pink syenite, cross cutting the older foliation.

The dominant mineral of the pink syenites is microcline, albite is present in variable subordinate amounts (Table 14, Appendix I) and quartz is important in appropriate compositions. In augen bearing varieties coarse microcline perthite is present set in a fine recrystallised two feldspar matrix. Augite, hornblende, biotite are the main mafic minerals. Magnetite, apatite and sphene are important accessories. In most varieties mafics form less than 10 percent of the rock. A minor, but ubiquitous, exception is a biotite syenite with a colour index up to 20. Where present, very coarse microcline perthite is recrystallised to form a fine two feldspar matrix free of intergrowths. Discontinuous albite rims are present at plagioclase-microcline grain boundaries. Quartz, where present, forms the common granulitic type ribbons.

Hornblende appears to be of metamorphic origin. Replacement by clinopyroxene of amphibole is ubiquitous via a stage of complex, spongy, symplectic intergrowths which is widely preserved.

<u>Foliated Syenitic and Quartz Syenitic Pegmatites</u>: The pegmatites are present throughout the heterogenous syenite gneiss (Unit 5B) and have a similar cross-cutting but deformed relation to the buff syenite (Unit 5A) as do the pink syenites. They occur as isolated bodies generally no more than a few metres wide.

The pegmatites vary from brick red to pale pink, from strongly cross cutting, coarse and poorly foliated to sub-concordant and augen-gneissic. Although several ages of pegmatites are probably present, some show great variations of fabric strength within one body. Pegmatites which are not strongly recrystallised are dominated by microcline perthite, free albite and variable amounts of quartz. Clinopyroxene (partially replaced by amphibole), biotite, sphene, allanite, calcite, magnetite are among the minor and accessory constituents.

<u>Miscellaneous Syenites</u>: Albite syenite is a minor constituent of the Drag Lake Syenite and the heterogeneous syenite gneiss to the south of that body. Hewitt (1957a) mentions it as the oldest of the syenites but Hewitt (1957c) does not precisely locate it on his map. None was observed by the author within the confines of Hewitt's map. None occurs north of Farquhar Lake and east of the Drag Lake grey gneiss complex. This medium to fine grained granoblastic rock is composed of albite, sometimes with pink strands of microcline. Magnetite is an important accessory. At some localities coarse corundum grains are present.

FIGURE 2.3 Chemical variation in syenitic rocks. Symbols: 1a, buff syenite, Drag Lake syenite; 1b, buff syenite from small body south of west end of main Drag Lake syenite; 1c, Deer Lake syenite (Hewitt 1957a); 3, albite syenite, Drag Lake syenite. 2a, pink syenite, 2b. quartz syenite, 2c. granite, 2d. syenitic pegmatites from heterogeneous syenite gneiss south of Drag Lake. M, average mugearite, compiled from Carmichael et al. (1974).

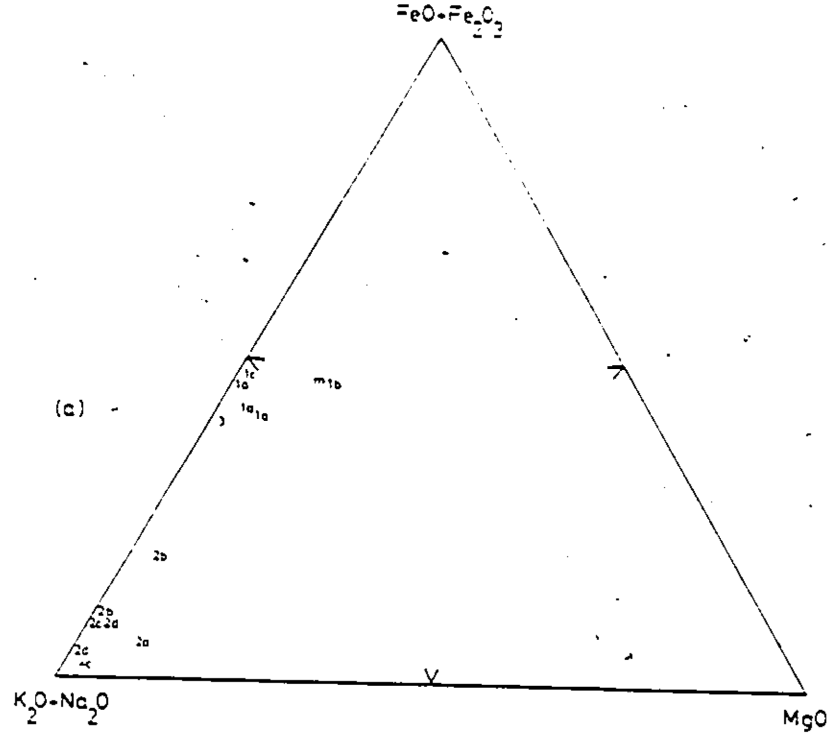
FeO+Fe2O3
(a)
K2O+Na2O
MgO

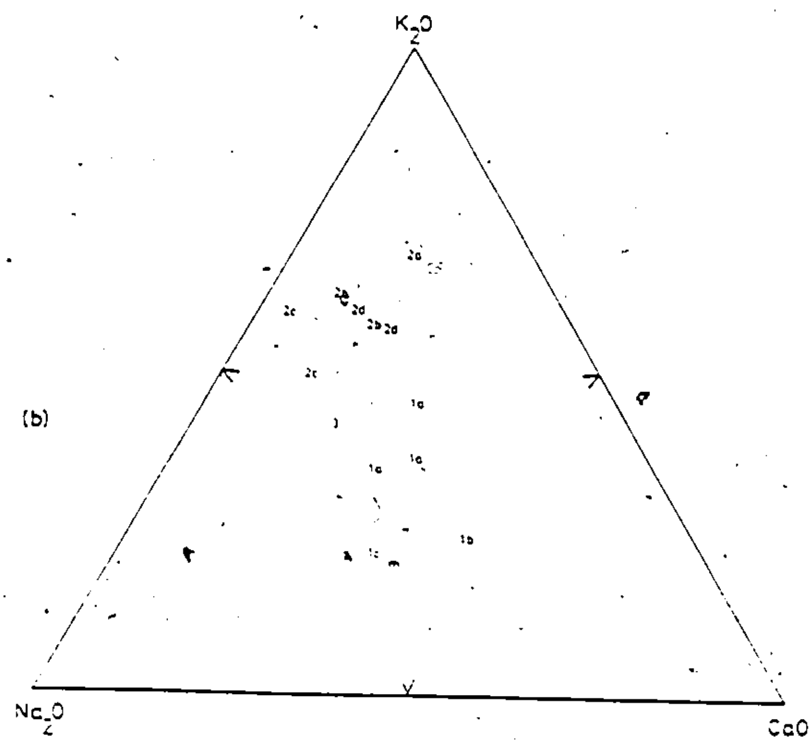
K2O
(b)
Na2O
CaO

North of Farquhar Lake a curious but rare scapolite rock occurs closely associated with syenite gneiss and the diopside rock. It is a massive white rock formed of coarse grained scapolite and minor diopside. It is cross-cutting. Under the microscope the scapolite shows moderate undulatory extinction and minor recrystallisation.

2.5.4 Geochemistry:

Analyses of all the major syenite and related rock types are presented in Table 15 (Appendix I). On the AFM diagram there are two distinct clusters (Fig. 2.3) demonstrating the iron enrichment of the buff syenites (and the albite syenite) relative to all the others. A buff quartz syenite lies between the two clusters. A comparable clustering is shown on the CKN diagram where the buff syenites (and the albite syenite) are located closer to the calcium apex. K_2O/Na_2O in pink syenites and quartz syenites (2.25 average) and pegmatites (2.38 average) is much higher than that of the buff syenites (1.07, Drag Lake; 0.5, Deer Lake).

The major element geochemistry of the buff syenites is comparable to that of a mugearite, an intermediate member of the alkali basalt-nephelinite magma series found in both continental and oceanic environments (Fig. 2.3, Table 15, Appendix I).

2.5.5 Conclusions

There is considerable field and petrographic evidence that the syenitic rocks are magmatic in origin: (i) the occurrence of xenoliths in the pink syenites; (ii) the cross cutting relations; (iii) the mutual close spatial association of buff and pink syenites and pegmatites, the more felsic varieties (K_2O richer) always cross-cutting the more iron and calcium rich buff syenites.

Likewise there is much evidence for modification by syntectonic metamorphism: (i) ubiquitous tectonite fabric; (ii) reduction of grain size due to recrystallisation of large perthitic grains; (iii) recovery and recrystallisation in plagioclase of the buff syenites; (iv) hydration of clinopyroxene to form amphibole.

The chemistry may have been modified to an unknown extent by contamination by marbles, as witnessed by the fairly common occurrence of sphene and crystals, patches and blocks of diopside.

As with the gabbroic rocks the sheet-like form of these bodies is compatible with a pre- or syntectonic emplacement as sills into an already stratiform pile. The lack of flattening fabrics and dominance of down-dip plane-strain to prolate fabric types indicates their dimension parallel to the strike has not significantly changed and they were originally sill-like. Also syntectonic emplacement is argued for by the rare presence of unfoliated to moderately foliated pink syenites, cross-cutting foliated syenite. Since they cross-cut the strong foliation in the host rock and are themselves foliated their time of emplacement must have been preceded and followed by deformation.

Since alkali-gabbro comparable to alkali-basalt and syenite comparable to mugearite occur close together it is tempting to suggest that they are plutonic equivalents of a continental alkali-basalt-nephelinite magma series. This is compatible with Armstrong and Gittins' (1968) suggestion that the hypersolvus nepheline syenites of Monmouth Township may be related to the alkaline Glamorgan Gabbro. It may be noted that the syenites themselves may well have been one feldspar hypersolvus syenites before recrystallisation of perthites and grain size reduction.

A second level of speculation would link the occurrence of continental alkaline magmatism to continental rifting (Miller and Gittins 1982).

2.6. Unit 6: Granitic Rocks

2.6.1. Introduction

Granite gneiss forms most of the Cheddar batholith and part of the Cardiff plutonic complex, where it occurs as conformable sheets. The western end of the Faraday granite underlies part of the east of the map area. It is composed of two sheets of granite gneiss. Granite and pegmatitic granite is an important member of the heterogeneous syenite gneiss unit (Unit 5B) and also forms isolated small bodies throughout the area.

The Cheddar batholith and the Cardiff plutonic complex are the northernmost members of a series of bodies which form the Harvey Cardiff Arch. This plutonic-structural feature has an exposed length of almost 60 kilometres in a north - northeasterly direction. Hewitt (1962) describes the Arch as a series of autochthonous and parautochthonous granites of the catazone, implying that the deep level at which they were generated anatectically is near that now exposed. Buddington (1959) used them to exemplify his concept of 'catazonal granite'. Hewitt (1962) noted the difference in character of the bodies, contrasting the sheeted nature of the Cardiff complex with the relatively homogeneous nature of the Cheddar batholith and the heterogeneous migmatitic nature of the Anstruther batholith to the south.

Bright (1980) generally agreed with earlier opinion stating that the Cheddar batholith was a gneissic body generated anatectically although his map denotes it as the basal feldspathic arenite of the Grenville Supergroup. This presumably implies that it was derived anatectically from such an arenite.

Working within a regional framework Lumbers (1967) assigned the granites to the quartz-monzonite group. This group was considered to have been emplaced during the last plutonic event in the Bancroft-Madoc area, the emplacement, for the most part, being synchronous with the culmination of high-grade metamorphism.

Fowler and Doig (1979) state that the Rb/Sr whole rock age for the Cheddar pluton is 1200 Ma., but it is not clear if this is the age of metamorphism or of the initial formation of the granite. The 1200 Ma. age is considerably older than both the age of metamorphism and emplacement of the nearby Silent Lake pluton, 1118 ± 12 Ma. (Heaman 1982, Rb/Sr) and the age bracket proposed for the emplacement of the quartz monzonite suite, 1125 ± 25 Ma. (Silver and Lumbers 1966). Note however that a considerably wider time bracket for emplacement of this potassic group is implied by the Rb/Sr dates of 1060 ± 25 Ma. and 1185 ± 25 Ma. for the Addington and Mazinaw Lake Plutons, respectively (Bell and Blenkinsop 1980). Moreover, different workers have arrived at dates with as much as 100 Ma. difference for the same body reflecting, perhaps open-system behaviour during metamorphism (Moore and Thompson 1980).

The petrography in this chapter emphasizes the importance of the syntectonic metamorphic history. It is suggested that the bulk of the granite gneiss originated as a hypersolvus granite which was similar in composition in every body and shows a modest amount of fractionation.

2.6.2. Composition of the Granitic Bodies

Although the Cheddar batholith has been described as relatively homogeneous (Hewitt 1962), it contains three distinct lithological assemblages:

1) Parts of the southeast dipping central portion are formed of a fine to medium grained equigranular alaskite (Unit 6A) devoid of shape-fabric and in which magnetite is an

important accessory. It is interlayered with substantial conformable units of hornblende-biotite paragneiss. These are both cross-cut by deformed pegmatite and a medium grained to pegmatitic granite (Unit 6C) which has a well developed quartz shape fabric. On the west side this alaskite interfingers with hornblende-biotite granite and paragneiss. One thin layer of a feldspar rich quartzite is located here.

2) At the northeast end of the alaskite is an anticlinorium of relatively mixed lithologies, comprising supracrustal rocks, alaskite, pegmatite, migmatite and mafic layered clinopyroxene granite gneiss. A semipelite is the dominant supracrustal rock. Minor garnet-sillimanite-plagioclase schist, calc-silicate marble and pyroxene granite gneiss outcrops on the west side of this zone. At the north west corner of the zone there is a sheet of purple alkali granite (Unit 6B).

3) Hornblende-biotite and biotite granite (Unit 6D) with minor alaskitic granite (Unit 6A) make up the bulk of the remainder of the body. These rocks usually have a distinctive planar-linear metamorphic fabric. There are no thick stratiform units of paragneiss within these rocks although there are occasional mafic layers especially at the margins. There are several podlike groups of xenoliths. Medium grained to pegmatitic granite (Unit 6C) are important minor constituents. These are always present at the margins of the pluton where they cross cut the country rock

foliation. The same rock type is found cutting the alaskite.

In the Cardiff plutonic complex (Fig. 1.2b) the Centre Lake and Monck Lake granite is the most important component. It is comprised of alaskitic (Unit 6A), hornblende-biotite and biotite granites (Unit 6D) as in the Cheddar batholith. All have a well developed planar-linear fabric of quartz. Medium-grained to pegmatitic foliated granite (Unit 6C) forms small cross cutting bodies. On the southwest side there are small conformable bodies of biotite-hornblende gneiss. On the northwest side conformable amphibolite layers are important. Compared to the dominant lithology in the Cheddar batholith this granite is somewhat finer grained, more leucocratic and has a more strongly developed fabric, otherwise they are petrographically and chemically similar.

The Lower Faraday granite is a fine grained very strongly deformed sheet. Otherwise it is similar to the Centre Lake and Monck Lake granite, of the Cardiff plutonic complex.

The Upper Faraday granite is separated from the Lower granite by a metasedimentary septum. The upper granite is part of a larger body which extends for fifteen kilometres out of the map area to the east. Within the map area it is represented by a medium grained granite identical to the medium grained to pegmatitic granite (Unit 6C) of the Cheddar batholith and Cardiff complex. In most places it displays the southeast plunging lineation, but it is heterogeneously and weakly deformed in comparison to the other granites.

2.6.3 Unit 6A: Alaskite

This rock type underlies much of the central portion of the main body of the Cheddar batholith. Here it is uniform, medium to fine grained, equigranular, and, on a small scale appears massive since it has no quartz shape fabric. It has a sparsely developed grain-size or mafic layering. Similar looking equigranular alaskite, devoid of layering, is present in very minor amounts throughout the other granites of the Cheddar and Cardiff complexes. Very rarely this rock contains mafic pods, which may be interpreted as xenoliths.

In the alaskite microcline, oligoclase (An_{10-11}) and quartz are subequal. Biotite and magnetite may be present as accessories. The quartz and feldspar form an equigranular mosaic in which grain boundaries are indentate and irregular. Quartz occurs as isolated grains, rarely forming polygrain aggregates. Microcline is free from intergrowths. In some plagioclase grains microscopic peristerite lamellae are developed. Discontinuous albite rims are found at some microcline-plagioclase boundaries. There are extremely rare occurrences of isolated medium grained microline with plume and bead perthitic intergrowth and of myrmekitic and kinked plagioclase.

The biotite has a spongy texture of spherical and worm-like inclusions (quartz?). It has a brown to green pleochroism and is often associated with an amorphous yellow serpentine-like mass. Magnetite if the typical accessory mineral of this unit.

Rare conformable quartz layers, no more than 3 cm wide, have coarse grains with exaggerated grain-growth microstructure and contain albite.

Examples of alaskite from the main body of the Cheddar pluton but not from the central portion have been sampled geochemically. These have notably higher K_2O/Na_2O than the hornblende-biotite granite, comparable to the medium grained to pegmatitic granites (Table 16, Appendix I).

2.6.4 Unit 6B: Alkali Granite

Alkali granite is completely restricted to a conformable sheet near Hook Lake near the centre of the Cheddar batholith (Fig. 1.2), where it outcrops for about 2.5 km along strike and forms the tallest hills in the area. It is mostly a gneissic rock with a purple hue. There are a few outcrops where it is undeformed. At its margin it appears to grade into pink gneiss typical of the main granites.

In an unstrained sample of alkali granite quartz forms one third of the rock. Microcline, with plume perthite intergrowths, greatly exceeds albite (An_{7-8}), which resembles "Chessboard Albite" (Smith 1974). Aegirine is present and magnetite is an accessory. In some gneissic samples of LS2 microstructures are observed which are described in Section 4.3.4.

The alkaline nature of the granite is evidenced by the normative acmite, the low Al_2O, which is subequal with MgO + FeO, and the very high total Fe (Table 16, Appendix I).

2.6.5 Unit 6C: Medium Grained to Pegmatitic Granite

These medium to coarse grained granites form minor bodies which cross-cut the hornblende-biotite granite and alaskite in the Cheddar batholith. As noted previously, they are very common at the margins of this body, where they cut the gneissosity of the country rock. In the southern part of the Cardiff plutonic complex, they have a similar relation to the host granite. They may well be present elsewhere in the complex in a deformed less recognizable state. They form most of the Upper Faraday granite which is exposed in the map area. In the Lower Faraday granite there are small cross cutting, highly deformed bodies which are slightly coarser than the host granite. These may be the medium grained granite in a recrystallised form. There are granitic members of the heterogeneous syenite gneiss unit and occasional small isolated bodies which are the probably equivalent of this rock.

These rocks are distinguished from the host granite in being more leucocratic, coarser grained and generally less recrystallised, although they too usually bear the regional lineation.

In these granites quartz, perthitic microcline and albite (An_{5-8}) are subequal. These rocks are distinguished by the presence of two feldspars which, in contrast to many of the other granites, are not the product of recrystallisation of a single perthitic feldspar. The feldspars are medium grained (2-5 mm). Microcline contains a small amount of bead-perthite. It is often cracked and displays an undulatory extinction. Albite is often myrmekitic, it shows signs of incipient recrystallisation and grain-size reduction due to a kink related process (Plate 6a,b). The size of these incipient neocrystals is comparable to that in more extensively recrystallised granite gneisses. Discontinuous albite rims are observed on some plagioclase boundaries at contacts with microcline. Microcline and plagioclase from the Upper Faraday granite both show a maximum degree of ordering (Table 17, Appendix I). Spongy biotite is present in accessory amounts together with minor opaques. Quartz microstructures and microfabrics are dealt with in Sections 4.2 and 4.3.

The primary geochemical characteristics of this group is that K_2O/Na_2O is > 1 and that K/Rb is significantly lower than that for the biotite and hornblende biotite granites (Table 16, Appendix I).

2.6.6 Unit 6D: Biotite and Hornblende-Biotite Granite
Unit 6E: Layered Pyroxene Granite Gneiss.

Rocks of this group form the bulk of the Cheddar batholith, The Monck Lake granite in the Cardiff complex and the Lower Faraday granite. In the main part of the Cheddar batholith they interfinger with the Alaskitic equigranular rocks and the metasedimentary inliers at the southeast and southwest sides. Mafic layered pyroxene granite gneiss (Unit 6E) occurring most abundantly at the margin of the inlier of intermixed metasediments and granites is included with this group.

In the Cheddar batholith most of the rocks of this group are medium grained. They have a planar-linear fabric which is more or less well developed depending on the amount of mafics present and the grain size of the quartz. Some varieties have a weak augen texture. The mafic layered pyroxene granite gneiss is an equigranular medium grained rock becoming lineated in the neighbourhood of Hook Lake.

In the Centre and Monck Lake granite the rock is more leucocratic than in the Cheddar batholith, and was termed alaskite by Hewitt (1957a). Generally the rock is penetratively lineated. Its grain size varies from fine to medium grained, with most fine grained. Although parts of it have a similar aspect and grain size as in the Cheddar batholith (for example that exposed on Highway 121 north of Paudash Lake) it is mostly finer grained and appears more strongly deformed (Table 18, Appendix I). The extremes of this grain size reduction and planarity of fabric may be seen on the west shore of Jordan Lake at the north of the Cardiff complex.

The Lower Faraday granite is uniformly fine grained (Table 18, Appendix I). As in the Centre and Monck Lake granite the grain size decreases and the fabric strengthens from south to north (see Table 18, Appendix I, Plate 12). In the northern half it is a very fine grained sugary gneiss with delicate, extremely attenuated quartz ribbons. This grades southward into a gneiss comparable to that in the Cardiff complex.

Quartz forms between one quarter and one third of the rock. The feldspar is either perthite with minor albite, or perthite and varying amounts of fine intergrowth-free microcline and plagioclase or it is entirely a fine grained aggregate of the two latter. Biotite and hornblende and biotite are present in minor to accessory amounts and may replace clinopyroxene. Titano-magnetite, sphene and apatite are common accessories.

In most of the granites quartz forms polycrystalline quartz ribbons of the "granulite" type. They are described and discussed in Sections 4.2.1. and 4.2.2.

In the three granite bodies similar feldspathic components are present but in different proportions. Loss of perthite coincides with grain-size decrease which correlates with a strengthening of mesoscopic fabric. A comparable process of grain-size reduction and unmixing of perthites is seen in the mylonitized grains of the Cheddar batholith (Appendix II). In samples from a traverse across the central part of the Cheddar batholith north of Hook Lake medium-grained microcline perthite is dominant in hornblende-biotite granite. In biotite granite medium grained albite (An_{2-9}) is also present. In some samples of the former the perthite lies in a matrix of equant fine grained microcline and plagioclase, free from intergrowths. In a narrow concordant shear zone with a very well developed fabric only fine grained microcline and plagioclase is present. Perthite types include braid, plume, ribbon, (Deer et. al. 1966), mesoperthites (Plate 6d). Perthite coalesces with a rim of albite which may be segmented, continuous or interpenetrated by similar albite from neighbouring grains (Plate 6c). Chessboard albite sometimes accompanies mesoperthite in the biotite-hornblende granite.

In the Centre and Monck Lake granite medium grained augen of perthite are always subordinate to a matrix of fine grained, equant, intergrowth-free microcline and plagioclase The fine grained plagioclase is in the An_{5-14} range with most near An_{10}. Discontinuous albite rims are common. One or two grains with microscopically visible peristerite are present in most sections. In the perthite augen intergrowth morphologies are similar to those in the Cheddar batholith, braid mesoperthites being most common. Chessboard albite is present in a relatively perthite rich sample. In general there is less perthite, a finer grain size and a less albitic plagioclase at the north than at the south of the complex.

In the Lower Faraday granite, perthite is absent. Very fine grained plagioclase (An_{9-12}) and microcline (0.5 - 0.1 mm) is present, comparable to the fine grained feldspars of the neighboring granites. These feldspars show a maximum degree of ordering (Table 17, Appendix I).

In all the bodies, there is evidence for the metamorphic origin of biotite and amphibole: 1) they form the planar linear metamorphic fabric; (ii) hornblende is intergrown with clinopyroxene in some samples from the Cheddar (Plate 7a) and Lower Faraday granites. In the Cheddar, unaltered clinopyroxene is present in the mafic layered gneiss in which there is no destruction of medium grained perthite and no planar-linear fabric. (iii) there are many examples of skeletal amphibole and biotite in which these minerals are intergrown with a variety of other very fine grained minerals (serpentine (?), magnetite, sphene, carbonate, apatite, quartz) (Plate 7b-d). In the Lower Faraday granite and the Centre and Monck Lake granite these symplectic textures are not present in the northernmost rocks, where only well formed biotite, or hornblende and biotite are found.

The major elements of all the hornblende-biotite and biotite granites are very similar (Table 16, Appendix I). K/Rb values in the 300 to 400 range are only slightly higher than the normal range for igneous rocks of 160-230 (Heier

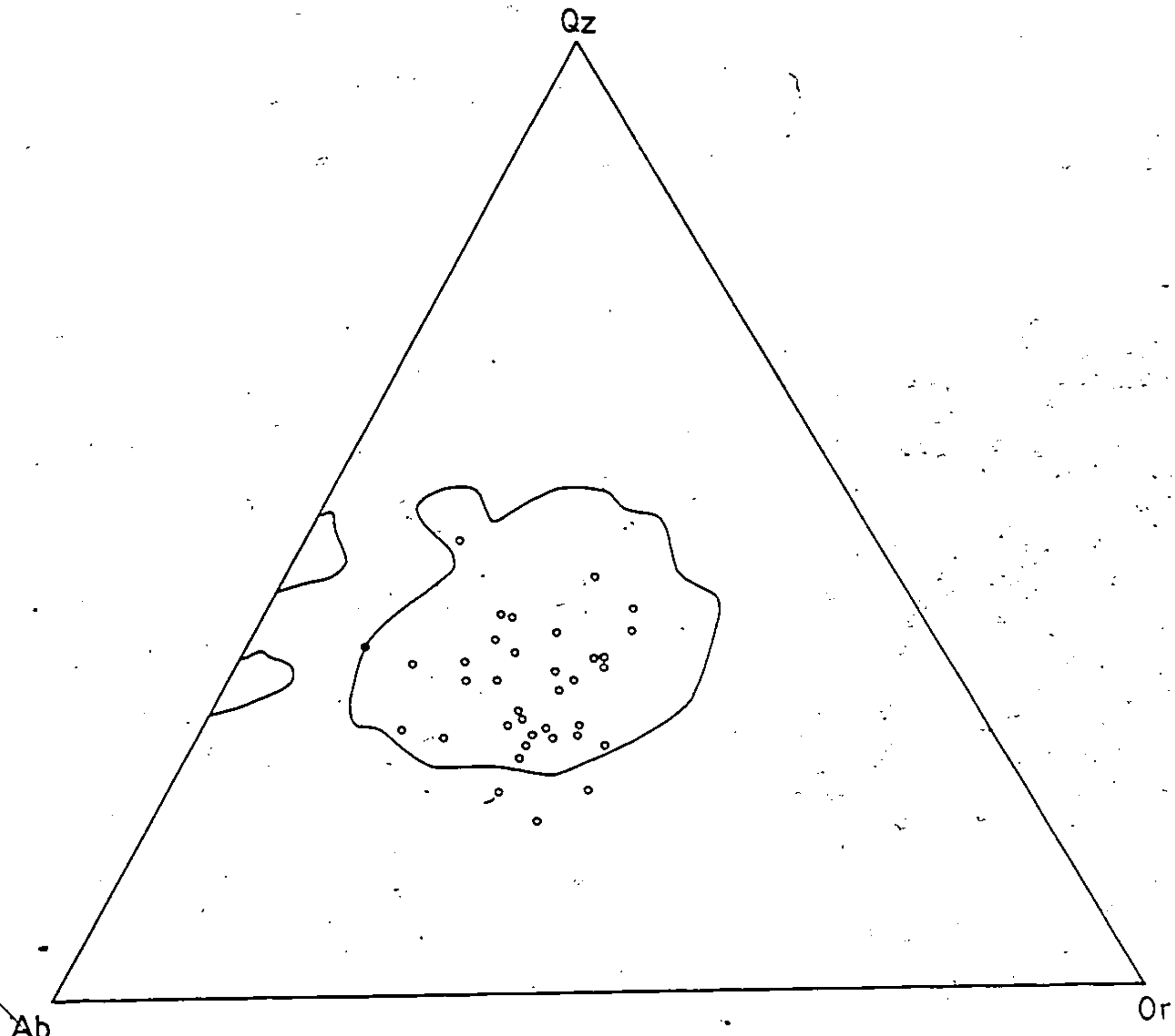

FIGURE 2.4 Normative QZ : Ab:OR of Cheddar, Centre and Monck Lakes and Faraday granites. Contour contains 86% of all granites (from Winkler and von Platen 1961).

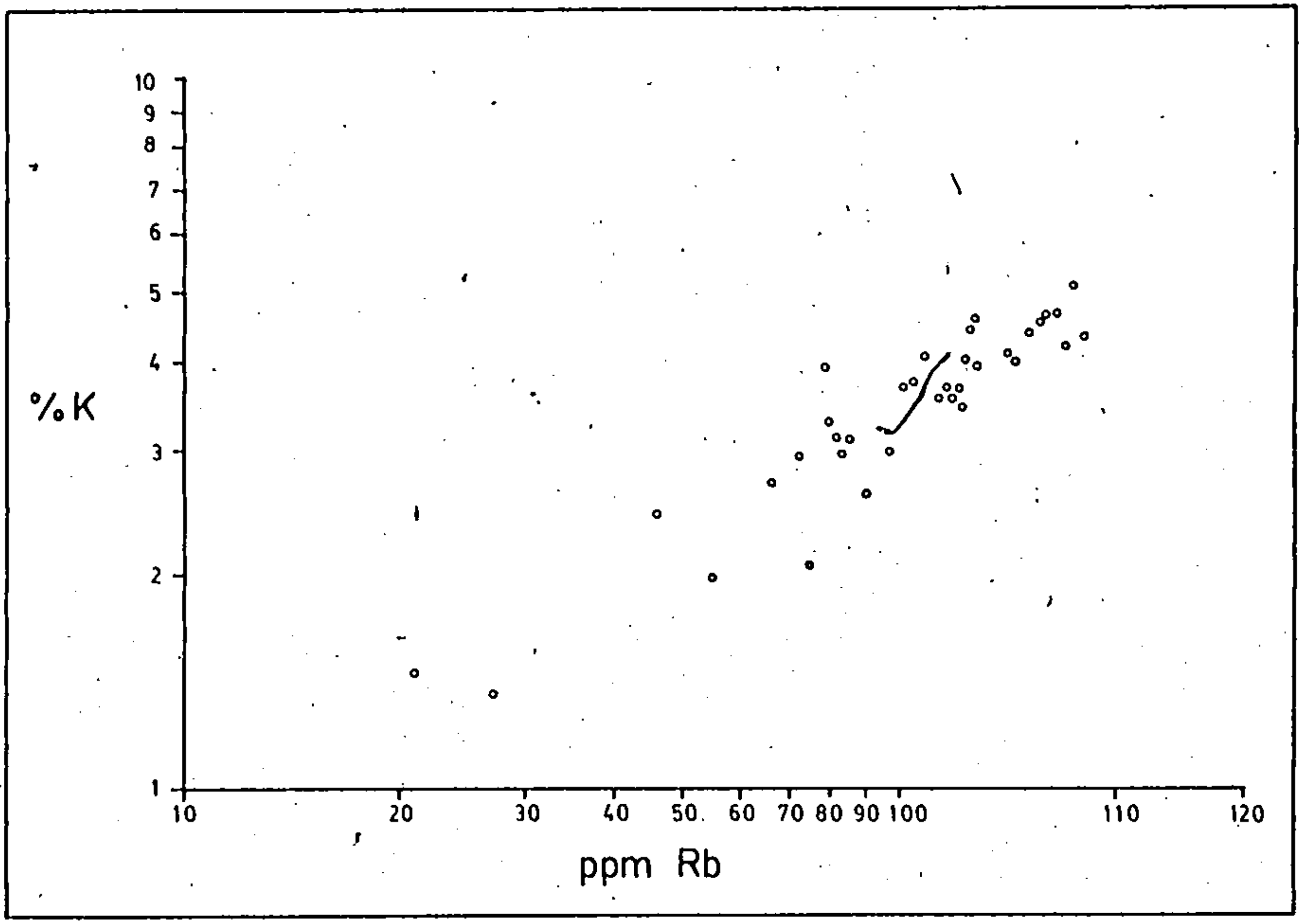

FIGURE 2.5 K vs Rb variation in granites of Cheddar and Cardiff complexes.

and Adams 1964) and average for igneous rocks, of 280 (Shaw 1968). The Centre and Monck Lake granite of the Cardiff complex is a little different from the Cheddar granite in certain respects. For example the former has relatively elevated K/Rb values, perhaps reflecting the lesser amount of amphibole in it than in the latter (Shaw 1968). The mafic layered pyroxene granite of the Cheddar batholith is notable for its low K_2O/Na_2O and high iron.

2.6.7. Geochemistry

All the granite fall in or near the maxima of the haplogranitic system (Fig. 2.4). However, they do not define any recognizable trend within this system. On a K vs. Rb plot they form a well defined trend (Fig. 2.5). Later cross cutting granites show enrichment in K and lower K/Rb (Table 16, Appendix I).

2.6.8. Conclusions

(i) The rocks have had an important solid state metamorphic history as witnessed by the well developed mesoscopic fabrics.

(ii) Much amphibole and biotite are metamorphically derived from the breakdown of augite. Additional components, such as Na and K are possibly contributed by the unmixing and recrystallisation of perthite. In this regard the more calcic composition of plagioclase in the more extensively recrystallised (finer grained) granites is relevant.

(iii) Feldspars show two lineages depending on whether the original rock is (a) an hypersolvus one feldspar granite (the perthitic biotite and hornblende biotite granites) or (b) a subsolvus two feldspar granite (the high-K medium grained granites). Complete recrystallisation of both these types results in a fine grained two feldspar granite free of perthite.

Mesoperthites with highly indentate grain boundaries similar to those in the Cheddar granite have been interpreted as exsolution microstructures (e.g. Yund and Ackermand 1979). In this type of granite (a) recrystallisation of the perthite and grain-size reduction with increasing strain is evident from: 1) the occurrence of fine, perthite-free two feldspar granite in a shear zone in perthitic granite of the Cheddar batholith; 2) the occurrence of segmented albite rims continuous with perthite braids in the least deformed perthitic granites (Plate 14b); 3) the inverse correlation of the amount of fine intergrowth-free feldspars with medium grained perthitic augen. The amount of the former increases with increasing strain judged from inspection of hand samples, taking into account, for example, attenuation of quartz ribbons, fineness of grain size (Table 18, Appendix I, Plate 14); 4) perthite unmixing and recrystallisation with increasing strain is known from other rocks (Deer et. al. 1966). (b) The complete evolution of the two feldspar medium grained to pegmatitic granite cannot be documented, although the initial stages of plagioclase recrystallisation are clearly recorded e.g. Plate 7.

Several other points favour the interpretation of the fine-grained two feldspar aggregate as being the product of dynamic recrystallisation. For example, peristerite is restricted in occurrence to the fine grained two feldspar aggregate. Although in Smith's (1974) opinion peristerite formation is posttectonic, Wenk and Wenk (1977) dissent, pointing to the catalyzing effect of deformation on the otherwise sluggish migration of M and T atoms and Marshall and Wilson (1976) demonstrated the formation of peristerite during dynamic recrystallisation. A second feature is the presence of discontinuous albite rims at plagioclase-microcline boundaries which Byerly and Vogel (1973) interpret as indicating grain-boundary migration.

These recrystallised feldspars may be further modified in an LS2 zone (Section 4.3.5) or a discordant mylonite zone (Appendix II).

(iv) Since recrystallisation and grain-size reduction correlate with increasing strain it may be concluded that the order of increasing strain from greatest to least is: Lower Faraday granite, Centre and Monck Lake granite, Cheddar granite, Upper Faraday granite. In addition, the south of both the Centre and Monck Lake and Lower Faraday granite is less strained than the north (Table 18, Appendix I, Plate 12).

(v) The alaskite of the central part of the Cheddar batholith is totally different from the other granites in that it:

1) is interlayered with paragneiss; 2) does not have a shape fabric of quartz, which is made up of fine single grains; 3) it has an almost complete lack of perthite. Although these may be taken as an argument for the rock being a recrystallised arkose, neither its sheetlike form nor its texture is necessarily diagnostic. The Centre and Monck Lake granite, for example, is interlayered with amphibolite at its northern end. The microstructure of the alaskite may be a result of extreme recrystallisation, as indicated by the occurrence of peristerite and two fine grained intergrowth free feldspars. Quartz may never initially have been coarser grained. However, the nearby Silent Lake Pluton has been interpreted on geochemical grounds to be a remobilized arkose (Breaks and Shaw 1973) and texturally and mineralogically the alaskite resembles this pluton. Therefore on the basis of the present evidence it is not possible to satisfactorily give a genetic interpretation of this unit.

(vi) All the granites may be reasonably interpreted to belong to one magmatic suite (disregarding the alaskite on acccount of the ambiguities descibed above and lack of chemical data). The following reasons can be cited: 1) later (cross cutting) fractions are more K and Rb rich than earlier; 2) the rocks show a well defined K vs Rb trend; 3) K/Rb ratios compare with magmatic rocks.

The history of these granites involves crystallization from a melt of one feldspar pyroxene granite, subsequent, syntectonic, crystallisation of the two feldspar granites.

2.7. Mafic Dykes

Thin mafic dykes, usually foliated amphibolites, are found throughout the area. Although sparsely developed, they have been found cutting all rock types, predating the regional lineation. Two examples of unfoliated partly amphibolized diabase are known, cutting the crest of the Deer Lake Structure in the Cardiff complex and the poorly foliated Upper Faraday granite.

Francoeur (1975) described similar mafic dykes which were found throughout Monmouth and Glamorgan Township. Lumbers (1967) noted that dykes in the almandine-amphibolite terrain were foliated and metamorphosed, whereas in the lower grade terrains deformation is weak or absent and primary textures are widely preserved in dykes which may be tens of metres wide.

The dykes are thin amphibolite sheets, rarely more than 15 centimetres wide. Often they may be observed to cross-cut the country rock foliation only in surfaces near perpendicular to the lineation. Some dykes contain deformed and recrystallised plagioclase phenocrysts, whose original shapes may be seen in this section. Such dykes may have a marginal zone free of phenocrysts, which is interpreted as a chilled-margin.

In the Drag Lake Grey Tonalitic Gneiss, the southern part of the Cheddar pluton and the crest of the Deer Lake structure, the dykes are cut by foliated pegmatite. Elsewhere the foliated dykes cut pegmatite, for example, in the supracrustal envelope on the east side of the Cheddar pluton. Foliated and unfoliated dykes are found in the crest of the Deer Lake structure. Evidently several generations are present or, possibly the dykes are syntectonic.

The unfoliated dykes strike southeast and are somewhat thicker (up to 1 m) than the foliated variety which also strike southeast.

The foliated dykes are normal amphibolites comprising hornblende and plagioclase, with variable amounts of scapolite, clinopyroxene and biotite and accessory sphene and magnetite.

The partly amphibolized dykes have preserved primary plagioclase, which is corroded and partly recrystallised. Skeletal hornblende replaces clinopyroxene. Magnetite is abundant.

2.8. Metamorphism

2.8.1. Introduction

The study area lies within a larger region which consists of rocks of the upper amphibolite facies (Lumbers 1967, Armstrong and Gittins 1968, Divi 1972, Chesworth

1971). It is but a small part of the southern Grenville Province which is characterized by rocks of this facies over large areas.

Lal and Moorhouse (1969) considered the rocks of Fishtail Lake to be transitional between the garnet-amphibolite and granulite facies.

Chesworth (1971) and Dostal (1975) suggest that the region belongs to a facies-series of intermediate pressure. The following are cited as evidence:
1) the occurrence of staurolite, typical of the higher pressure series of Miyashiro (1973) together with cordierite (Lal and Moorhouse 1969, Chesworth 1972, Shaw 1962) representative of the lower pressure series; and 2) occurrences of all three aluminosilicates (andalusite, Lumbers 1967; sillimanite and kyanite, Best 1966; Hewitt 1957a; sillimanite, kyanite and andalusite, Lal and Moorhouse 1969).

Chesworth (1971) suggested that the pressure and temperature limits for metamorphism in the Haliburton Highlands were between 3.5 and 7 kb and 580 and 700° C.

2.8.2. Metamorphic Events within the Map Area

Two features of the metamorphism which are of fundamental importance are that it was syntectonic and that it affects all but the latest plutonic rocks.

Mineral assemblages (Table 19, Appendix I) and many mineralogical features confirm most of the conclusions quoted above. Evidence that the rocks belong at least to the upper amphibolite facies is: i) In pelites, potassium feldspar and sillimanite, although rare, are present. Orthoamphibole rather than orthophyroxene is stable. ii) In mafic compositions (gneissic metagabbro) hornblende (green) and andesine-labradorite are stable, typical of high grade amphibolites (Winkler 1976). iii) In marbles diopside and tremolite are ubiquitous. Forsterite is rare. These are typical minerals of higher grades (Turner 1981, Kretz 1980). Wollastonite, typical of the highest grades, is absent. The assemblages present (Table 19, Appendix I) suggest the following reactions: tremolite + calcite + quartz = diopside + CO_2 + H_2O; tremolite + dolomite = forsterite + calcite + CO_2 + H_2O; dolomite + quartz = diopside + CO_2 (in quartzites). The first two reactions in particular belong in the field of high-grade metamorphism (Winkler 1976). iv) Several of the feldspar microstructures are restricted to high grade rocks. For example, huttenlocher and boggild-type intergrowth are found in andesine and labradorite in meta-supracrustal amphibolite, in amphibolite pods from the grey tonalitic gneiss, in gneissic metagabbro and meta-anorthosite and in pelitic and semipelitic paragneiss. Similar features are considered to have been formed at elevated temperatures ($600^{\circ}C \pm 100$, Nissen 1968; greater than $600^{\circ}C$, Wenk and Wenk 1977). Discontinuous albite rims, so common at microcline- plagioclase boundaries in all two feldspar rocks, may be restricted to rocks of the middle amphibolite facies and higher grades (Byerly and Vogel

1973). Moreover Goldsmith (1982) considered peristerite to be formed in metamorphic rock at relatively high temperatures but pressures not higher than 6-7 kb. v) The ranges of plagioclase compositions for specific róck composition ranges are comparable to other medium to high grade terrains (Table 20, Appendix I). In particular the similarity of the compositions to the two high-grade areas from the Swiss Alps may be noted.

Regarding the possible transitional amphibolite to granulite facies nature of the rock it is relevant that: 1) the assemblange almandine-cordierite-biotite-sillimanite is present, similar to other rocks in the Grenville Province, transitional to the granulite facies (Dallmeyer 1972). The assemblages are very similar to those recorded for the amphibolite-granulite facies transition in the Adirondacks, where a pressure range of 3-5 kb. was estimated (Turner 1981).

Armstrong and Gittins (1968) recorded orthopyroxene bearing coronas in the Glamorgan Gabbro, similar to those in the Farquhar Lake Gabbro. They wondered why this evidence for granulite facies metamorphism was limited in extent while the surrounding rocks were of lower grade. In Section 2.4.6., it is suggested that this effect is not necessarily due to repeated episodes of metamorphism but to limited access of water to the undeformed cores of the gabbroic bodies.

The principal evidence for polymetamorphism is the replacement of diopside and forsterite by tremolite, in the marbles and related rocks, and the destruction of LS1 quartz microstructures by the LS2 microstructures. Although evidence for the first event is widespread the timing and physical significance is not clear. The second event is localized within concordant zones (Section 4.3.2.) and it has kinematic significance. However it is not clear whether it took place at a significantly lower temperature or later time than the main metamorphism, perhaps at the same time as the retrogression in the marbles, or simply at a higher strain rate.

Finally there is the occurrence in the Drag Lake complex of layered gneiss with clinopyroxene partly replaced by amphibole of the main metamorphism. This hints at an earlier high grade event, possibly restricted to the grey gneiss. In this regard it is worth recalling the ca. 1400 Ma. age of the granulite facies orthogneiss situated in probable basement gneiss some 50 km northeast of the map area.

2.8.3. Metamorphic Fabrics

The microstructure of the minerals record processes which started during a dynamic metamorphism and, probably, continued after it. In Section 4.2.7 it is suggested that the very coarse microstructures in the quartzites are exaggerated-grain-growth microstructures (Wilson 1973).

This kind of microstructure is the end-product of grain-growth initiated during dynamic recrystallisation and continued in the static environment until all strain and grain boundary energy is dissipated. The same process may be invoked to explain the microstructure of the coarse grained marbles (Plate 1c). This explanation is compatible with many features of the marbles: (i) Mesoscopic and microscopic inclusion fabrics which show evidence of extreme strain (Plate 1a,d); (ii) The presence of the coarsest grain sizes in the purest marble; (iii) The inclusion of silicate minerals, often drop-like, within the carbonate grains as well as on the grain boundaries (Plate 1c); (iv) The lack of intracrystalline strain shown by the carbonate grains; (v) The occurrence of the finest carbonate grains in marble very rich in graphite, the presence of which presumably hindered grain growth. This explanation is compatible with the observation of Lumbers (1967) that marbles in the Bancroft- Madoc area become coarser with increasing metamorphic grade.

Likewise the decussate textures of biotite, hornblende and biotite-hornblende aggregates (Plates 8b,c) represent the end-product of essentially similar processes. They show equilibrium boundary configurations in which many of the grain-boundaries are rational, low energy planes (Spry 1969, Nicolas and Poirier 1976).

3. MAJOR AND MINOR STRUCTURES

3.1. Introduction

The most important structural feature of the region is the well known down-dip, southeast plunging lineation (Culshaw 1981, Divi and Fyson 1973, Best 1966, Hewitt 1962) and the northwest leaning Cheddar and Cardiff granitoid plutons, type 'catazonal' granites (Buddington 1959). The lineation distinguishes it from the Hastings Lowlands to the southeast, where lineations of low rake (many trending NE) are found (Hewitt 1962 and Fig. 1.1)

The southeastern border of the map area (Fig. 1.1) lies near the border of the regional zone of SE plunging lineations and includes the two northernmost bodies of the Harvey-Cardiff Arch, the Cheddar batholith and Cardiff Plutonic complex (Fig. 1.2). To the north dips flatten whereas to the southeast and south a steepening of foliations coincides with a change in lineation trend to predominantly northeast along the regional strike (Hewitt 1962, 1957 a and b, Divi 1972, Bright 1980). Divi, in an area just east of Bancroft, demonstrated that F2 minor folds showed increased flattening of their profiles as their axes were progressively swung with an increase of rake within the foliation from northeast to southeast. In that area major F2 isoclines with steep northeast trending axial surfaces occur.

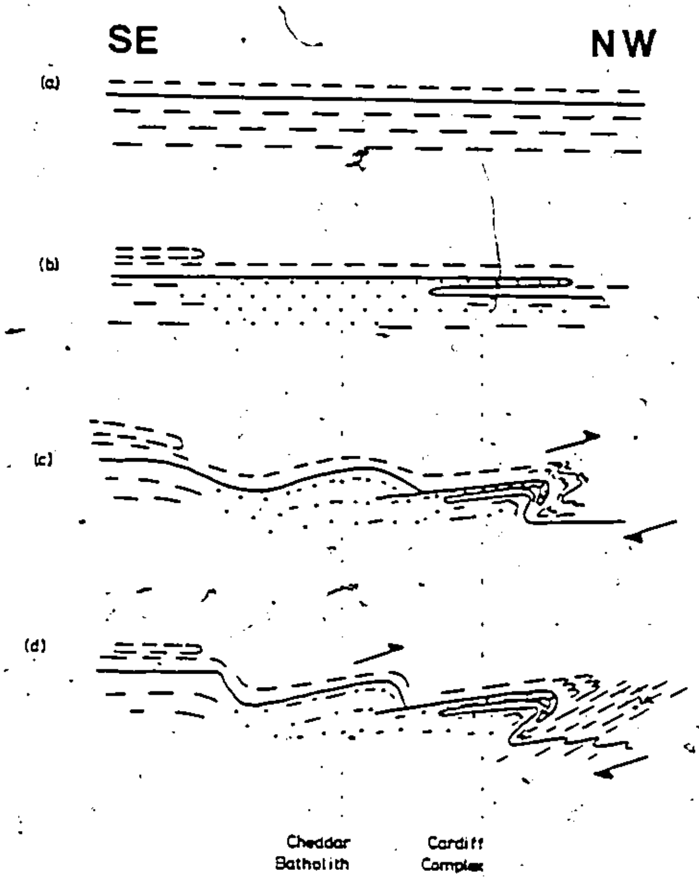

FIGURE
3.1
Postulated sequence of events in the map area at the northern end of the Harvey-Cardiff Arch. This is a schematic projection of sections of the plutonic complexes onto a NW - SE vertical plane. (a) Early configuration of basement and cover; (b) cover is thickened by early large scale folding; granite is generated along the axis of the Arch, forming migmatitic and homogeneous bodies; (c) in response to the lowering of the ductility contrast by high grade metamorphism the bouyant granitoid rises diapirically into the denser cover; the northern extremity is deformed by ductile shearing; (d) the shear zone widens, deforming the Cheddar batholith.

The map area (Fig. 1.1) affords sections across and parallel to the strike of the zone of southeast plunging lineations. It is naturally divisible into three structural units: (i) & (ii) the Cheddar batholith and Cardiff Plutonic complex (~~Fig.~~ 1.1), which are northwesterly verging structures; and (iii) the northern segment of possible basement, plutonic gneiss and Grenville Supergroup gneiss extending from Drag Lake to Elephant Lake. Locally strikes run northwest in zones of folding coaxial with the lineations. The lineation is imposed on rocks forming the Cardiff-Harvey Arch whose formation postdates the large F_2 folds (Fig. 1.1).

This chapter demonstrates that the SE lineation exerts a fundamental control on the geometry of the major and minor structures, that it is both a stretching lineation and an axis of rotation and that the tectonic history of the area may be interpreted in terms of a displacement of material in a ductile environment toward the northwest towards the close of a structural history which included early large scale isoclinal folding and the emplacement, probably syntectonic and diapiric of the Harvey-Cardiff Arch of catazonal gneissic bodies (Hewitt 1962). A postulated sequence of structural events is shown in Figure 3.1.

For the purpose of analysis of major and minor structures the map area has been divided into twenty-one

Domains (Fig. 1.3). The Domains represent areas which have been recognized from the structural map to be homogeneous with respect to some structural element and distinct from neighbour(s) with respect to that element. Several Domains make up a structural unit such as the Cheddar batholith, or a single Domain may encompass a significant large-scale structure, for example zones of folded envelope rocks between the Cheddar, Cardiff and Faraday bodies. The Domains also provide an easy geographic reference for location of minor structures.

3.2. Description of Minor Structures

3.2.1. Foliations

Foliations include compositional layering, schistosity (either S1 or S2) and shape fabrics which are planar-linear of the LS type.

A stratiform compositional layering exists in most rock types as described in the petrography section. It is most common in the supracrustal rocks where it probably includes original bedding, in the tonalitic grey gneiss and in the heterogeneous syenitic and granitic gneisses. It is of subordinate importance in the granites and syenites of the main plutonic bodies and absent in the meta gabbro bodies. In most cases the layering, schistosity and the planar component of the LS shape fabrics are parallel.

An S1 schistosity is formed of aligned biotite in quartzo-feldspathic rocks, phlogopite in marbles and biotite, feldspathic aggregates and, rarely, calcite in quartzites. In some rocks it is the only fabric element present, for example in some granites in the north of the Cheddar Body (Domain 3). In the great majority of cases it lies parallel to the layering. Foliations shown in Figs. 1.2 and 1.3 are dominantly S1 foliations, parallel to the compositional layering.

Second foliations (S2) which transect layering and layer parallel S1 are rare and almost entirely restricted to zones of northwest striking foliations where folding co-axial with the regional lineation has taken place. In all cases S2 dips moderately to the southeast sub-parallel to the regional foliation and transects a steeply dipping layering sometimes associated with an open wrinkling of this layering. It is best developed in Domain 21. (Fig. 1.2, Plate 8a).

3.2.2 Shape Fabric

Shape fabrics are the quasi-ellipsoidal aggregates of minerals found in many orthogneisses which are assumed to indicate the orientation and type of finite strain ellipsoid (Schwerdtner et. al. 1977, Grocott 1979). LS fabrics (mainly LS1) are the most significant fabric element in the area since they indicate the stretching direction of the rock and serve as a time marker relative to which other structures may be dated.

In the grey tonalitic gneisses (Unit 3A) quartz-ribbons and aggregates of light and dark minerals (hornblende-biotite and plagioclase-quartz) are present in rocks of appropriate compositions. The granites (Unit 6) including many pegmatites, typically display quartz ribbons and sometimes a shape-fabric consisting of mineral aggregates (Plate 9a). This latter is common in syenites (Unit 5) where even mafic-poor varieties have tiny clusters of hornblende or clinopyroxene, and is ubiquitous in metagabbroic rocks (Unit 4). Comparable shape fabrics are found in mafic dykes cutting metasupracrustal rocks in Domains 6 and 7. In these, polygonal plagioclase aggregates retain the tabular outlines of phenocrysts in the sections perpendicular to the lineation (YZ).

Inclusions of varied origin contribute to the shape fabric in several rock types. In syenitic gneisses (especially in Domains 13, 14, 16 and 20) ellipsoidal green diopsidic inclusions are found, sometimes with dimensions of several metres. A second example is the occurrence of elongate gabbroic patches in gabbroic anorthosite (deformed oikocrystic texture).

3.2.3. Lineation

There are two main kinds of lineation besides the long dimensions of LS shape fabrics: intersection lineations and the dimensional orientation of elongate minerals. All may occur together in a single rock and are not distinguished on stereoplots (Fig. 1.3). For the most part lineations measured are L1. L2 features are rare, restricted to intersections of S2 on compositional layering or to the narrow concordant zones of LS2 tectonites.

Mineral Lineation: Amphibole lineations are ubiquitous in all appropriate rock compositions. In syenites, granites, metagabbros and grey tonalitic gneisses there is petrographic evidence of replacement of clinopyroxene by amphibole indicating formation of this lineation during syntectonic metamorphism. There are rare examples of some amphibole growing within the foliation at a high angle to amphibole with a linear orientation. This is best displayed in the syenite gneiss in the southwest corner of Domain 22. Other minerals with dimensional orientation include clinopyroxene in syenites and quartzites, feldspar augen in syenites, granites, pegmatites and quartzites and rare sillimanite.

Intersection Lineation: There are three categories of intersection lineations: (i) the intersection of a deformed vein or dyke with a foliation (usually S1); (ii) intersection of layering with S1 or S2 which may be expressed as the physical intersection of two foliations or as a very small scale plication of layers and parallel S1 (Plate 8); (iii) the intersection of mica-flakes which display a decussate microstructure on foliations (Plate 8), the mica-edge lineation (Fyson 1970).

(i) This type of lineation results from the homogeneous deformation of a single vein (granitic or syenitic) or system of veins and the rotation of suitably oriented vein intersections on foliations towards the direction of maximum extension (Watterson, 1968 and section 3.2.5.), or the syntectonic instrusion of veins (Plate 10).

(ii) The intersection of layering that is original bedding with S1 has not been identified with certainty. The best candidates are ridges lying parallel to hinges of intrafolial isoclines (Plate 9b-c) in tightly folded and finely layered calc-silicate rocks.

The intersection of S2 on layering is mostly associated with zones of northwest trends. It is produced by either a physical intersection of two foliations or the deformation of an old foliation by F_2 or both. In an example of this type in Domain 7 (Plate 8d,e), rocks dipping shallowly to the southeast are surrounded by steeply dipping northwest striking rocks. This gently dipping foliation is crenulated by very open upright folds of a few centimetres wavelength. Comparable open plications with axial surfaces which dip moderately southeast are very common on steeply dipping foliations from zones of northwest trends and on steep limbs of many asymmetric minor folds (e.g. in Domains 4,6, and 2).

An example of the combination of crenulation of an old foliation with intersection of it by a new one is seen in some folded calc-silicate marbles (Plate 9d,e; Hewitt 1957,

p. 17). S1 is transposed parallel the axial surfaces of asymmetric F_2 folds producing a streaking on S0 which is parallel to crenulation axes. At right angles to this compound lineation tension gashes filled with late carbonate and calc-silicates show that it also lies in an extension direction.

A second example is found in the thick quartzite body of Domain 21. A low dipping S2 schistosity, marked by tiny slits of weathered-out calcite, transects a steeply dipping layering on which a ribbing of the quartz is conspicuous. In thin sections cut perpendicular to the layering and parallel to the lineation the long axes of all mineral grains lie parallel to the mesoscopic lineation. In sections cut perpendicular to the lineation many of these grains are observed to be deformed into more equant shapes. It is the intersection of the grains with equant shapes on the layering which produces the excellent quartz ridging in this rock. The long axes of pyroxenes, feldspars and calcites also lie at a high angle to the layering in this section, forming S2 dipping at a moderate angle to the SE.

Mica and amphibole foliations transect steeply dipping layering in the grey tonalitic gneiss and the garnet gneiss in Domain 17 (Plate 8a), producing an intersection lineation which is parallel to the axes of folds and small plications with southeast dipping axial surfaces.

(iii) A very common type of lineation in mica-rich rocks is formed by the intersection of the edge of mica flakes on the

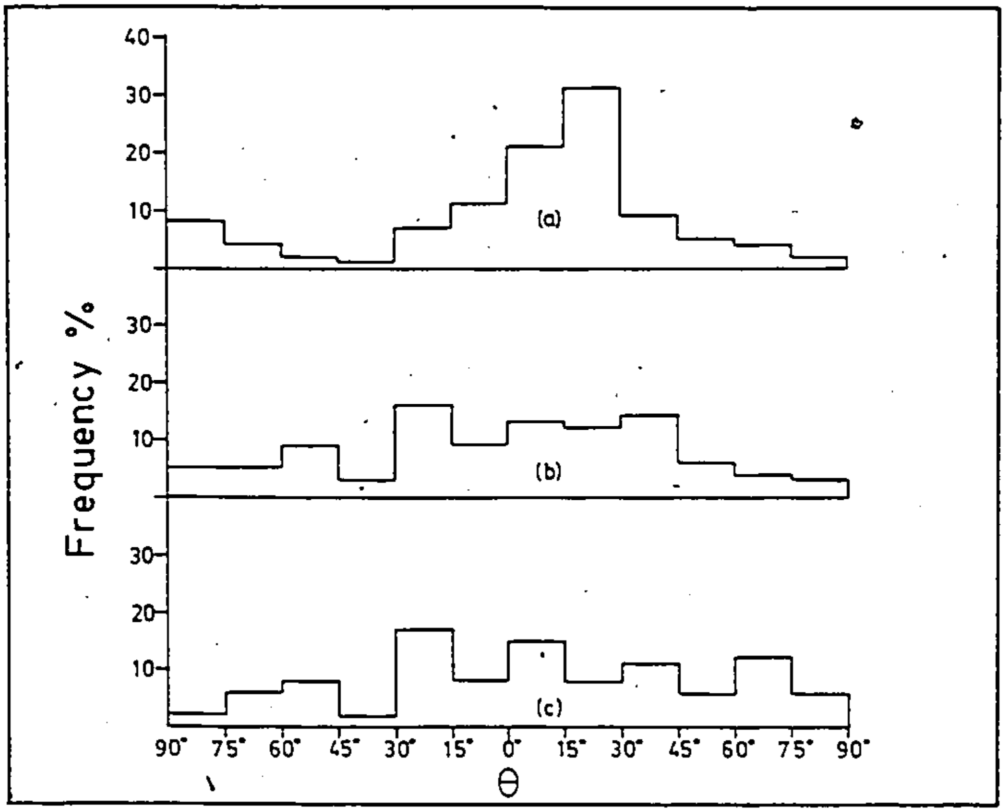

FIGURE
3.2

Trace of biotite basal planes on YZ plane perpendicular to lineation in paragneiss which has mica edge lineation. θ is the angle between trace of basal plane & mesoscopic layering. 100 measurements in all diagrams. (a) biotite gneiss from Eels Lake, lineation is down dip, type I mica edge lineation, domain 5. (b) hornblende- biotite gneiss from northwest of Colbourn Lake, domain 7, lineation has low rake on steeply dipping layering, type II mica edge lineation. (c) calcsilicate gneiss from southeast of Colbourn Lake, domain 7; low rake on steeply dipping foliation, type II mica edge lineation.

layering, the mica-edge lineation. This is the result of the decussate texture of mica (Vernon 1976). Since in this texture (Plate 8b) the interfaces of neighbouring grain-pairs in biotite aggregates are parallel to (001) of only one of the grains of the pair, neighbouring (001) planes will not be parallel. Since most of the flakes appear to contain the stretching lineation, all the flakes not lying perfectly parallel to the layering will contribute to the mica-edge lineation in the case where layering and S1 are mesoscopically parallel (Fig. 3.2). This type of distribution (Type I) is typical of the moderately southeast dipping tectonites. A second type of distribution (Type II) is found only in zones of predominant northwest strikes where it is widely developed in steeply dipping layering (Fig. 1.2). The (001) traces in the section perpendicular to the lineation approach a uniform dispersion (Fig. 3.2, Plate 8c). Both types of distribution are easily recognizable in hand specimen.

Strain in the weakly deformed Upper Faraday granite on the eastern side of Domain 9 is dominantly prolate (see Section 3.2.5) and biotite has an axial type II distribution. However the trace of this linear mica fabric on the XZ plane of the mesoscopic fabric is oblique to the long axis of LS1 quartz ribbons (Fig. 3.3). The trace of the mica fabric plunges more steeply than the quartz towards the southeast. This asymmetric fabric has only been found in this unit and is interpreted as indicative of northwest

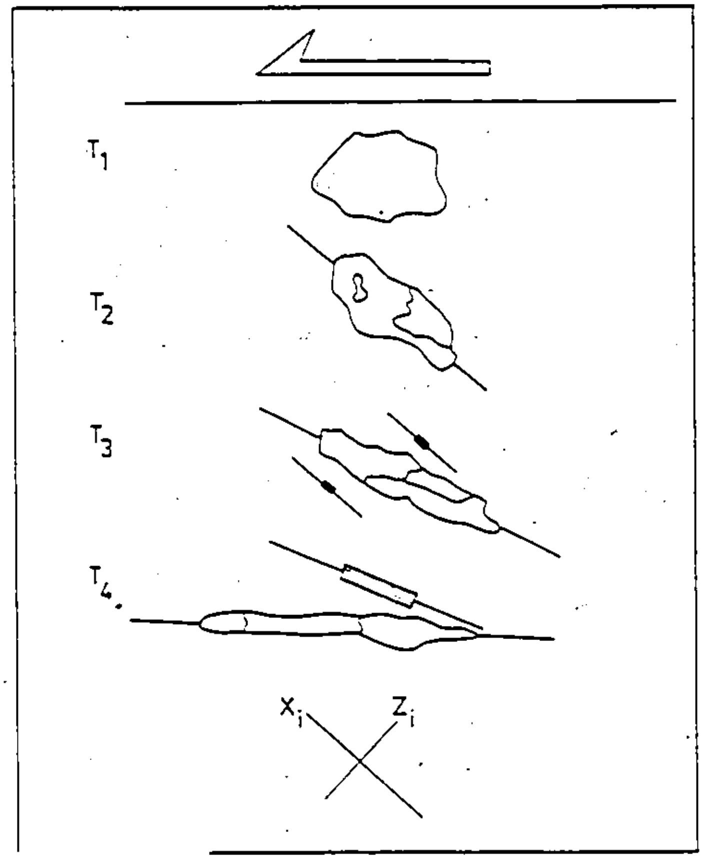

FIGURE
3.3

Interpretation of development of asymmetric biotite and quartz fabrics in granite gneiss from Upper Faraday granite near Albion Lake. Diagram of XZ plane of mesoscopic fabric, north-west to left. A quartz-eye, undeformed at T1, is subject to shear and elongates near parallel to the principal axis of the incremental strain ellipse (Xi) at T2. The long axis of the quartz swings progressively closer to the shear plane (T2-T4). At T3 metamorphic biotite has nucleated and grown near parallel to Xi. Owing to its late nucleation and growth its long dimension lags behind that of the quartz as both are rotated towards the shear plane.

directed shearing during the formation of metamorphic biotite (Fig. 3.3).

3.2.4. Minor Folds

There are two categories of minor folds: Type (i) intrafolial folds with axial surfaces parallel to the layering and Type (ii) with the axial surfaces at a low to moderate angle to the surrounding layering that are noticeably asymmetric (Plate 11). Both types are moderately common in all layered rocks.

Type (i) fold styles vary from Class Ic to Class 3 with Class 2 folds (similar style) estimated to be the most common fold styles (after Ramsay 1967). Type (ii) fold styles vary from 1B to 2. Type (ii) fold tightness varies from open (interlimb angle 120° - 70°, following Fleuty 1964) to tight (30° to 0°) with most belonging to the close class (70° - 30°).

Type (ii) folds from Domains with northwest trending foliations have different patterns of orientation of axes and axial surfaces from those from Domains with predominantly southeast dipping foliation (Fig. 3.4 and 3.5). The latter have axial surfaces which tend to dip more consistently southeast; axes, although predominantly plunging southeast have a wide scatter and may lie anywhere near a plane which dips moderately to the southeast parallel to many of the axial surfaces. Axes from folds in Domains of northwest trending foliations all plunge moderately to

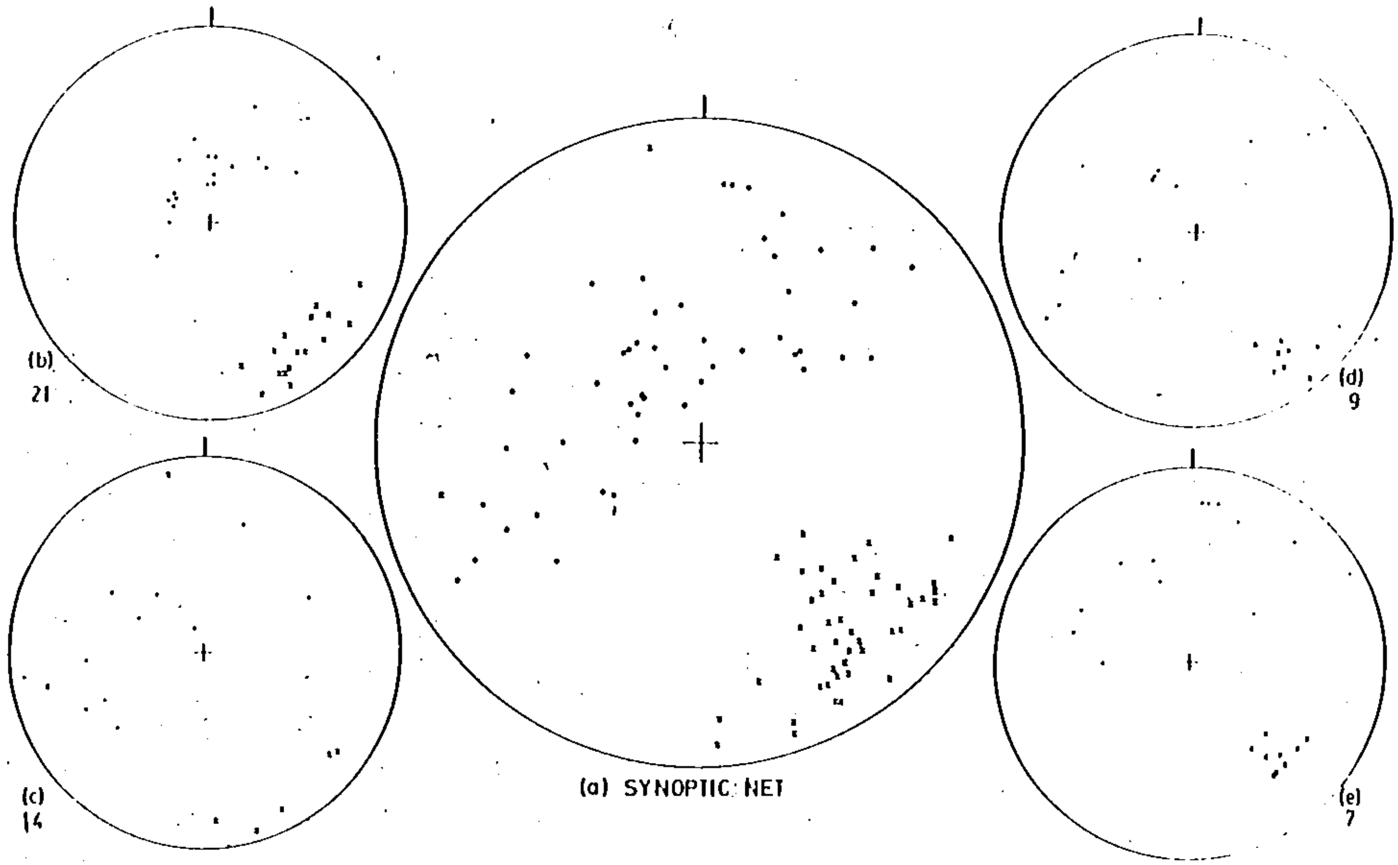

FIGURE 3.4 Orientation of asymmetric folds from zones of northwest trending foliations. Crosses, fold axes, circles, axial surfaces. (a) combination of data from northwest trending zones in domains 21, 14, 9 and 7; (b) domain 21; (c) domain 14; (d) domain 9; (e) domain 7.

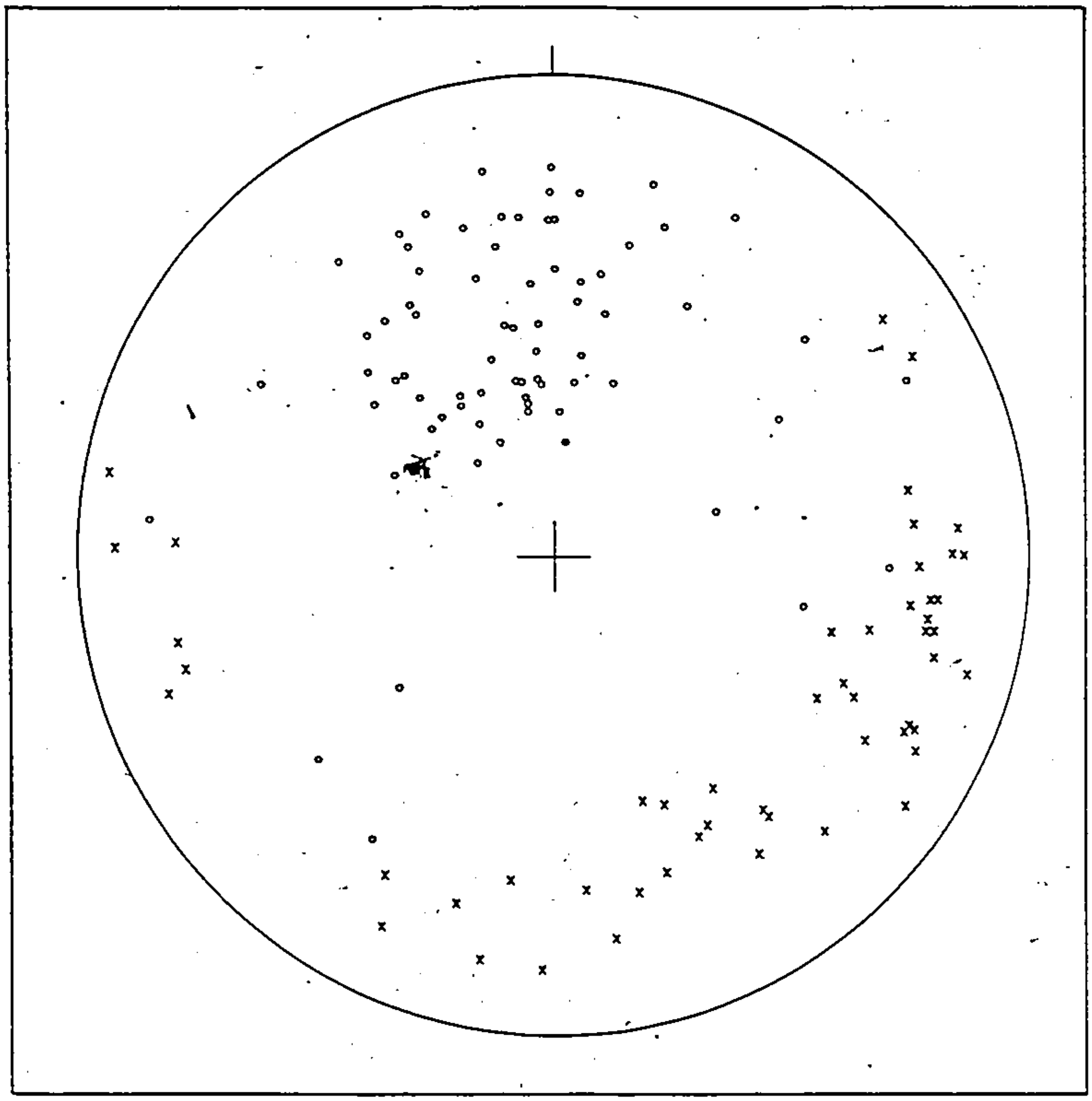

FIGURE 3.5

Orientation of asymmetric folds from whole area exclusive of zones of northwest trending foliations. Crosses, fold axes; circles, axial surfaces.

the southeast, while axial surfaces tend to be polyclinal (Fig. 3.4). The folds of Domain 21 (Fig. 3.4) are an exception, for although all the axes plunge to the southeast the axial surfaces are also relatively constant in orientation.

Most folds appear to be broadly synchronous with respect to the metamorphism and the development of the regional stretching lineation. Several lines of evidence may be cited: (i) Most folds have a lineation parallel to the fold axes, including those with axes at a high angle to the regional lineation, which very often have axes parallel to the local lineation. Examples of this are found in and around the Eels Lake dome (Domain 14) and in the western part of the crest of the Deer Lake Structure (Domain 11, Figs. 1.2 and 1.3). (ii) Lineations are very rarely refolded. (iii) Granite and pegmatite formation occurs before, during and after fold forming (Plate 11). (iv) Rarely, similar minerals lie in both S0/S1 and S2 (Plate 8) e.g. in Domain 17, a zone of NW trends in the Drag Lake complex, lineated granitic leucosome formed syntectonically.

Some other folds have axes at a high angle to the regional lineation and to the local lineation. The best examples are found in the northern part of Domain 13 in tonalitic grey gneiss and quartzite (Fig. 1.2). These are asymmetric folds with rounded near parallel profiles, amplitudes of one or two metres, moderately dipping axial surfaces and axes east-west to southwest-northeast. These folds may be related to folds of intermediate scale which are responsible for sudden local dip and plunge reversals in the northern Domains, for example in Domain 16 (Fig. 1.3).

There is some evidence for the existence of folds with curved hinge lines. Two examples from Domains 21 and 13 have axes on the same outcrop diverging by up to 45° within a southeast dipping plane; axes from an isoclinally folded calc-silicate rock which borders a marble tectonic breccia show a comparable variation within a single hand-specimen; a rather well exposed fold in feldspathic gneiss in the northern part of Domain 13 has a curved hinge (Plate 11f), and may be related to nearby asymmetric folds with axes at a high angle to the regional lineation.

On the other hand there are many folds which have apparently rectilinear axes parallel to the regional lineation, but which do not have the tight profiles expected of folds which first formed at a high angle to the lineation and were subsequently rotated towards the stretching direction. Many asymmetrical folds from within and outside of the Domains of northwest trending foliation belong to this class. The mullion-like lineation formed by gentle folding of steep foliations around southeast plunging axes may be included here. An hypothesis for the formation of those in zones of moderate SE dips is described in Section 5.1.3.

Refolding of folds is rarely observed. In relicts of shallowly southeast dipping supracrustal rocks within the

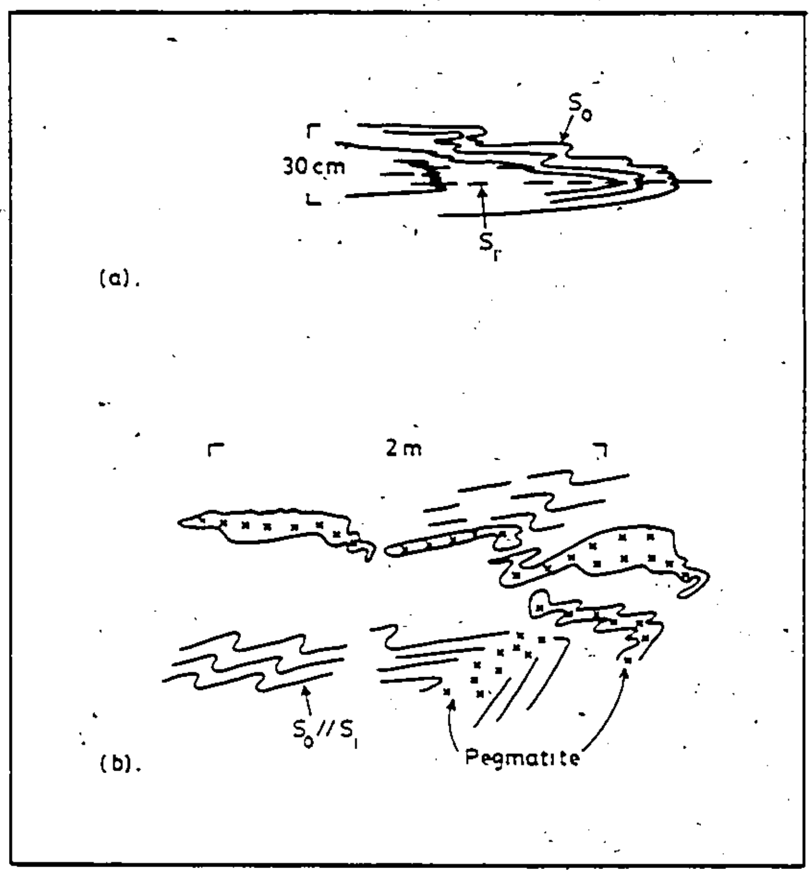

FIGURE
3.6

Structural relations in supracrustal rocks of the roof pendant of the Cheddar batholith (domain 2). Isoclinal fold of layering in biotite gneiss, near Eels Lake North, biotite forms S1 which lies on the axial surface. (b) asymmetric fold of layering (So) and foliation S1 from location near (a). Boudinaged pegmatite is folded and later pegmatite lies on the axial surface.

inter-plutonic steep zone of Domain 7 an upright crenulation co-axially refolds mesoscopic isoclines (Plate 10). Asymmetric folds on the flanks of the synform which surrounds the pyroxenite body of the Farquhar Lake complex (Domain 14) include one which refolds an earlier fold in a migmatitic layering. Both these examples are clearly related to the forming of the northwest structures.

In the crest of the Deer Lake structure there are many asymmetric minor folds related to the major structure (see Section 3.2.9). In one case these refold a boudinaged and isoclinally folded migmatitic layering and schistosity in feldspathic gneiss (Plate 11b). A similar case is found in infolded supracrustal rocks of the Cheddar Body (Domain 2) where asymmetric folds deform a layering, micaceous schistosity (S1) and boudinaged granitic veins (Fig. 3.6b). Nearby there are isoclinal folds of the layering in which the S1 schistosity is axial-planar (Fig. 3.6a) other isoclinal folds deform a granitic component. The scarcity of fold interference prohibits the confident designation of fold ages. Nevertheless, the examples given above do show that folding affects an already highly evolved stratiform foliation and formation of granitic material occurred during and prior to all phases of folding (Plate 11).

3.2.5 Strain

Deformed Vein Fabrics: In rocks cut by mafic dykes or systems of granitic or syenitic veins which have been deformed, the relation of the trace of the rock fabric to the margin of the veins varies according to the location of the erosion surface on which it is exposed relative to the principal axes (XYZ) of the rock fabric. In the map area, especially in the northern Domains (13 to 22), there are many examples of heterogeneous gneisses formed of layers of igneous and/or supracrustal rock of varied origin. Many have an extremely planar aspect and many show signs of crystalline strain such as sugary fine grained feldspars, relict feldspar augen and extremely drawn out quartz ribbons. Only a minority of these are exposed well enough to show the geometry of the layers. In sections in zone with the lineation vein margins are characteristically parallel to the trace of the host rock fabric (Plate 10). In sections perpendicular to the lineation cross-cutting relations between veins and host rock fabric are preserved.

Examples of these relationships are found in most rock types apart from the marble mainly in the northern Domains (Table 21, Appendix I), and in the Burleigh fold (see Section 3.3.2.). Watterson (1968) suggested that the geometry of vein fabrics is related to the shape of the bulk strain ellipsoid, the homogeneity and magnitude of the strain and the initial orientation of the veins. Systems which have suffered high homogeneous plane strains will show cross cutting relationships and profiles of isoclinal folds with axial planes parallel to the flattening foliation only in the section perpendicular to the lineation. Polyclinal folding will be evident in this section with constrictional strain. Presumably this relationship of vein geometry and strain holds whether vein emplacement is pre- or syntectonic. Accordingly most of the vein fabrics seen display approximate plane-strain fabrics (Table 21, Appendix I). A noteworthy exception is that of the northeast shore of Drag Lake where polyclinal folds of veins in sections perpendicular to the lineation indicating constrictional strain occur (Plate 10). This example is in a zone of northwest trending foliations (Domain 17).

Marble Fabrics: In the layer of impure marble which forms a concordant envelope almost completely surrounding the Cheddar batholith, the great ductility of the marble in comparison to other materials is shown by boudinaged structures in pegmatitic, granitic and amphibolitic layers and by the high degree of amplification of folds in them. These features are best seen on the northwestern and southern tip of the body, where boudinage structures show apparent extensions in excess of 400% parallel to the strike. Oblate and somewhat elongate boudin tablets occur.

Marbles in which many boudinaged fragments have variably oriented long axes are common throughout the northern Domains 13 to 22 (Plate 1a,b). Such fabrics have been called Tectonic Breccias (Hewitt 1957). A well exposed example on Elephant Lake Road (Domain 13) shows instructive relationships. The breccia is a concordant layer not more than 1.5 m wide. The calcitic matrix is isotropic and fine grained and contains ovoid and rounded silicate inclusions with variably oriented long axes in which there is no lineation or foliation. At the upper margin layers of fine grained, sugary pink and green calc-silicate gneiss are folded in open asymmetric northeasterly verging folds of a few decimetres amplitude or in highly amplified isoclines with very sharp hinges whose axial orientation may vary on the scale of a hand specimen. In places these layers are broken up and included in the marble. Below the breccia a biotite feldspar gneiss is folded in asymmetric southeast plunging folds with highly deformed long limbs (Plate 11e).

In most tectonic breccias the carbonate matrix forms a mosaic of equant centimetric grains. Silicate fragments vary in size and shape considerably. Boudinage and rotation may be observed in all stages. Elongate boudinaged fragments are often subsequently folded. There is evidence that some of the fragments are also produced by a plucking of the margins of large bodies of plutonic gneiss by the ductile marble. An excellent example is found near the western side of Dudmon Lake on Highway 121. Here proportions of buff syenite to marble decrease in an easterly direction in a section oblique to the strike. At the western end marble is absent. Fragmentation and engulfment of the syenite increases until marble forms 60 per cent of the outcrop. Fragments of syenite range from half-metre rectangular blocks to tiny millimetric ovoids spread evenly throughout the marble. Carbonate fills gashes in the syenite. The gneissosities of neighboring syenitic framents are highly misoriented, attesting to considerable rotation.

These fabrics reflect the very high ductility contrasts which must exist between marble and silicate rocks at metamorphic temperatures. The blocks with variably oriented gneissosity or sigmoidal feldspathic tails are interpreted as reflecting a history of simple shear (Ghosh and Ramberg 1976) and in some cases may indicate a sense of shear (Plate 1b).

Strain in the Granitic Gneiss (Unit 6): The granitic rocks of the Cheddar, Cardiff and Faraday Plutons (Unit 6) are all rather similar petrographically and geochemically (see Section 2.6.7). A qualitative idea of variation in magnitude and type of strain can be gained from field observations of grain size, which is assumed to decrease with increased strain (see Section 2.6.8), homogeneity of development and orientation of LS fabrics and, more rarely, the angular relationships of fabrics to deformed pegmatites or mafic dykes. Relying on the first two criteria it appears that granitic rocks of the Cardiff complex are generally more strongly deformed than those in the Cheddar batholith; that strain increases from south to north in the Monck Lake granite of the Cardiff complex, that strain also increases from south to north in the Lower sheet of the Faraday granite and that the Upper Faraday granite is much less deformed than the Lower. Inspection of relevant photomicrographs (Plate 12) and measurement of the size of

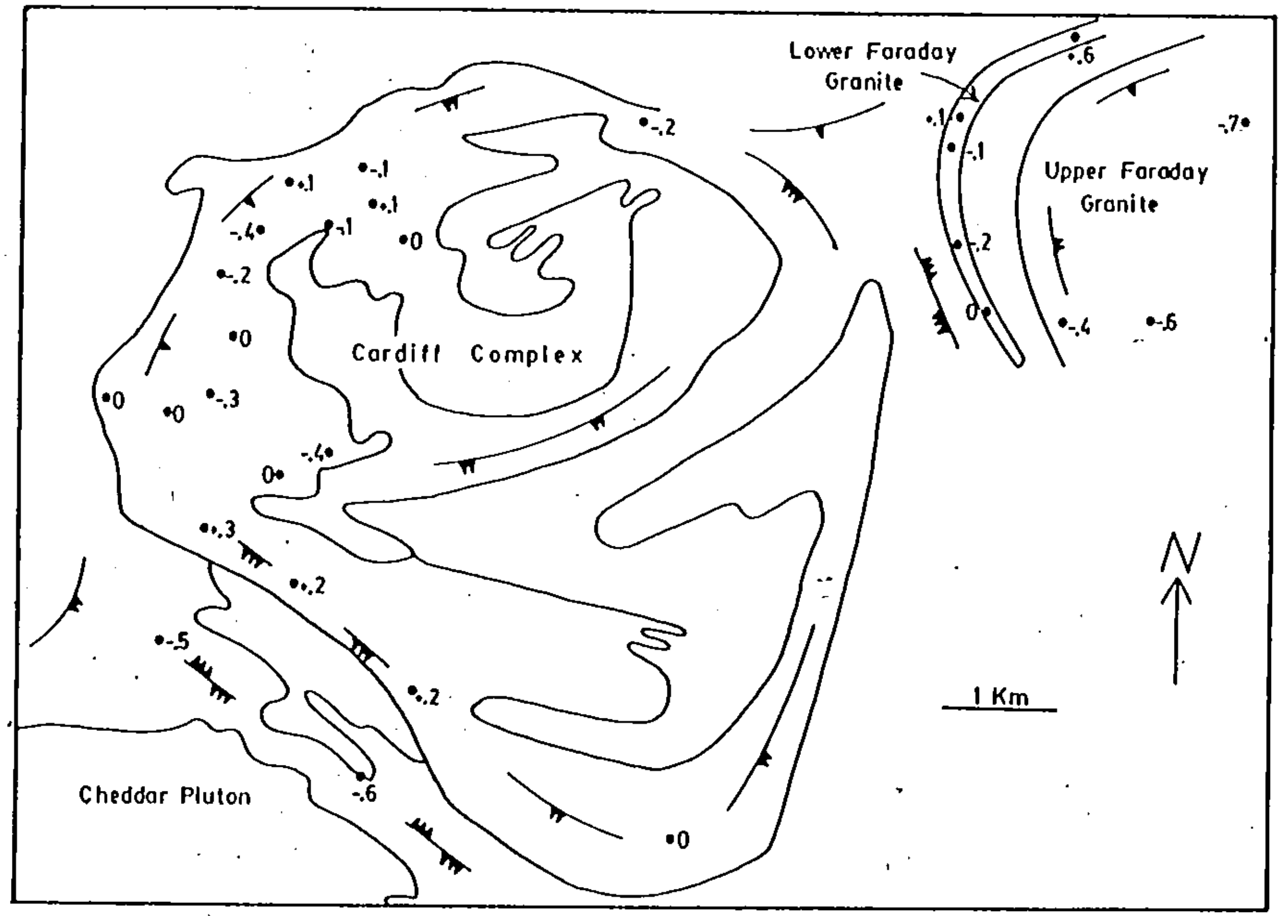

FIGURE 3.7 Strength of foliation relative to lineation in shape-fabrics of Cardiff Complex and Faraday Granites. Lodes numbers approaching +1 represent oblate fabrics, 0 are plane strain and -1 are prolate. Form lines as in Fig. 1.3.

feldspar grains (Table 18, Appendix I) illustrate this variation in grain size and the concomitant decrease in grain-size range and number of large perthite grains within and amongst the granites. The decrease in feldspar grain size is also accompanied by an increase in quartz ribbon aspect ratio. The principal conclusion is that strain judged qualitatively from field inspection of the rock fabric increases from south to north across the plutons.

It is common practice to regard shape fabrics in plutonic gneiss as directly related to the shape of the strain ellipsoid of the whole rock (e.g. Schwerdtner 1977, Grocott 1979). In the granites of the Cardiff and Faraday plutons and in adjacent rocks shape fabrics of quartz aggregates have been measured in order to validate field estimates of the relative strength of foliation and lineation. The resultant Lodes numbers show some variation of fabric shape with structural position with respect to the plutons (Fig. 3.7). (i) shallow to moderately southeast dipping rocks on the western and northern flanks of the Cardiff complex and on the southern flank have values close to 0, a plane-strain fabric, although three examples have prolate fabrics (negative Lodes numbers). (ii) Prolate fabrics are present in syenite gneiss and a mafic dyke between the Cardiff and Cheddar plutons where foliations are steeply dipping and strike southeast whereas adjacent granite of the Cardiff complex also with steep foliation striking southeast, has weakly oblate fabrics. (iii) There is a great contrast between the Upper Faraday granite where strain appears to be low, which has pronounced prolate fabrics, and the more strongly deformed Lower Faraday granite which for most of its length has values indicative of plane-strain.

The plane strain fabrics of the moderate to shallow southeast dipping foliations on the northern flank of the Cardiff pluton and the shallow fabrics of the Lower Faraday granite are compatible with the simple shear model envisaged for the whole region in which the shear plane dips moderately southeast. In this case the Y direction is subhorizontal. The prolate fabrics in the syenite and the mafic dyke between the Cardiff and Cheddar plutons could reflect the superimposition of two plane-strains with X directions parallel and NW but successive Z and Y directions mutually perpendicular. The stage with Y subvertical developed when the envelope rocks were crumpled between the steep NW trending walls of the plutonic complexes, presumably during emplacement. These increments may have been successive or synchronous, an interference between the pluton emplacement strain and the regional shearing strain. The weakly oblate fabrics in the adjacent granitic gneiss would have been formed during the emplacement of the granites. Likewise the constrictional strain in the Upper Faraday granite may result from a similar interference of emplacement and regional strain due to shearing. In the Lower Faraday granite the influence of the latter is clearly greater.

It is of note that in both the Domains with apparent constrictional strain there is the well developed type of mica-edge lineation (Type II) in which mica plates are uniformly distributed around the lineation (Fig. 3.2), lending strength to the idea that this type of mica-edge lineation reflects constrictional strain.

Mesoscopic Fabrics in Northern Domains (13-22): The rocks of the northern Domains exclusive of the grey tonalitic gneiss complex and the mafic plutonic gneisses, comprise a heterogeneous mixture of granitic, syenitic and supracrustal gneiss, interlayered on all scales. The rocks appear to be more strongly deformed than all but the most northerly of rocks in the Cardiff and Cheddar Complexes and some zones in the grey gneiss (Unit 3) and form a zone of high strain transecting the map from the Faraday granite to the west side of the area, north of the Glamorgan gneiss.

The main feature is the very straight layered often flaggy aspect of the rocks. This is caused in the buff syenite by the presence of a strong vein fabric of fine pink syenitic, granitic and pegmatitic veins. Other straight layered mixtures comprise pink granite and syenite and concordant highly deformed pegmatite with augen texture with the foliation flowing around drop-like inclusions of varied composition. granite, syenite and augen pegmatite form layers within any of the supracrustal rocks forming systems of very planar aspect.

On the hand specimen-scale, several features indicate strong deformation. Augen and fine sugary textures are present in many of the syenites, granites and pegmatites. In a few examples the presence of large isolated feldspar augen (up to 5 cm in length) in a fine equant feldspar matrix attest to a high degree of grain size reduction during recrystallization. Quartz ribbons are generally very delicate and finely drawn out.

Many or all of these features occur together forming an association which typify the rocks of the area. An excellent example is found in neighboring outcrops near the extreme southwest corner of Baptiste Lake (Plate 1b,e). The main rock types are marble, hornblende-biotite gneiss and calc-silicate gneiss. Granitic, syenitic and pegmatitic veins penetrate the silicate rocks forming very planar vein fabrics with a southeast plunging lineation. The veins have very fine grained sugary feldspar textures and quartz ribbons. The pegmatitic layers are marked by augen textures. The coarse grained marble tectonic breccia is replete with misoriented boudinaged layers and blocks of supracrustal and intrusive gneiss. The nearby outcrops of the Lower Faraday granite show all the textural features displayed by the granite veins.

The mesoscopic fabrics of the grey tonalite gneiss and the garnet gneiss show a structural history broadly divisible into two parts: (i) the earliest stage which encompasses the period before the emplacement of the syntectonic granitic veins and may have predated amphibolization of the whole complex. (ii) The second stage which involves all events during and soon after the emplacement of the granitic veins which occurred during the lineation forming event, the main metamorphism and the formation of the zone of northwest striking foliations. This second stage generally was only locally as strong in the grey gneiss as in the enveloping supracrustal, granitic and syenitic gneiss.

(i) The presence of a strong deformation which predates the emplacement of the granite veins is demonstrated where the granite, although lineated has a medium grained, weakly recrystallised texture of feldspar but cross cuts gneiss with a more planar deformed aspect, or cross cuts or engulfs an amphibolite layer which has a lensoid highly attenuated form. A straight layered gneiss with square terminated boudins is present where amphibolization is not complete (see Section 2.3.2) indicating that the boudinage predated the amphibolite facies metamorphism, and hence the granite veins and the lineation.

Since some of these older high strain features appear to predate the lineation and none of the gabbroic, syenitic or granitic orthogneisses have any deformation fabric but the lineation, this earlier fabric may have been formed at a period predating the emplacement of the gabbros and syenites, possibly even predating the appearance of the Grenville Supergroup.

(ii) The degree of deformation which took place in the grey gneiss during and after the emplacement of the granitic veins is shown by the strength of various fabrics, for example fineness of grain size and planarity of the gneiss, expressed by the parallelism of the mafic, gneissic and granitic layers. Concordant with the regional gneissosity, several high strain zones are known, none of which appear to be wider than a few tens of metres. Examples of these zones are found near the boundaries of the complex, for example on the eastern and southeastern shores of Elephant Lake, near its western shore in the isolated sheet of grey gneiss, near the southern shore of Farquhar Lake and on the southern shore of Drag Lake. Rocks in these zones have a very well foliated flaggy aspect, often delicately laminated with strong vein fabrics. The granitic veins form concordant layers of augen gneiss. In several cases these zones contain concordant schist ("tectonic schist" in Fig. 1.2 and henceforward) horizons which vary in width from a few centimetres to two or three metres (near west side of Elephant Lake). They commonly contain isolated feldspathic augen and stringers and truncate isoclinal folds of the layering of the host gneiss. In an example from near the southern shore of Farquhar Lake the schist zone has an asymmetric biotite planar-linear fabric (LS2). The sense of asymmetry of the biotite fabric is the same as that of quartz in the surrounding gneisses, indicating localized southeasterly directed shear of upper layers.

In the garnet gneiss (Unit 3C) there is, in more micaceous members, a fabric of dismembered pegmatite which resembles a tectonic schist, being charged with feldspathic augen and stringers, although it lacks the strong planarity of the schists and is less micaceous. Adams and Barlow (1910 Plate IX, Figure 2 and p. 78) called an example from Fishtail Lake: "conglomerate gneiss produced by intense motion ...." and envisaged it as the end product of a process marked by "extreme motion with an unusual plasticity ....". It resembles the "tectonite gneiss" of Davidson et al. (1982), and probably has the same significance.

To the north reconnaisance shows that a broad belt (> 10km) of similar strong syn-lineation deformation is present in interlayered probable basement and supracrustal rocks. The emplacement of the grey gneiss must accompany or precede this deformation.

3.3. Description of Major Structures

3.3.1 Comparision of Net Projections of all Domains.

All domains in which intermediate and map scale folding is absent are characterized by southeast dipping foliations (Domains 1,13,19, Fig. 1.3). The contoured stereoplots of poles to foliations of many of the domains with intermediate and map scale folds have maxima of similar orientation to that of the unfolded southeast dipping foliation, (Domains 2,3,5,7-9,11,12,17,18,20-22, Fig. 1.3) and π-axes which lie either sub-parallel to the SE plunging regional stretching lineation (L1) or in a plane which lies roughly parallel to unfolded southeast dipping foliation (Fig. 3.8). The point

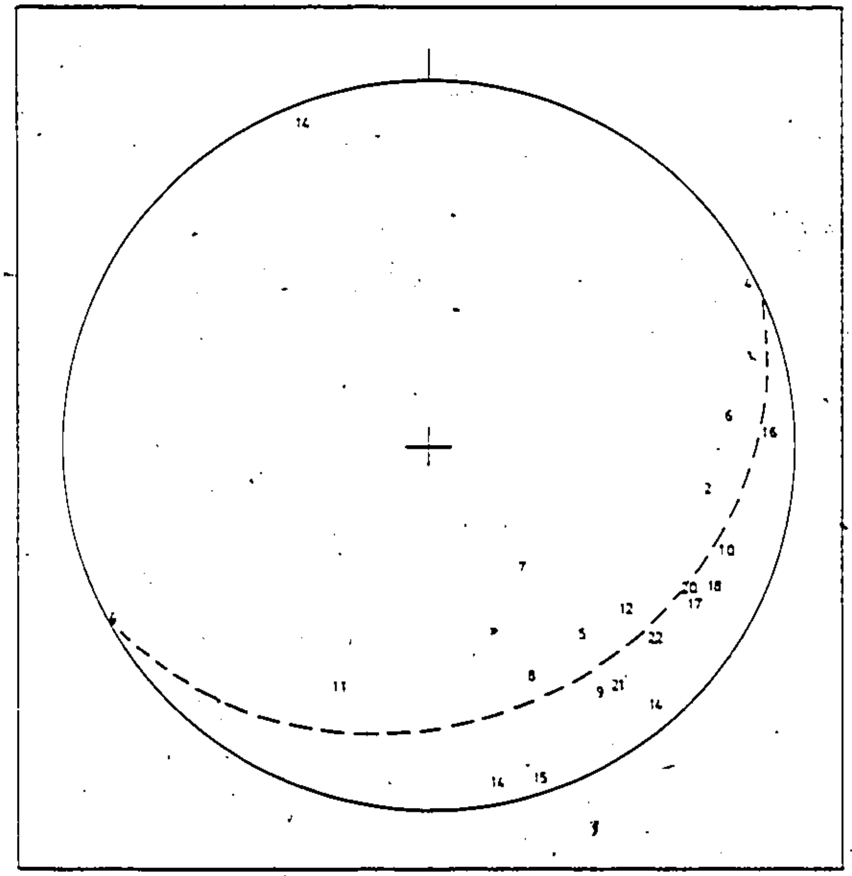

FIGURE 3.8 Axes of intermediate and large scale folds (axes of all Domains). π axes numbered by Domain.

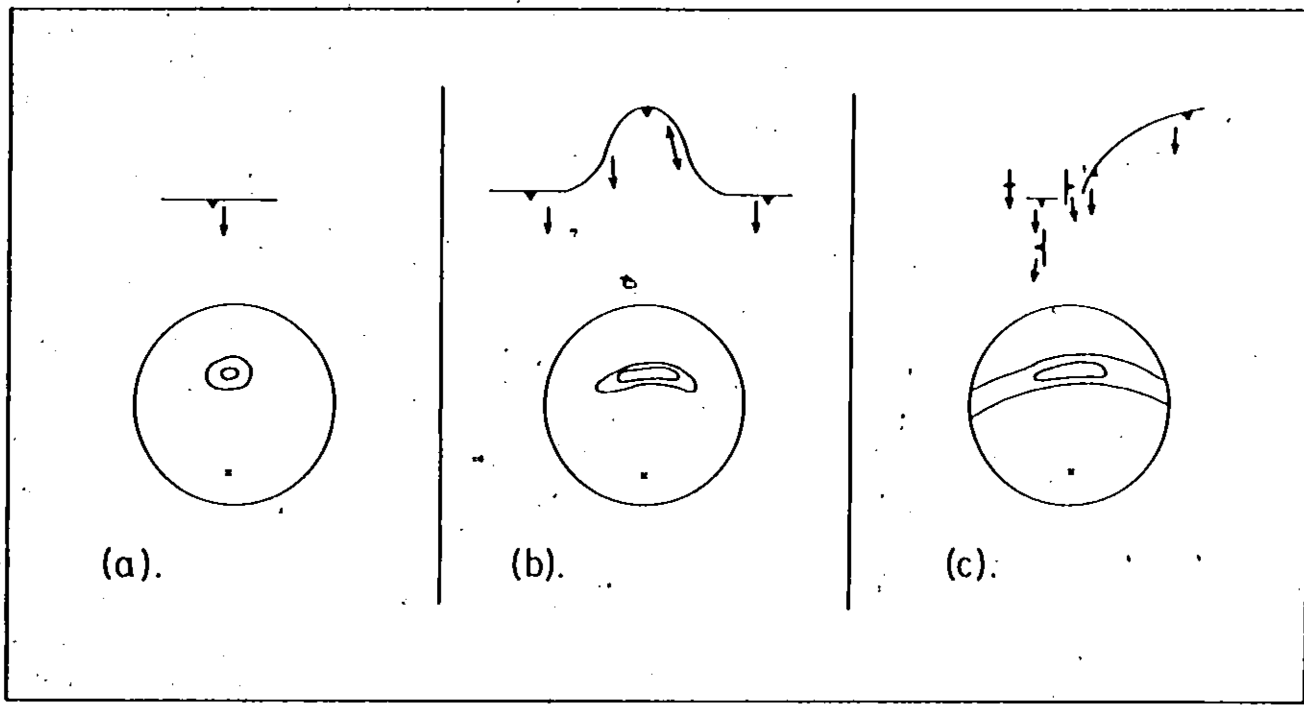

FIGURE
3.9
Macrofabrics of structural domains. Three main types of domains defined by poles to foliation and lineation(X). (a)homoclinal domain with down-dip lineation. (b)gentle large scale cylindrical folding, coaxial with the stretching lineation. This type is transitional to (c) which is formed by gentle large-scale cylindrical folding and well developed intermediate scale folding. The latter is responsible for the complete girdle of the low value contour. Fabrics comparable to (a) and (c) have been called by Lisle (1977) 'S' and 'L' macrofabrics.

maxima of poles to foliations may be modified by open upright large and intermediate folding which slightly disperse the distribution (Fig. 1.3, Domains 14-16 and Fig. 3.9). Transitional to a girdle is a partial girdle (Domains 18 and 22) usually formed by gentle large scale folds. Well defined girdles (Domains 2,7,9,17,21) are formed in Domains where intermediate scale and mesoscopic scale NW trending folds are important, in these Domains the dominant trend of the foliation is NW along the strike of the fold limbs.

Since cylindrical folding is present it is profitable to regard the Domains as macrofabrics, following Watterson (1968) and Lisle (1977). The configuration on the nets is thus referred to the type of bulk strain in the L/S fabric scheme. Point maxima will reflect ellipsoids with no contraction in Y, in the plane of flattening perpendicular to the maximum extension, indicating oblate to plane strain fabrics. Girdles will represent the range with contraction in this direction, indicating near plane-strain to prolate ellipsoids.

It is argued that the two types form a mosaic of plane strain and fairly prolate ellipsoids and that this pattern is essential to the interpretation of the map area as being formed in a tectonic regime of low angle transport. The plane strain macrofabrics may be interpreted to reflect the regional shearing strain whereas the prolate macrofabrics form from interference of regional and local (eg. pluton emplacement) strains.

3.3.2 The Burleigh Fold.

The Burleigh fold lies at the eastern margin of the Harvey Cardiff Arch some 15 km to the south of the main map area (Fig. 1.1). Regional mapping (Hewitt 1957b) leaves the exact nature of the fold uncertain, it is difficult to decide from the form lines whether it is a flattened tube or a Z-shaped fold. Its position on the flank of the arch and its intimate mixture with rocks of granitic and pegmatitic composition leave no doubt that is must have been effected structurally by the arch-forming event. Structural data from the northern nose (Fig. 3.10) show that it is unlikely that it was made by the arch-forming process.

The stereoplot of foliations reveals a cylindrical fold (Fig. 3.10) with an axis plunging 102/40 at right angles to the arch flank. The axial surface lies roughly parallel to the arch flank. It is thus a reclined isoclinal fold draped on the side of the arch. The form-surface of the fold is a compositional layering and a micaceous schistosity which lies in the axial-surface of minor folds. The latter transpose a layering, quartz-sillimanite veins and early granite leucosome. The major and minor fold axes are sub parallel (Fig. 3.10).

A second generation of granite and pegmatite forming bodies varying from half to one or two metres wide has a mode of occurrence which is controlled by the shape of the fold. In the nose of the fold granites commonly both cross-cut the foliation with dihedral angles of near 90° and

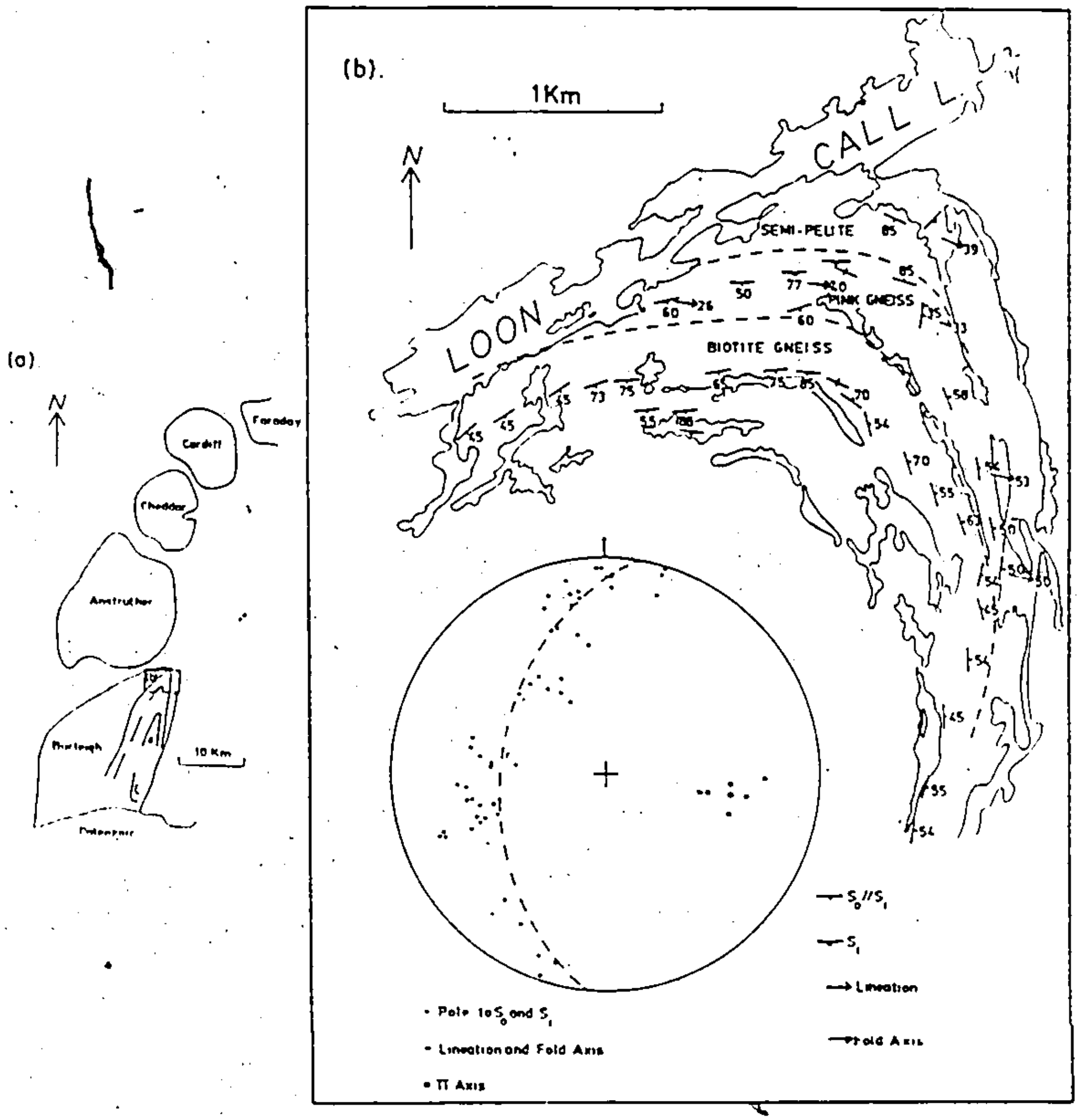

FIGURE
3.10

Burleigh fold. (a) shows form lines on map of Harvey-Cardiff Arch (from Hewitt 1957b) (b) geological map of fold nose.

are concordant. In the limbs cross-cutting relations are less common and the granitic bodies have a pinch and swell structure. Veins striking at high angles to the axial trace are only weakly folded and foliated. These observations are made in the most common plane of erosion, at a high angle to the lineation. On rare erosion surfaces in zone with the lineation the veins lie near parallel to the lineation (Plate 10), and thus form a "vein fabric".

It may be concluded that: (i) since it is difficult to conceive how such a large fold could be formed during arch uplift, that the formation of the fold predated the emplacement of the granitic material which accompanied the emplacement of the arch; (ii) that the arch was preceded by two deformations, that forming the fold and that forming the folded schistosity; and (iii) that the fold and the granites cutting it were deformed together during and possibly after the arch uprise to impose a linear ESE trending fabric.

It is reasonable that the large F_2 fold of Divi (1972), some 45 km along strike to the northeast (Fig. 1.1) which is similar in history, shape and size is of the same age. Both may represent a major folding event which predated the arch. The regional structural succession is compatible with those of other studies (e.g. Francouer 1975, Glamorgan and Monmouth Townships).

3.3.3 The Cheddar batholith and Its Envelope (Domains 1-7).

The outcrop pattern of each of the two granitoid masses of the Cheddar batholith, the Eels Lake granite in the south and the Cheddar granite to the north is elliptical (Axes 13 and 10 km) with the longer axis running northwest-southeast at an angle to the axis of the Harvey -Cardiff Arch, (Fig. 1.1, 1.3 and 3.11). The northerly Cheddar granite has a "D" shaped map pattern, the upright of the D running northeast perpendicular to the long axis of the complex. The Eels Lake granite is elliptical (axes 6 and 3 km), its long axis also trending northeast.

Monoclinic symmetry is displayed by the margins of the whole granitic complex which is also evident in the net projection of poles to foliations for the northern part of the Cheddar batholith (Domains 1,2,3). Fig. 3.12 shows a very broad girdle whose axis plunges moderately to the southeast roughly parallel to the trace of axis of symmetry of the outcrop pattern and the regional lineation.

In general foliations in the Cheddar pluton conform to the shape of the margin like layers of an onion, but there is little evidence for a complete dome form such as a central area of horizontal foliation. Smoothly curving form-lines may be readily constructed for the north, south and west segments but are abruptly terminated in the east (Domain 2) where foliations are variable in attitude, forming an LS macrofabric.

FIGURE
3.11

Lines which approximate the traces of planes of symmetry of the Cheddar Batholith and the Cardiff Complex (C-C' and B-B') are inclined at a high angle to the trend of the Harvey-Cardiff Arch (A-A') and near parallel to the trend of the regional lineation (heavy arrows).This is interpreted to indicate that the regional strain,as opposed to the local diapiric strain,has a dominant influence on the gross geometry of these bodies.(Foliation triple points TP). Form lines as in figure 1.3.

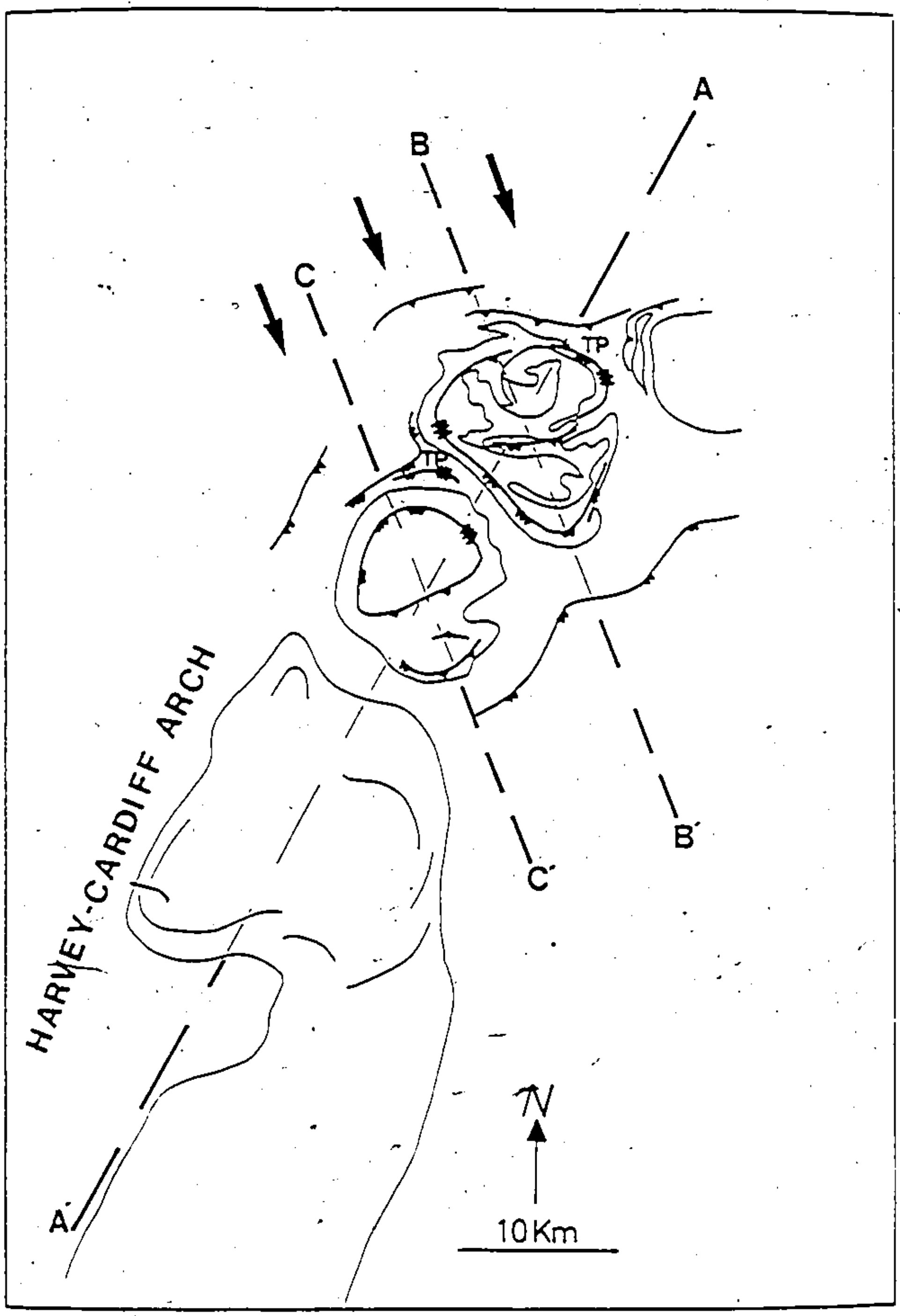
A
B
C
TP
TP
HARVEY-CARDIFF ARCH
B'
C'
A'
N
10 Km

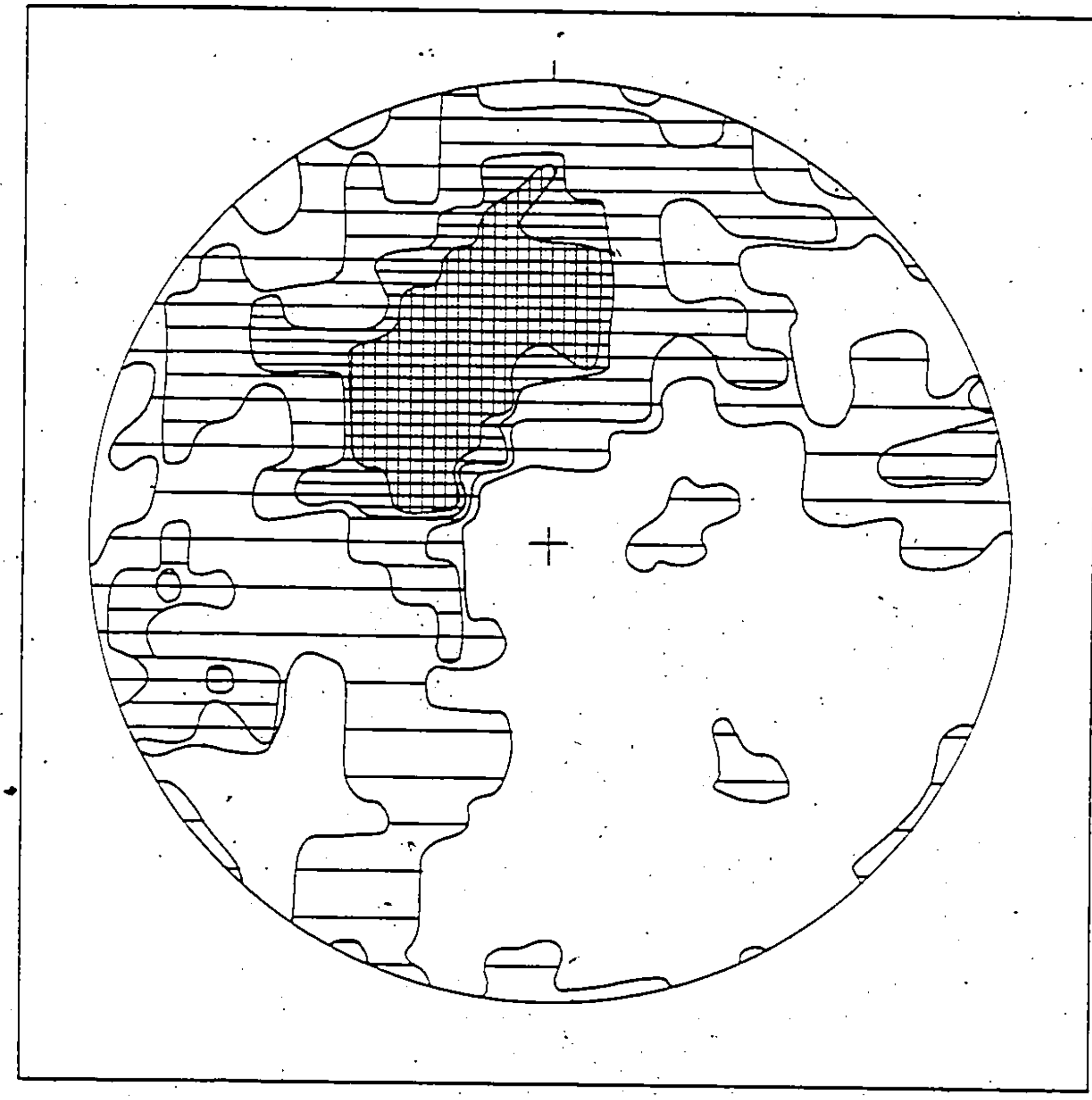

FIGURE 3.12 Synoptic diagram of poles to foliations of the Cheddar body (Domains 1,2,3). Contours at 0.4, 1.1, 2.1, 3.2%/1% area. N = 285.

Domain 1 forms the upright of the "D" shape which is a monocline dipping gently southeast (Fig. 1.2 and 1.3). It is composed of stratiform alaskitic sheets and less frequently hornblende-biotite gneisses. Although the alaskites lack shape fabrics some component of post-granite flattening across the foliation must be present since the foliation is cut at a low angle by pegmatites with augen textures and pinch and swell structures.

There are rare reclined folds with the same style, vergence (N) and axial trend as that in the Eels Lake Body (Domain 4) and the neighbouring projection of supracrustal rocks (Domain 6).

Domain 2 is composed of an estimated 60 percent granite and 40 percent supracrustal rocks occurring in a synclinorium (Fig. 1.2 and 1.3) which is characterized by the presence of abundant mesoscopic and intermediate scale folds plunging east to the southeast which is reflected in a girdle of poles to foliation with an east-southeast plunging axis (Fig. 1.3).

Minor asymmetric folds (Type (ii)) verge predominantly northwards with axial surfaces subparallel to the regional foliation maximum. These folds deform a schistosity axial planar to early isoclines where granite veins were produced before and during this folding.

Domain 3 consists of the north part of the Cheddar batholith granitic rocks to the north of a prominent northeast trending lineament and those in a strip to the

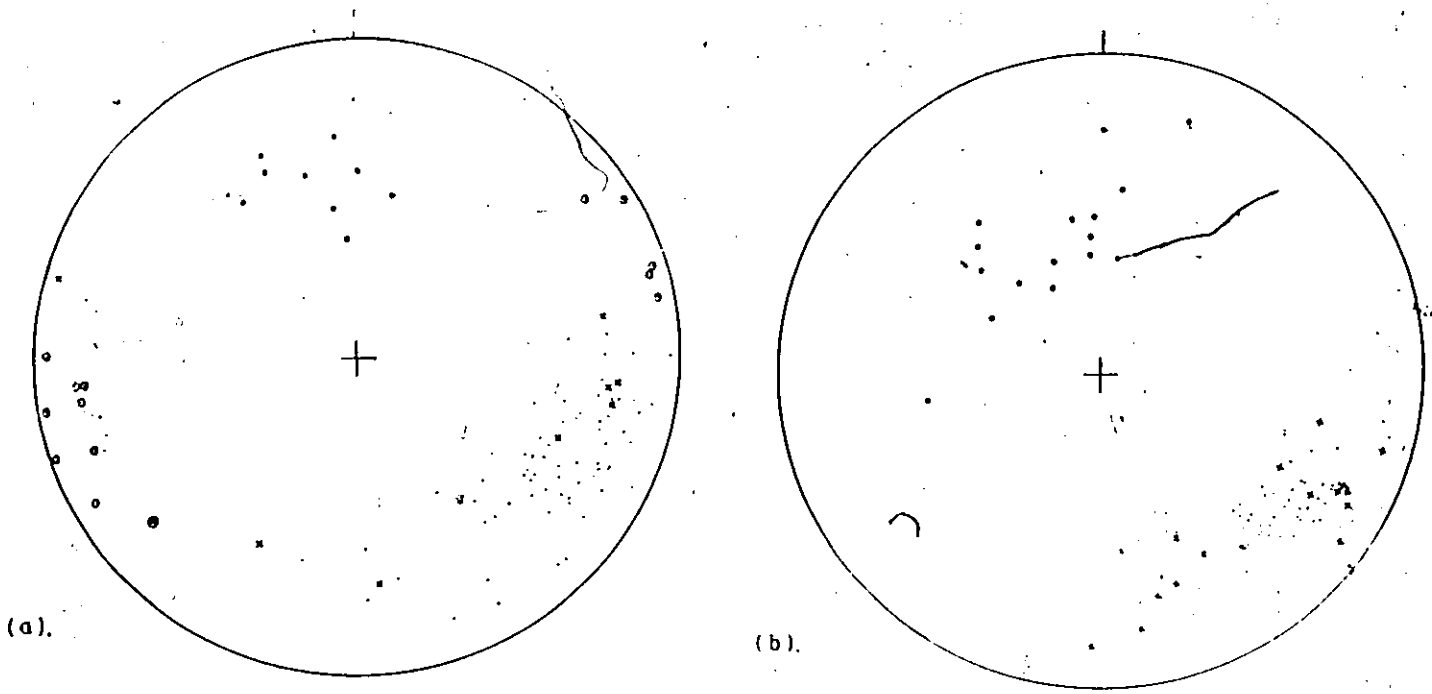

FIGURE 3.13 Attitude of fold axial surfaces (circles), fold axes (crosses) and lineations (dots) in (a) Cheddar batholith (symbols for Eels Lake granite are circled) (b) Cardiff complex (domains 8,10,11,12).

west of Domain 1 running parallel the western margin.

The net projection (Fig. 1.3) shows a dispersed pattern. As in Domain 1 this northern segment of Domain 3 contains little evidence for a dome form. Occasional steep dips in areas of moderate dips, as on the north shore of Hook Lake, or shallow dips in areas of steep, as near the northern margin, are suggestive of folding.

On the net projection for the Eels Lake granite (Domain 4, Fig. 1.3) poles to gently dipping foliations form a partial great-circle girdle the axis of which coincides exactly with the northeast trending long axis of the elliptical outcrop. Lineations also coincide with this axis (Fig. 1.3), as does the axis of the single northwesterly verging minor fold. The attitude of the margins and the shallow inclinations in parts of the interior are compatible with an elongate dome form.

Lineations from the entire batholith have either the same trend and plunge as minor fold axes and the girdle axis or lie dispersed within a plane lying parallel to the axial planes of the minor folds (Fig. 3.13), they do not necessarily coincide with the plunge of the body.

For the most part supracrustal rocks lying south of the Cheddar batholith (Domain 5) form a moderately southeast dipping monocline curving with the margin of the Eels Lake body. As this margin curves to the northwest, the dips steepen. On the net projection (Fig. 1.3) this curving and steepening has a cyclindrical geometry with a southeast plunging axis, comparable to other inter-pluton belts (e.g. Domains 7 and 9). Lineations generally lie within a southeast dipping plane at high angle to those in the crest of the Eels Lake body.

Domain 6 consists of a synform which separates the eastern extremities of the Eels Lake and Cheddar granites. Layering and foliation poles lie on a well defined great circle (Fig. 1.3) indicating it has a cylindrical macrofabric comparable to other interplutonic structures (e.g. Domains 5,7,9). The axis of the girdle plunges gently east parallel to the lineations. A down-plunge view of the marble band in this Domain reveals a somewhat reclined northerly vergence comparable to the minor folds present in the batholith. Minor NW verging asymmetric folds (Type (ii)) are comparable to that in the Eels Lake body and those in Domains 1 and 2 of the Cheddar Body. Quartz shape fabrics in folded granitic veins indicate extension parallel to the fold axes in a direction comparable to that of shape fabrics within the Eels Lake body.

Rocks in Domain 7 on the westerly side of the Cheddar batholith are generally conformable with a wide belt of southeast dipping rocks which strike parallel to the western flank of the Harvey-Cardiff Arch. As the envelope rocks swing round the northern flank of the Cheddar pluton and the western flank of the Cardiff complex they become steeply dipping and change to a NW-SE strike quite abruptly (Fig.

1.2) forming a foliation triple-point (Hanmer and Vigneresse 1980). The net projection of foliations for Domain 7 (Fig. 1.3) has a well formed girdle consistent with isoclinal folding of the northeast trending rocks about an axis plunging southeast, coincident with the lineations and fold axes in the Domain. Shallow foliations striking north-northeast related to larger than outcrop scale folds are locally preserved within the steep belt where they are severely crenulated. It is in the crest of these folds that the coaxial refolding of isoclines and development of axially symmetric mica-edge lineation previously referred to is found, demonstrating that the mica fabrics represent additions of regional and local strain (emplacement related).

3.3.4. The Cardiff complex and Faraday granite (Domains 8-12).

The Cardiff complex is a set of structures which like the Cheddar complex is folded about moderately south to southeastward plunging axes (Fig. 1.3, Domains 8,9,10,11, 12). Dips along the northwestern margin are generally shallow compared to those at comparable locations in the Cheddar batholith. In both cases southeast striking foliations are steep. Like the Cheddar batholith, the complex can be regarded as a planar-linear macrofabric plunging moderately southeast.

The complex differs from the Cheddar batholith in being formed half of syenite and supracrustal rocks besides granite. The presence throughout much of the complex of a lithological layering is a major contrast with the Cheddar complex where a gneissic shape fabric (LS1) is much more common. The layering makes possible the recognition of a deformed crestal region.

The Cardiff complex has an outcrop pattern like a rounded triangle with 10 km sides, its axis of symmetry is at an angle to the of the Harvey-Cardiff Arch (Fig. 1.1 and 3.11). The component granite, syenite and supracrustal gneisses are interlayered on a large scale. The outermost layer, the semi-continuous Monck Lake and Centre Lake granites, envelopes the complex defining the shape of its margin (Fig. 1.3). From the northern side, striking northeast to east-west and dipping gently southeast, the layer curves southward to where it strikes NW-SE parallel to the steep zone of envelope rocks lying between the complex and the Cheddar batholith. On this side the foliation dips steeply outward (SW). From the southeast end of this steep-zone the layer curves to the northeast forming a broad antiform plunging south-southeast. The folded nature of the southeastern portion contrasts with the gently curving nature of its northern flank. Dips are somewhat steeper in the southeast than in the northwest. The outer layer of granite thus defines a triangular tube-like body plunging and steepening to the southeast. Internal foliations and lithological boundaries are generally conformable with the shape in an onion layer fashion.

The antiform forming the southern part of the complex (Domain 8) dies out northwestward along its axial trace where it is replaced by foliations dipping more uniformly southeast. This change marks the edge of an oval structure, centred on Deer Lake, which comprises Domains 10 and 11 and parts of 9 and 12.

The eastern half of this structure (Domain 10 and west part of Domain 9) is a reclined fold (Fleuty 1964) with a moderately inclined SE dipping axial surface and a southeast plunging axis. Within the layered paragneisses of the core area, northeast of Deer Lake, the pattern of asymmetry of minor folds is consistent with the antiformal nature of this part of the structure (Fig. 1.2). A broad zone of S folds is succeeded by narrow zones of M's and Z's close to the northern steep limb of the structure. The axial surfaces of these folds dip moderately southeast (Fig. 3.13b). In the area around and including the east end of Deer Lake foliations have very variable attitudes reflected in the two prominent maxima on the net projection (Domain 10), and interpreted as resulting from folding on the intermediate scale, of the same age as the mesoscopic folds, of a rather flat crestal region. The heterogeneous deformation of the layered core contrasts with the homogeneous deformation of the large mass of syenite overlying it to the east, which is uniformly lineated.

Domain 11 comprises the western half of the central oval structure. As shown from the foliation poles (Fig. 1.3) This part is roughly cylindrically folded on a moderately plunging southwesterly axis. There is a small area where stretching lineations have a similar plunge.

Across strike in a northerly direction in Domains 10 and 11 dips change from shallow to steep and back to shallow. To the west the dips change from westerly to easterly across a synformal structure which dies out rapidly to the north and south. The Deer Lake syenite is uniformly lineated in both these areas.

Lineations and fold axes from Domains 10 and 11 lie approximately within a plane that corresponds to the average axial surface of the mesoscopic folds (Fig. 3.13b). Lineation and fold axes are parallel but diverge somewhat from those in the rest of the body. The foliation which is deformed in this structure has an extended history since the asymmetric folds at the northern margin of the core zone in Domain 10 deform a boudinaged migmatitic layering (Plate 11b). The micaceous foliation lying in this layering is already isoclinally folded.

Domain 12 includes the northwestern and southwestern sides of the curved Monck Lake granite sheet, and extends southeastward to join Domain 8. At the northwest side of the complex foliation dips moderately southeast beneath the central oval core. At the western shoulder of the complex the foliation quickly changes attitude to very steep, striking southeasterly parallel to the trends in Domain 7. Again this reflects a cylindrically folded form, about a moderately southeast plunging axis which is parallel to the stretching lineations. The granite is uniformly lineated throughout, the strength of the fabric decreasing from northwest to southeast.

The eastern side of the Deer Lake syenite, the west end of the Faraday granite and the enveloping rocks in between are included in Domain 9. A narrow well defined girdle of foliation poles (Fig. 1.3) reflects the geometry of all scales of structures. The main feature is a disharmonic synform between the two plutonic complexes in which shallow southeast dipping rocks curve around the flanks of the complexes and appear to converge, steepen and strike northwest forming a foliation triple-point. This again is a cylindrical structure with the lineation and the girdle-axis parallel. The attitude of the girdle-axis is very close to that of Domain 12 on the other side of the complex (Fig. 1.3), demonstrating that the northeastern and the southwestern sides have very similar geometry.

In Domain 9 folding on the mesoscopic and intermediate scales is concentrated in a zone between the southeast dipping rocks and an area located where the two plutonic complexes are closest together and the foliations are uniformly steep and striking northwest. The folds are polyclinal, the poles to their axial surfaces fall in a poorly defined girdle (Fig. 3.4), the π-axis of which lies parallel to the fold axes and lineation. As in the centre of the Deer Lake structure and Domain 7 the layering which is folded contains a micaceous layering, occasional boudinage structures and isoclinal intrafolial folds. Within the southeast dipping foliations the presence of open folding with axes at a high angle to the regional lineation is betrayed by occasional reversals of dip in which the lineation plunge is reversed.

The western end of the Faraday granite is composed of an upper and a lower plutonic unit. For most of their outcrop length the units have shallow dipping margins and are separated from each other by a supracrustal layer composed dominantly of marble. Strain within the two granites, is much greater in the lower unit; although fabric trends are in both bodies similar.

The easternmost tip of the northern lobe of granite gneiss of the Monck Lake granite outcrops in the northwest corner of Domain 9 on the shores on Jordan Lake. This granite is of similar highly deformed aspect as the lower Faraday granite. This fine grained highly tectonised body contains several layers of tectonic schist containing rotated feldspathic augen. The two highly deformed granites on both sides of Domain 9 occupy similar structural levels and may be interpreted as having a history of being over-ridden from the southeast by large masses of plutonic gneiss.

3.3.5 Heterogeneous Deformation and Sense of Shear in Gabbro.

At the southern tip of Farquhar Lake two lenses of heterogeneously deformed metagrabbo lie en échelon (Fig. 3.14). The two bodies are separated by a narrow belt of homogeneously foliated metagabbroic gneiss which strikes north-northeast. The northern lens and its southeastern foliated carapace are continuous with the long sheet of gabbroic gneiss which strikes northeast for several kilometres beyond the south shore of Farquhar Lake (Fig. 1.2). Country rock, calcareous, tonalitic and syenitic gneisses dip moderately toward the southeast. Lineation in all rocks plunges to the southeast except for local reversals in the underlying tonalitic gneisses (Unit 3A). To the south a large S-shaped curve in the country rock foliation marks a divergence in the northeast striking attitudes. The curve follows the outline of the metagabbro (Fig. 3.14). It is present up to two and a half kilometres south of the body.

On the northern side of the foliated belt there is a rapid transition into unfoliated gabbro which is relatively poorly amphibolized with a wide-spread preservation of subophitic textures and coronas. A single shear zone observed within the generally unfoliated gabbro is narrow (> 50 cm) and dips moderately to the southeast, with a southeasterly lineation. Asymmetry of foliation curving into the shear zone indicates shear of upper layers to the northwest which is in accord with LS1 fabrics discussed later. The southern lense is more thoroughly amphibolized, there is little relict clinopyroxene and no coronas are present. Subophitic textures are recognizable although plagioclase is partly recrystallised. In this lense there are several narrow (5-30 cm) and steep southeast striking shear zones (Fig. 3.14). These zones have a gently south-east plunging lineation and a sinistral shear-sense. The details of fabric development is described in Section 4.4.

The gabbro forms steep-sided knolls which allow some of the features of the three dimensional geometry of the foliated zone to be observed. The main features of this geometry are that foliation curves from moderately steep at the highest structural levels to shallow and flat at the lowest levels. This transition can be seen in the steep western side of the southern lense.

The steeper foliations on the western side of the southern lense are cut by several narrow shear zones which dip gently southeast. These shear zones have a southeast plunging lineation and a fabric asymmetry which indicates a northwesterly transport of upper layers.

The main features to be explained are the en echelon arrangment of the two lenses, the evidence that they are physically continuous, the lineation which transects their trend, the shear directions of the small scale shear zones (northwest for the thrust faults and left lateral for the strike-slip faults) and the curving nature of the foliated

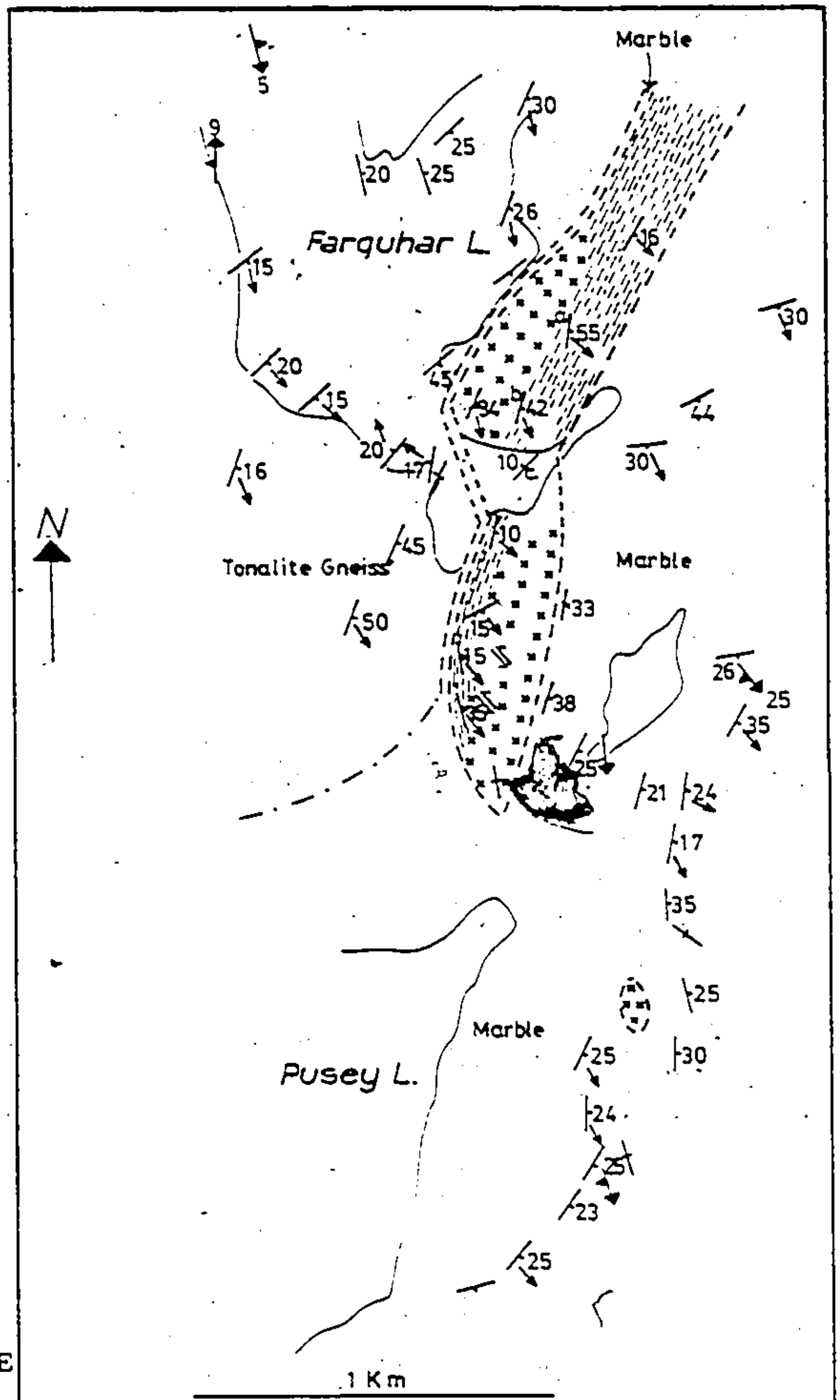

FIGURE 3.14 Structural setting of gabbros at south end of Farquhar Lake. Symbols: solid arrow, fold axis with vergence; crosses, unfoliated gabbro; lines, foliated gabbro; subvertical shear zone; shear zone with upper layers moved NW with minimum dip. Foliations at a and b are topographically 30 m higher than c.

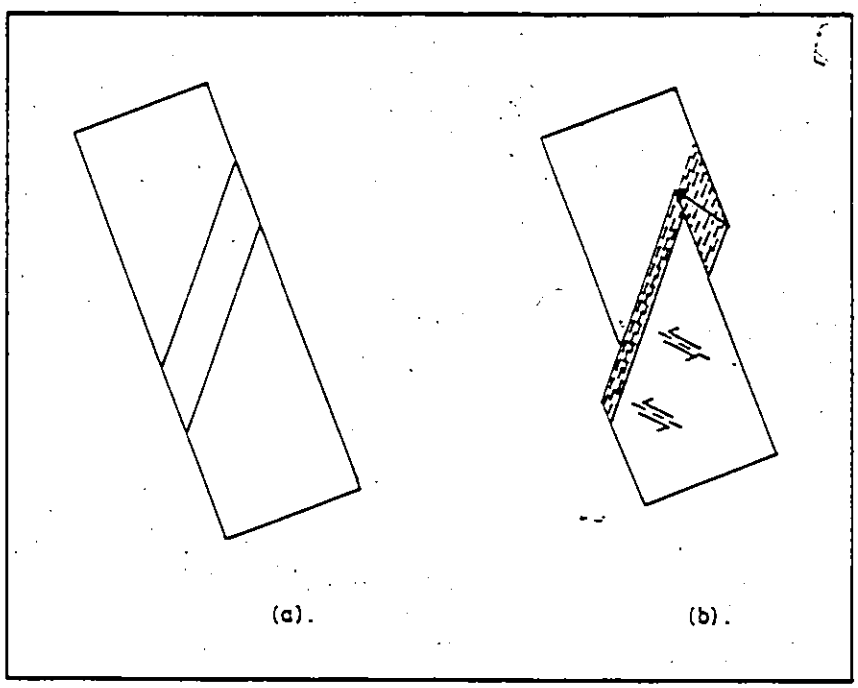

FIGURE 3.15 Model for deformation at metagabbro body at the south of Farquhar Lake. (a) undeformed shape. (b) ductile thrusting directed to the northwest, oblique to the length of the body along a thickening shear zone (dash ornament), produces an en echelon array of undeformed rocks. Steep sinistral minor shear zones have same shear direction as flat-lying main zone.

zone. The shape of the foliated belt is interpreted as a curving shear zone or as the curving foliation in the leading edge of a propagating shear zone (see Ramsay 1980, Fig. 17). A model compatible with both of these interpretations is shown in Fig. 3.15 in which a body elongate north-northwest parallel to the trend of the undeformed pyroxenite body which lies in a syncline to the north (Fig. 1.2a), is cut by a shear-zone with a NW transport direction somewhat oblique to the length of the body. Northwest directed thrusting on this zone would account for the en echelon arrangement of the blocks.

3.3.6 Large Scale Structures in the Northern Domains (13-22)

The largest scale structure in the northern Domains is a gentle synform cored by pyroxenite separating the Drag Lake and Straggle Lake complexes of grey gneiss (Fig. 1.2 and 1.3). This major structure is bounded on the west side by two zones (Domains 17 and 21) of northwest trending foliations in which folding is coaxial with the southeast plunging regional lineation. All these structures are disharmonic to under and/or overlying structures. To east and west of this major structure the foliation dips to the southeast. Several plunge reversals of the southeast trending lineation are present. A comparison of equal area nets (Fig. 1.3) shows that the structures may be derived by folding of a gently southeast dipping homocline about axes lying within this plane. Deformation is concentrated in supracrustal rocks and granitoid gneisses of this folded homocline, forming a belt of high strain which traverses the area (Section 3.2.5).

There are several important structural relations between the major lithostratigraphic units. The grey tonalitic gneiss (Unit 3A) centred on Drag Lake (Domains 16-19) dips under supracrustal rocks (Units 1 and 2) to the south but overlies similar rocks to the north. Similar tonalite gneiss unit outcropping around Farquhar, Allen and Yankton Lakes (Domains 14 and 15) appears to lie within supracrustal rocks at a higher structural level than the Drag Lake and Straggle Lake complexes (Fig.1.2). Likewise in the southwest corner of the map area, supracrustal rocks and syenitic gneisses dip gently south beneath the Glamorgan Gneiss complex, which has a large component of the grey tonalitic gneiss. The relations of the grey tonalitic gneiss units with the supracrustal rocks along their northern edges is comparable to that of the Cheddar and Cardiff bodies which also lean towards the northwest. These relations may indicate that the grey gneiss has been thrust over and into the supracrustal rocks.

The area in the east bounded by Baptiste, Farquhar and Fishtail Lakes and includes structural Domain 13 is largely homoclinal (Fig. 1.3). The eastern side of this area, in particular the boundary of the grey gneiss with supracrustal rocks is only known from reconnaissance mapping. It is continuous with the homocline of LS tectonite gneisses which is along the northern edge of the Cardiff complex and is dominated by the highly deformed heterogeneous gneisses described in Sections 3.2.5. The rocks are perfectly homoclinal except in a zone to the west of Elephant Lake in the environs of the grey gneiss contact where intermediate scale folds are present. This folding causes wide swings of strike between neighbouring outcrops but dips remain low. In the neighbourhood of these folds there are also, in the supracrustal rocks and the grey gneiss, mesoscopic folds with east-west to northeast - southwest trending axes. These folds are asymmetric reclined to recumbent, with a rounded profile, and are less than two metres wide. They are most common in the grey tonalitic gneiss where their long limbs are sometimes very strongly deformed, locally grading into tectonic schist.

The boundary of the grey tonalitic gneiss cuts obliquely across the regional trend forming the eastern limb of a regional synform. At its northern end, southeast of Fishtail Lake, it is irregular.

A system of upright disharmonic folds centred on a synform containing the Allen Lake Pyroxenite lies in the centre of the regional synform. These upright folds are large scale features which have limited expression on the intermediate and mesoscopic scale when compared to the zones of northwest trending foliation (e.g. Domains 17 and 21).

Zones of intermediate scale folding indicated by large attitude changes between outcrops do occur in places on the east and west sides of the upright structures (east Domain 14 and Domain 16). The axes for these upright structures and the zone of intermediate scale folding (Domains 14 and 16) all have very shallow plunges suggesting upright folding of a previously shallowly inclined plane (Fig. 3.8).

To the north of the fold system the east side of the main synform is well defined. The boundary of the grey tonalitic gneiss sweeps round forming an antiformal promontory south of Fishtail Lake. The west side has a comparable, but, in detail, more complex geometry (Figs. 1.2 and 1.3).

The central synform of the fold system (Domain 14) joins eastward with the homoclinal rocks of Domain 13 in a zone of intermediate scale folds. The strike swings from northeast to north-northwest between outcrops. Mesoscopic folds of this generation have not been identified. The surface folded is the composite layering and gneissosity which is the product of extreme deformation, lineations have low plunge and low rake on the southwest dipping foliations, plunging predominantly to the northwest.

The limbs of the central synform are both moderately dipping, indicating a nearly upright symmetrical structure. However, the axial trace in the foliation of the pyroxenite is displaced towards the east limb. The synform is boat-shaped with a blunt stern at the northern end and a sharp bow at the south. The axis is very gently doubly plunging, which is reflected in the plunge reversal of the lineations. South of the 'bow' a very gentle antiform, with an axial trace at a high angle to the synform axial trace, warps the structure, exposing the migmatitic gneisses which underlie the grey tonalite gneiss along the isthmus which separates Grace Lake from Farquhar Lake. South of this culmination the grey tonalitic gneiss, which is overlain by metagabbro, dips southeast. An S-shaped trace of foliations curves around the gabbro at the south end of Farquhar Lake over a width of several kilometres (Fig. 3.14). In some respects this structure is analagous to that on the east side of Domain 9 in the Lower Faraday granite and its enveloping gneisses. The similarities are: the curving shape which is essentially a refolding that is coaxial with the lineation; the constituent rocks show signs of great deformation, for example graphite bearing mylonitic marbles, coarse marble tectonic breccias, concordant augen pegmatites, quartzites and a very planar syenitic migmatite gneiss; mesoscopic folds have moderately inclined axial surfaces and are coaxial with the lineation; rare intermediate scale folding forms local steep zones of northwest striking foliation (Fig. 3.14).

To the north of the main synform data is scarce. Foliations with moderate southwest dips are present. The main synform is separated from the next synform to the west by a very narrow antiform. This structure is asymmetric, being somewhat steeper on its eastern flank. The scant data suggest two domal culminations. In the northerly one supracrustal rocks are exposed (Unit 1b), while in the southern one gabbroic gneiss (Unit 4B), apparently the lowest level of the mafic complex, is exposed.

To the west of this narrow antiform is a much broader synform in grey tonalitic gneiss around Yankton Lake. This is a broad structure with shallowly dipping limbs, much gentler than the folds to the east. It too is disharmonic, since the folded grey gneiss merges southward along the synformal axis with southeast dipping grey gneiss. This is possibly in part due to the same open upright folding with approximately east-west axes which is postulated at the southern end of the central synform.

The central system of large-scale folds is separated from structures in Domain 16 to the west by a southeast dipping homoclinal swath which extends west to the south shore of Drag Lake and contains a large sheet of syenite. Domain 16 comprises the eastern extremity of the mass of grey tonalitic gneiss centred on Drag Lake and its enveloping supracrustal rocks. Open, upright, intermediate scale folds affect all rocks in the Domain. The net of poles to foliations (Fig. 1.3) shows that the folds have axes which plunge very gently eastward. These folds cause some plunge reversal of the lineation.

The central system of open folds is bounded on the west and southwest sides by northwesterly trending structures which are formed by folds which are coaxial with the southeast plunging lineation (Domains 17 and 21). These structures are disharmonic with respect to each other and with respect to the system of open folds. The NW trending structures run from north of Drag Lake southeast to Esson Lake where they terminate in a NE trending belt of syenitic gneisses dipping SE under the Cardiff and Cheddar Complexes. The zone of northwesterly structures is continuous with the T-shaped eastern termination of the Eagles Lake marble belt which lies to the north of Drag Lake (Hewitt 1957b). This termination continues northwest for some six kilometres north of the map area.

In the grey tonalitic gneiss of Domain 16 which is affected by northeast trending folds, foliations on the western side pass into the zone of northwest trends with a gentle swing to the southwest. In the boundary between the grey gneiss and the overlying supracrustal rocks this swing is marked by an abrupt step showing an apparent sinistral displacement in the plane of the map. There is no other evidence of interference between the northwest and northeast trending structures.

This belt is disharmonic, since down plunge, to the southeast it is truncated by the boundary of the grey gneiss and by the large southeast dipping sheet of syenite and northwestward it makes a wishbone pattern around the salient of marble and garnet gneiss. Westward the belt of northwest striking foliation merges across a narrow strip of intermediate scale folding with the western area of southeast dips. The net for Domain 17 shows that the southeast lineation is the axis of all the folds (Fig. 1.3).

A zone of northwest structures comprises Domain 21 and forms a belt which is relatively wide compared to its length parallel to the lineation trace (Fig. 1.3). It is composed fundamentally of an antiformal and a synformal structure. The former is a simple structure defined by a thick quartzite (See Fig. 1.2), the latter is more complicated. It has an irregular western boundary composed of several different rock types. In its core intermediate scale and mesoscopic folding is important. To the east of the antiform there is more intermediate scale folding about similar axes. The entire zone is disharmonic with respect to structures above and below. The net shows the dominance of folding coaxial with the regional southeast plunging lineation (Fig. 1.3).

In the synformal area and in the irregular protuberance of south dipping amphibolite which forms a southwestern boundary, reclined to recumbent mesoscopic folds are important (see Fig. 1.2). They are less frequently developed near the western boundary of the amphibolite. In steeply dipping quartzites a second foliation of mineral inclusions lies near parallel to the axial surfaces of these folds and the regional SE dipping foliation (Fig. 1.2). In the amphibolite the shape fabric varies from blade-like to prolate as its eastern margin is approached, matching the prolate mica fabric common in the steeply dipping rocks of the synform.

The area comprised of Domains 18-20 is a southeast dipping homocline with a southeast plunging lineation. There are narrow belts of northwest trending foliations which are reflected in weak girdles in the nets of Domains 18 and 20 (Fig. 1.3).

3.3.7. Summary

The fundamental feature of the area is the development throughout of the southeast trending lineation. The area is part of a larger region with this lineation, which itself is one of several similar zones in the western Grenville province (Lumbers 1975, Davidson et. al. 1982).

The lineation and all structures are imposed upon a northeasterly striking homocline. Foliation in this homocline gradually steepens in a southeasterly direction. Northwest leaning granitic and plutonic bodies plunge southeastward parallel to the lineation. Zones of northwest trending foliations are zones of folding coaxial with the stretching lineation and may be considered as linear macrofabrics (Watterson 1968, Lisle 1977).

The lineation postdates large folds of kilometric proportions which fold a micaceous foliation. For example, south of the map area near Apsley (Fig. 1.2), granites and pegmatites related to the formation of the Cardiff Harvey arch postdate the large Burleigh Fold and are deformed together with it to form the lineation during or after arch emplacement. To the northeast (south of Bancroft) minor folds of the same age as large F2 folds have their axes swung into a southeast direction during the lineation forming event (Divi and Fyson 1973).

3.4. Origin of Structures

3.4.1 Comparison with Regimes of Low Angle Ductile Tectonic Transport

Many features of the area are comparable with examples of low-angle tectonic transport. Such regimes include nappes, thrusts and ductile shear zones, all of which have structural features in common. All these systems involve large scale translation along a low-angle transport direction in which all or part of the material being moved is plastically deformed. The occurrence together of many of these features is advanced as circumstantial evidence for such tectonics, in the absence of stratigraphic proof of translation.

There are many examples of stretching lineations in such systems. In the study area the shape fabrics forming the stretching lineation are present where the foliations are northeast striking and have an estimated, and locally measured, plane-strain morphology. This strain type is comparable to those in shear zones in gneissic terrains (Escher and Watterson 1974, Watterson 1968, Bak et.al. 1975) where it is considered to be a necessary feature and to strain in conglomerates in nappes (Hossack 1968, Chapman et.al. 1979). In the sheared gneissic terrains, as in the study area, vein fabrics expressing large homogenous bulk strains are common.

The characteristic feature of the structural Domain map (Fig. 1.3) is that it is a mosaic of Domains in which poles to S-surfaces either form a single maximum, which reflects a moderately southeast dipping foliation, or form a girdle normal to the stretching lineation and which contain the same maxima. This pattern is found in many tectonic systems with low plunging transport directions. For example, in the thrust terrain which includes the Moine thrust, several Domains close to the trace of the main thrust plane show this variation of geometry (Christie 1963) in which the maxima of poles to foliations is subparallel to the pole to the thrust plane. A similar arrangement of girdles of poles to foliations and stretching lineation is found in the Bergell granite and its envelope, part of an alpine nappe structure (Wenk 1973) and in an alpine peridotite at Lanzo (Nicolas and Boudier 1975). The effect is equally common in large-scale transcurrent shear zones (Nicolas et.al. 1977, Bak et.al. 1975) and in regions of gneissic rocks whose structural pattern has not been related to any one of these specific situations (Watterson 1968, White 1966).

Asymmetric minor folds from outside of the belts of northwest striking foliation have a common axial surface and axes which lie spread out in this gently southeast dipping surface. This "average" axial surface lies close to the maximum found in the pole figures of foliations of most structural Domains. The stretching lineation has a near constant rake in this surface. Examples of this arrangement are well documented in low angle thrust environments (Bryant and Reed 1969, Christie 1963, Johnson 1957). This is usually explained by assuming that rocks near a thrust plane undergo simple shear with the shear direction lying near parallel to the stretching lineation. Folds formed with axes at a high angle to the shear direction will have the axes progressively rotated within the axial surface towards the stretching lineation (Flinn 1962, 1965, Sanderson 1973, Williams 1978, Escher and Watterson 1974). It has been pointed out (Ghosh et.al. 1979) that folds which have been so rotated will appear more flattened than those formed with their axes initially parallel to the stretching lineation.

Quartz C-axis microfabrics from LS1 and LS2 tectonites show girdles which are perpendicular to the stretching lineation (see Section 4). There are numerous examples of this basic geometry from regions of low-angle tectonics. For example, it is present in mylonitized quartzites from the Moine thrust (Johnson 1957, Christie 1963). It is common in quartzites from nappe complexes, eg. in quartzite from the envelope of the Bergell granite (Wenk 1973), in quartz pebbles from a Caledonide nappe (Strand 1945) and Lister (1974) mentions several from Australian nappe and thrust complexes and it is reported from transcurrent shear zones (Bouchez 1977).

3.4.2 Structures Indicating a Component of Simple Shear.

All of the above features found in the study area are compatible with some form of tectonic system with a low plunging transport direction. There are additional structures which are compatible with a state of simple shear on various scales. The most obvious is the shallowing in a northwesterly direction of the regional homocline. Related to this is the northwest lean of the tonalitic and especially the granitic bodies. Passing from the Cheddar northward to the Cardiff complexes there could be an increase in shear-strain marked by flattening in dip of the northern margins of the complexes and a syntectonic refinement of grain-size.

Other indications of simple shear are the structures in the heterogeneously deformed metagabbro south of Farquhar Lake in which large and small scale structures indicate northwest directed ductile thrusting while steep northwest striking shear-zones have a sinistral sense. Structural lithological types such as the tectonic schists found sporadically in the syenites and grey tonalite gneiss and the marble tectonic breccias also probably record components of simple shear. In some cases there is direct proof of this, as for instance in the LS2 tectonic schist within the grey gneiss (Unit 3A) from south of Farquhar Lake or rotated silicate inclusions with sigmoidal tails in marble tectonic breccia (Plate 1b). It has been argued that the transecting quartz and biotite fabrics from the Upper Faraday granite record simple shear (Fig. 3.3).

3.4.2 Gravity and Shear Tectonics.

Structures such as the Cheddar batholith, which are quasi-circular granitoid plutons, surrounded by marbles which are more dense suggest diapirism. Likewise the occurrence of extremely dense pyroxenite sitting inside a synform strongly suggests gravitational sinking.

There are two indications that vertical movement due to contrasts in density could have happened during the main thermal-structural event. Firstly, it is clear that the ductility contrast between most rock types was low. This is shown by the occurrence in all rock types including parts of the gabbroic rim of the pyroxenite of strong tectonite fabrics. Secondly, density contrasts between candidate diapirs or anti-diapirs and their envelopes is of the right magnitude when they are compared with those of model and natural diapirs (Table 22, Appendix I). Note that the densities which have been measured and estimated are those which the rocks have now and not necessarily those which they had during metamorphism. It is evident that diapirism would be possible for the Cheddar Cardiff complexes. For the Allen Lake pyroxenite part of the Farquhar Lake complex the density contrast with the heaviest possible envelope rock is very high (Table 22, Appendix I) much higher than that estimated for any other lithological pair. In contrast, the grey tonalite gneiss of Drag Lake requires a cover of supracrustal rocks devoid of granite and syenite in order for a density contrast comparable to natural diapirs to be generated.

One of the most often cited criteria for the occurrence of diapirism (or its converse) is that less dense material fills the interior of circular or oval complexes, or vice-versa for anti-diapirs (Coward 1981, Pitcher 1979, Stephansson and Johnson 1976). This is met by the Cheddar and Cardiff structures. A second criterion cited by the same authors is that structures such as lineations and foliations inside and outside of the proposed diapir should be concordant. This is certainly true for the Cardiff complex structure. It is also true of the marginal foliations in the Cheddar and Eels Lake bodies, although crestal lineations in the latter are discordant to the regional trend. However it must be emphasized that this regional lineation is not restricted to pluton margins. It is present over a very wide area in all rock types, has a constant attitude and cannot be regarded as simply an effect of diapirism.

Stephansson and Johnson (1976) state that the proposed diapir should show evidence for solid state flow, a condition fulfilled by the granitoids. Circular structures could also be formed by cross-folding. Proposed diapirs should show no evidence for this such as occurring in regular arrays or having pairs of axes of axial surfaces at a high angle to one another (Stephansson and Johnson 1976, Coward 1981). The complexes certainly do not show such features.

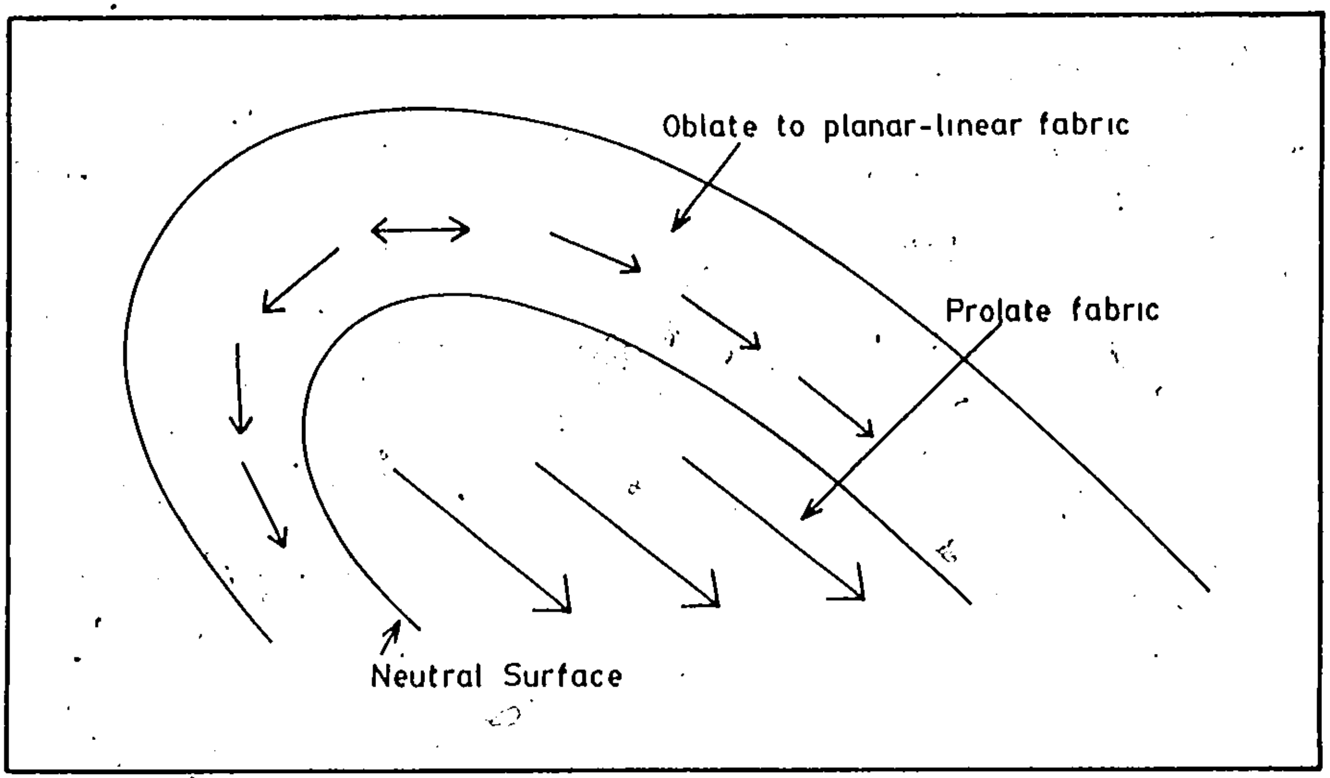

FIGURE 3.16 Distribution of fabric in an immature inclined diapir.

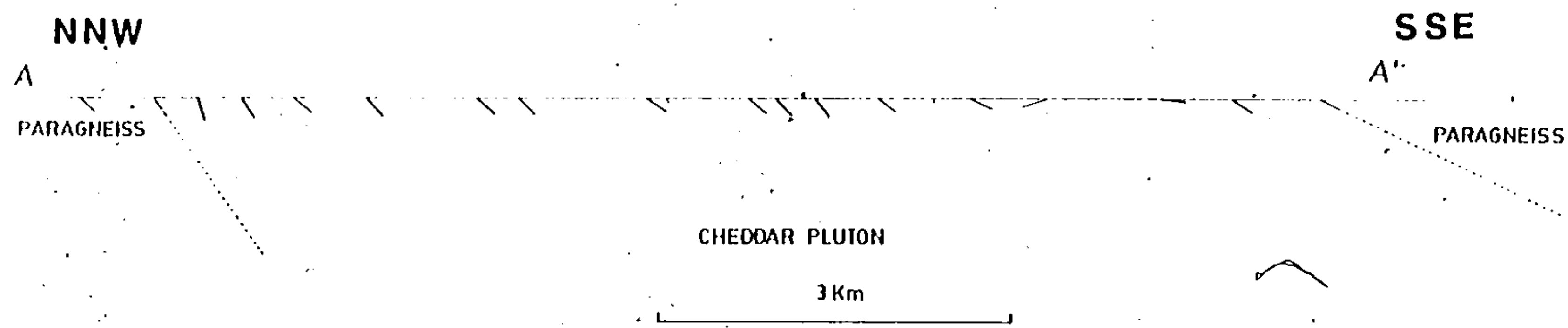

3.17.

Cross section of the Cheddar pluton. Foliations indicated by heavy lines. See fig.1.2 for line of section.

The most intensely discussed criterion for recognition of diapirism focus on the distribution of strain (Coward 1981, Ramberg 1967a and b, 1973, Fletcher 1972, Dixon 1975, Schwerdtner et.al. 1978). The expected pattern is constructed using mathematical or centrifuged scale models. For an immature diapir, one which has not mushroomed, a crestal region with sub-horizontal extension is separated by a neutral surface from a neck region with lineation plunging parallel to the neck. Within the neck region folds with radial axial surfaces are possible. For an inclined immature diapir the fabric distribution observed would depend on the level through which the erosion surface cut (Fig. 3.16). Superficially a cross-section through the Cheddar complex resembles a section through the lower part of an inclined immature diapir (Fig. 3.17). However lineations are not parallel to the trunk of the body and folds do not have radial axial surfaces (Fig. 1.2). On the contrary, lineations in the Cheddar body vary from sub-horizontal in various directions to moderately plunging to the southeast while the few folds measured have axial surfaces dipping southeast (Fig. 3.13a). In the subsidiary mass, the Eels Lake body, there is a sub-horizontal stratiform foliation and sub-horizontal lineation trending NE-SW, which is axial to the single reclined fold observed. Moreover, as noted above, pluton and envelope lineations are not entirely conformable. In the Cardiff complex, lineations are parallel to the SE plunge of the structure. However, it

FIGURE
3.18

The effect of shearing of an immature upright diapir. (a) Cross section of an immature upright diapir (after Fletcher 1972); an inherited formerly horizontal layering is cross-cut below the neutral surface by an imposed shape fabric; above the neutral surface the layering and shape fabric are more nearly parallel. (b) The upright diapir is deformed by an homogeneous simple-shear ($\lambda \approx 2$, shear plane dips 15°); the cross-section may be divided into areas where the layering has a history of continual extension (E), early contraction, late extension and overall extension (E>C), early contraction, late extension, overall contraction (C>E), overall contraction (C); in the latter area folding may occur in layers above and below the initial neutral surface. (c) map section showing half of trace of a single layer from upper part of an upright immature diapir. (d) map section of trace of same layer after a simple shear as in (b). In (b) ES is erosion surface.

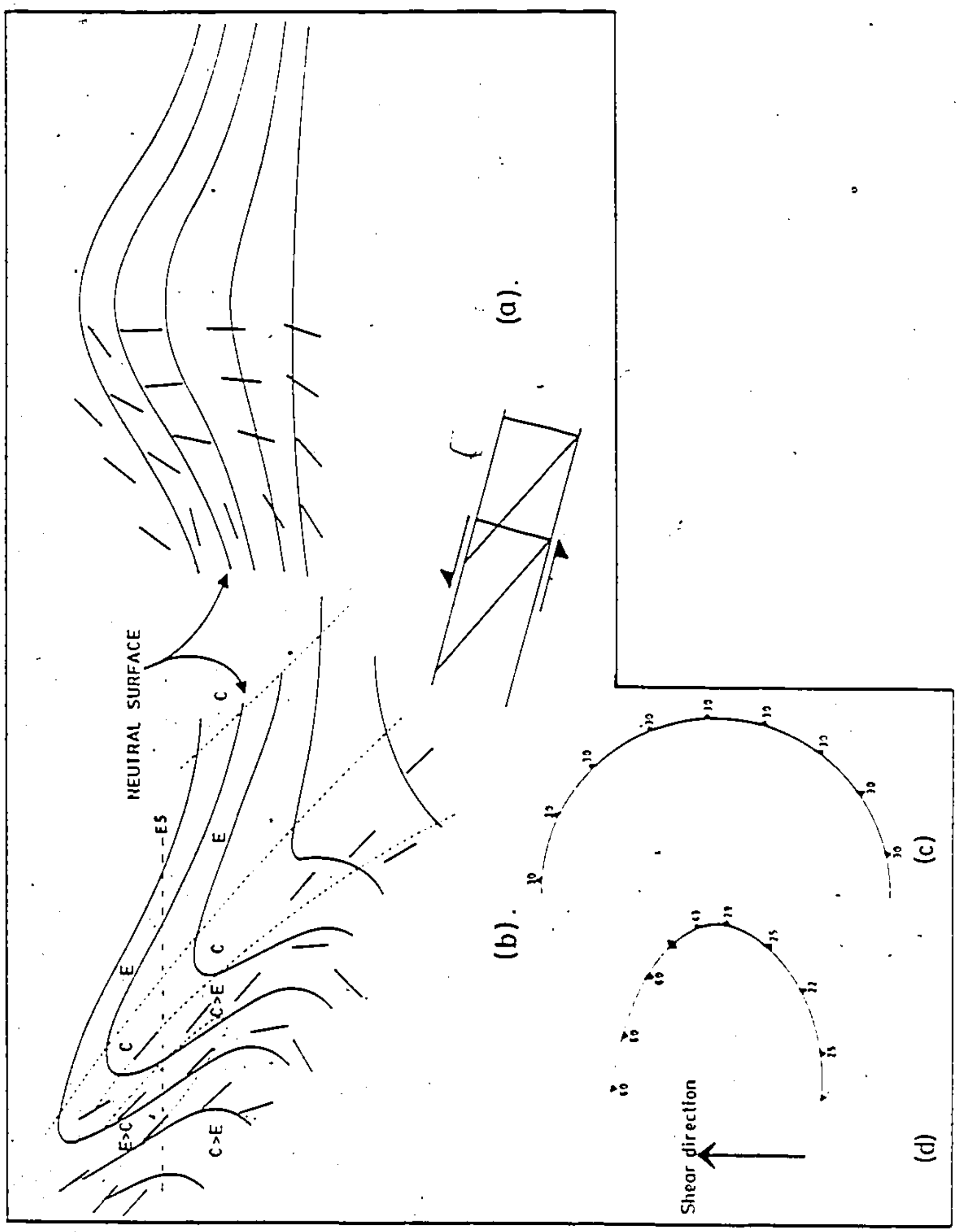
NEUTRAL SURFACE
ES
C
E
C>E
E>C
(a)
(b)
(c)
(d)
Shear direction

does not seem likely that this is a section through the trunk of an undeformed diapir since there is a sub-horizontal foliation which is deformed by reclined folds with axial surfaces mainly dipping southeast and axes slightly oblique to the overall plunge of the structure.

To account for the asymmetry of the bodies and their structural relations, a model can be made in which an immature diapir is subject to simple shear (Fig. 3.18). The model has many simplifying assumptions but indicates the type of structural relations to be expected in such a body. The assumptions include: that simple shear was homogeneous; that the shear plane dips 15° with respect to today's erosion surface and the base of the initial dome and that the shear direction is down the dip of the shear plane somewhat oblique to the trend of the arch. The choice of the initial dome cross-section is arbitrary and based on a model of Fletcher (1972); the magnitude of shear strain is also arbitrary ($\gamma = 2$). Deformation of the cross-section which contains the shear direction and a surface trace of an arbitrarily chosen horizontal plane is accomplished using equations for reorientation of planes and lines given by Skjernaa (1979).

The general result of the deformation of the cross-section is that all fabrics are reoriented but their history and final state depends on whether they are an imposed fabric, which tracks the axes of the finite strain ellipsoid or an inherited fabric such as an initially sub-horizontal layering (Fig. 3.18). As a result of the shearing all the imposed fabrics are made nearly mutually parallel and are moderately inclined to the erosion surface. All, except some lying above the neutral surface in the crest of the dome, have a history of continual extension.

In contrast, most of the inherited fabrics, that is to say, the layering, have a history which includes a period of contraction (Fig. 3.18). Those in the centre of the dome suffer continual contraction and will therefore be folded with axial surfaces (and parallel foliations) dipping moderately with respect to the erosion surface. Similar relations are found in the granitoid plutons. For example, in the Cheddar body which is largely devoid of layering in its northern part, imposed shape fabrics and schistosity dip moderately to steeply southeast. Folds are dominant in the eastern part where there is a continuous layering in the supracrustal rocks. In the crest of the Deer Lake body an inherited layering is present in the central supracrustal gneisses. It is here that the mesoscopic and intermediate scale folds are developed.

This model does not specify what the history of the imposed fabrics located initially above the neutral surface in the crest would be apart from indicating early contraction. If extension were allowed to take place at right angles to the plane of the section in order that this contraction be accommodated, then an extension lineation at right angles to the shear direction and parallel to the fold axes may be expected in the early parts of the history. These linear elements would then rotate towards the shear direction. This is possibly the reason for the dispersion within a plane of fold axes and lineations. Moreover, this explains well why lineations and fold axis in the Eels Lake body trend NE near perpendicular to the SE regional lineation (Fig. 1.3), and why the body itself is also elongated NE and why intermediate scale folding (Fig. 1.2) on this axis is found here. This would happen if part of the southeastern extremity of the dome dipped more shallowly than the shear-plane so that a second area of continued contraction existed (Fig. 3.18b). If, as suggested (see Sections 2.6.8 and 3.2.5), shear strain increases from south to north in the area, structures in the south would have orientations appropriate to earlier stages of the shear history.

Following Skjernaa (1979) an oval map pattern can be derived by shearing a circular domal structure with a thirty degree outward dip (Fig. 3.18c and d). The result is an oval structure with its long axis at right angles to the shear direction trace. This pattern is poorly shown by the main mass of the Cheddar batholith but is present in the Eels Lake body and the core of the Cardiff complex. It must be pointed out that if the plutons were simply inclined undeformed cylinders, then the long axis of their outcrop pattern would be parallel to the axis of tilt of the cylinders.

A feature unexplained in the foregoing model is the layered nature of the Cardiff complex. A possible mechanism is shown in Fig. 3.1 in which a granite sheet was intruded into denser cover rocks above granitoid basement. Under conditions of high grade metamorphism and a lowered ductility contrast, the granitoid basement then rose to form the quasi circular complex.

The open large and intermediate scale structures centred on the Allen Lake pyroxenite syncline are local structures that do not form part of a regular regional pattern. Their causes may be sought in the density and hardness of the pyroxenite and metagabbro and the interaction of these properties with the regional bulk strain history. As regional metamorphism increased and reduced the ductility of the surrounding rocks the pyroxenite would have begun to sink owing to its great density relative to the surrounding rocks (Table 23, Appendix I). At the same time northwest directed tectonic transport was taking place. It is suggested that a combination of the effects of sinking of the pyroxenite and the regional push from the southeast against the hard resistant mass of the pyroxenite produced the very open warps whose axes lie in a shallow SE dipping plane (Fig. 3.8).

3.4.4 Zones of Northwest Trending Foliation

Deformation in the zones of northwest trending foliation is essentially synchronous with that outside with respect to the metamorphism and formation of the regional stretching lineation. Formation of the zones must therefore be related in part to the postulated low angle tectonics. This is more readily demonstrable for some zones than for others.

It is justifiable to regard most of the zones as planar-linear to linear macrofabrics (Lisle 1977, Watterson 1968) where intermediate scale folding dominates the structural pattern (see Section 3.3.4). Moreover, on the mesoscopic scale many of the minor structures restricted to these zones have more linear than planar-linear aspect (see Section 3.2.5). Examples of these are the prolate shape fabrics measured in rocks between the Cardiff and Cheddar bodies (Fig. 3.7). Also, the type of mica fabric (type II mica edge lineation) in which the mica flakes are cylindrically and uniformly distributed around the lineation may be regarded as a linear fabric and is found predominantly in these zones (Fig. 1.2). Fold axial surfaces from these zones also have, like the mica flakes, a more nearly radial orientation with respect to the lineation, a linear macrofabric (see Section 3.2.3). Features in the zones of NW trends, such as the prolate fabrics, can be regarded as due to interference between local pluton emplacement related strains (with Z subhorizontal) related to syntectonic emplacement of plutons and the regional ductile shear strain (with Z perpendicular to the interplutonic Z). In this model the X directions of both components are parallel, compatible with the synchronous imposition of both components (compare Hanmer and Vigneresse 1980).

Some minor structures from the zones of northwest trends have an orientation which appears to be related to the attitude of layering and foliation outside the zones. Examples include second foliations which transect steeply dipping layering in Domains 17 within the Drag Lake complex and 21 to the southeast (see Section 3.2.3). These, the axial surfaces of reclined to recumbent asymmetric mesoscopic folds in Domain 21 and small reclined open folds which plicate steeply dipping earlier foliation in several domains (e.g. Domains 4,6,2,7,9,17), often have moderate dips toward the southeast and could be explained by a minor flattening, which deformed fold limbs steeply inclined to the shear-plane during continued deformation.

The northwest structures of Domains 7 and 9 are relatively easily understood. Both form between neighboring plutonic complexes. In both, there is a zone of folded supracrustal rocks overlying southeast dipping rocks warped on a large scale and lying beneath steeply dipping rocks located where the plutonic masses are closest together. The major difference between the two zones is in the eastern margin of Domain 9, which is more moderately dipping than the others. The zones clearly share the structural history of the plutonic masses, being an expression of the combined history of diapirism and ductile northwest directed transport.

The NW structures of Domain 21 southeast of Drag Lake are best interpreted as wide zones of contraction comparable to the much narrower inter-plutonic structures of Domains 7 and 9. In this case the plutonic masses would be the Glamorgan Gneiss complex to the west (see Fig. 1.1) and the Cardiff complex to the east.

The zone of northwest trends encompassed by Domain 17 within the Drag Lake grey gneiss complex is enigmatic. It is not a structure within supracrustal rocks formed between major bodies of plutonic gneiss. Equally enigmatic is its postulated regional extent (Fig. 1.1), the presence of neighbouring upright structures with northeastern axes at a high angle to the regional lineation (Domain 16). A possible explanation for this zone of northwest trends is that it represents a contraction undergone by the sheet of grey gneiss when it was emplaced into the supracrustal rocks. An alternative, arrived at when considering the regional picture, is given in Section 5.12.

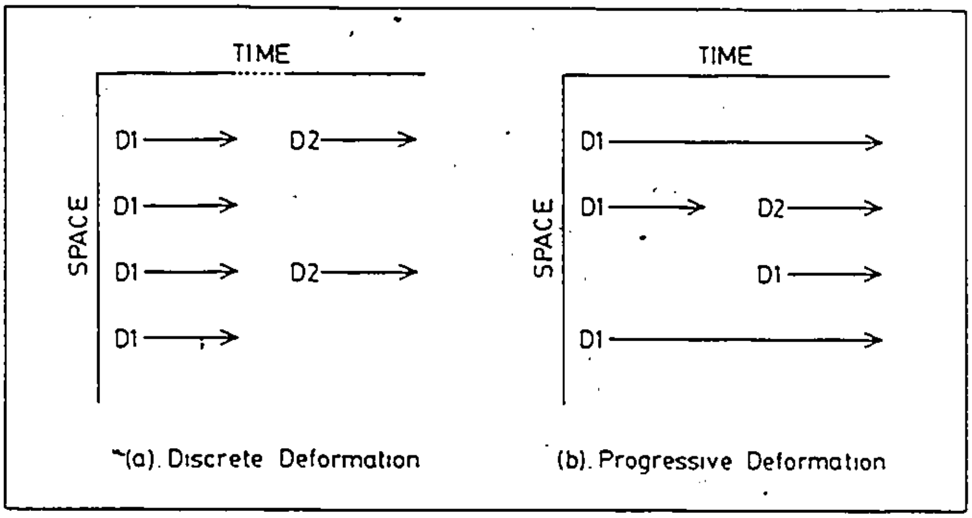

FIGURE
3.19
Possible relations between deformation phases in space and time. (a) in a discrete deformation, structures of the D1 system are formed everywhere before structures of the D2 can be formed anywhere; a considerable interval may separate the two deformations; an example is the overprinting of Archean structures in Proterozoic shear zones. (b) in a progressive deformation, structures of different systems are successive at a particular location, but at different locations they may occur simultaneously and even initiate simultaneously; an example of a process involving a polyphase progressive deformation is the emplacement of a diapir; polyphase progressive deformations may be part of a longer history of discrete deformation.

3.4.5. Summary of Structural Time Relations and their Significance.

It has been argued that the prolate strain within the zones of NW trending foliation is the result of additions of regional shear strains to the local pluton emplacement related strains. Because the two strain components have a common stretching direction and rocks inside and outside the zones of NW trending foliations are metamorphically indistinguishable, the formation of these zones of NW trending foliations and the evolution of structures outside of them appear to be essentially coeval, i.e. the structures are locally polyphase but regionally progressive (Fig. 3.19). Since some of these zones can be related primarily to the emplacement of the Cheddar and Cardiff granitoids regional deformation and emplacement must be essentially synchronous.

There are other features, too, where expressions of the regional strain are imposed on structures related to pluton emplacement compatible with the progressive nature of the evolution of the structures. These features are: (i) on the very large scale the regional strain appears to be imposed upon emplacement related strain in that the axes of symmetry of the Cheddar and Cardiff complexes are at an angle to the long axis of the Harvey-Cardiff Arch but parallel to the regional lineation. (Section 3.3.3 and 3.3.4, Fig. 3.11). (ii) it has been argued that several structures, such as the deformation of the crestal region of the Cardiff complex

(Section 3.3.4) and the presence of a strain gradient across the two bodies, represent the imposition of regional strain on emplacement related structures.

(iii) Likewise, minor structures in zones of NW trends such as the wrinkling of steep foliations about moderately SE dipping axial surfaces and the formation of similarly oriented S2 in steep limbs may represent the reimposition of regional shear strain (Section 3.2.1).

FIGURE 4.1

Summary diagram of relations between LS1 and LS2 microstructures and quartz c-axis microfabrics in the area. Actual sample is a granite gneiss from northern Cardiff Complex, Jordan Lake (24101B). Granite gneiss with LS1 quartz ribbons gives different quartz microfabric patterns when sampled in YZ (a) and XZ (b) planes; data from both are presented in XZ plane. Asymmetry of YZ sample suggests rotational strain, upper layers moving NW. A concordant quartz vein has an oblique planar-linear fabric, LS2, which is visible to the naked eye; within the vein a rutile lineation lies sub-parallel to L1; LS2 quartz has a strong preferred orienation, the girdle is asymmetric with respect to LS2 (c), and the asymmetry suggests movement of upper layers SE.

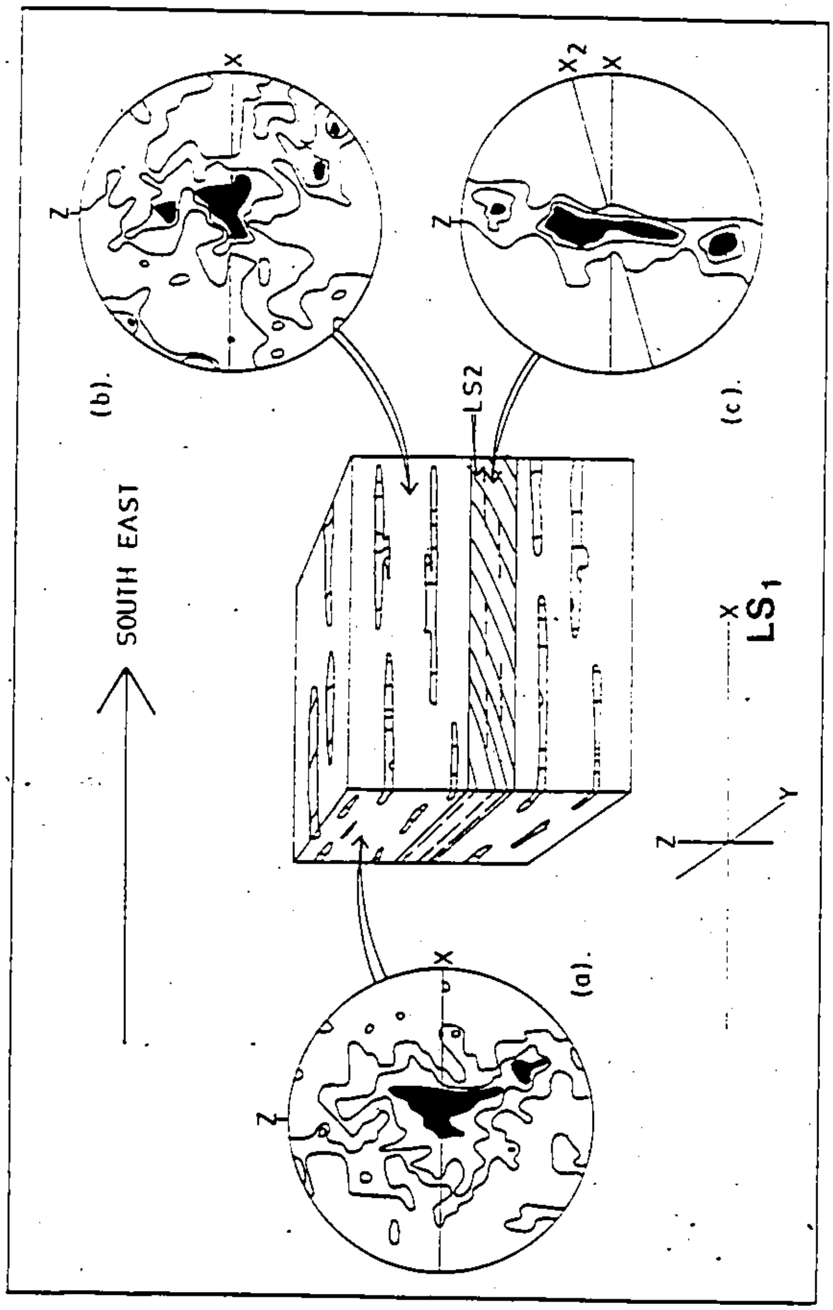
SOUTH EAST
(a).
(b).
(c).
Z
X
X_2
LS2
LS_1
Y

4. MICROFABRICS

4.1. LS1, Quartz Microfabrics, Introduction

Several types of quartz microstructures and quartz C-axis microfabric are found in the area. The particular type depends on rock type and age of the microstructure. The varieties present resemble those found in other gneissic terrains e.g. the Saxony Granulites (Behr 1978, 1980), where the principal variations purportedly depend on successive decreases in temperature and pressure.

The earliest quartz microstructure, LS1, is the most widespread and is the expression of the southeast trending penetrative lineation in the area. The second microfabric, the LS2, is concentrated in narrow zones of centimetric to metric width which are concordant with the LS1 foliation. This microstructure is usually characterized by an asymmetric quartz foliation which unequivocally indicates the sense of shear with upper layers moving SE (Fig. 4.1). The LS2 dynamically recrystallised microstructure is formed at the expense of the LS1 microstructure. The geometry of the LS1 and LS2 tectonites are closely related, L2 always lying in the plane containing L1 and the pole to S1 (XZ in Fig. 4.1). Many of the differences between LS1 and LS2 microfabric and microstructures are most easily explained by the probably lower temperature and pressure of formation of LS2 and hence a lack of post-tectonic grain-growth (Fig. 4.2).

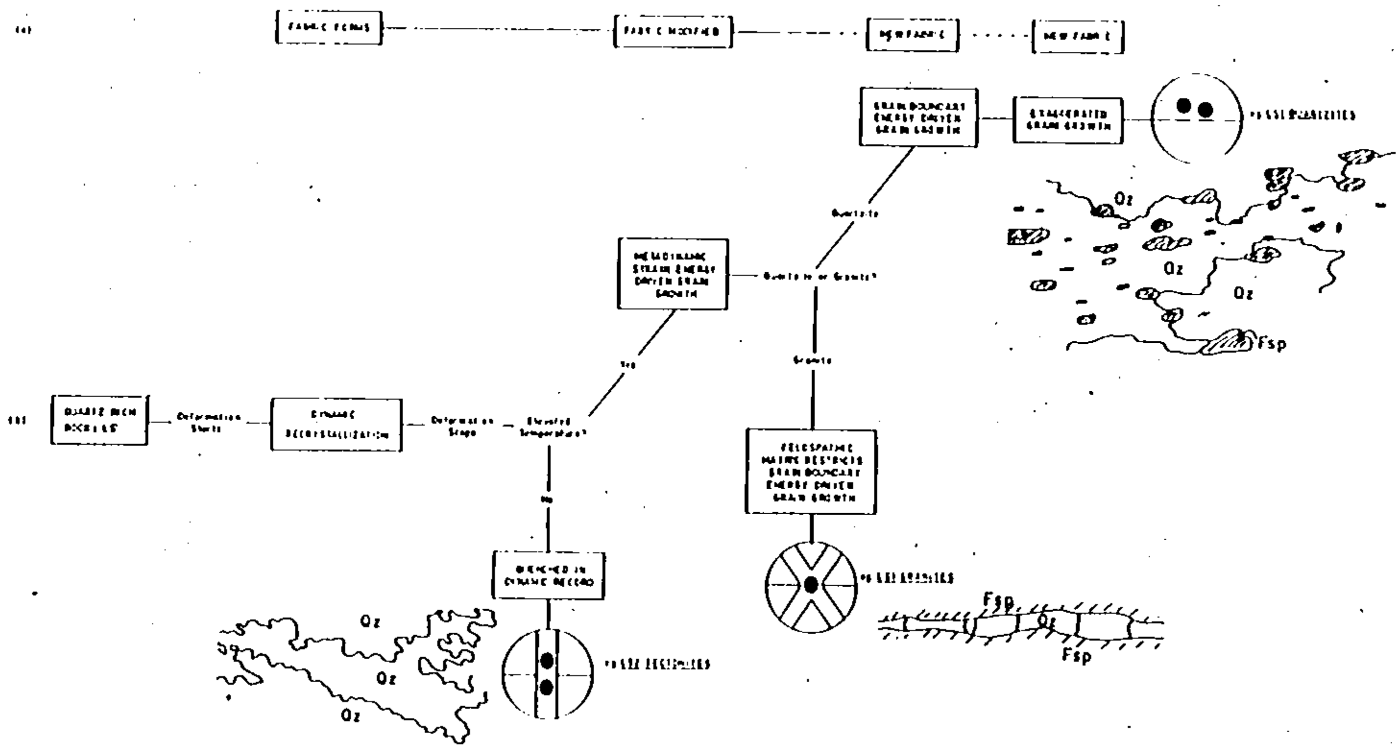

FIGURE 4.2 Flow diagram of proposed evolution of quartz c-axis microfabrics and microstructures. (a) indicates steps in formation of microfabric when the rock undergoes the successive steps shown in (b). The main line of (b) depicts the processes which a quartzite passes through when the temperature remains elevated after deformation and grain growth is unimpeded at all stages. The first branch is probably typified by LS2 tectonites.

Strain rate may also be a controlling factor. LS2 microstructure and quartz C-axes are more fully treated in Section 4.3. The postulated complete LS1-LS2 sequence of microstructural and C-axis microfabric development of a granitic quartz ribbon is shown in Fig. 4.3.

A third type of microstructure and microfabric is present in mylonites along lineaments which are discordant with respect to the regional foliation trend. Microstructurally, they most closely resemble the LS2 tectonites and may be related in age.

Within quartz bearing LS1 tectonites there are two major types of microstructure which are found, respectively, in quartzites and granite gneiss. The quartzites in most cases have a coarse grained microstructure due to exaggerated grain-growth and a C-axis microfabric with a very sharp preferred orientation which is geometrically unrelated to the mesoscopic fabric axes and which retains no memory of the dynamic recrystallisation (Fig. 4.2). In contrast, the granite gneiss has a shape-fabric of polycrystalline quartz ribbons which, despite resembling the quartzite substructurally, have C-axis microfabrics which are strongly controlled by the mesoscopic fabric axes. These two microstructural and microfabric types are occasionally found together in outcrop and even thin-section (Plate 15) where granite sheets and quartzite are interlayered.

FIGURE 4.3

Diagram of postulated sequence of development of LS1 and LS2 microstructure and c-axis microfabric of quartz ribbons in granite gneiss. (a) in LS1 microstructure, at low strains, quartz-quartz boundaries are very indentate, due to strain-energy driven grain-growth, and show no preferred orientation with respect to the fabric axes. Small new grains are present which do not impinge upon the feldspar and intracrystalline distortion is high, accommodated by elongate subgrains. The c-axis preferred orientation is weak. (b) in LS1, at increased strain, grain boundaries are now sub-perpendicular to the lineation, minimizing grain boundary area and indentations have disappeared. All grains have grown until they impinge on feldspar. (Note attitudes of (0001) varying from parallel to XZ to dipping steeply with respect to XZ for the indicated grains). (c) preferred growth of grains with c-axes parallel to Y (of (b) with respect to (a) and (c)). These grains are possibly those with the softest slip system lying in a position of maximum resolved shear stress. This stage is envisaged to be both dynamic and metadynamic. The oriented grain growth is reflected in the YZ sampled c-axis microfabric (Fig. 4.9). (d) an asymmetric microfabric, LS2, is formed by recrystallisation of LS1. The initial formation of LS2 is by kinking of the coarser LS1 quartz. A large volume of LS1 quartz is favourably oriented for basal <a> slip during kinking in which kink axes lie subparallel L2 (c.f. LS1 YZ sampled microfabric, Fig. 4.10). This kinking and subsequent preservation of the geometrical kink relationship during recrystalllisation is reflected in the LS2 c-axis microfabric.

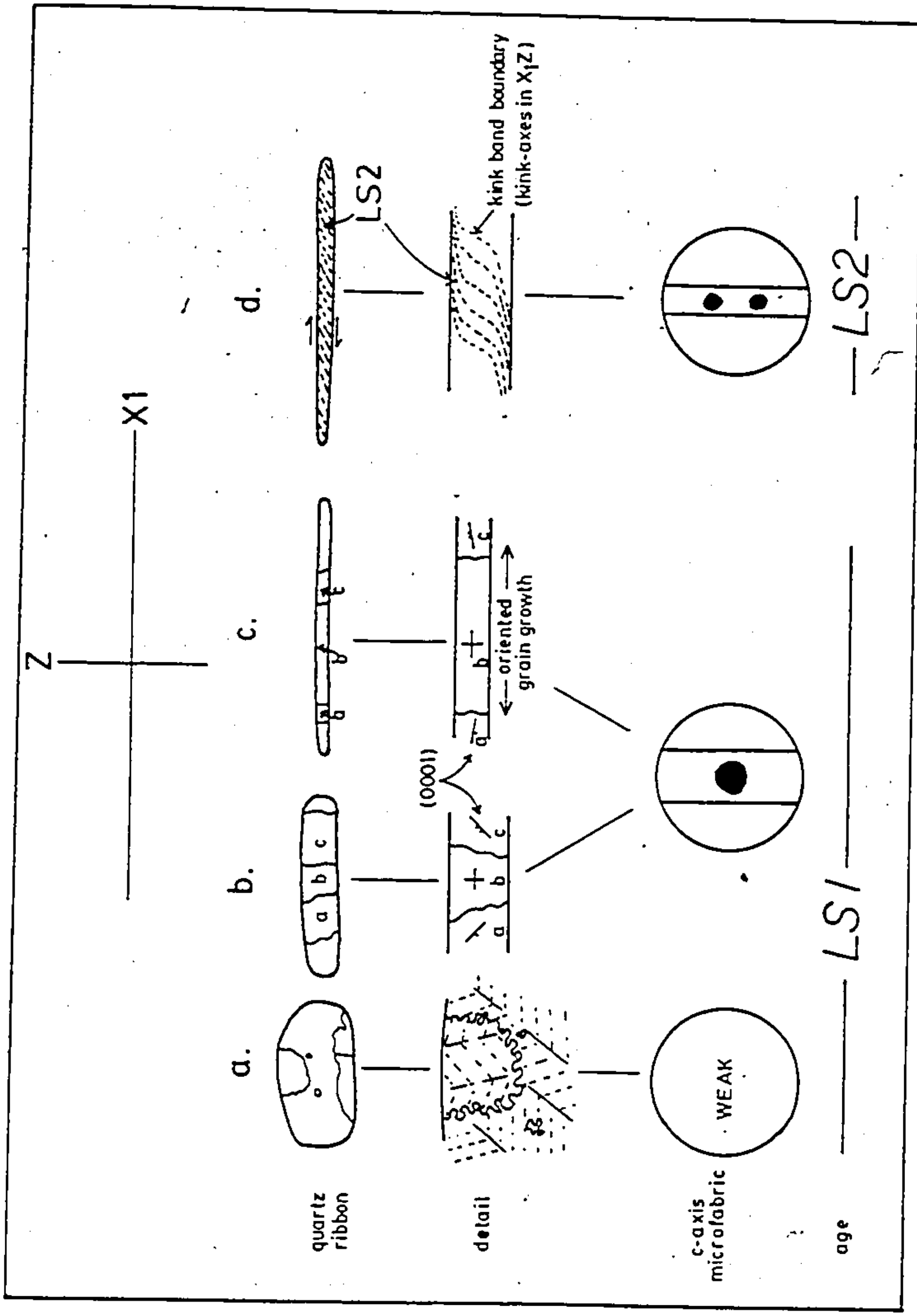

Z
X1
a.
b.
c.
d.
quartz ribbon
detail
c-axis microfabric
age
WEAK
(0001)
oriented grain growth
LS2
kink band boundary
(kink-axes in X1Z)
LS1
LS2

In 1910 Adams and Barlow noted the ubiquity of the granite gneiss in the Haliburton-Bancroft region and perspicaceously remarked on the highly developed quartz shape fabrics that it was "looking ... as if the mineral had been spread ... like streaks of butter on a slice of bread" (Ibid, p. 80) and that there was a crystallographic fabric since "... in the great majority of cases the direction of extinction makes an angle of between 25° and 30° with the long axis of the quartz leaf" (Ibid, p. 80).

This section pursues these two themes of microstructure and quartz C-axis microfabric using granitic gneiss samples from the Cardiff and Faraday complexes and quartzite mostly from locations north of the Cardiff complex. Evidence is presented that there was metadynamic recrystallization (Sellars 1978) and that the microfabric and microstructural evolution of the quartz ribbons in the granites records in part the early history of crystalline slip and dynamic recrystallisation and in part an episode of static grain growth. In particular, C-axis microfabric data are presented which show a systematic variation of pattern which is dependent on the plane of the granite gneiss fabric the sample was taken from (Fig. 4.1). This variation is shown to be related to the proportion of the ribbon that an individual grain comprises and may be explained as an effect of oriented grain growth. Since the microfabrics bear some record of their syntectonic history an interpretation of the strain history is feasible in which an episode of simple shear is postulated during which upper layers moved northwest over lower layers, the lineation being a stretching lineation with its axes near parallel to the axes of the strain ellipsoid.

However in the quartzites since the exaggerated grain growth seems to destroy any record of dynamic recrystallisation (Fig. 4.2), the C-axis microfabrics are of little use in kinematic interpretation despite the evidence that these rocks have undergone profound deformation. However, when LS2 age substructural modification is advanced the C-axis microfabrics may be of kinematic utility.

4.2. LS1 Microstructures and C-Axis Microfabrics

4.2.1 LS1 Microstructures in Granite Gneiss

There are two distinct types of quartz microstructure in the lineated granite gneisses which are considered to be members in a gradational series (Plate 12). The main microstructural differences of the quartz and feldspar fractions are summarized in Table 23, Appendix I. In the most common type interpreted as representing an advanced stage of microstructural development (henceforeward "MCT"), the ribbons are composed of blocky quartz grains with straight grain-boundaries subparallel to YZ (Plate 12). The less common type, found mainly in a large mass of the Upper Faraday granite near Albion Lake and rarely in the least deformed southern part of the Cardiff complex and interpreted as representing an early stage of microstructural development (henceforward "ALT"), has grain boundaries which are, in part, highly indentate and not parallel to any fabric plane (Plates 12, 14). The field setting of MCT suggests elevated and homogeneous strain judging by uniform fine grain size and high aspect ratio of quartz ribbons and the near concordance to the trace of the lineation of deformed dykes and pegmatites. In contrast, ALT is found in zones of heterogenous and generally weak deformation in the Upper Faraday granite where the fabric may even be absent. The low strains are witnessed by the low aspect ratio of the quartz ribbons and the moderate grain-size of the unrecrystallized feldspathic matrix (Plates 12,13,14).

In the MCT the quartz ribbons have aspect ratios measured in the XZ section of up to 10 to 1 with most between 5 and 6 to 1. Typically the ribbons are made up of subrectangular grains whose mutual boundaries tend to lie perpendicular to the ribbon length (Table 24, Appendix I, Plates 12,13). Circular or semi-circular grains are scarce. Rarely, portions of the ribbons are two grains thick, in which case a feldspar often lies on the intervening grain-boundary. The boundaries are generally free from very small scale irregularities. Occasionally ribbons are made up of a single grain, however polycrystal ribbons are the rule. For example, in sample 1296B 60 percent of all quartz grains belonged to ribbons with three or more members and only 15 percent of the grains formed single-grain ribbons. The distribution of aspect ratios measured in the XZ section

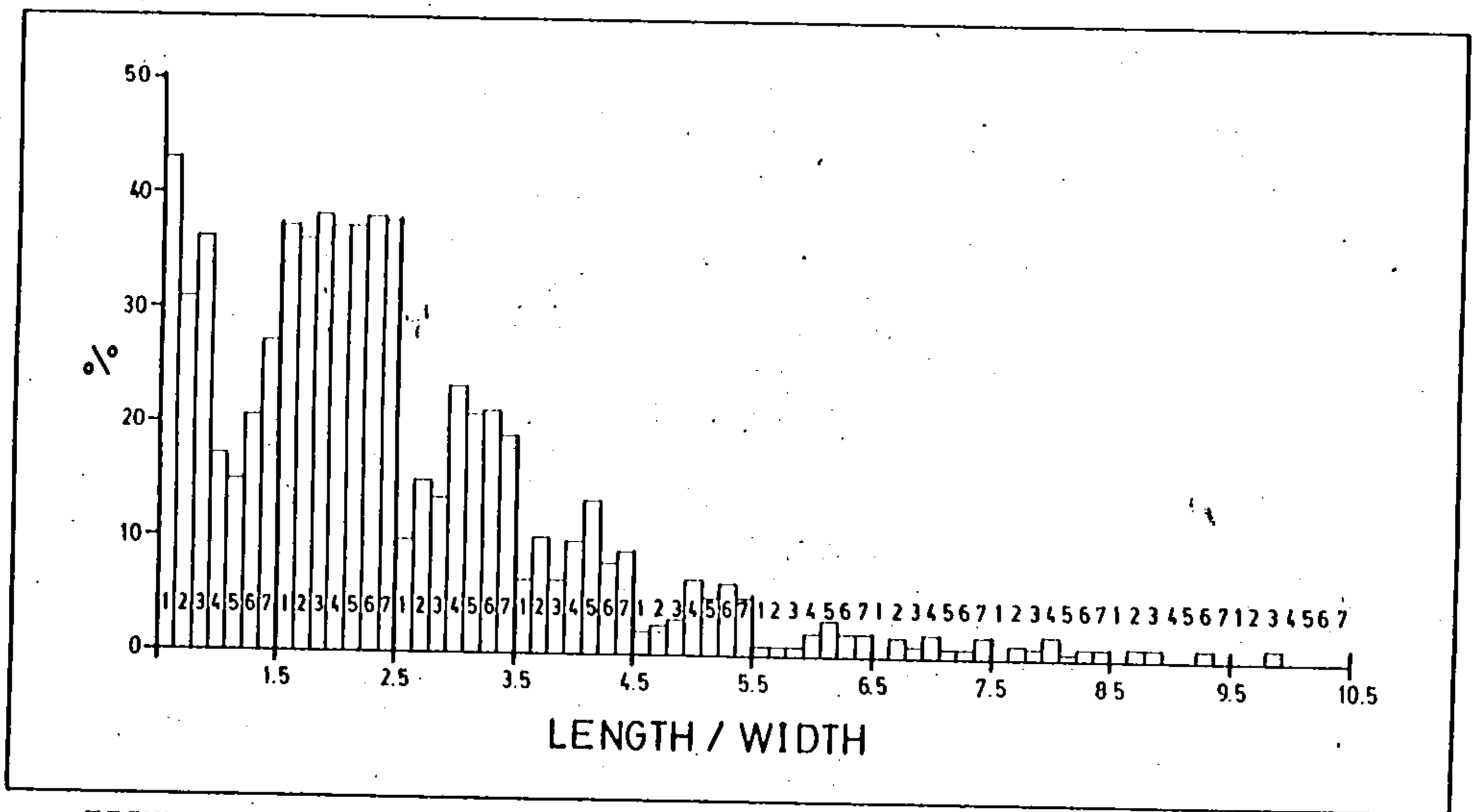

FIGURE 4.4 Frequency distribution of aspect ratios of single quartz grains from quartz ribbons in samples of granite gneiss from Lower Faraday Granite and Cardiff Complex. (Sample identification: 1 = 22104B, N = 192; 2 = 22103B, N = 174; 3 = 497C, N = 194; 4 = 1293B, N = 142; 5 = 1296B, N = 214; 6 = 1691B, N = 198; 7 = 24101B, N = 213.) All measured in XZ section of MCT microstructure.

is skewed (Fig. 4.4), most of the grains (70 to 90 percent) being stubby with aspect ratios less than 3.5:1. Amount of strain (estimated from ribbon aspect ratios, Fig. 4.5c) appears to have little effect on distribution of grain size (Fig. 4.5a).

Undulatory extinction is common and elongate subgrains with boundaries parallel the prism cut across the entire width of the grain. Misorientation across the subgrain boundaries is usually small, less than 5°. Deformation lamellae are absent.

In contrast to the MCT quartz microstructure the grain boundaries of the ALT microstructure show little tendency to lie perpendicular to the ribbon trace in the XZ plane (Table 24, Appendix I). Moreover, in detail, many of the grain boundaries are highly irregular (Plates 12 and 14) displaying lobes and embayments of great complexity. Some grain boundaries are free of small scale irregularities (Plate 14d) as in the MCT. The two types of grain boundaries may coexist in the same ribbon.

Associated with the very irregular grain boundaries in the ALT are small equant sub-grains and new grains, both approximately 50μm in diameter. New grains also occur on deformation band boundaries and near feldspar inclusions, where some of the greatest lattice distortion is found (see Humphreys 1977 for comparable recrystallisation near hard inclusions in metals). New grains are rare, however they are observed in several stages of growth. The smallest are

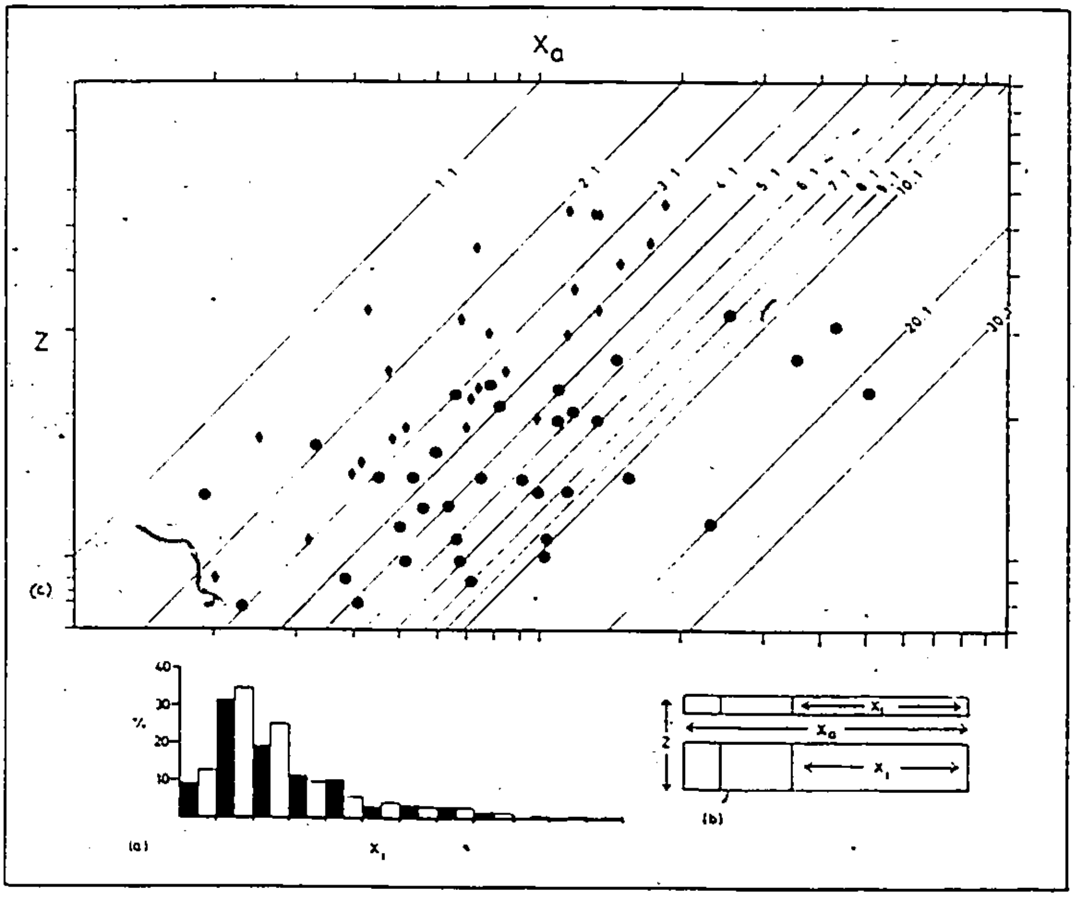

FIGURE
4.5

Variation of shape parameters of ribbons and component grains in granite gneiss from Lower Faraday Granite; (a) frequency distribution of relative grain length (X_1) in 22103B (Black) and 1691B (White); (b) distinction between ribbon length (X_a) and grain length (X_1); (c) aspect ratios of quartz ribbons measured in XZ plane, 22103B (diamonds) and 1691B (circles).

polygonal, above a certain size their grain-boundaries are very irregular (Plate 14b,c). The preservation of grains whose boundaries have not impinged on the feldspathic matrix is restricted to the ALT microstructure.

Deformation band-like subgrains are highly developed in the ALT microstructure (Plates 13a,14b). These substructures may be equant or, more commonly, elongate, measuring up to 1 x 0.25 mm. The longer substructures have tapered ends and rarely cross the whole grain; their length is near parallel to the C-axis trace. They appear to be analagous to propagating kink-bands. Misorientations across the substructural boundaries are mostly in the 5°-10° range with a few of 25° to 30°.

Bright lamellae lying subperpendicular to the C-axis trace are occasional features in the ALT microstructure. These are interpreted as subbasal deformation lamellae.

4.2.2. Interpretation

The two microstructural types seem to be members of a transitional sequence since they all are of similar age, both forming the southeast plunging LS shape fabric. In the field they appear to be gradational and in thin section microstructural features typical of both types may appear in the same rock (c.f. variety of grain-boundary morphologies in ALT).

This sequence appears to be related to variations in strain. Apart from the clear differences in degree and homogeneity of deformation observed on all scales several microstructural features lend weight to this and the contention that they are members of a sequence of increasing recrystallization. The occurrence of deformation lamellae exclusively in ALT compares ~~with~~ their exclusive occurence in the least strained members of sequences of progressive deformation in quartzites (Christie 1963, Crampton 1963, Wilson 1973, Bouchez 1977, MacClaren and Hobbs 1970). The differences in the relative homogeneity of intragranular strain shown by the differences in deformation band misorientations between the ALT and MCT types and the presence of large cumulative lattice distortions in ALT which are absent in MCT are comparable to differences between new and old grains (Wilson 1973, see also Section 4.3.4., Specimen 30103B). Related to the latter is the difference of the grain boundaries in the two types. The morphologies of grain boundaries has been related to the driving force of crystal growth in metals and in naturally and experimentally deformed minerals (Cahn 1965, White 1976, Nicolas & Poirier 1976, Wilson 1973). Highly irregular lobate boundaries are considered to form when the driving energy is the residual strain energy of deformation whereas smooth boundaries form after the dissipation of most of this energy when the aggregate is simply attempting to minimize grain boundary energy. This minimization of grain boundary energy is achieved by decreasing the grain boundary area per unit volume thus not only smooth grain boundaries but grain boundaries tending to lie parallel to the YZ fabric plane will result since this is the orientation in which grains will have the smallest area in blade-shaped ribbons, as is observed (see also Spry 1969).

It is generally considered that the presence of deformation bands, sub-grains, undulatory extinction and deformation lamellae are indicative of the operation of dislocation dominated recovery processes (White 1973, 1976) and that lobate grain boundaries, new grains and a polygonal substructure indicate dynamic recrystallization (Nicolas and Poirier 1976). The microstructure of ALT may then be attributed to the stage of primary recrystallisation in a history which at least in part contained an episode of dynamic recovery and recrystallisation. Evidence for secondary, static, recrystallisation is strong, comprising not only the morphology and, in MCT, the orientation of the smooth grain boundaries but also the close association of exaggerated grain growth microstructures and MCT on the thin-section and outcrop scale where quartzites and granite gneiss are interlayered. The static grain growth which must have occurred, especially in MCT, would be very limited in extent in comparison to the quartzites on account of the very large area of quartz-feldspar boundaries surrounding a quartz ribbon.

The static grain growth must be metadynamic (Sellars 1978), in the sense that nucleii of recrystallisation which were present and boundaries which were mobile before the deformation stopped, continued growing and moving after it has stopped. In such a case the final grain-size will be independent of strain and larger than that produced by dynamic recrystallisation alone (Sellars 1978). In light of the lack of dependence of grain-size on ribbon aspect-ratio (Fig. 4.5) and the contrast between new grain-size in ALT (Plate 14b) and MCT grain size (Plate 12b) this condition appears to be met.

In summary, the microstructure of the quartz ribbons in the granite gneiss appears to show the imprint of a sequence of metadynamic recrystallization the position of each rock in the sequence depending on the amount of deformation suffered. Rocks with ALT microstructure, indicative of dominant primary metadynamic recrystallisation, show evidence of low strains, in contrast to the higher strains of rocks with MCT microstructure, indicative of limited secondary metadynamic recrystallisation.

The quartz ribbons compare very well with examples of "Platten Quartz" found in many high-grade terrains (e.g. Behr 1961,1965,1980, Starkey 1979, Boullier and Bouchez 1978). Opinions on the origin of the microstructure are rare and diverse: Spry (1969) considered it the result of static annealing of a cold-worked rock; Starkey (1979) presented evidence of dynamic recovery. The present interpretation partly agrees with that of Boullier and Bouchez (1978) who considered the microstructure to have developed statically.

FIGURE 4.6

Quartz c-axis microfabrics of Lower Faraday Granite, mature (MCT) microstructure. Southeast is to the right of all nets. X = L1

(a) 1691B; contours at 1.33,2,2.66,4%/1% area; maximum 4%; XZ sample; N=150

(b) 1296B; contours at 1.2,1.9,2.6,3.2%/1% area; maximum 4.5%; YZ sample; N=156

(c) 1092B; contours at 1,2,3,4%/1% area; maximum 6%; XZ samples; N=200

(d) 497C; contours at 1,2,3,4%/1% area; maximum 4%; YZ sample; N=200

(e) 895C; contours at 1,2,3,4%/1% area; maximum 6%; YZ sample; N=200

(f) 22103B; contours at 1.7,2.5,3.3,4.2%/1% area; maximum 5.8%; 106 YZ data, 14 XZ data

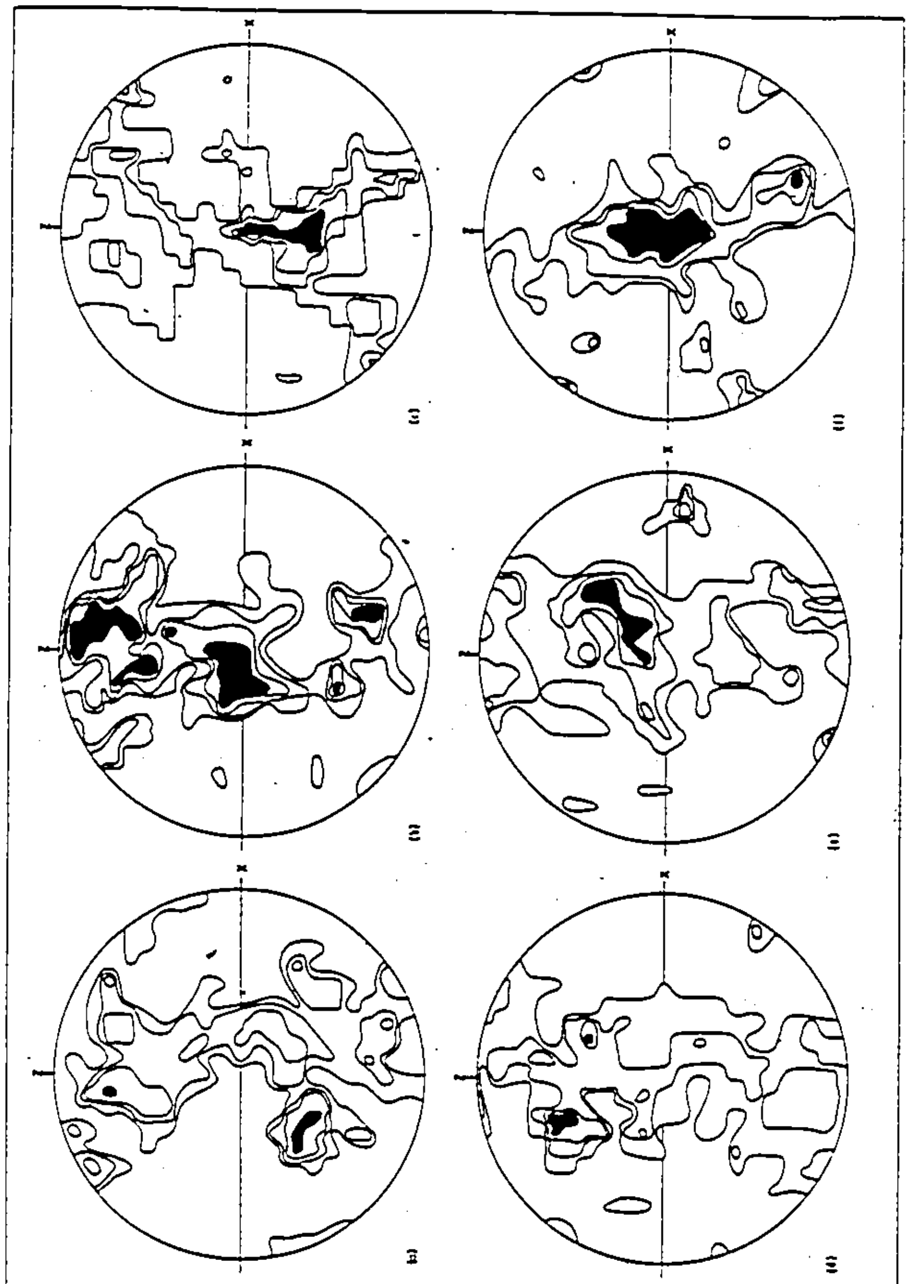

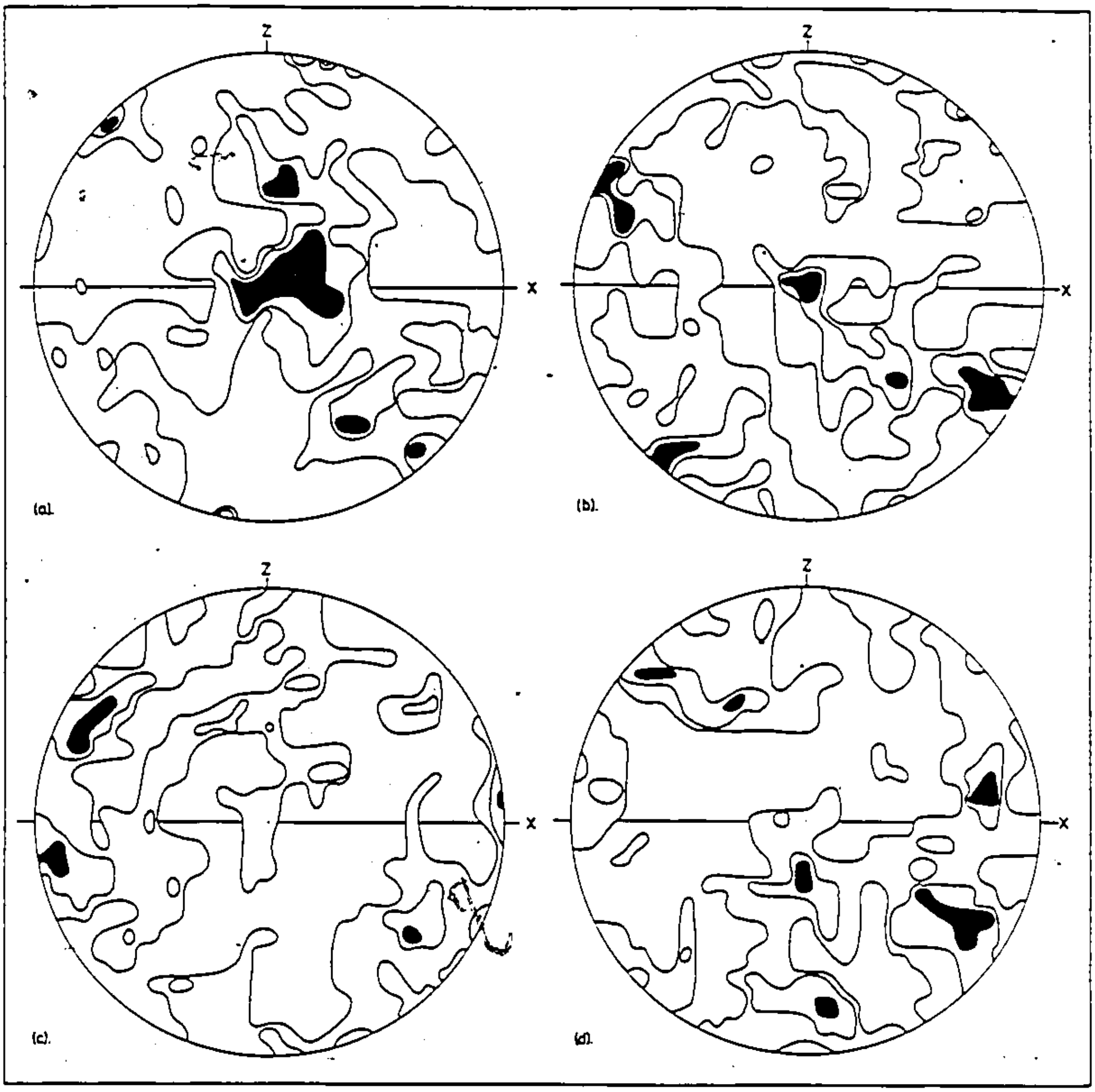

FIGURE
4.7

Quartz c-axis microfabrics from Cardiff Complex, mature (MCT) microstructure, XZ samples. All contours at 1,2,3%/1% area; N=200. (a) 24101B, maximum 7%; (b) 25101B, maximum 4.5%; (c) 30105B, maximum 3%; (d) 30101B, maximum 6%. Southeast to right on all nets. X = L1

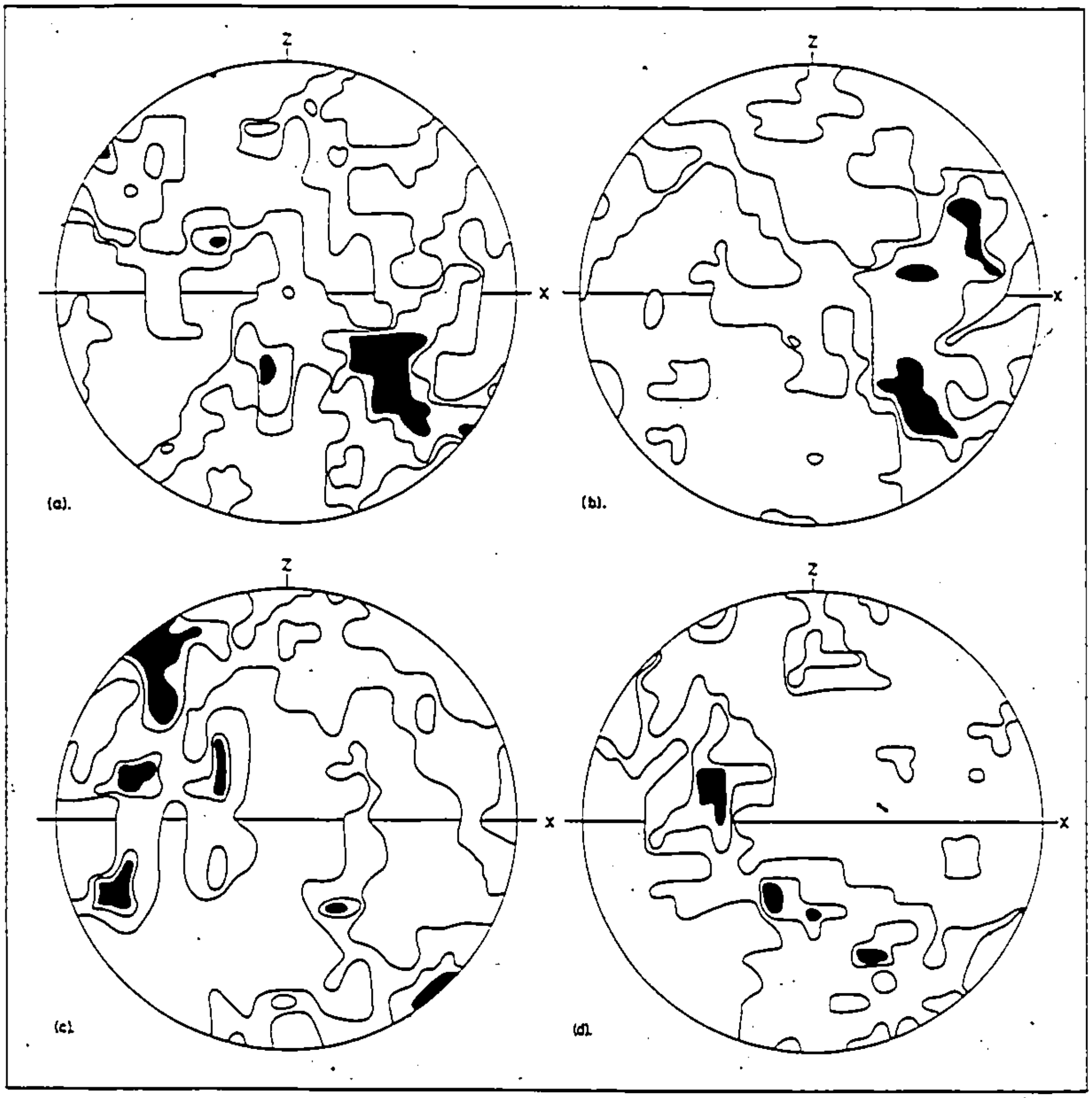

FIGURE
4.8

Quartz c-axis microfabrics from Upper Faraday Granite, immature (ALT) microstructure. All contours at 1,2,3%/1% area. (a) 1113D, maximum 5%, XZ sample, N=200; (b) 2111D, maximum 4%, XZ sample, N= 200; (c) 1491C, maximum 6%, XZ sample 150 data, YZ sample 50; (d) 1395C, maximum 3%, XZ sample 76 data, YZ sample 95. Southeast to right on all nets. X = L1

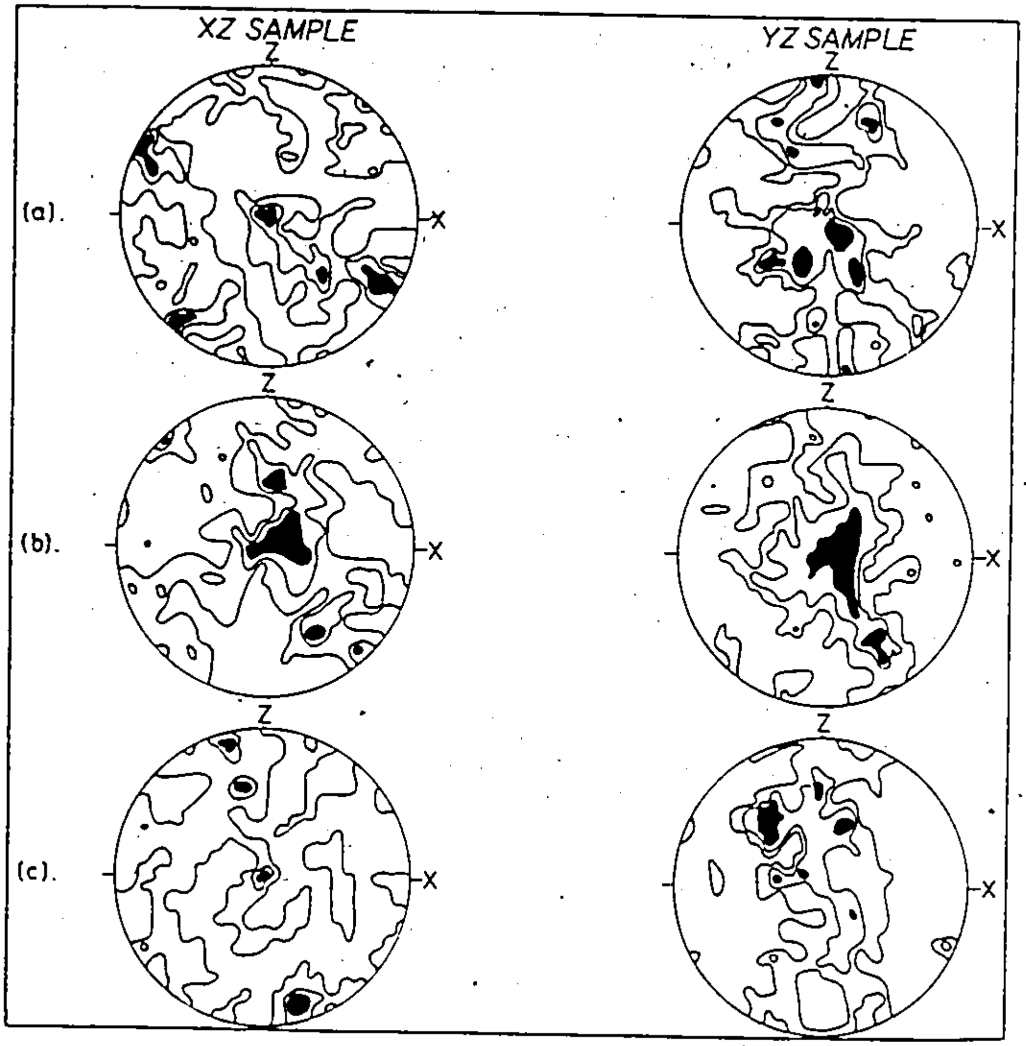

FIGURE
4.9

Comparison of quartz c-axis microfabrics sampled in the same rocks in the XZ and YZ fabric planes, mature (MCT) microstructure. All contours at 1,2,3%/1% area; 200 data in each. (a) 25101B, north Cardiff Complex, maxima at 4.5% (XZ), 4% (YZ); (b) 24101B north west Cardiff Complex, maxima at 7% (XZ), 5% (YZ); (c) 497C, Lower Faraday Granite, maxima at 3% (XZ), 4% (YZ). Southeast to right on all nets. X = L1

4.2.3. LS1 Quartz C-Axis Microfabrics in Granite Gneiss

Quartz C-axis microfabrics were measures in 14 granite gneiss samples bearing the LS1 quartz microstructure of both MCT and ALT varieties (Figs. 4.6-4.9). All but two of the samples come from rocks with the southeast plunging lineation on the north and west side of the Cardiff and western part of the Faraday complexes (Fig. 1.2). Rocks here are thought to have had a comparatively simple structural history; relatively homogeneous and intense LS1 deformation produced tectonites with a moderately southeast plunging lineation and shape fabrics range from quite prolate to dominant plane-strain types.

Microfabric data was collected from sections cut parallel to the XZ plane in order to simplify comparisons and facilitate visualization of the relationships between microfabric and shape-fabric axes. Nets were contoured by hand according to the Schmidt or Starkey (Starkey 1977) methods.

All grains present in a section were sampled with the exception of one member of any pair of grains which were suspected of being joined out of the plane of the section.

When possible, two hundred grains per sample were measured. Nevertheless, it was found that the basic pattern emerged at around one hundred and twenty grains. The adequacy of such a sample size is underscored by the general similarity of microfabrics from several rocks sampled in the same plane and having similar shape fabrics though the

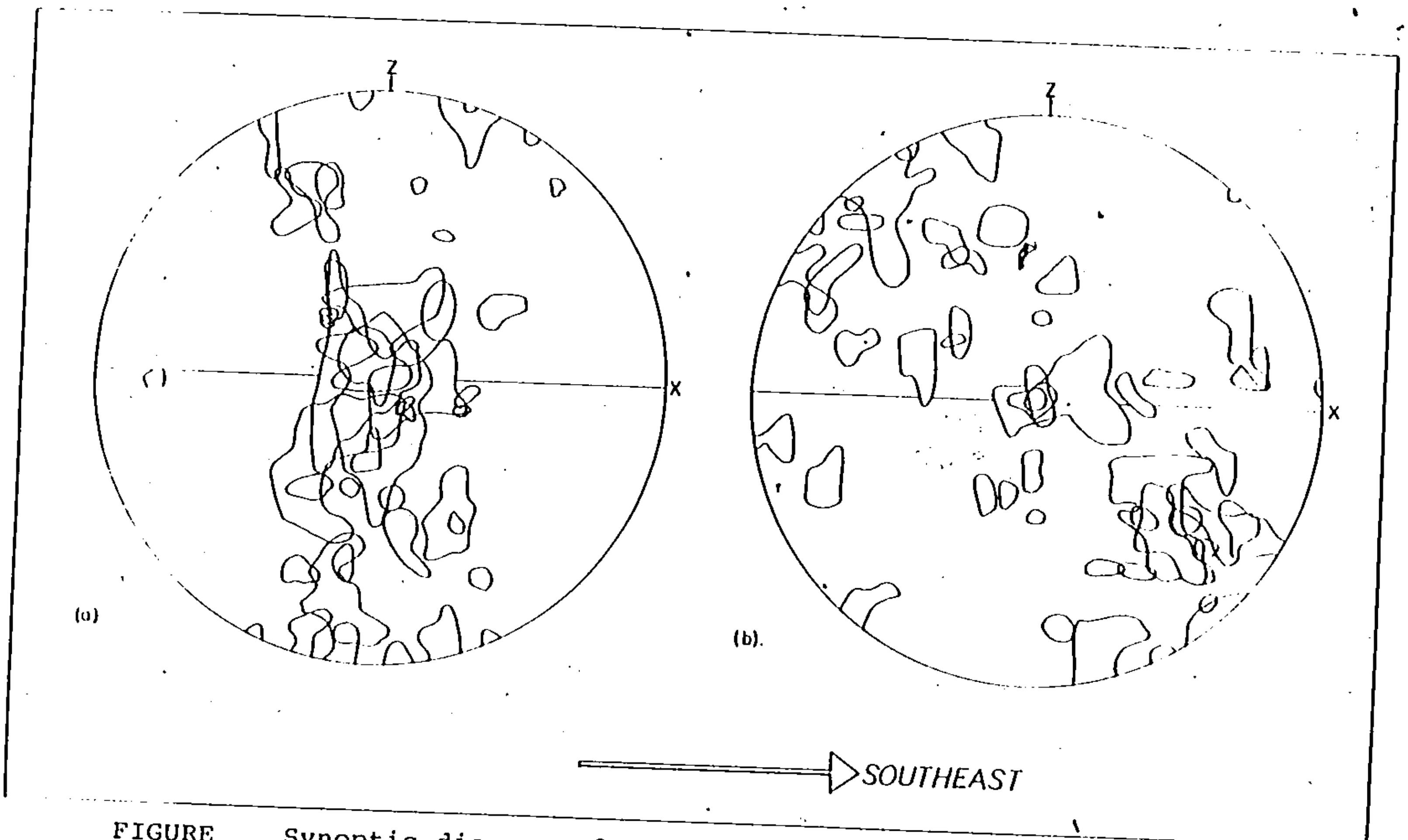

FIGURE 4.10 Synoptic diagrams for quartz c-axis microfabrics of granite gneisses sampled in YZ plane (a) and XZ (b). Both diagrams and constructed by combining all 3%/1% area contours from many samples; 6 samples contribute to (a), 9 to (b). X = L1

sample size varies from 106-200 (e.g. Fig. 4.6b,d,e,f). In most rocks this amount of data was available from one section cut in the YZ plane or from two cuts in the XZ plane. In the coarser less strained rocks of the Upper Faraday granite, between four and eight sections were required.

The most striking features of the C-axis microfabrics are: (i) the presence of YZ girdles in microfabrics sampled in the YZ plane (Fig. 4.6b,d,e,f; Fig. 4.9a,b,c); (ii) rocks with MCT microstructures sampled in the XZ plane may have well defined cross girdles (Fig. 4.6c, Fig. 4.7a) or poorly to very poorly defined (Fig. 4.7b,c,d, Fig. 4.9c); (ii) in both fabric types a maximum in Y is common (Fig. 4.6b,c,e,f; Fig. 4.7a,b; Fig. 4.9a,b,c); (iv) rocks with ALT microstructure sampled mainly in XZ section have poorly defined patterns, compatible with the relatively low finite strains they have suffered (Fig. 4.8).

Several features of the XZ and YZ sampled patterns are brought out by synoptic diagrams prepared by presenting on one diagram all the 3 percent contours of all the specimens sampled in a particular plane (Van Roermond et.al. 1979, Lister and Williams 1979). The YZ girdle, perpendicular to the lineation and the maxima in Y is highlighted in the YZ sample diagram (Fig. 4.10a) whereas the XZ sample diagram shows one inclined girdle (Fig. 4.10b) comparable to a single girdle of a pair of cross girdles with an opening angle of the magnitude (~ 90°) of that found in some of the XZ samples (e.g. Fig. 4.7a,b).

The reality of the differences between the XZ and YZ sampled populations is clearly shown in patterns from rocks that have been sampled in both planes (Fig. 4.9), the change from cross-girdles to YZ girdles is confirmed.

4.2.4 Oriented Grain Growth in Quartz-Ribbons

It is clear from the frequency distribution of individual grain aspect ratios (Fig. 4.4) that the XZ sampled population consists of a large number of stubby grains as compared with those of high aspect ratio. Thus, the XZ sample has a C-axis microfabric highly biased towards that of the stubby grains. The YZ sample must be selected on the basis of the factors that determine which grains have the highest probability of being cut by a plane perpendicular to the ribbon length. Assuming that the size of the grains measured in the XZ section reflects the real three dimensional shape of the grain, such factors could be aspect ratio, length or the proportion of a ribbon which a particular grain comprises (all measured in XZ plane). In order to find which of these factors or combination of them determines the make-up of the YZ sample it is obviously worth examining in the XZ plane the effect of variations of them on the microfabric and the implications of any significant variations on the microstructural history of the ribbons.

The MCT sample examined has distinct XZ and YZ sampled C-axis microfabrics (Fig. 4.9c). The aspect ratio (length

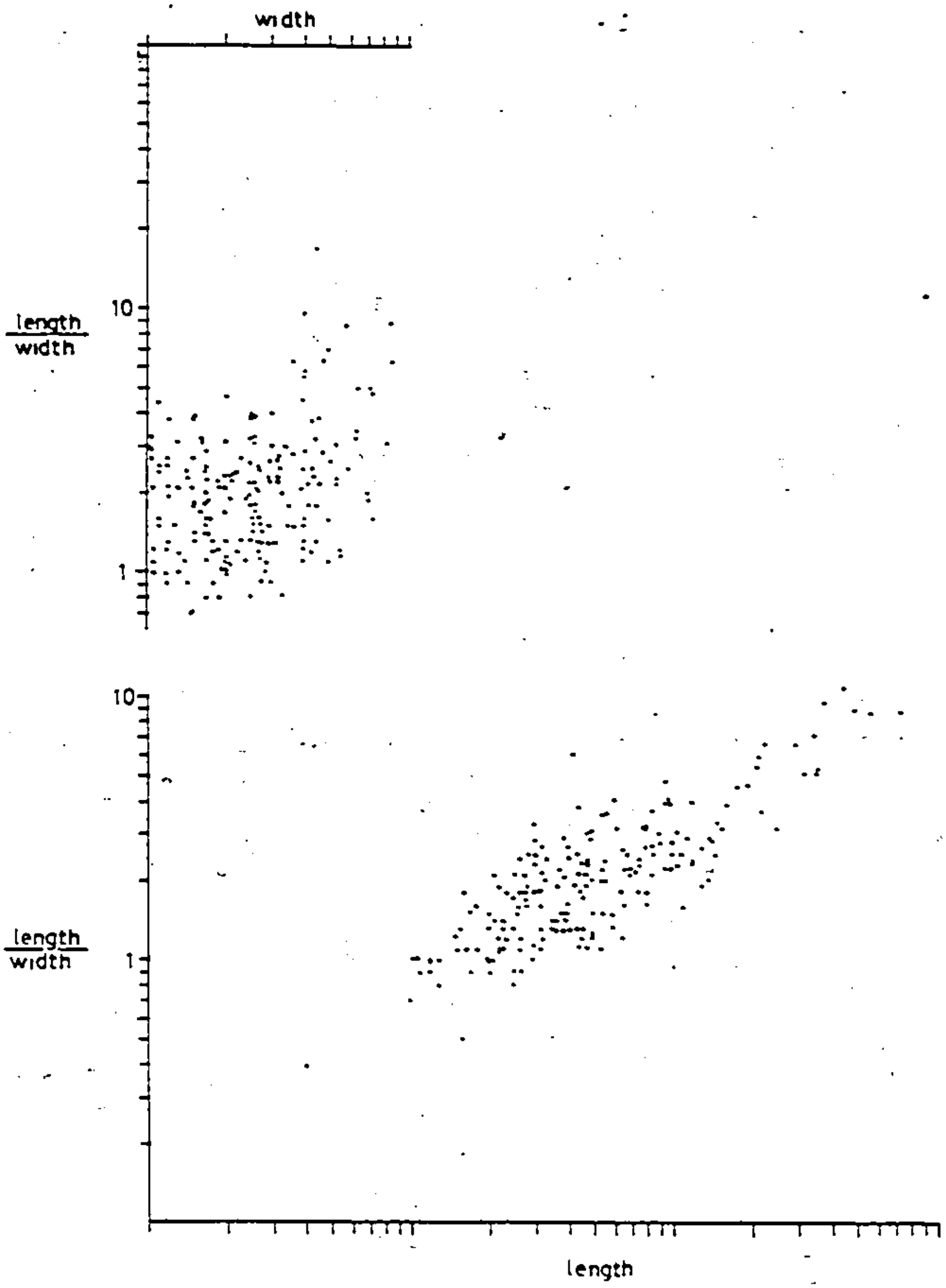

FIGURE 4.11 Variation of aspect ratio of quartz grains comprising LS1 ribbons with length and width of grains in granite gneiss from Lower Faraday Granite (497C). XZ cut of mature (MCT) microstructure.

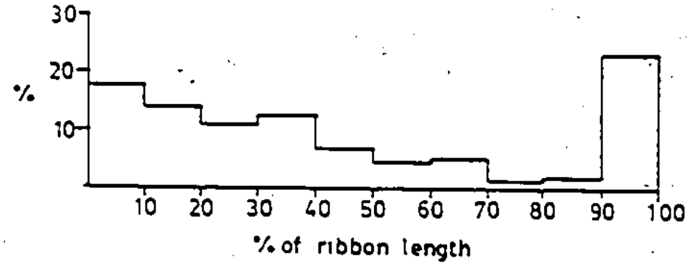

FIGURE
4.12
Frequency distribution of quartz grains according to the proportion of the quartz ribbon that they comprise. Granite gneiss from Lower Faraday Granite (497C). XZ cut of mature (MCT) microstructure.

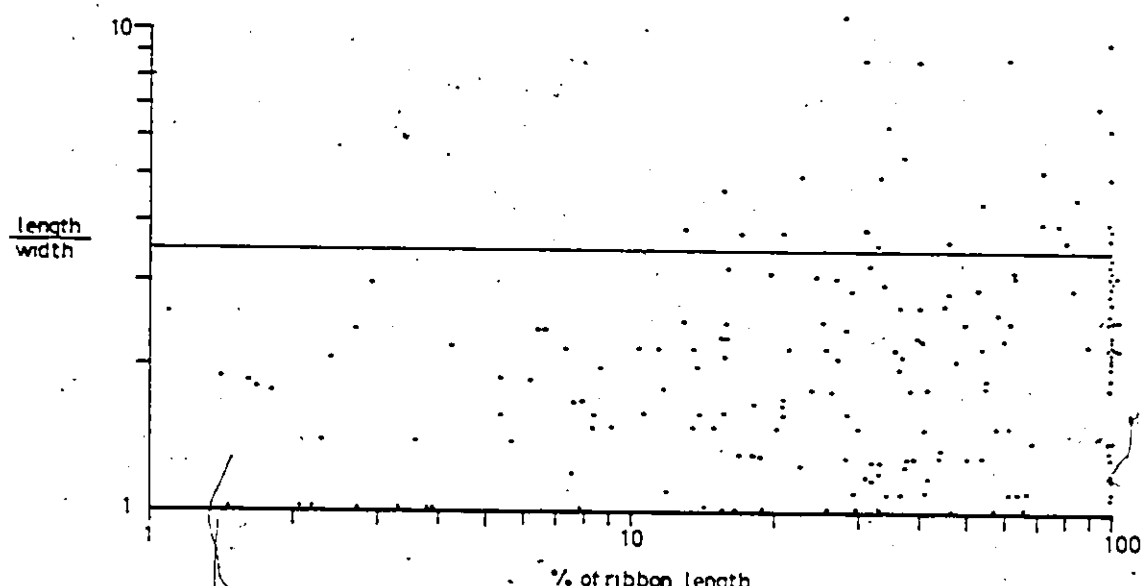

FIGURE
4.13
Variation of quartz grain aspect ratio with proportion of the quartz ribbon that they comprise. Granite gneiss from Lower Faraday Granite (497C). XZ cut of mature (MCT) microstructure.

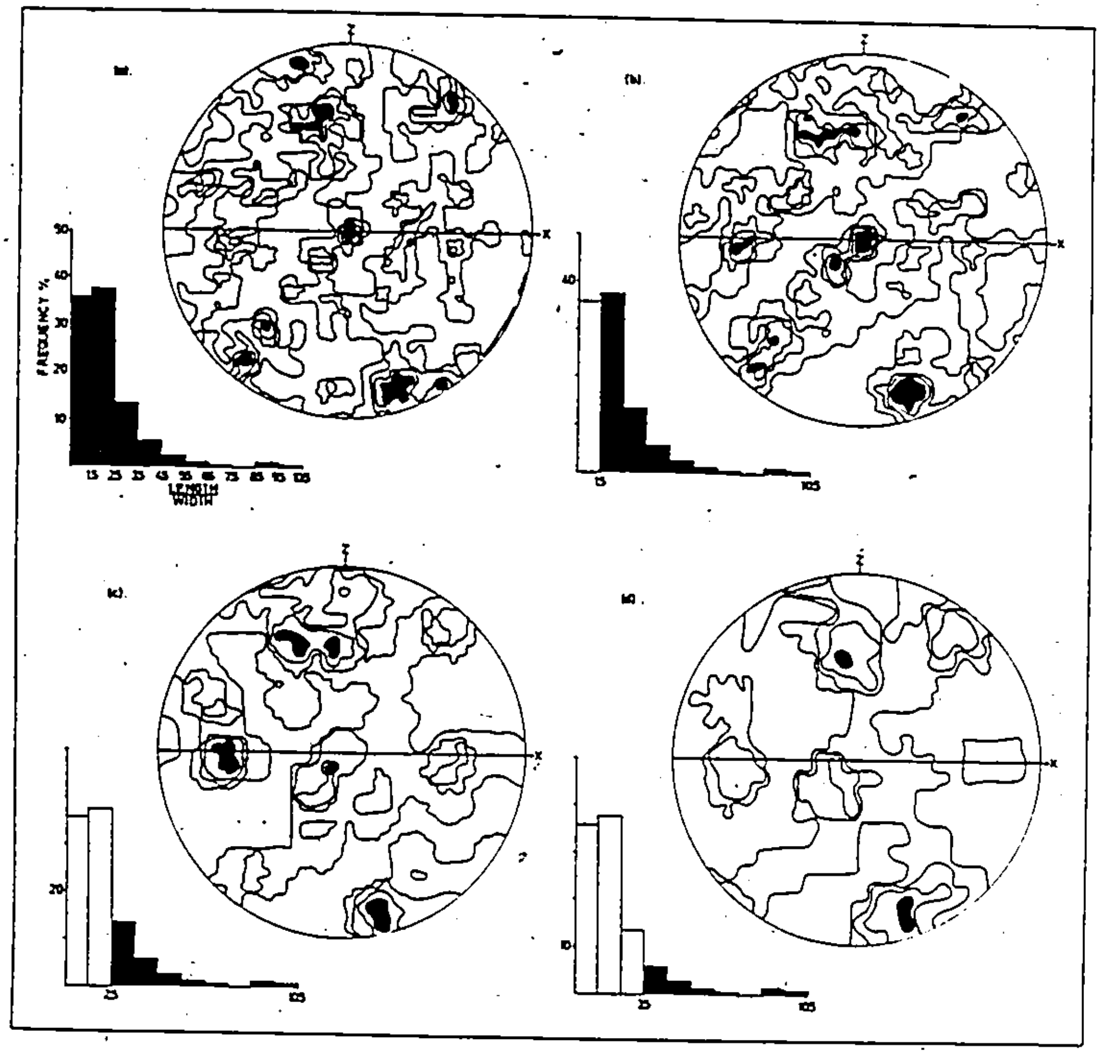

FIGURE
4.14
The cumulative effect of varying elongation of quartz grains on quartz microfabric of granite gneiss cut in XZ section, southeast to right (Specimen 497C, Lower Faraday Granite). X = L1 The sequence of microfabric diagrams is constructed by subtracting successively more elongate grains; each diagram is composed of grains in the blacked- out areas of the histograms. All contours at 1,2,3,4 points/ $\frac{100}{N}$ % of the net area; (a) maximum 8 points, N=194; (b) maximum 8 points, N=121; (c) maximum 4 points, N=49; (d) maximum 4 points, N=25

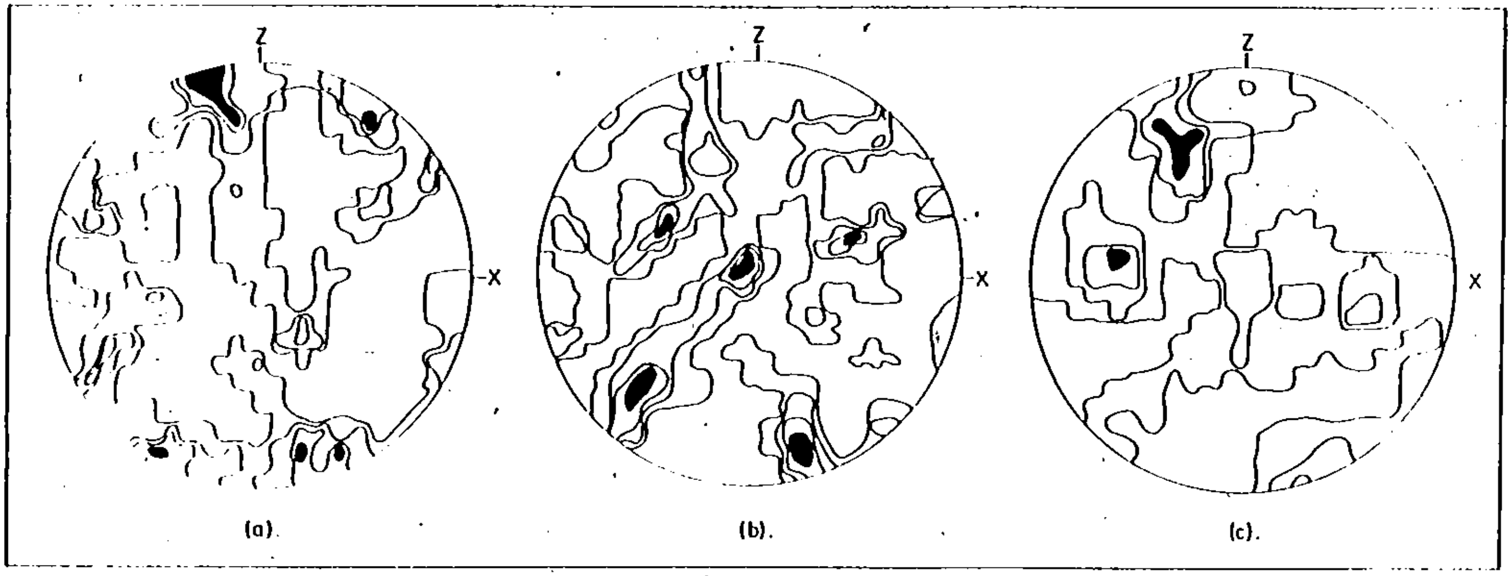

FIGURE 4.15 The effect of varying elongation of quartz grains on quartz microfabric of granite gneiss (specimen 497C, Lower Faraday Granite). X = L1 The sequence of microfabric diagrams is constructed of classes of successively more elongate grains. (a) L/W < 1.5, maximum 5 points, N=73; (b) L/W > 1.5, < 2.5, maximum 5 points, N=72; (c) L/W > 2.5, < 3.5, maximum 4 points, N=24.

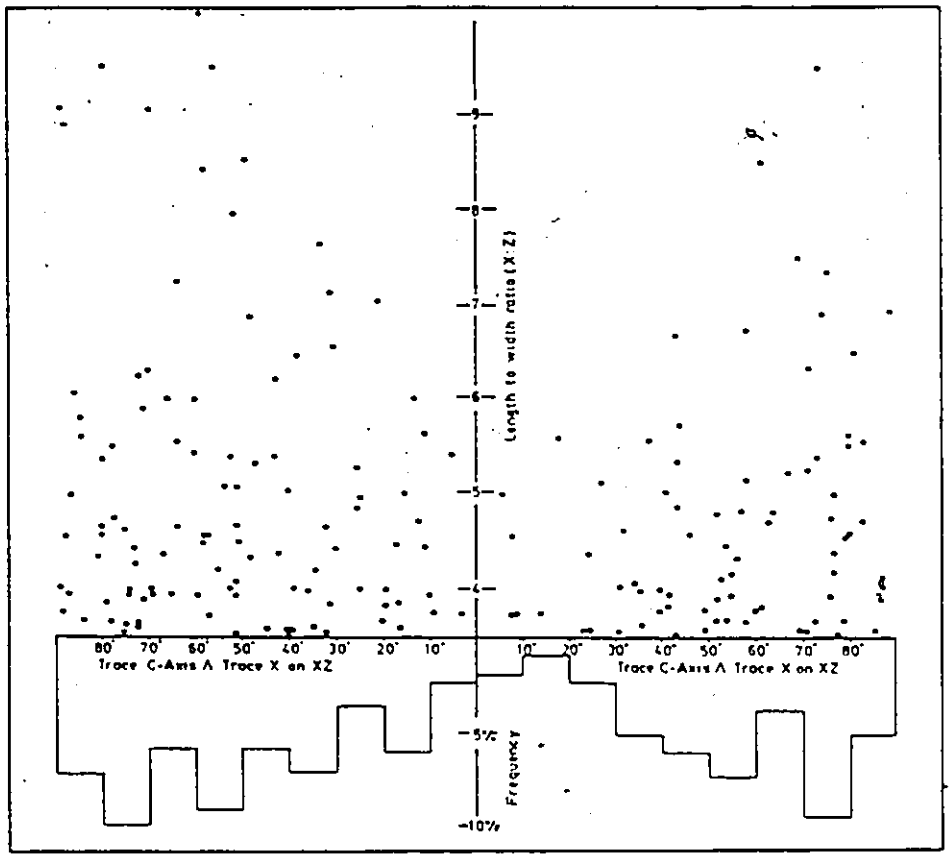

FIGURE
4.16

Trace of c-axis (flat stage) of quartz grains with aspect ratios > 3.5 in XZ plane. Measured in five specimens in granite gneiss from Lower Faraday and Cardiff Granite with MCT microstructure (1296B, 1293B, 1691B, 24101B, 22104B). In upper diagram aspect ratio is plotted against angle of trace of c-axis with lineation in XZ plane.

to width) distribution in the XZ plane is similar to that of other gneisses (Fig. 4.4, column 3). Aspect ratio shows a simple correlation with absolute length (Fig. 4.11). Longer grains have higher aspects but changes in ratio are not accompanied by a large variation in width. This reflects the overall parallel-sided shape of the ribbons and also strengthens the validity of the assumption that grain length (measured in XZ parallel to X) is simply correlated with the volumetric proportion of the ribbon comprised by that grain. The distribution of grains according to the proportion of the length of the ribbon they comprise in the XZ section (Fig. 4.12) is doubly skewed with a surprisingly high number of grains which comprise 90-100 percent of the length of a ribbon. Aspect ratio is not simply related to a grain's share of the ribbon length (Fig. 4.13). Although there is a trend toward higher aspect ratio the more a grain comprises of a ribbon there is also a family of stubby grains which make up large proportions of ribbons and, in particular, numerous single grain ribbons with a variety of aspect ratios.

The effects of varying elongation (aspect ratio) of the grains does not make an easily understandable pattern in terms of C-axis microfabrics (Figs. 4.14 and 4.15). Noteworthy is the excellent cross-girdle displayed by the most elongate grains (Fig. 4.14d). This has a strong asymmetry of maxima. This girdle is probably present in the elongate grains of many samples (Fig. 4.16).

FIGURE 4.17 The quartz c-axis microfabric of quartz grains plotted according to the percentage of a ribbon length which they comprise, in granite gneiss from Lower Faraday Granite (497) cut in XZ section with mature (MCT) microstructure. Each diagram is composed of grains in the blacked-out areas of the histograms. All contours at 1,2,3,4 points/$\frac{100\%}{N}$ of net area; (a) maximum 5 points, N=89; (b) maximum 4 points, N=46; (c) maximum 6 points, N=16; (d) maximum 7 points, N=44; (e) maximum 8 points, N=195

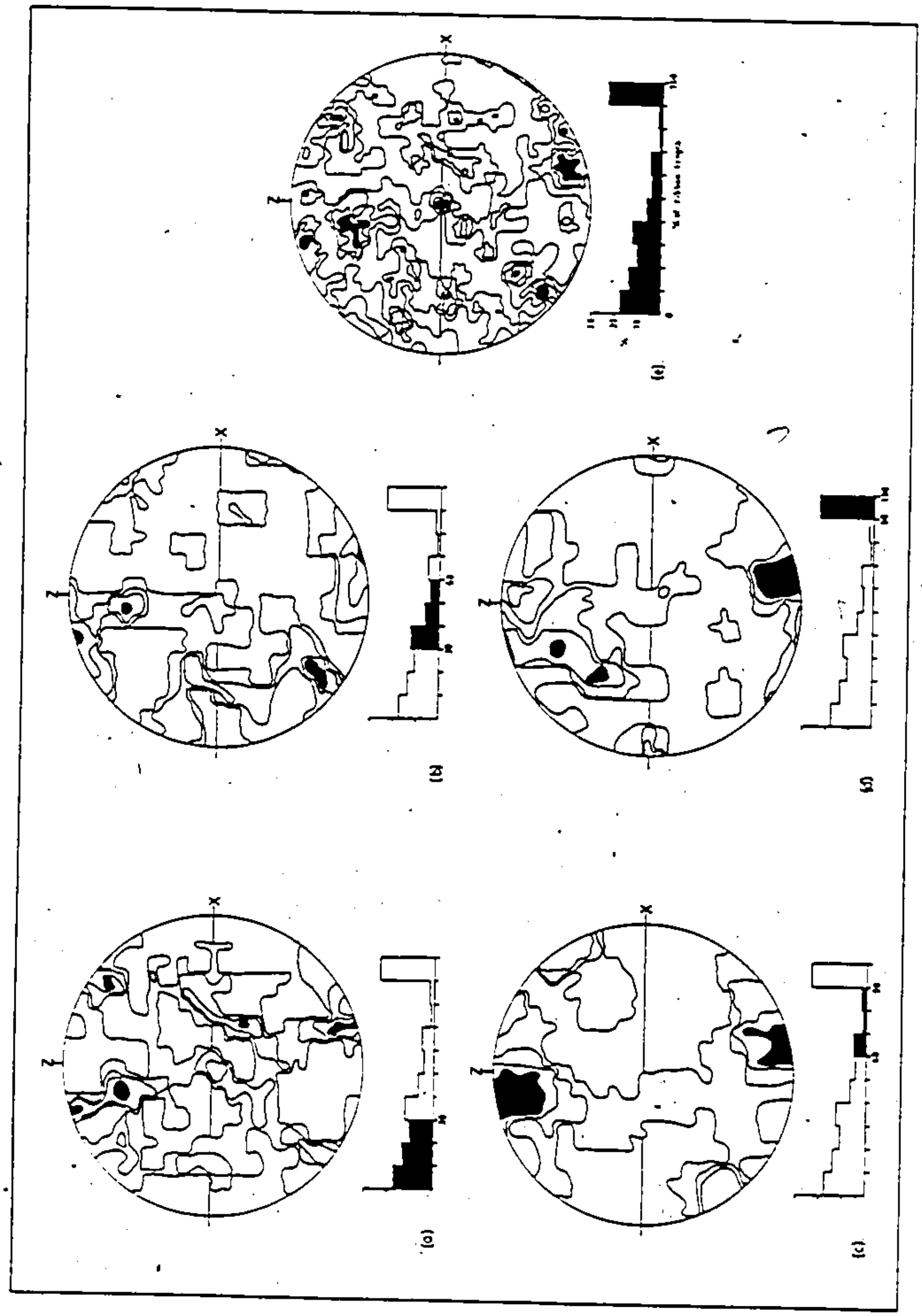

Microfabrics plotted according to their share in a ribbon's total length in XZ show an easily discernible pattern (Fig. 4.17). Grains which form 30 percent or less of the length of a ribbon display a well developed cross-girdle with two maxima symmetrically disposed to Y in the XY plane (Fig. 4.17a). (This population of grains is almost entirely distinct from that of the elongate grains showing a comparable cross girdle.) Successive groups of grains show a stripping away of elements of the modified cross-girdle until a single girdle with maxima asymmetrically disposed to Z remain in the grains making the highest contribution to ribbon-length (Fig. 4.17b,c,d).

The foregoing data suggests that the best explanation for the differences between the XZ and YZ microfabrics is based on the supposition that the YZ plane is most likely to cut those grains which occupy the greatest percentage of their parent ribbons' length. It is these types of grains which, in the sample studied, when measured in the XZ plane, have C-axis microfabrics most similar to microfabrics measured in YZ plane.

The microstructural data and the existence of a strong relationship between contribution to ribbon length of a grain and quartz C-axis orientation may be interpreted as resulting from oriented grain growth during metadynamic recrystallization. That is to say those grains making the highest contribution to ribbon length, which have particular microfabrics, grew during metadynamic recrystallisation at the expense of grains of the type which make the least contribution to ribbon length, which have a distinct but related microfabric. This is a confirmation of the hypotheses of Bouller and Bouchez (1978).

The cross-girdle of the grains which form less than 80 percent of the ribbons of which they are members may be interpreted as a record of the microfabric of dynamic recrystallisation, if, as appears to be the case, its component grains are being consumed during a metadynamic stage of primary recrystallisation.

There is experimental evidence that dynamically recrystallised quartzites deformed at high temperature in plane strain will produce cross girdle microfabrics similar to that of the low percentage grains (Green et.al. 1970). It is relevant that microfabrics produced during dynamic recrystallization are considered to be essentially little altered, somewhat more diffuse, versions of their parents (Cahn 1965, White 1976, Wilson 1973) and that continuing intracrystalline slip very quickly readjusts the microfabric (Lister and Price 1978). However the reason why certain orientations have less strain energy than others, and therefore grow at their expense, is not immediately clear. We may speculate that this is related to the relative ease of slip on the various slip systems operative during the deformation and to the orientation of grains with that slip-system relative to the flow direction. More specifically we may speculate that grains lying with the softest-slip system parallel to the plane of highest resolved shear stress (the flow plane in simple shear) will grow at the expense of other grains during dynamic and metadynamic primary recrystallisation. This model is analagous to that proposed by Urai and Humphreys (1981) to account for dynamic oriented growth of camphor. Furthermore it is informative to compare the possible dynamic fabric (Fig. 4.17a) with that produced by computer simulation of a model quartzite deformed by simple shear (Model quartzite C of Lister and Hobbs 1980, Fig. 4.15), not only is one arm of the cross-girdle better populated than the other (that near perpendicular to the XY plane) but there is a similar clustering of grains in the XY plane. In this model quartzite of Lister and Hobbs the basal <a> slip system is one of the softest, metadynamic growth of grains with the basal plane in the flow plane would result in a pattern of preferred orientation comparable to that shown by grains forming the highest proportions of the ribbons (Fig. 4.17c, d).

From the synoptic diagrams of the XZ and YZ samples (Fig. 4.10) and from the microfabric-microstructural relationships described, it may be inferred that for most of the samples, the grains which grew the most during metadynamic recrystallisation had their C-axes oriented parallel to Y (Fig. 4.10a). Likewise most probably the dynamic microfabrics may be represented by the stubby grains of the XZ sample (Fig. 4.10b). Again comparing with the simulations of Lister (1979, 1981) a model quartzite is found

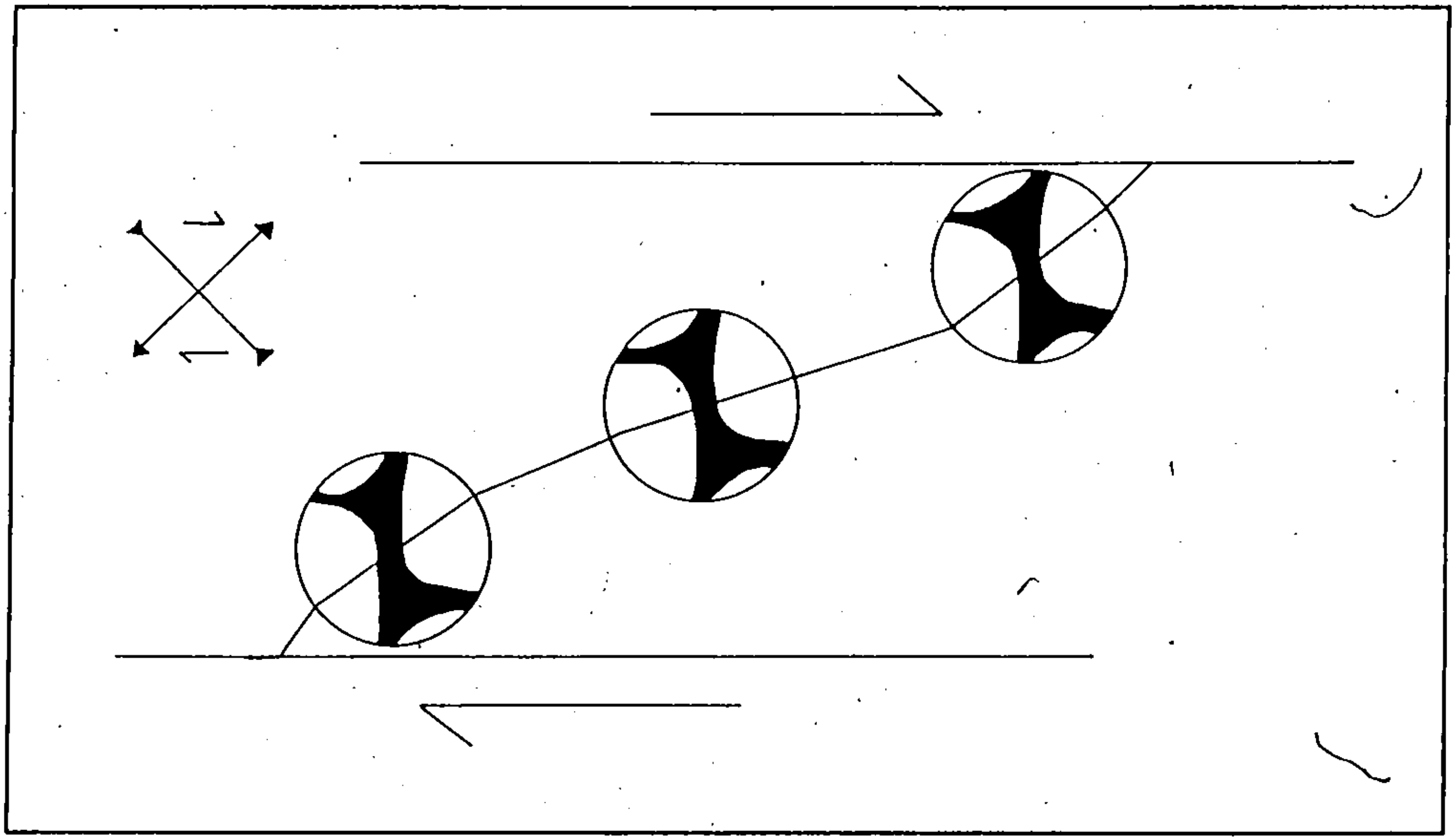

FIGURE 4.18 Illustration of theoretical control of microfabric by kinematic framework. Here the case of simple shear is shown, with instantaneous stretching axes. The angle between the girdle and the shape-fabric varies with strain; the direction and sense of shear is uniquely indicated. After Lister and Williams 1979.

which has a cross-girdle with a wide opening angle and an extremely soft prism <a> slip system (Lister 1979, Fig. 4.4d). Those grains with this slip system lying perfectly oriented in the flow plane (i.e. those with the C-axis parallel to Y) would be candidates for metadynamic oriented growth populating the YZ sample. If the strain history were non-coaxial, one arm of the cross-girdle would be overpopulated (Fig. 4.10b), a pattern which would appear in the XZ sample.

4.2.5. Microfabrics and Strain History of LS1

C-axis microfabrics may be interpreted in terms of their strain history, if they have been primarily produced by intracrystalline slip. Computer simulations of microfabric development (Lister 1974, Lister et al 1978, Lister and Paterson 1979, Lister and Williams 1979, Lister and Hobbs 1980, Etchecopar 1977) show that the important distinction between coaxial and non-coaxial strain histories may be made on the basis of the microfabric since the preferred orientation is controlled by the kinematic framework and not by the axes of finite strain. In general, the presence of a non-coaxial event is shown by the asymmetry of elements of the microfabric with respect to the axes of finite strain, which may be approximated by the shape fabric axes. The computer simulations predict that for all model quartzites there will be an asymmetry of microfabric skeleton with respect to shape fabric and, for some models,

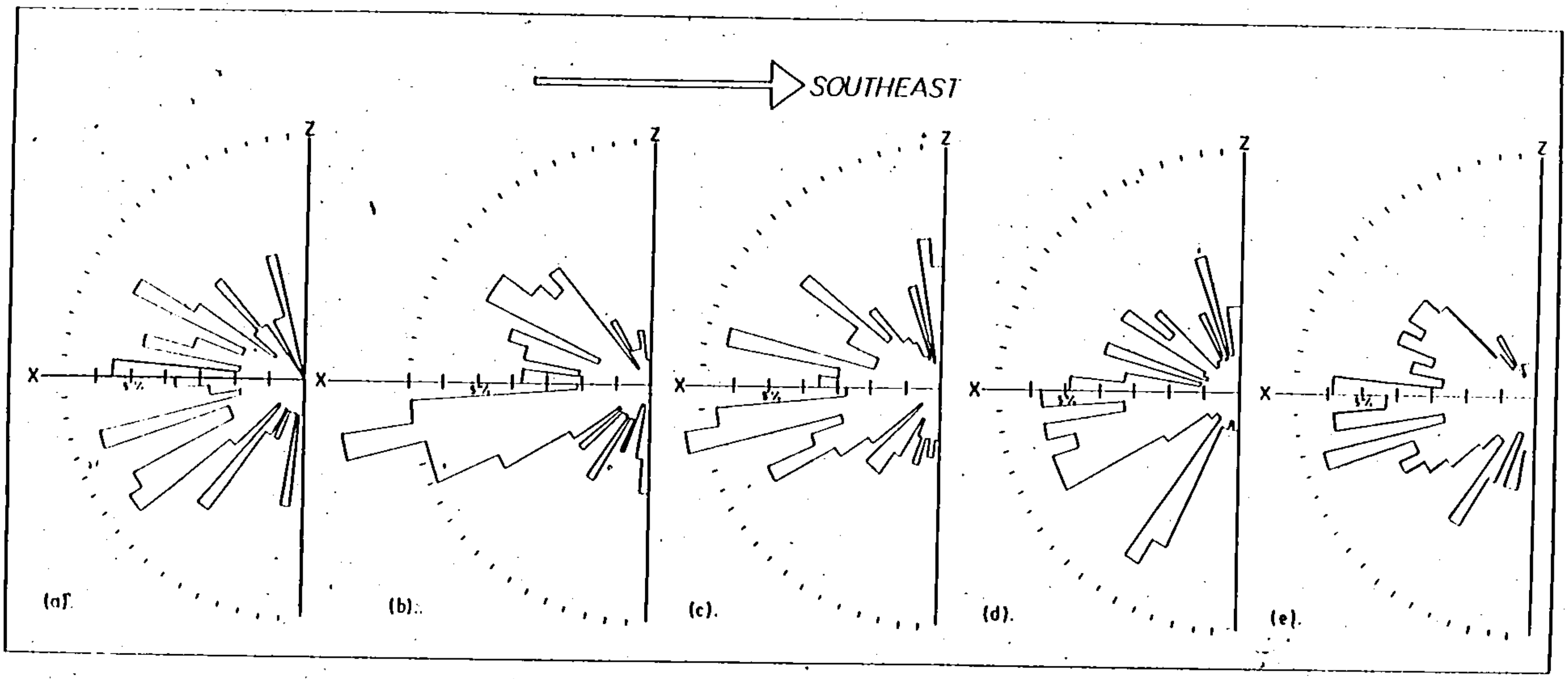

FIGURE 4.19 Rose diagrams of trace of basal planes of quartz on XZ (LS1) plane of granite gneiss from Lower Faraday granite; (a) 1296B, YZ sample; (b) 1092B, XZ sample; (c) 497C, YZ sample; (d) 22103B, YZ sample; (e) 895C, YZ sample. Number of data as in c-axis diagrams (Fig 4.6).

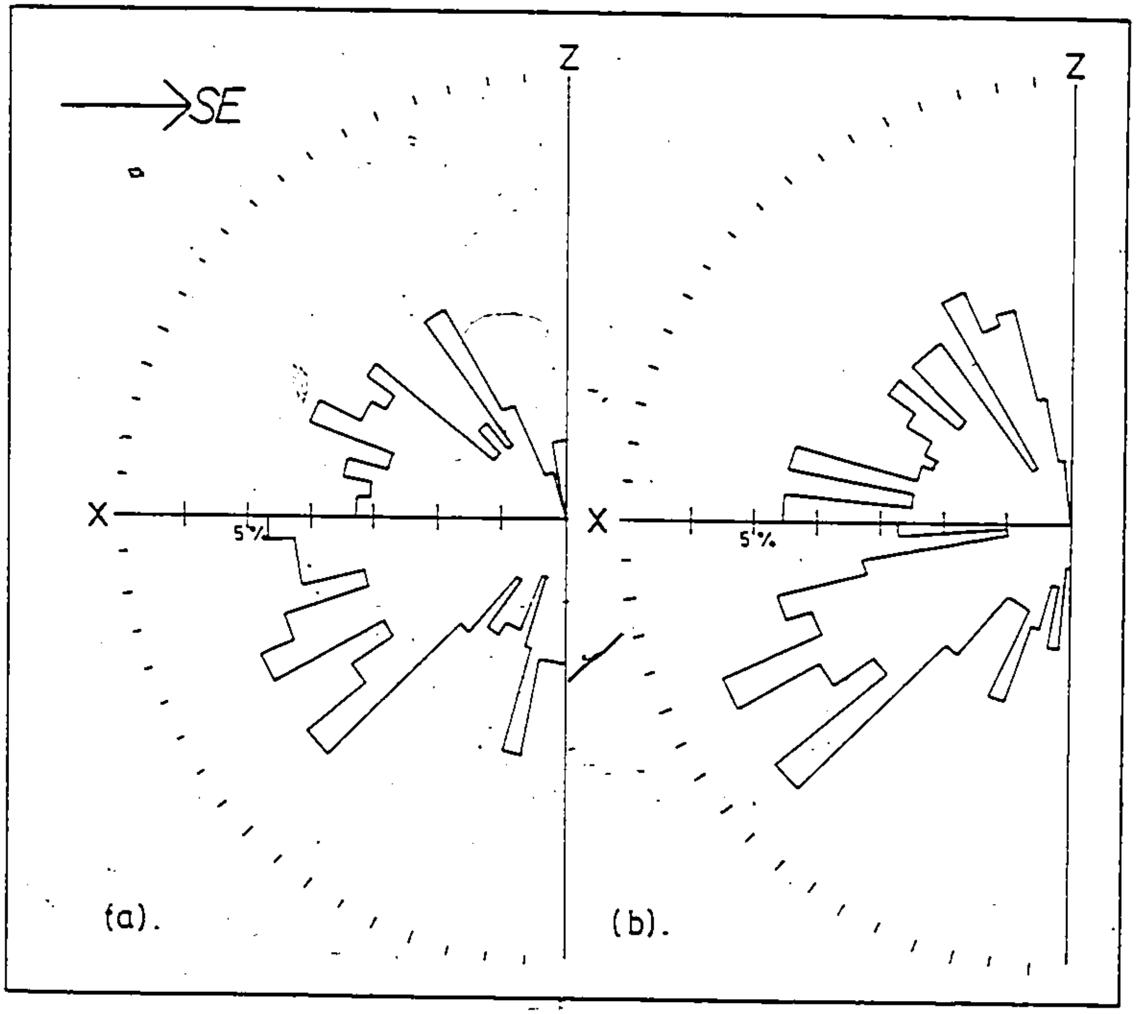

FIGURE 4.20 Rose diagrams of trace of basal planes of quartz on XZ (LS1) plane of granite gneiss from Cardiff Complex; (a) 25101B, YZ sample; (b) 24101B, YZ sample.

the majority of basal planes would lie in the flow-plane (Lister and Hobbs 1980, Etchecopar 1977).

Natural examples of microfabrics in shear-zones of known displacement strongly favour the contention that C-axis girdles tilt toward the shape fabric in the shear sense (Fig. 4.18) and that the girdles are perpendicular to the flow plane (Eisbacher 1970, Lunardi and Baker 1975, Bossiere and Vauchez 1978, Burg and Laurent 1978, Bouchez 1977, 1978, Berthé et al. 1979, Brunel 1980, Bouchez and Pêcher 1981, this study, in relation to LS2 microfabrics). Such girdles should also dispose a maximum of traces of basal planes parallel to the trace of the shear plane on the XZ plane.

Of the individual microfabric diagrams half of the well defined girdles (YZ sample) are orthorhombic at a low contour value level with respect to the shape fabric axes; of the YZ sampled microfabrics two have asymmetric high and low value contours (Fig. 4.6f, Fig. 4.9b). The best defined XZ sampled cross-girdles are all either asymmetric (Fig. 4.7a,b) or unequally populated (Fig. 4.9a,b,c); the synoptic diagram of the XZ sample (Fig. 4.10b) has a strongly defined southeast tilted girdle. Rose diagrams of the trace of the basal plane of quartz on the XZ plane brings out the asymmetry very clearly for the Lower Faraday Granite and the northern part of the Cardiff complex (Fig. 4.19, Fig. 4.20). In all cases, the asymmetry is consistent with shear of upper layers to the northwest (Fig. 1.1b).

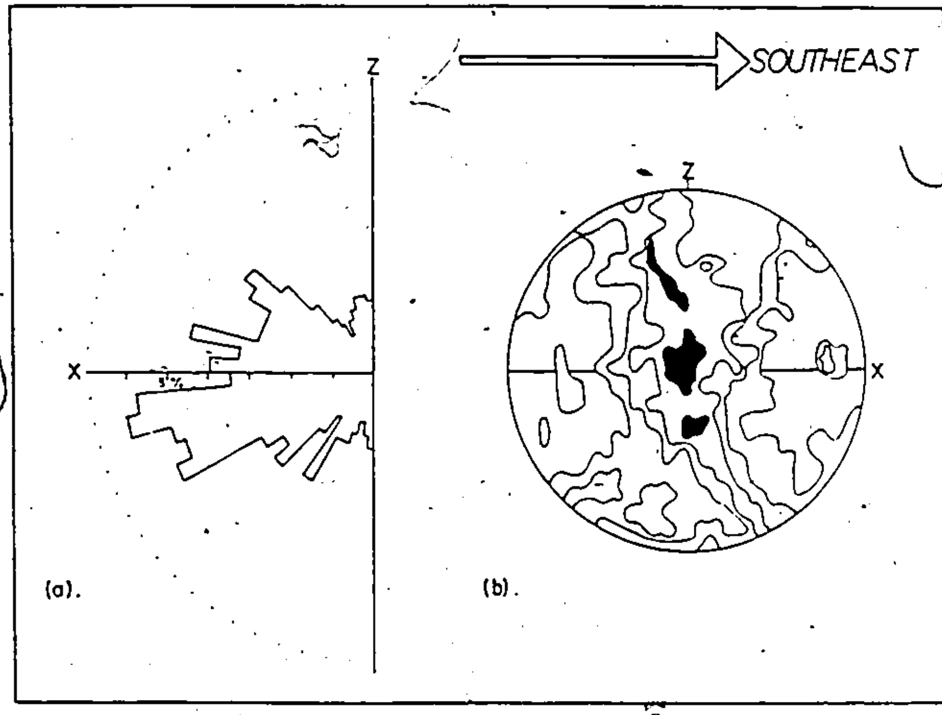

FIGURE
4.21

Synoptic microfabric diagrams for quartz of the Lower Faraday Granite, formed by combining data from individual diagrams of figure 4.6, b-f, (N 876); (a) rose diagram of trace of basal planes on XZ section; (b) quartz c-axis diagram; contours at 0.5, 1, 1.5, 2%/1% area; maximum 4%.

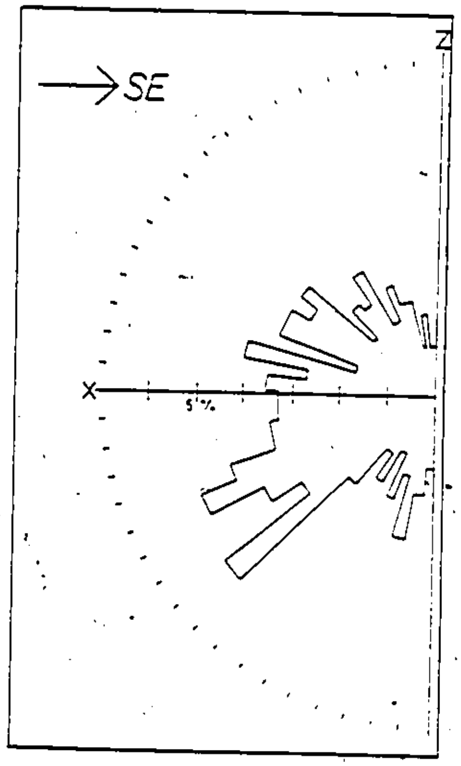

FIGURE 4.22 Synoptic rose diagrams of trace of basal planes of quartz on XZ (LS1) plane for Cardiff Complex (N=400).

An important constraint of the Taylor-Bishop-Hill model used in the computer simulations of microfabric development (Lister 1974) is that the undeformed aggregate has no initial fabric. An initial asymmetry will be reflected in the final microfabric leading to possibly erroneous conclusions concerning the kinematic regime. In order to ensure as large a number as possible of initial orientations Van Roermond et.al. (1979) recommend that data from a large number of specimens be combined in one synoptic diagram, providing that all the samples appear to have suffered a similar strain history. This constraint of homogeneous deformation at all points is probably met by the Lower Faraday granite gneiss (Fig. 1.2). It is marked by only minor variations in the relative strength of the planar and linear elements of the shape fabric (Fig. 3.7). The amount of strain variation judging qualitatively from grain size and quartz ribbon aspect ratio (Fig. 4.4) is probably appreciable but not an important factor, affecting fabric strength and not fabric type (Lister and Hobbs 1980).

Five samples from along the strike of the granite sheet (Fig. 4.6b,c,d,e,f) contribute to the synoptic diagram (Fig. 4.21). The YZ sample plane is strongly favoured (>75% of all data). The resultant well defined microfabric of this substantial gneiss sheet (Fig. 4.21b) is asymmetric at all contour value levels, increasingly so at the higher values. A rose diagram of the basal trace on the XZ plane highlights the asymmetry (Fig. 4.21a). A comparable asymmetry is shown by a synoptic rose-diagram for samples from the north of the Cardiff complex (Fig. 4.22). The relatively weak asymmetry of the microfabric outline, the lowest value contour in (Fig. 4.21b) compared to that of the maxima may be attributed to the imposition of a late coaxial strain on a microfabric produced mainly by northwest directed simple shear of upper layers relative to lower (Lister and Williams 1979).

4.2.6 LS1 Microstructure of Quartzites

The typical quartzite of the area is coarse grained and has a strong planar linear fabric (LS1) formed by the dimensional orientation of mafic minerals (Plate 15). This coarse grained structure is interpreted as having been formed by exaggerated grain-growth (Wilson 1973, Bouchez and Pêcher 1981) at the same time as the LS1 ribbons in the granite gneiss. Superimposed on this structure are a variety of substructures interpreted as being of LS2 age, and in some cases possible precursors of LS2 quartz foliations.

The coarse quartz grains have at best a crude shape fabric. The impression that these rocks have been strongly deformed is gained mainly from the excellent fabric of non-quartz minerals such as biotite, clinopyroxene, feldspar, carbonate, sphene, amphibole or magnetite (Plate 15). These usually have a strong preferred orientation of shape, the long axes of elongate minerals lying parallel to the regional L1 lineation. The foliation so defined lies parallel to layering and the long axes of the weak shape-fabric of the quartz grains. An exception to this is found in Domain 21, a zone of steeply dipping northwest striking foliation. In these rocks in sections perpendicular to the lineation a moderately inclined foliation defined by the inclusions of calcite, clinopyroxene and feldspar transects the steeply dipping layering and vestiges of a quartz shape fabric. This foliation dips southeast with a trace on the layering lying parallel to the southeast plunging L1 lineation formed of quartz-ridges and aligned clinopyroxenes.

Feldspar and pyroxene inclusions show some interesting variations in morphology. Although they are always extremely well aligned, in some specimens they are rectangular whereas in others they are lense or cigar-shaped and have high aspect ratios. In some of the latter cases perfectly aligned trails of tiny fragments extend in the foliation like minute boudins (Plate 15d), obviously marking an extension direction. This fragmentation is comparable to that of clinopyroxene in a LS2 quartzite tectonite. The biotite in these rocks also has a high degree of preferred orientation, indicated by the high aspect ratio and the sharpness of the trace of the basal cleavage (Plate 15e). Undoubtedly these rocks have been strongly deformed.

The size and shape of the quartz grains appears to be strongly dependent on the number and arrangement of non-quartz phases present. Variations in the number of non-quartz grains (feldspar, clinopyroxene, biotite, sphene) in one thin section can result in large variations of grain size (Plate 15b,c). This control does not apply to second generation LS2 grains which are uniformly fine. The commonest grains, coarse and very coarse, vary from a half centimetre up to several centimetres in their longest dimension. Inclusions of non-quartz phases may "float" within the grain or sit on the grain-boundary (Plate 15), very commonly at the locus of a change in direction of the boundary. Such changes are very often orthogonal giving the grains an irregular stepped and blocky character to their somewhat elongate outline. The stepped and box-shaped three dimensional outline bears no resemblance to a clastic texture (Plate 15).

Some samples have layers of considerable feldspar content. Depending on the dispersion or continuity of this feldspathic matrix the quartz grains may form long aggregates which are identical to the ribbons of the granite gneiss (Plate 15).

The variation of the grain size with the density of other minerals and the location of these minerals at boundary steps indicates that these minerals pinned the grain boundaries during grain growth. That most of the grains exceed by far the size of the original grains is indicated by the numerous inclusions within the large grains (Plate 16). A rare fine grained sample (1-0.5 mm) has equant quartz grains with 30-40 percent evenly dispersed amphibole located at the grain boundaries. The lack of amphibole inclusions within the quartz indicates that minimal grain growth occurred, possibly hindered by a critical density of the second phase.

In detail the grain boundaries are smooth to moderately irregular. Lobate very irregular boundaries are increasingly frequent with the appearance of a strongly developed subgrain substructure and evidence for recrystallisation which postdates the main grain-growth phase.

In a sample from a northwest striking steeply dipping quartzite, in which the inclusion fabric transects the layering, the quartz grain shapes are modified. In sections perpendicular to the lineation grains with irregular but equant outlines are common. In sections parallel to the lineation all grains are elongate and grain boundaries are regular to moderately lobate. In these specimens it seems likely that the formation of the equant (in YZ section) grains is simply a function of strain history and occurred during the main growth period, since the intersection of these grains on the layering forms a ridging lineation, absent in SE dipping quartzites, and substructure in these rocks is otherwise identical to that in other LS1 quartzites.

In all samples, quartz grains have a variably developed sub-grain substructure. These subgrains, several hundred microns across, have square, rectangular or lensoid shapes. Misorientations between traces of C-axes are often as high as 10°. Such substructures are usually considered to mark a period of deformation later than the exaggerated grain growth phase (Wilson 1973, Bouchez and Pêcher 1981).

A set of small grains, from 50 to 500 μm in size, is present in varying proportions (from less than 1 percent to 30 percent). They are evidently related to the subgrains since they often appear within areas of old grains where lattice distortions are highest. Above a certain size these new grains have undulatory extinction and very irregular lobate grain boundaries. Irregular mobile boundaries are always accompanied by a strongly developed substructure regardless of whether or not new grains are present. Occasionally these boundaries may be observed to transect and remove features such as boehm lamellae which are related to the first grain growth.

This substructure of subgrains, highly irregular grain boundaries and/or small new grains is probably equivalent to the LS2 microstructure, which it closely resembles in detailed grain-boundary morphology although the LS2 quartz foliation is lacking. The clearest evidence for this is in an example of significant microstructural change which takes place on the scale of the outcrop in samples of quartzite from near the east shore of Pusey Lake, north of Wilberforce (Fig. 1.2). The sample site is in a broad swath of gently southeast dipping foliation which flanks the northern side of the Cardiff complex and in which three of the LS2 samples are situated. The most microstructurally altered specimen comes from near the contact of a thick quartzite unit with an overlying highly deformed syenite gneiss. The second sample, which shows a well preserved LS1 microstructure, was taken some three metres structurally lower. There is no discernible difference between the samples in hand specimen.

In thin section the second sample shows all the features typical of the exaggerated grain growth microstructure, coarse quartz grains with stepped outline, moderate undulatory extinction and grain boundaries free from small-scale irregularities (Plate 16a,b). In the quartzite from close to the syenite the quartz microstructure is radically different: grain boundaries are irregular, indented and lobate (Plate 16c,d); although the broad outlines of the LS1 grain shape is still discernible new grains with ragged outlines project into and transect old ones (Plate 16c,d); subgrains, undulatory extinction and deformation bands are now very well developed with misorientations in excess of 10°. In this sample, in contrast to the unmodified sample, plagioclase and biotite are altered to a very fine micaceous aggregate.

The similarities of this microstructural modification with that generally effecting the exaggerated grain growth microstructures are great. The main differences are in the great extent of grain boundary migration in this sample. Likewise, the differences with LS2 tectonites are mainly those of degree, a quartz foliation is not developed although the detailed grain boundary shape is very similar and the microstructure clearly post-dates the LS1 microstructure. A correlation is therefore probable on temporal and some morphological grounds between the widespread and relative minor alteration of the LS1 quartz microstructure and the formation of LS2 tectonites.

4.2.7 LS1 C-Axis Microfabrics of Quartzites

Only six quartz C-axis microfabrics were measured, enough to establish that kinematic information was not easily forthcoming from them and that they are essentially similar to others from quartz tectonites displaying exaggerated grain-growth microstructures.

All the microfabrics have very strong maxima most of which are not readily related in any consistent fashion to the foliation (e.g. Figs. 4.23b, 4.25b). Among these there are patterns with both large and small pole-free areas (Figs. 4.23b, 4.25b and 4.25a respectively). It is noteworthy that the patterns with large pole free areas are displayed by rocks with microstructures in which the exaggerated grain growth microstructure, although still recognisable, has been extensively affected by the second recrystallisation and grain growth event. In the case of the two samples from the outcrop-scale microstructural transition (Plate 16, Fig. 4.25) it is evident that the development and movement of very irregular grain boundaries, is accompanied by the development of the large pole free area and the consolidation of the pattern which, while

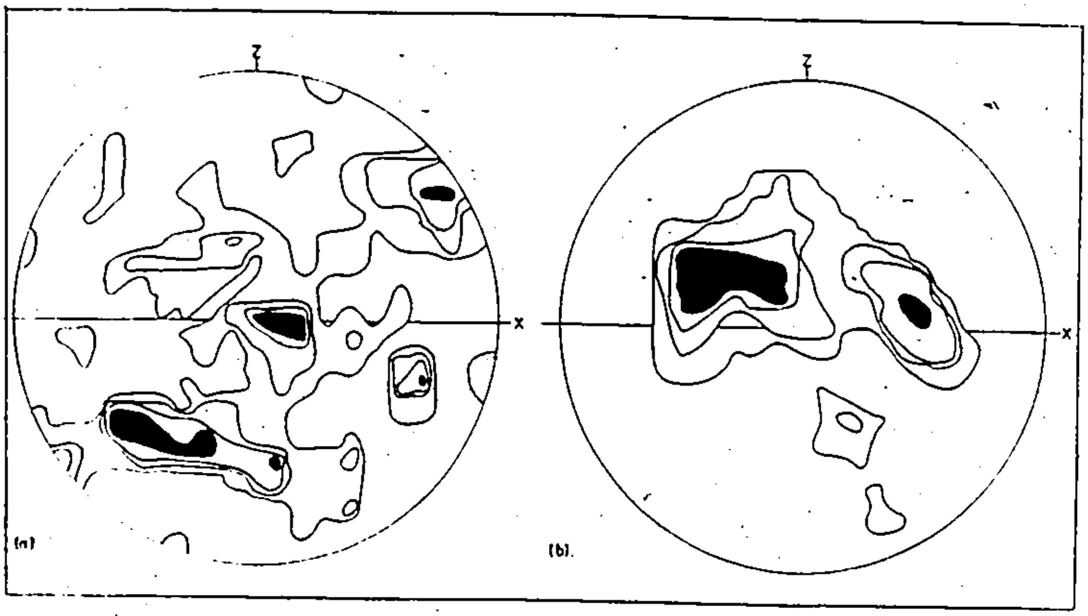

FIGURE
4.23

Quartz c-axis microfabrics from quartzites with LS1 fabric. (a) quartzite with pink feldspathic layers from west of Grace Lake (1391C); contours at 1,2,3,4%/1% area; maximum 8%; N=200. Coarse, medium and fine grained quartz of the first phase of grain growth (LS1) is sampled. (b) quartzite from northeast of Farquhar Lake (2465C); contours at 1,2,3,4%/1% area; maximum 13%; N=200. Coarse-grained quartz of the first phase and fine-grained of the second phase of grain growth is sampled. South east to left.

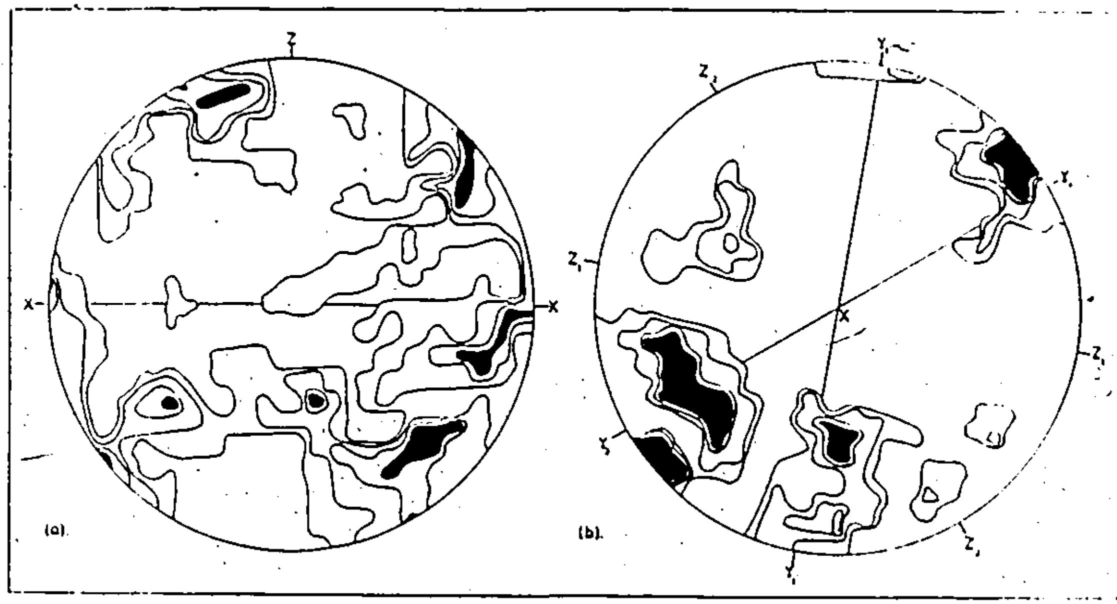

FIGURE
4.24

Quartz c-axis microfabrics from quartzites with LS1 fabric. (a) quartzite from Burnt Creek Area; contours at 1,2,3,4%/1% area; maximum 8%; N=100. Fine-grained quartz of first phase of grain growth is sampled. South east to right. (b) quartzite from south of Miskwabi Lake; contours at 1,2,3,4%/1% area; maximum 6%; N=200; a foliation of elongate clinopyroxene, sphene and carbonate (XY_2) transects an earlier foliation (XY_1) defined by the layering and the elongation of some quartz grains.

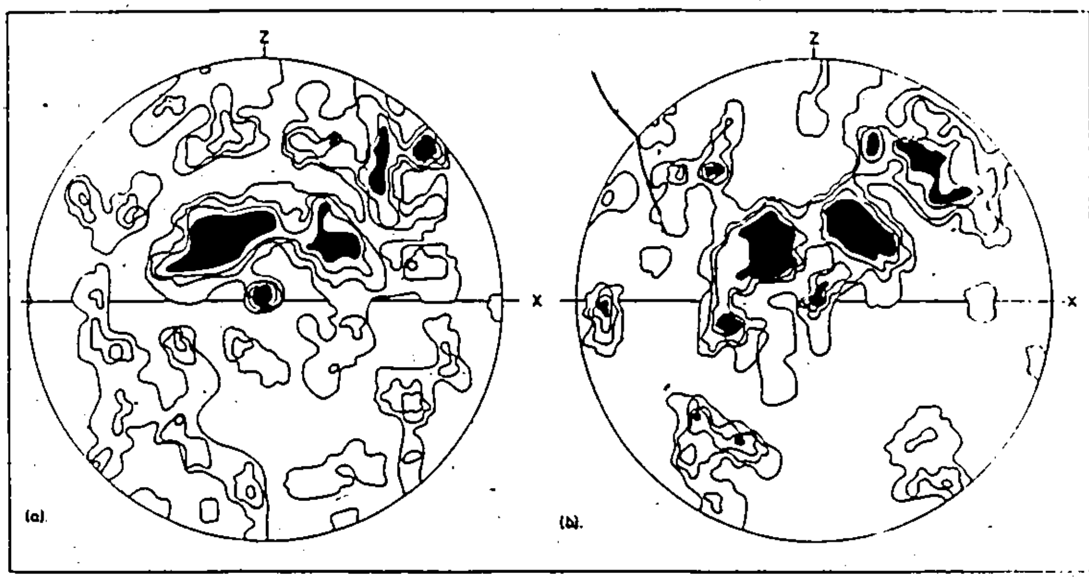

FIGURE
4.25

Quartz c-axis microfabrics from quartzites. (a) and (b) quartzite from east of Pusey Lake (12101D); sampled at same outcrop, (b) is the closest to an overlying gneissic syenite; contours in both at 1,2,3,4 points/0-5% of area; maximum in (a) 14%, in (b) 20%; N=200; (a) has typical coarse grained microstructure of LS1; (b) has this microstructure modified by second phase grain growth of probable LS2 age, southeast to the right.

retaining the strong maxima of the original microfabric, now has an asymmetric girdle.

A quartzite in which both very coarse grains and medium to fine first generation grains are present (Fig. 4.23a) has a highly asymmetric girdle with several very strong sub-maxima, the girdle appears to split at one end into a small circle girdle with a wide opening angle, asymmetrically disposed around Z. The microfabric of a uniformly fine-grained sample (Fig. 4.24a) has in common with the previous pattern the asymmetric small circle girdle around Z. Both may be described as embryonic cross-girdle patterns.

A sample with transecting foliations from folded quartzite has a preferred orientation most strongly related to the fabric axes (Fig. 4.24b), maxima are located close to the Y direction of both foliations, large pole free areas are present.

The patterns with strong maxima unrelated to the meso-scopic fabric are comparable to patterns reported in Australian quartzites which had exaggerated grain-growth micro-structures (Wilson 1973). Also broad girdles with subsidiary maxima are reported from the Australian rocks as well as from Himalayan quartzites with exaggerated grain growth (Bouchez and Pêcher 1981). It must be noted however that the present example of this pattern (Fig. 4.23a) has much input from medium and fine grained quartz and that the resemblance of this pattern to that of the fine grained quartzite in which exaggerated grain growth has not taken place cannot be accidental (Fig. 4.24a).

4.2.8 C-Axis Microfabric and Microstructural Evolution of Quartzites

Since most of the quartzites in the area are coarse grained, it is likely that as in the samples examined they have exaggerated grain growth microstructures. This type of grain growth is well known to be the last stage of secondary recrystallisation (Fig. 4.2), the final process in the post deformational evolution of a monomineralic or metallic aggregate (Cahn 1965, Wilson 1973, White 1976, Bouchez and Pêcher 1981). It may thus have some use as a time marker, of value in polycyclic terrains.

There is general agreement that the driving force for grain growth at this stage is surface energy and that the end result is a strong preferred orientation unrelated to the mesoscopic fabric. There are several theories why a limited number of grains should grow so large at the expense of so many others. The theory that is considered most suitable for these rocks envisages a very strong microfabric of primary recrystallisation seeded with a few 'rogue' grains which have a misorientation with respect to the majority of the grains such that grain-boundary mobility is at a maximum. Note that such 'rogue grains' would most probably not be lying in or near a symmetry plane of the mesoscopic fabric unlike the grains contributing to the earlier microfabric (Cahn 1965, Wilson 1973). This explanation fits well in rocks such as those in which there is much evidence for plastic strain. An unfortunate result of the development of a new microfabric so late in the history is a complete loss of kinematic memory.

Samples with a high percentage of medium and fine grains (Fig. 4.23a, Fig. 4.24a) have a large proportion of non-quartz inclusions which would have ended grain growth quickly and thus the microfabric will record a stage of microstructural evolution earlier than exaggerated grain growth (Fig. 4.2).

It has been shown that significant microstructural and microfabric changes caused by late deformation can occur at the outcrop scale in the quartzites. The microstructural change may be interpreted as the beginning of a strain energy driven grain growth event wherein lobed irregular grain-boundaries have formed in order to multiply grain boundary area (Nicolas and Poirier 1976). The accompanying C-axis microfabric change agrees well with the conclusions of Lister and Williams (1979) that the skeletal outline of a pattern of preferred orientation is very sensitive to late stage movements which should however leave already formed point-maxima undisturbed. The microfabric may therefore be considered a compound LS1 and LS2 fabric. The newly formed asymmetric girdle (Fig. 4.25b) should be compared to microfabrics from nearby LS2 tectonites (Fig. 4.26b,d,e), the main differences being that this girdle has LS1 type maxima and is asymmetric with respect to LS1, whereas LS2 girdles are asymmetrical with respect to LS2 and orthogonal to LS1, although the sense of asymmetry, and thus the kinematic significance, is the same as that in the LS2 tectonites.

The folding present in zones of north west striking foliations modifies the original exaggerated grain growth microstructure. The new microstructure, although distinct morphologically, is similar to the earlier one in other respects there being no drastic reduction in grain size. It is probable that this reflects similar temperature and pressure conditions before and during the folding. This is in agreement with the fact that throughout the area similar minerals are found in S1 and S2.

4.2.9 Why Quartz Ribbons in Granite Gneiss Remember Dynamic Recrystallisation and Quartzites Do Not.

The obvious differences between the coeval LS1 quartzite and granite microstructures and C-axis microfabrics may be understood if they are related to a continuous process of recrystallisation. This may, if the temperature is high enough, continue, despite cessation of deformation, through a discrete series of steps, which can only occur in one particular order and each of which is characterized by a distinctive microfabric and microstructure (Fig. 4.2). Interruption of this process at any point, such as due to a lack of sufficient heat for static grain growth or as a result of intrinsic qualities of the deformed aggregate, such as insufficient quartz-quartz grain boundaries (as is the case in the granites), will result in the inheritance of the C-axis microfabric and microstructure characteristic of the stage at which the process was stopped (Fig. 4.2).

Such a 'one-way' sequence of recrystallisation has been recognized in metals (Cahn 1965), in experimentally deformed quartzites (Green et.al. 1970) and in naturally deformed quartzites (Wilson 1973, Bouchez and Pêcher 1981, White 1976.) The sequence is expressed by the variations in C-axis microfabrics and microstructures. These authors make a basic distinction between "primary-" and "secondary-" recrystallisation, terms which express the difference between earlier grain growth driven by strain energy and later growth, which decreases grain boundary energy. These terms have been applied indiscriminately to hot-worked and cold-worked metals which have been held at an elevated temperature after deformation. Sellars (1978) shows that significant microstructural differences are found between metals deformed and recrystallised in these ways, calling static recrystallisation in which nucleii and mobile grain boundaries formed during dynamic recrystallisation continue to grow and move "Metadynamic Recrystallisation". This is an appropriate term to use for the initial modification of a dynamically recrystallised rock microstructure which must occur after deformation has ceased if the temperature is high enough (Fig. 4.2).

In experimental deformation of quartzite, dynamic and metadynamic recrystallisation has been achieved at a variety of temperatures and strain rates with significant microfabric and microstructural differences at each stage (Green et.al. 1970). Documented microfabric and microstructural changes in rocks usually correlate with changes in grade (Behr 1980). However there appear to be several episodes of the best documented sequences which are confined to the same grade and may represent sequences of metadynamic recrystallisation (Wilson 1973, Bouchez and Pêcher 1981).

Microfabric and microstructural variations may occur within each of the major steps of recrystallisation. For example as strain increases the number of new grains increases and the C-axis microfabric changes in a dynamically recrystallised quartzite (Carreras et.al. 1977); duplex structures mark the early stages of exaggerated grain growth (Wilson 1973).

The major differences between quartz microstructures and microfabrics of LS1 age are ascribed primarily to the stage which grain growth has achieved during a single metamorphism which had both a dynamic and a static component (Fig. 4.2). Quartzites and granites have probably undergone very similar deformations, both having the regional mesoscopic LS1 fabric. Details of quartz microstructure in both, such as grain-boundary morphology, are quite similar yet quartz microfabrics are very different (compare Fig. 4.9 with Figs. 4.23-4.25). This difference is judged to be due to the obvious limits on metadynamic quartz grain-growth in a granite exercised by the large volume of feldspar, metadynamic grain growth in the granite being thereby halted before the dynamic fabric could be erased (Fig. 4.2).

4.3 LS2 Tectonites

4.3.1 Introduction

The LS2 tectonites are those rocks which in hand specimen have a well developed LS1 fabric, but which in thin section are marked by the presence of a second planar-linear fabric, LS2 (Plate 17). The fabrics are only completely distinguishable in sections cut parallel to the XZ plane, a fact which underlines the importance of choosing the plane of observation in microstructural geology (Nicolas and Poirier 1976). The LS2 tectonites yield unambiguous kinematic information from both the geometry of the microstructure and the C-axis microfabric.

The LS2 fabric in many cases is difficult to distinquish in the field from the regional LS1 fabric which it overprints. Its presence may be suspected when the host rock is increasingly delicately laminated, grain size is greatly decreased and quartz acquires a frosty appearance. It is only locally developed, being restricted to quartz bearing rocks in concordant zones a few metres or tens of metres wide, or to narrow quartz veins a few centimetres wide.

In the XZ section, in all samples studied, LS2 has a gently curving or straight trace and shows the same sense of asymmetry, dipping more steeply to the SE than LS1. The XZ plane of LS1 contains L2 and L2 approaches L1 with increasing shear strain. The Y direction of both fabrics is identical. In favourable cases the distribution of extended rutile needles shows that the quartz fabric lies subparallel to the XY plane of the finite strain ellipse at the initial stage of its development (Fig. 4.27). There is evidence for rotation of non-quartz inclusions previously parallel to LS1 (Plate 20), allowing interpretation of the fabrics as shear fabrics in which, on the scale of hand specimen and outcrop, upper layers moved southeast over lower layers. L1 was the shear direction and the XY plane of LS1 was the shear plane.

This section describes the rock types and field setting, the nature of the microstructure, both of quartz and non-quartz minerals and the nature of the C-axis fabric. All photographs and diagrams, except when otherwise stated in captions, refer to the XZ fabric plane of LS1 and LS2. The main features to be discussed are shown in Tables 28 to 32.

4.3.2 Rock Types and Field Setting

All rock types studied are quartz bearing, ranging from quartz rich types such as quartz veins and impure quartzites (Plate 17b,f and a,d respectively) to quartz bearing granitic and tonalitic gneisses (Plate 17c,e). The location of the samples is shown in Fig. 1.2b.

The concordant zones of LS2 development are varied in character (summarized in Table 25, Appendix I). For instance a quartz vein (26102B) from the west central part of the Cardiff Complex is typical of many others found in the lineated granite gneiss. It has a mesoscopic fabric of elongate aligned feldspars which is parallel to that in the surrounding gneiss. A granite gneiss (30103B) with LS1 recrystallised in curving ribbons (Plate 17c) comes from a narrow ravine which forms a prominent topograhic lineament concordant with the gneissosity on the western side of the Cardiff granite. The specimen has a finer grain size than the normal granite gneiss but a mesoscopic fabric which is otherwise identical. In alkali granite (20102B), from part of the Cheddar granite where the regional LS fabric is variably developed, unfoliated, moderately and highly foliated zones coexist, the latter have LS1 (MCT) type of microstructure in most cases; the sample with an LS2 micro-structure is indistinguishable in hand specimen from these.

In contrast a quartz vein (24101B), a quartzite (695C) and a granite gneiss (194C) come from the zone to the north of the Cardiff complex where the regional LS fabric is most strongly developed. Feldspathic rocks are finer grained, augen textures more common, vein fabrics more 'straightened' and fabric development more homogenous here than elsewhere. In places this strong fabric is a composite of LS1 and LS2. The quartz vein (24101B, Plate 19, Fig. 4.1) is a few centimetres wide and set in a fine, highly deformed granite gneiss which is only recrystallized at its margin with the vein. The quartzite (695C) grades over a few metres into rock with LS1 quartz microstructure. At two sample locations (24101B and 194C at Jordan and Farquhar Lakes) tectonic schists with rotated feldspar augen lie parallel to LS1 in the granitic gneiss.

At Farquhar Lake both the schist zone and the grey tonalitic gneiss within which it lies have the LS2 fabric. A pink granitic gneiss also displaying LS2 (194C Plate 17e) is from the leucosome of a migmatite unit lying several metres below the grey gneiss indicating a minimum thickness 20 m for the LS2 zone.

A quartzite from Tory Hill (THQ, Plate 17a) comes from a thick band of quartzite striking north-northeast through Monmouth Township (Fig. 1.2a). Much of this unit has the typical LS1 fabric dominated by exaggerated grain growth microstructures. The map of Francoeur (1975) shows several such localities where 'mylonitic' quartz was found. Rocks with similar mesoscopic fabrics underlie a prominent ridge for more than 1 km. along strike.

In hand specimen LS2 samples are not greatly different from similar rock types with LS1 fabric, making field recognition difficult. Some of the specimens do have features which are either unique to or typical of LS2 bearing rocks, features summarized in Table 26, (Appendix I). The diagnostic asymmetric LS2 fabric is visible to the naked eye in cuts near the XZ plane in relatively few specimens, notably in the quartz vein from the northeast margin of the Cardiff Complex (24101B) as a thin milky streaking, in a quartzite (695C) as the outline of deformed LS1 grain boundaries and in a "tectonic schist" (1131C Table 25, Appendix I) as the disposition of mica flakes. In some specimens a frostiness of the quartz, distinct from the usual glassiness, is apparent (e.g. 24101B, 695C, 20102B, THQ). Typical, but not unique, in quartzo-feldspathic LS2 gneisses is the fine grain size of the feldspathic matrix (~ 0.1mm), the development of augen textures and delicate lamination (e.g. 30103B, 194C, 192C, but not 20102B). Although under the microscope all the quartz rich rocks are fine grained, this is only obvious at hand-specimen scale with certain samples (e.g. 24101B, THQ), in others only LS1 grain boundaries are obvious.

4.3.3. Quartz C-axis Microfabrics

All measurements were made and are presented in the XZ plane. The data are summarized in Table 27 (Appendix I) and Fig. 4.26. Most samples have partial or complete girdles

FIGURE
4.26

Quartz c-axis microfabrics of LS2 tectonites. All data measured in XZ plane of LS1. All samples have 200 data except (a), which has 100. Southeast is to right.

(a) Tory Hill Quartzite (THQ); contours at 1,4,8%/1% area (max 20%). (b) Quartz vein in granite gneiss, northeast Cardiff Complex (24101B); contours at 1,3,5%/1% area (max 14%). (c) Granite gneiss, western margin Cardiff Complex (30103B); contours at 1,3,5%/1% area (max 8.5%). (d) Quartzite, south shore of Elephant Lake (695C); contours at 1,3,5%/1% area (max 8.5%). (e) Granite gneiss, south shore of Farquhar Lake (194C); contours at 1,3,5%/1% area (max 6%). (f) Alkali granite gneiss, Cheddar Granite (20102B); contours at 1,2,3%/1% area (max 6%). (g) Quartz vein in granite gneiss in west-central part of the Cardiff Complex (26102B); contours at 1,3,5%/1% area (max 8%).

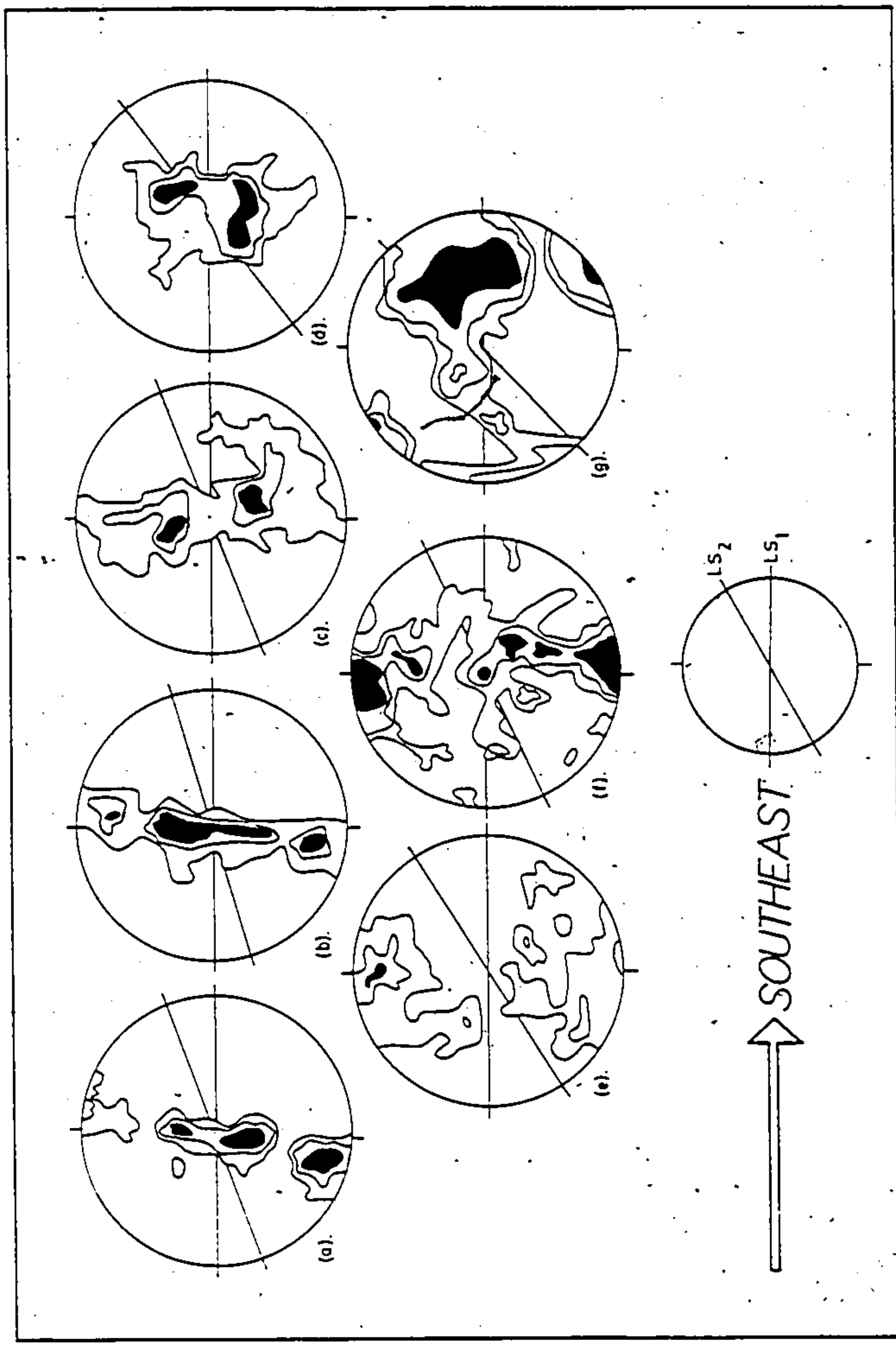
(a).
(b).
(c).
(d).
(e).
(f).
(g).
LS2
LS1
SOUTHEAST

subperpendicular to LS1. Several specimens (Fig. 4.26a,b, c,d) have modified versions of the well known pattern consisting of two maxima lying in YZ girdle near Y (White et.al. 1980). The granite from south of Farquhar Lake (194C) and the granite from the Cheddar batholith (20102B) (Fig. 4.26e,f) have types that can be considered as transitional between cross girdles and the YZ girdle. The quartz vein from the west central Cardiff complex 26102B (Fig. 4.26g) is a special case, it has two maxima irregularly disposed around X (compare Shelley 1980). In the pattern for the granite from the west Cardiff complex 30103B (Fig. 4.26c) the tail in the girdle is populated by C-axes of unrecrystallised augen. All of the girdles have an angle of less than 90° to the average LS2, while although two (Fig. 4.26d,e) are perpendicular to LS1 the assumed plane of shear, others are not perfectly so.

All the C-axes patterns except that for the vein from the West central Cardiff complex (26102B) (Fig. 4.26g) have the same asymmetry with respect to the shear system. The girdles lean towards the LS2 quartz shape fabric and are sub-perpendicular to the shear plane (LS1). The pattern is interpreted as indicating shear of upper layers to the SE parallel to L1. This geometry compares with several studies of fabrics in shear-zones (e.g. Eisbacher 1970, Bossière and Vauchez 1978, Burg and Laurent 1978, Lunardi and Baker 1975, Bouchez 1978, Berthé et.al. 1979, Brunel 1980, Bouchez and Pêcher 1981) and tends to confirm the theoretical prediction that the preferred orientation is not controlled by axes of finite strain in a non-coaxial deformation but by the kinematic framework (Lister 1974, Lister and Williams 1979).

The girdles with two maxima near Y displayed by several of the samples (Fig. 4.26 a-d) is common in shear and thrust regimes (e.g. Eisbacher 1970, Hara et.al. 1973, Christie 1963, Burg and Laurent 1978, Lunardi and Baker 1975, Wilson 1975, Carreras et.al. 1977, Berthé et.al. 1979, Brunel 1980, Behr 1978, 1980, Sylvester and Christie 1968) and appears to be confined to the greenschist and amphibolite facies. This is consistent with the fact that LS2 destroys LS1 and may have been formed in constant or waning amphibolite facies temperatures. The sense of shear deduced from the C-axis microfabrics (upper layers to SE, down dip to parallel to L1) is precisely opposite to that indicated by LS1 C-axis microfabrics and the asymmetry of major structures.

4.3.4 Quartz Microstructure

Description: The overall structural geometry in thin section is dominated by the presence of two planar-linear fabrics, a planar LS1 and an asymmetric LS2 which often curves (Plate 17). In all cases LS1 is parallel to the assumed plane of shear. In some cases discrete planes of shear may appear parallel to LS1 marked by extremely thin layers of very fine equant material transecting quartz or feldspar. Rocks with two such active transecting fabrics (30103B, 194C, THQ) are comparable with C-S tectonites

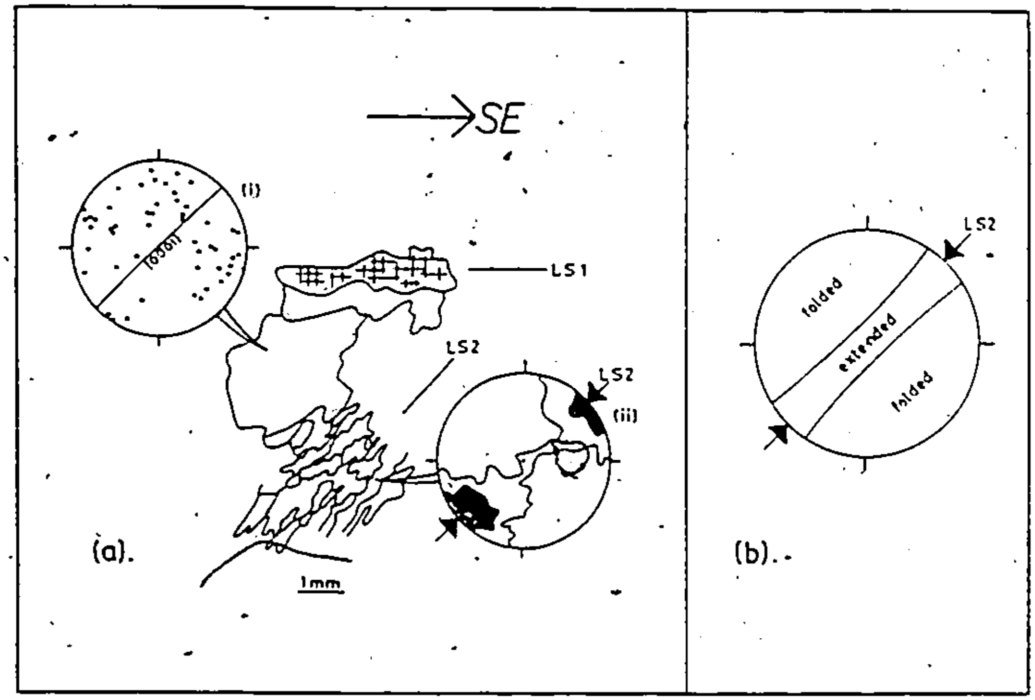

FIGURE
4.27

(a) Sketch of detail of microstructure of quartz vein showing LS2 recrystallisation (26102B from Cardiff Complex), XZ section. (Plate 17f). An unrecrystallised quartz grain is undeformed, as shown by the quasi-uniform distribution of rutile needles (i); (0001) lies in LS2, an "augen" position; recrystallised quartz, defining LS2 has a strong preferred orientation of rutile needles (ii). Kspar - cross hatch. (b) Stereonet showing distribution of folded and extended rutile needles in LS2 quartzite tectonite (specimen 695C). South of Elephant Lake XZ section (Plate 63d).

(Berthé et.al. 1979). There are also other features in some of the samples not of LS1 age which lie parallel the trace of LS1. For example the quartz vein in granite gneiss (24101B) a banding within the recrystallised quartz comprised of domains with contrasting extinction lies parallel to LS1; this feature possibly marks the traces of recrystallised deformation bands. In this sample boudinaged rutile also lies very close to L1 (Plate 18c,d).

LS2 has two significant geometries: the case where LS2 curves and is accompanied by a considerable proportion of unrecrystallised quartz and that where there is very little unrecrystallised quartz and LS2 is straight over large areas of thin section (24101B, THQ). The latter is considered to be the most mature microstructure, its significance is further discussed below.

The main features of the quartz microstructures are summarized in Table 28 (Appendix I). In the seven specimens analysed the amount of recrystallised quartz varies between 50 and 100%. The distinction between new and old material is straightforward in most cases. For example, in a quartz vein, (26102B) from the Cardiff complex a zone of equant grains of millimetric dimensions is surrounded by LS2 ribbons (Plate 18f). The undeformed nature of the equant grains is confirmed by the presence of numerous rutile needles which in contrast to those in the LS2 ribbons lack a preferred orientation (Fig. 4.27a). Specimens of granites from the Cardiff complex (30103B) and from near Farquhar

Lake (194C), have LS1 ribbons partly and completely replaced by LS2 grains (Plate 17e) and 'augen' of uncrystallised quartz surrounded on all sides by LS2 grains (Plate 19d). A quartz vein in granite gneiss from the northern margin of the Cardiff complex (24101B) has unrecrystallised material concentrated in a fringe along the vein margins (Plate 17b). In some samples of quartz veins (26102B, Plate 17f) and quartzite (695C, Plate 17d) it is difficult to tell whether fatter ribbons in LS2 are new grains which have grown or deformed unrecrystallised material since there is no difference in substructure between the two generations of material (see below). The quartzite (695C) has large (millimetric) irregular shaped grains which are probably old material (Plate 17d). By contrast another quartzite (THQ) is totally composed of LS2 grains.

An identical substructure is shared by new and old grains in the quartz vein (26102B) and the quartzite (695C) comprising undulatory extinction, elongate subgrains (deformation bands) with prismatic boundaries, rectangular subgrains and lobate grain boundaries. Subgrain misorientations range from 5° (26102B) to 10-15° locally (695B). In the quartz vein (26102B) new grains appear within grains on deformation band boundaries and on grain boundaries (Plate 18a,b) where new grains and grain-boundary lobes have comparable dimensions ("Bulge-nucleation", Bell and Etheridge 1976).

In several specimens (30103B, 24101B, 20102B, THQ and 194C) a distinction between substructures in new and old grains may more easily be made. In all cases except 30103B the LS2 grains are composed of equant polygonal subgrains ~ 50 μm in diameter with low mutual misorientations. The LS2 grains are rarely more than 3-4 subgrains wide and usually less. The irregular grain boundaries reflect the shape of the subgrains except in 30103B which has an unique saw-tooth grain boundary morphology.

In these specimens old grain substructure is quite varied. In 30103B (Plate 19c) and 24101B (Plate 17b) there is a continuous transition from relatively undeformed quartz though kink-like deformation bands into an array of LS2 grains. In 30103B, lattice distortion in deformation bands, marked by strong undulatory extinction, may be in excess of 40°. Deformation lamellae, lying between 5 and 20° from the basal plane occur in the old material (Plate 19a,b). Universal stage measurements of kinked LS1 quartz (Fig. 4.29) show the basal plane is an operative glide plane (after method of Christie et.al. 1964). Tabular as well as globular augen (Plate 19d) also show extreme lattice distortions (30° along length of augen). New grains are located on deformation band boundaries and at boundaries of recrystallised material of earlier generations.

Old unrecrystallised material in 24101B and 194C has undulatory extinction and deformation bands with misorientations across deformation band boundaries in excess of 10° but with no marked distortion along their length. Recrystallised grains have a distinctive location along 'recrystallisation fronts' lying subparallel to LS1 (Plates 17e, 18c), with some on deformation band boundaries. New grains project into old material parallel to LS2 from these "recrystallisation fronts" (Plate 18c), which in some cases may be deformation band boundaries which have become mobile. This mobilization is observed in the change in shape of deformation band boundaries from planar to irregular (Plate 18c).

Particularly interesting are the angular relations between rutile-needles, recrystallisation fronts and the bulges that occur on them in the quartz vein, 24101B, (Plate 18c,d). In the case illustrated a boundary between planar domains of very different orientation lies parallel to the direction of elongation of the rutile. This boundary is similar in orientation to several others nearby and appears to be a deformation band boundary. It, however, has many irregular elongate bulges which lie parallel to LS2, so that LS2 and the rutile are not parallel. This mobilization is interpreted as an example of bulge-nucleation (Bell and Etheridge, 1976).

Two of the LS2 granitic gneisses (194C and 20102B) have small domains composed of equant polygonal grains which are slightly larger than the subgrains which form the LS2 ribbons. These are interpreted as grains which have adjusted statically.

In all samples the LS2 ribbons viewed in the XZ section have a length to width ratio which varies from approximately 5:1 in the partially recrystallised microstructures to approximately 3:1 in the more completely recrystallised samples. The ribbons in the granite gneiss (30103B, Plate 18) have ratios considerably in excess of this value. The range of angles between LS1 and LS2 in the XZ section is quite constant, between 25 and 35° (again 30103B is considerably in excess of this, ribbon formation begins at between 45 and 55° to LS1).

In general, the presence of deformation bands, subgrains, undulatory extinction and deformation lamellae (in 30103B only) is evidence of dislocation dominated syntectonic recovery processes (White 1973, 1976, 1977). Moreover the lobate grain boundaries and the polygonal subgrain structure is indicative of a syntectonic episode of grain boundary mobility (Nicolas and Poirier 1976, Van Vlack 1965) when the volume driving force of grain boundary migration (the strain energy) is greater than the surface driving force (the need to decrease grain boundary area). The conclusion that the microstructure is syntectonic is strengthened by comparison with the grain boundary morphologies of hot-worked high-stacking fault energy metals which deform primarily by dislocation and recovery processes, e.g. aluminum (Leguet et.al. 1962) or with that of experimentally syntectonically recrystallised quartz (Hobbs 1968, Pl. VIIID.). The preservation of deformation lamellae in 30103B tends to strengthen this conclusion since a static post tectonic anneal would not selectively remove such work-hardening features (MacLaren and Hobbs 1970). An important observation is that in such a process of syntectonic grain-growth and recrystallisation the development of C-axis microfabrics will be partially governed by the motion of dislocations since new grains are relatively quickly deformed (Lister and Price 1978).

Mature Quartz Microstructures: As noted, some quartz microstructures are marked by a substantial percentage of unrecrystallised material coexisting with the new curving quartz foliation (Table 29, Appendix I). Others, notably the quartz vein, 24101B the quartzite THQ, and a late mylonite from the Cheddar batholith (Appendix II) are characterized by large areas free from unrecrystallised quartz, large areas where LS2 does not curve and there is a low angle between LS1 and LS2 (Table 28, Appendix I).

It is possible that these quartz foliations represent steady-state foliations, defined by Means (1981) as foliations with constant orientation and intensity. ("Intensity" in this case is probably best expressed as aspect-ratio.) Such foliations would only form under conditions of steady-state flow, flow at constant stress and strain rate. A significant consequence, especially for the case of steady-state foliations formed in simple shear, is that they would be strain insensitive. That is to say, that unlike, for example, a shape fabric in a shear zone, a steady state foliation, once it had been established, would not rotate no matter how large the shear-strain.

The condition that a stable microstructure has been attained may be argued from the presence of a mature micro-structure, in the sense explained above, which has been established at the highest shear strains found in the LS2 tectonites, as evidenced by the presence of the strongest C-axis preferred orientations (Fig. 4.26a,b) and the smallest angles between LS1 and LS2, both parameters being qualitative measures of the amount of strain (Miller and Christie 1981 and Lister and Williams 1979, respectively).

The strain insensitivity of the microstructure is clearly demonstrated in all the rocks. In the quartzite, THQ the quartz foliation is straight, non curving across large areas of a thin section and has rather low aspect ratios despite the considerable rotational strains witnessed to by rotated porphyroclasts (Plates 17a, 20a). In the quartz vein (24101B) and the mylonite boudinaged rutile needles do not lie parallel to LS2 but 15-20^{o} away from it and within 5^{o} of LS1 (Plate 18c,d). It is certain that the deformation of the needles is in part related to the LS2 recrystallisation since their extensions in recrystallised domains are 20% higher than in non-recrystallised domains. It is probable that the deformation of the rutile needles, only records the LS2 or the mylonite forming event, since the quartz (e.g. specimen 26102B) from undeformed parts of veins contains rutile needles with no preferred orientation

(Fig. 4.27a). Thus the rutile needles appear to have behaved like stiff and brittle rods with an initial scattered orientation, being brought into parallelism with the quartz foliation (S2) during its initial formation (as in 26102B and 695C) but rotating past the quartz foliation towards the shear plane with increased shear strain. Or the rutile may migrate past the initial orientation of LS2 before LS2 formed, as happens during the mobilization of deformation band boundaries in both the quartz vein and the granite mylonite (Plate 18c, Fig. 4.33, A.1). The final result is a set of two transecting coeval fabrics (compare Means 1981, Fig. 7).

Means (1981) states that for the foliation to be strain insensitive and constant in aspect ratio the processes tending to strengthen the fabric should be matched by those tending to weaken it. In the present case the cyclic process of dynamic recrystallisation may constitute such a set of events: grains elongating by dislocation glide and dynamic grain growth but continually strain hardening until recrystallisation releases the accumulating strain energy and produces a new equant grain. The ragged grain boundaries and polygonized substructure are evidence for dynamic recrystallisation (Nicolas and Poirier 1976, p. 169). In a simple-shear regime the direction of elongation of a grain formed at all but the earliest stage may be parallel to the instantaneous stretching direction and not related to the finite strain axes. It is thus the former

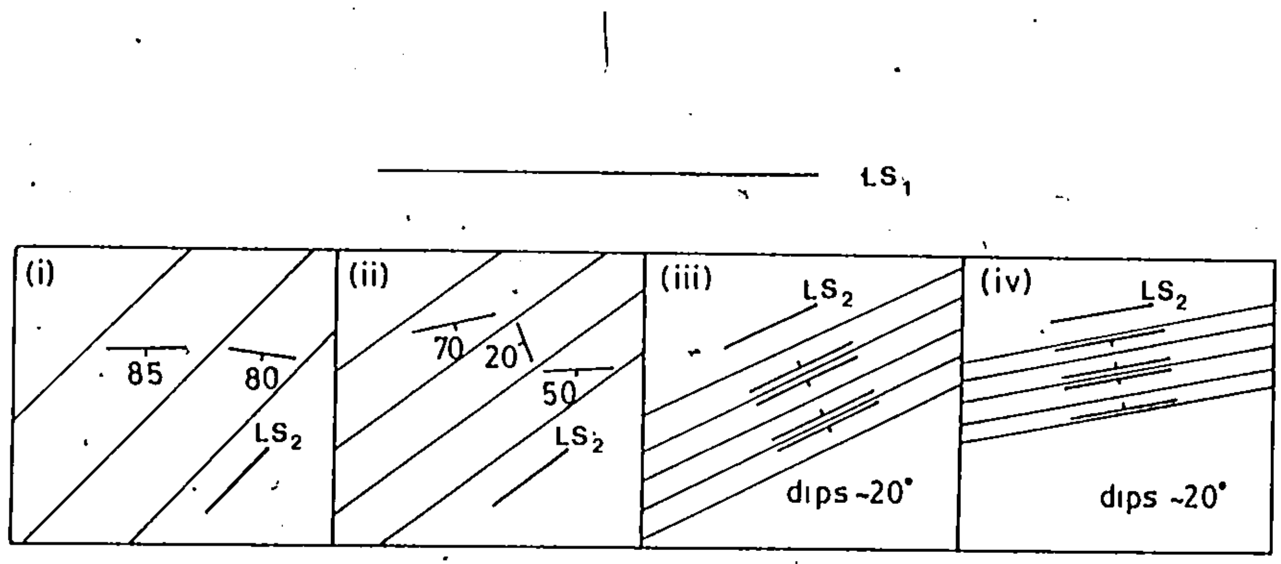

FIGURE 4.28 Diagramatic conception of evolution of quartz ribbons in LS2 granite gneiss (30103B) shown in XZ plane; (i) kink bands form with low misorientation between neighbouring slip planes (0001), trace of kink band boundary, LS2, is at high angle is LS1; (ii) with increasing strain kink band boundary is rotated further towards LS1, misorientation between neighbouring basal planes is low to moderate, intersection of neighbouring basal planes is parallel to LS2; (iii) and (iv) with increasing strain ribbons continue to rotate towards LS1, neighbouring basal planes have reached a stable orientation, intersection of neighbouring basal planes is parallel to L2 preserving the "kink- geometry".

It is apparent that new ribbons may form at any of these stages (Plate 19).

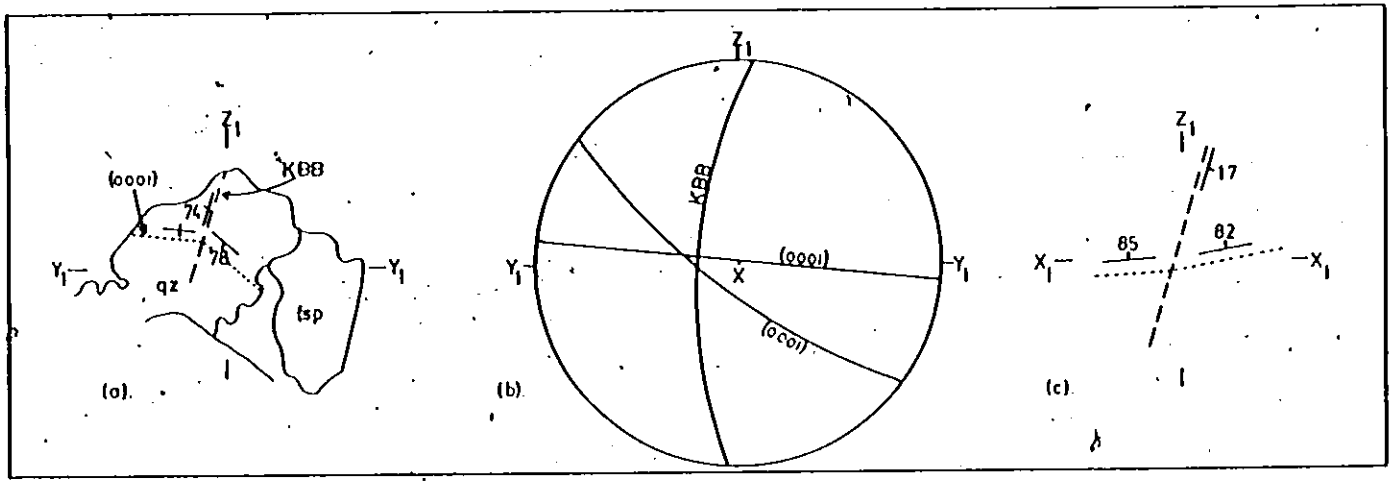

FIGURE 4.29 Geometry of kink-band in LS1 quartz of LS2 granite gneiss (30103B); (a) kinked old quartz in YZ section, kink band-boundary (KBB) and neighbouring basal planes have a high dip with respect to this section; (b) kink band-boundary and neighbouring basal planes intersect, defining axis of rotation and showing (0001) is, at this stage, the slip plane; (c) this kinked quartz as it might appear in the XZ section, KBB has a low dip with respect to this section, in contrast to the basal planes.

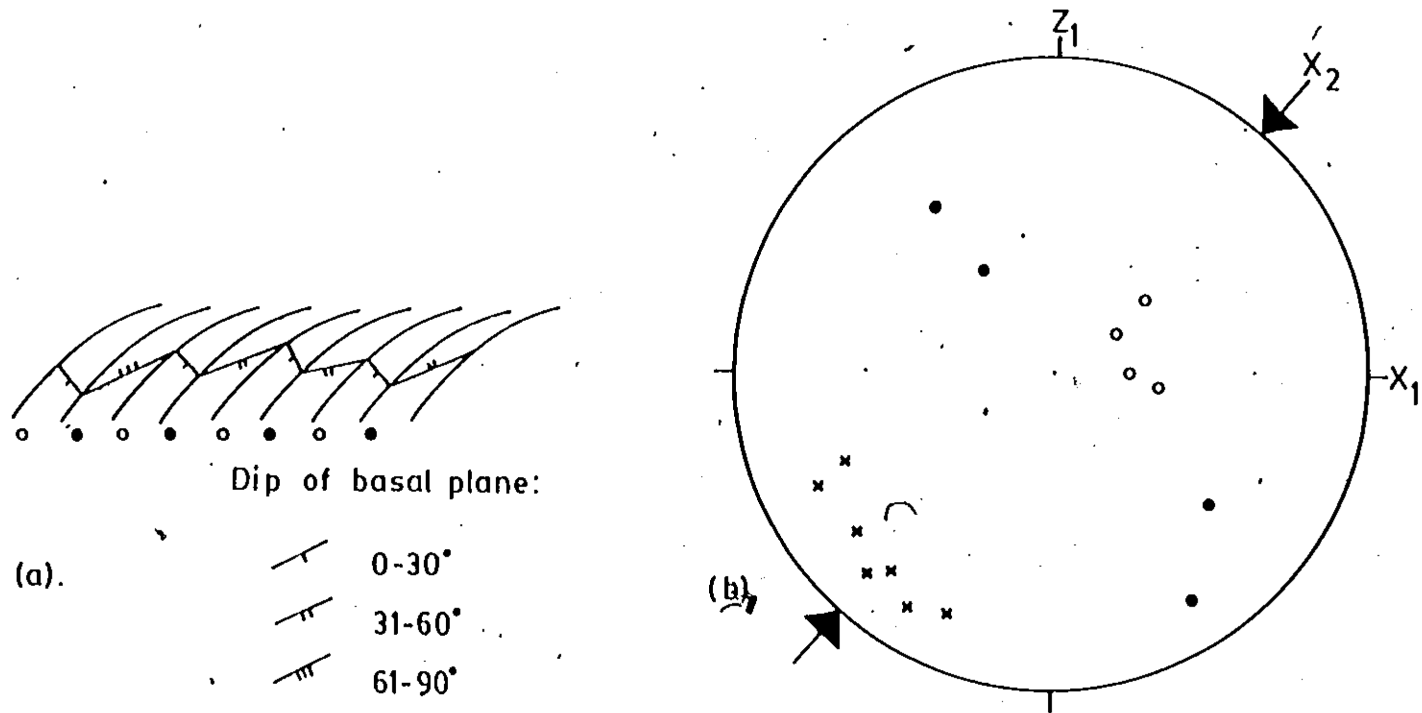

FIGURE 4.30 Geometry of quartz ribbons which retain a high angle to LS1 in LS2 granite gneiss (30103B); (a) diagram of disposition of basal planes in neighbouring ribbons; (b) disposition of poles to neighbouring basal planes (solid and open circles as in (a)); intersection of neighbouring basal planes (crosses) shows an axis of rotation close to the trace of the margin of the ribbons (local LS2),

direction that the mature LS2 and the fabric in the mylonite in all likelihood reflects.

The Influence of Microstructural Development on C-axis Microfabric Patterns: It could be argued that the LS2 quartz ribbons are shear-band like structures. If, for example, they are kinks and their axis of rotation lay perpendicular to the direction of flow, parallel to Y. In this case their kinematic significance would be quite different from that suggested here. However the evidence presented indicates that although the ribbons do originate as kink-like structures, the kink axes lie near L2 (Fig. 4.28 - 4.30). It is suggested that the kinking process is the most efficient way of rapidly softening a coarse-grained microstructure and leads quickly to a stable C-axis microfabric since recrystallisation processes preserve the kink geometry which produces a C-axis microfabric very common in quartz mylonites, the type 1 girdle (White, et.al. 1980). This YZ girdle with two maxima near Y is shared by 4 of the LS2 tectonites (Fig. 4.26a-d), a fifth (Fig. 4.26g) is a probable variation of it, there being maxima near X rather than Y in this case.

As a consequence of the partly unrecrystallised nature of the quartz microstructure in the granite gneiss from the west central Cardiff complex (30103B) many stages of the microstructural development and the attendant microfabric expression can be observed. At all stages of development the microstructure is dominated by kink-band like structures in which the axis of rotation of nearest neighbours lies near L2. The main change with increasing strain is the migration of basal planes toward the XZ plane from positions of variable dip with respect to that plane and a relatively small migration of the axis of rotation within that plane (Fig. 4.28).

The earliest stages include the formation of wide deformation bands (0.05 - 0.1 mm wide) often with sub-basal deformation lamellae (Plate 19a,b). These bands lying at a high-angle to LS1 are kink-bands (Plate 19a, Fig. 4.29). Kink-band boundaries lie sub-parallel to prism planes and sub-perpendicular to the slip plane (the basal plane) (Fig. 4.29). Misorientations between bands vary from 12 to 35°. Note that the axis of rotation of the kink-bands, shown in Fig. 4.29, lies near the L1 XZ plane. The kink-band boundary, when projected onto the XZ plane would make a high angle with LS1 comparable with those actually observed in the XZ plane (compare Fig. 4.26c with Plate 19b). Ribbons are also produced at the edge of families of deformation bands (Plate 19c) or at the edge of globular augen (Plate 19d). These wide deformation bands are replaced by several thinner ribbons 20-50 μm wide as they curve toward the shear plane, a result of the thinning with increasing strain of the original band and the growth of small lenticular new grains which nucleate both on the band boundaries and within the deformation bands.

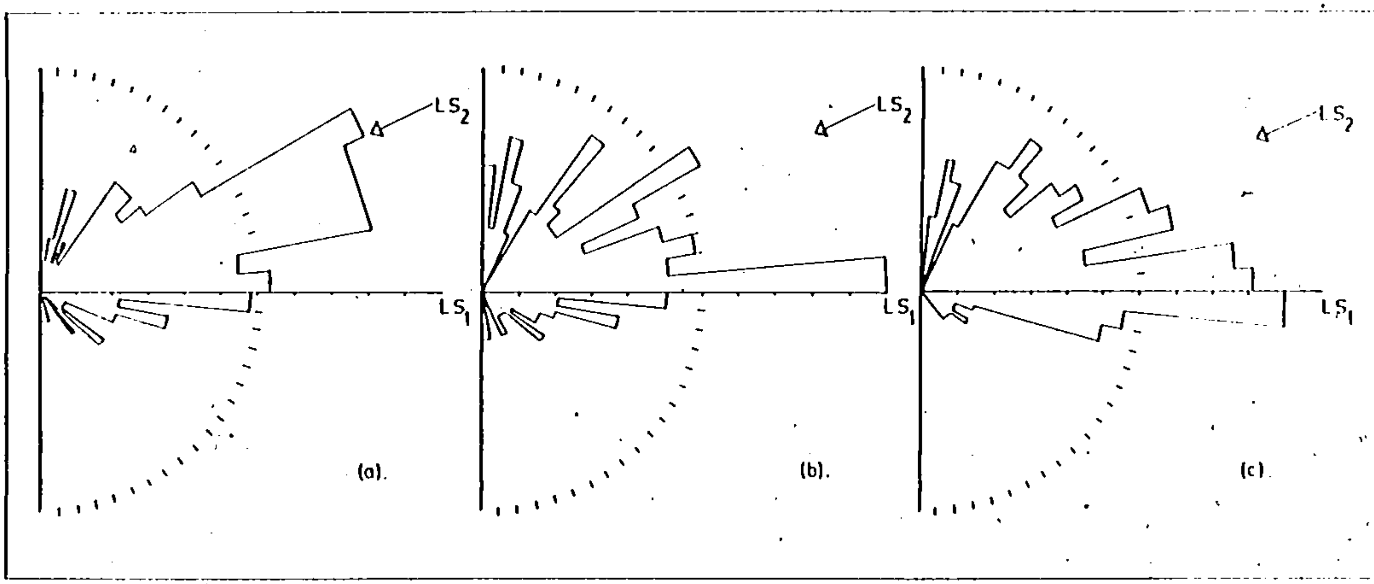

FIGURE 4.31 Relationship of basal planes in quartz ribbons of LS2 granite gneiss (30103B); rose diagrams shows trace on XZ of intersection of basal planes of nearest (a), second nearest (b) and third nearest neighbour quartz ribbons. Abscissa has 1% gradations.

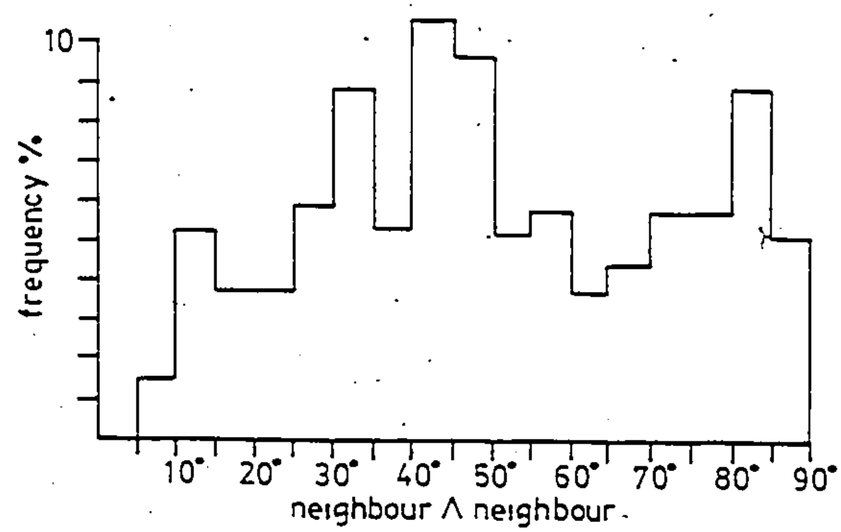

FIGURE
4.32

Histogram of misorientation between basal planes of nearest neighbour quartz ribbons in LS2 granite gneiss (30103B).

There is evidence that neighbouring ribbons retain the kink-band geometry in these subsequent stages of development. For example: (a) an intermediate stage of development may be represented by a family of grains, comparatively thick and retaining a high angle to LS1 (Fig. 4.30). In these the intersection of nearest neighbour's basal planes lies close to the ribbon margin's trace (LS2 of the micro-domain); and the angle between neighbouring basal planes is large and variable (35° - 75°); (b) The relationship of intersection of the basal-planes of nearest neighbour ribbons near the trace of the ribbon boundary holds for the entire measured population. This is demonstrated by the high degree of clustering of the trace of nearest neighbour basal planes' intersections near the trace of the LS2 maxima on XZ (Fig. 4.31a) as compared with that of second or third nearest neighbours (Fig. 4.31b,c). Moreover, the frequency distribution of angles between nearest neighbour basal planes has a maximum between 40 and 50° (Fig. 4.32). Thus the two maxima on the C-axis microfabric diagram actually reflect a specific relationship between neighbouring quartz ribbons which has been preserved from the earliest stages of development.

A comparable geometry and history is shown by quartzites from Central Australia (Mawer 1980, personal communication). In these rocks the two maxima lie in the XZ plane close to X, the "kink" axis thus being Y. Sample 26102B with its maxima near X (Fig. 4.26g) may be comparable to the Australian examples and thus essentially comparable to the samples showing double maxima near Y.

The kink geometry is essentially a rotation of one neighbour relative to the next about an <a> axis. This type and amount of rotation is very similar to a commonly found geometry of rotation of new grains relative to most grains of quartz with core and mantle structure (White 1976), the site of recrystallisation being grain-boundaries. For example, White (1976) found that most new grains had misorientations of 1-25° of twist about an <a> axis relative to the host grains. Those with misorientations in excess of 20° appear to have the highest rates of growth during primary grain growth (White 1976). Clearly, the cyclic dynamic recrystallisation of an aggregate in which the host-new grain relationship always follows the above rule, and the axis of rotation lies in the XZ plane, is compatible with the production of the microfabric which has two maxima near Y in a YZ girdle favourably disposing the aggregate for dominant prism <a> slip. The latter slip system has been found in this type of microfabric from quartz with a dynamically recrystallised microstructure (Carreras et.al. 1977), and a similar C-axis microfabric. In the present case kinking appears to play the same role in the earlier stages of microstructural development as those better known recrystallisation processes which function at grain boundaries. That is to say a population is produced in which mutual misorientations are of such a geometry that

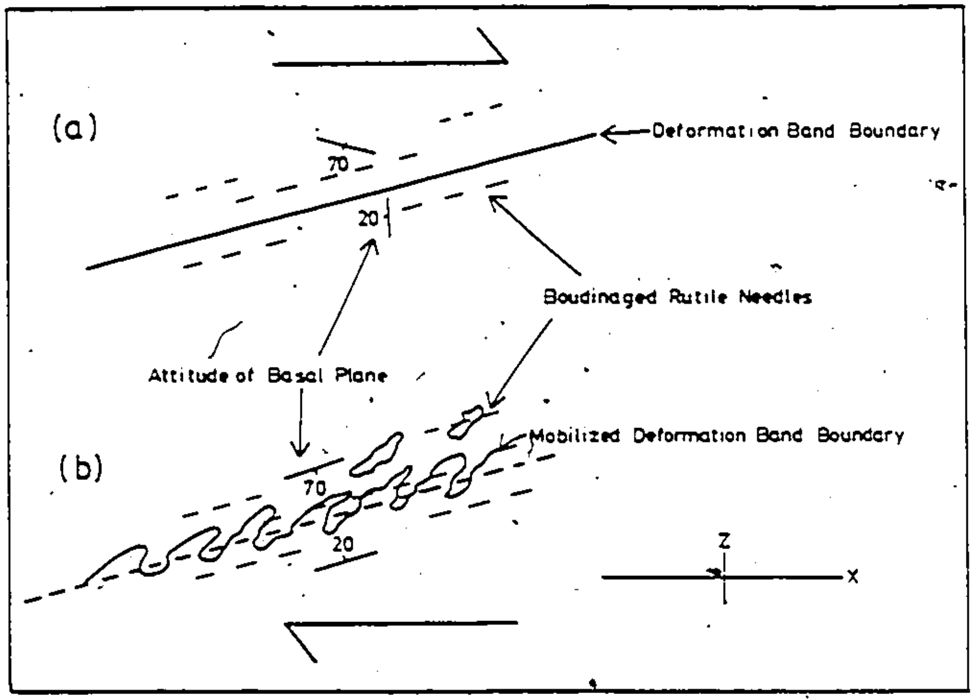

FIGURE
4.33

Formation of foliation of recrystallized quartz which is transected by boudinaged rutile.(a)in early stages of deformation of coarse grained quartz rock (e.g.24101B),quartz deforms by forming deformation bands (kink bands);Deformation band boundary and boudinaged rutile needles behave as quasi passive markers which rotate towards the shear plane.(b)deformation band boundary becomes mobile at critical value of strain and mutual misorientation of neighbouring quartz domains.Boundary migration is parallel to the instantaneous stretching axis.In subsequent cycles of recrystallization this type of crystallographic fabric is preserved by host grain control.

some of the kink band boundaries become mobile. The successive generations of dynamically recrystallised grains will, if they follow the same geometrical rule, reproduce these orientations whatever was the physical process of nucleation (e.g. grain-boundary bulging, sub-grain rotation). Bell and Etheridge (1976) suggest that nucleation by bulging of a subgrain on a kink band boundary will preserve the kink-geometry. The high angle boundary on one side of the subgrain will migrate during straining at the same time as the subgrain rotates relative to the host grain. The kink geometry will be preserved if the axes of rotation of the kink band and the subgrain relative to the host are the same. Among the present samples this process is probably taking place in the quartz vein from the north Cardiff complex (Plate 18c and Fig. 4.33) and the late mylonite from the Cheddar batholith where the mutual interfingering of material from either side of the mobilized deformation band boundary by growth of bulges parallel to LS2 should preserve a kink geometry between neighbouring new grains.

If kinking and recrystallisation preserving kink-geometry is a significant process in the development of the microstructure and C-axis microfabric a significant clue to the reason for the occurrence of this particular mode of recrystallisation may lie in the grain size of the unrecrystallized LS1 quartz and its preferred orientation (Fig. 4.3). All the microstructures have large grain sizes and quite regular grain boundaries, with consequent low grain boundary area per unit volume of quartz. The extreme example is the large grain-size of the exaggerated grain-growth microstructure in quartzites (Plate 15), quartz veins and ribbons being less coarse. Thus, since there is a low initial area of grain boundaries, the usual site of recrystallisation, a recrystallisation process specific to coarse grained microstructures may be envisaged analagous to that found in experimentally recrystallised single quartz crystals (Hobbs 1968). This is a production during a relatively high strain rate deformation of the large number of new grains required to keep the aggregate soft at the numerous deformation band-boundaries (in lieu of the scarce grain-boundaries) produced during the initial heterogeneous deformation. Moreover, if a large volume of the LS1 quartz has C-axes parallel to Y (Fig. 4.10), this will favour kinking with the axis in the XZ plane if the basal plane is the slip plane during kinking and if there is a component of flattening in the XZ plane.

4.3.5. Microstructure in Minerals other than Quartz

The main features of the microstructure of the non-quartz fraction is summarized in Table 29 (Appendix I). In many, but not all, instances there are differences between the state of the mineral in LS1 and LS2 tectonites.

The most noteworthy is the case of K-feldspar, which throughout the area in rocks affected only by LS1, whether perthitic or not, is a highly-ordered microcline. In contrast, in LS2 specimens 30103B, 20102B 194C and THQ (the first three being deformed granites, the other, quartzite) K-feldspar shows microcline twinning only very rarely in small patches and nearly always has a lunate albitic intergrowth (Plate 19e). The K-feldspar grains in the quartzite (THQ) have even more exotic microstructures such as rims and polygonal grains and sub-grains (diameter ~ 50 μm). In the same rocks plagioclase is quite strongly kinked. Universal stage measurements indicate that (010) was the active glide plane.

The clinopyroxene of quartzite THQ have tail-like trails of minute particles, lying in S1, clearly spalled off during LS2 deformation (Plate 20c). This is a noteworthy similarity to the microstructure of some of the quartzites showing LS1 exaggerated grain-growth.

4.3.6 Microstructural Evidence for Simple Shear

In all except the specimens with the highest proportions of recrystallised material the quartz LS2 fabric is moderately curved and asymmetrically arranged with respect to the discrete zones it occupies (Fig. 4.1). It is shown (Fig. 4.27) that the long axis of this fabric was near to the direction of maximum extension at least in the early stages of its development. This fabric, therefore has some of the characteristics of the foliation in a shear zone, and the microstructures record a history in part of simple shear, heterogeneous at the scale of observation in the case of strongly curved microstructures.

The evidence for the relation of the foliation shape to the strain ellipsoid is afforded by the presence in a few of the samples of fine hair-like needles, probably rutile, within the quartz (Plate 18, compare Mitra 1976, Mitra and Tullis 1979). In sample 26102B (Plate 17f), rutile needles are present in a quartz vein which has a large proportion of unrecrystallised quartz and is thus a microstructure in early stages of development. Within a large equant quartz grain which displays mild undulatory extinction and rectangular subgrains, the rutile needles are oriented with an approximately uniform distribution (Fig. 4.27a). Moreover these needles do not show signs of deformation such as boudinage, breaking or bending. In an immediately adjacent domain where LS2 is well developed, the rutile needles have a strong preferred orientation parallel to LS2 (Fig. 4.27a). This 'double-funnel' pattern is compatible with the plane-strain deformation of a randomly oriented set of rods (Ramsay 1967, p. 163). Needles lying in this orientation form linear trails of fragments of equal spacing and length which are evidently the boudinaged remains of the much longer hair-like needles in the unrecrystallised quartz. More rarely needles lie at a high angle to LS2, and are bent (Plate 18a). It may be concluded that in this very small domain, which is part of a much larger aggregate of heterogeneously deformed quartz, the long axis of the new quartz fabric lies close to the principal extension direction.

Likewise in specimen of quartzite 695C (Plate 17d), which also displays an incompletely recrystallised microstructure, a similar relationship is displayed between relatively scarce rutile needles and LS2: the range of orientations of exclusively boudinaged rutile coincides with that of the LS2 trace on the XZ plane (Fig. 4.27b). The LS2 strain ellipse must have been relatively oblate since aspect ratios of LS2 grains in sections parallel to XZ and YZ (of LS2) are similar.

It must be emphasized that this close alignment of rutile and quartz foliations appears to hold strictly only for microstructures with a relatively high percentage of unrecrystallised quartz. That is to say, it is true of the quartz foliations in an early stage of their development.

In granite gneiss specimen 30103B (Plate 18) there is indirect evidence that σ_1 lay in the XZ plane of LS1 lying at approximately 45° to LS1 and plunging SE, a position compatible with shear of tops to the southeast. This evidence comes from the attitude of the basal planes of unrecrystallised and therefore hard areas of quartz, "augen" (as in Plate 19d). The trace on the XZ plane of these basal planes (the poles to which are represented by the C-axes forming the peculiar cockscomb projection on the girdle in Fig. 4.26c) is at approximately 45° to L1. This arrangement is also true for the single unrecrystallised grain from

26102B shown in Fig. 4.27a. Now, since in the augen of 30103B basal slip can be demonstrated from analysis of kinking in quartz (Fig. 4.29) it follows that the grains remained undeformed and unrecrystalised because their slip planes are in positions of minimal resolved shear stress, perpendicular or parallel to σ_1 (Tullis et.al. 1973).

Minerals other than quartz show evidence for deformation by simple shear. For example, in the specimen of granite gneiss (30103B, Plate 20b) a biotite, originally at a high angle to LS1 is transected by a narrow shear surface which lies parallel to S1 and is deformed into a spectacular sigmoid which indicates southeast directed shear of upper layers. In the quartzite from Tory Hill (THQ, Plate 20a) a foliation of very fine comminuted biotite lies parallel to S1, occasionally it is dragged by rotated feldspar porphyroclasts forming a pattern whose sense of twist indicates the same sense of shear. More often, in this quartzite and that from Elephant Lake (695C) feldspar, clinopyroxene and sphene inclusions appear to be rotated out of the S1 foliation plane without any indication of the sense of shear such as is afforded by an entrained micaceous foliation. The rotation is compatible with the analysis of Ghosh and Ramberg (1976) who demonstrated that providing the rigid particle had a low enough aspect ratio (the exact value of which was determined by the relative amounts of simultaneously applied pure and simple shear) it would rotate in a more ductile aggregate indefinitely.

In Tory Hill quartzite (THQ) some of the clinopyroxene porphyroclasts have an asymmetric lozenge-shape when viewed in the XZ plane (Plate 20c). This shape contrasts with the symmetric elongate morphologies of porphyroclasts in other samples. The shape may itself be evidence of simple shear since the experiments of Ghosh and Ramberg (1976) produced identical shapes in inclusions which were relatively stiff, but deformable, subject to simple shear in a ductile matrix.

The exact combination of simple and pure shear contributing to these microfabrics cannot be ascertained on the basis of the available information. However, in the light of the somewhat oblate shape fabric of the Elephant Lake quartzite (695C) and rutile fabric of the vein-quartz (24101B) (K=0.8) it is probable that strain histories were not simple. For example, a 'rolling-dough' with extension perpendicular to the shear direction deformation (Lister and Price 1978) comprised of simultaneous simple shear and flattening across the shear plane would explain the shape fabric of the quartzite 695C.

4.3.7. Summary and Hypotheses

The LS2 tectonites have only been sampled in and around the Cheddar and Cardiff complexes. It is certain that there are other examples as has been recognized in thin-sections from non-oriented samples from between Elephant Lake and Drag Lake.

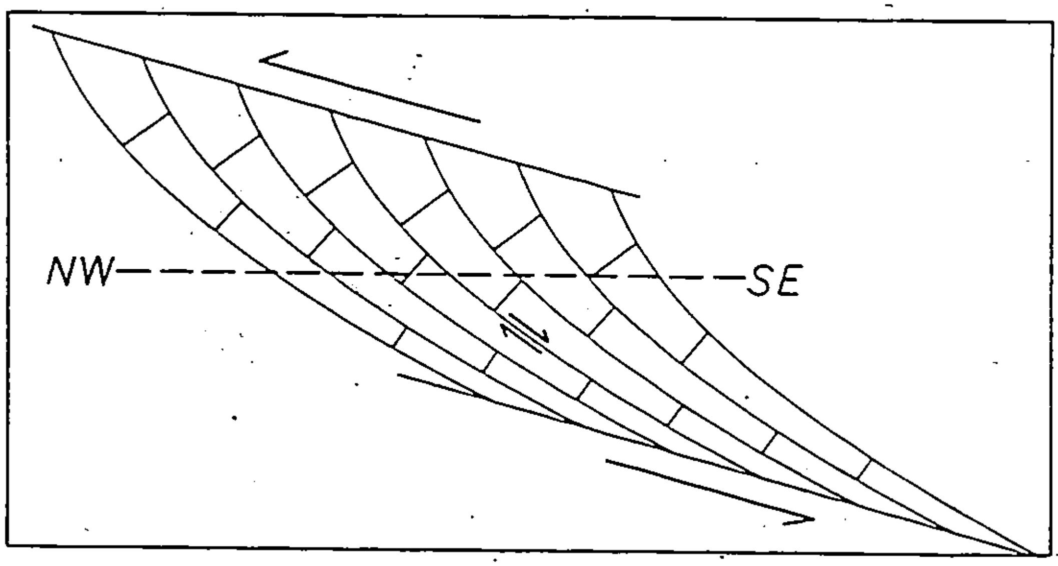

FIGURE
4.34

Model showing how a bulk northwesterly directed shear of upper layers can be accommodated by shear of opposite sense on thin discontinuities which lie parallel to an earlier foliation formed during the early stages of NW directed shearing, before the discontinuities were active. Discontinuities represent LS2 shear zones; the earlier fabric is LS1 (adapted from Lister and Williams 1979).

C-axis microfabrics and microstructures in the LS2 tectonites both indicates the same shear sense: upper layers have been sheared down dip to the southeast parallel to L1, S1 was the shear plane. The particular problem posed by the LS2 tectonites is that although they share many geometrical elements with the LS1 tectonites, the shear sense within the narrow zones is precisely reversed. This reverse in shearing sense along narrow concordant zones may be accommodated in a model in which bulk shear is towards the northwest (Fig. 4.34). In this model it is envisaged that initially the rock pile is sheared toward the northwest. Subsequently, as this shearing continued, deformation became concentrated in narrow zones as parts of the pile hardened, perhaps as temperatures fell. The pile now behaved as a sheared row of books in which antithetic shear takes place between volumes as they tilted. This history is necessarily episodic in order to account for the observed static grain growth in LS1 quartz. An alternate interpretation of the relationship of the two fabrics is that the bulk shearing sense in the two episodes was not the same and the LS2 zone represents the deep ductile level of a late, listric, normal fault system.

4.4 Microstructural Evolution of a Metagabbro

4.4.1 Introduction

The petrographic descriptions in Section 2.4 are ordered according to rock type and the degree of recrystallisation, modification of primary texture and development of tectonite fabric. The details appear to be quite complex involving: i) development of coronas of olivine and clinopyroxene and the subsequent evolution of these to amphibole aggregates; ii) the development locally of amphibole inclusions within primary plagioclase and the evolution of these domains involving plagioclase recrystallisation, zoning and amphibole and plagioclase growth; iii) the recrystallisation of plagioclase within pure plagioclase domains such as on kinks or at mutual boundaries of plagioclase grains. The third process also corresponds to changes observed in the anorthosites, which have microstructures similar to those which have been described in anorthosites by Kehlenbeck (1972).

Changes are described in samples taken from a vertical shear zone in the gabbro. The shear zone, which has a south-east trending lineation, developed during the formation of LS1 and deformation of the most southerly lobe of gabbro at the south shore of Farquhar Lake (Section 3.3.5, Fig. 3.14). With evidence of increasing strain the microstructure evolves towards a simple configuration in which there are some indications that a chemical equilibrium was also achieved. Changes parallel to those outlined above are found throughout the gabbro. This study elucidates the mechanical behaviour of gabbro, explaining in part why such bodies remained hard resistant masses; deformation of the gabbro depended not only on an influx of OH but also on subsequent diffusion of several chemical species over distances greater than grain-size.

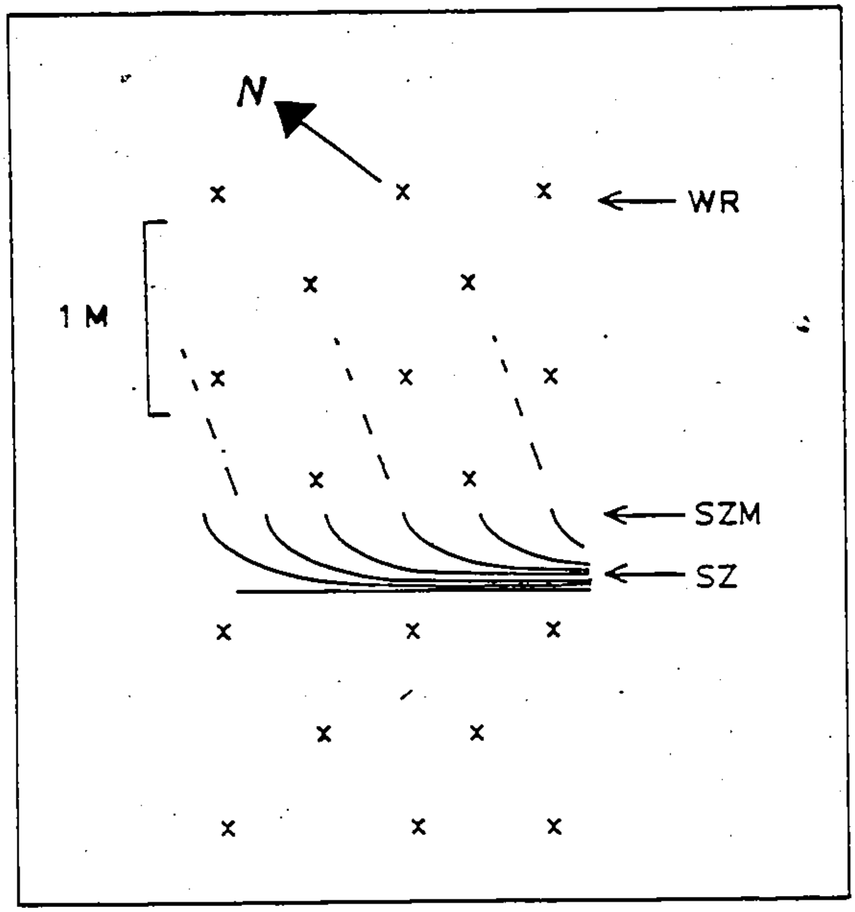

FIGURE
4.35

Diagram of shear zone showing approximate location of samples. Foliation: solid line; subophitic texture: crosses; direction of weak elongation in subophitic texture: dashed line. See Fig. 3.14 for location.

4.4.2. The Shear Zone

The main foliated part of the shear zone is no more than fifteen centimetres wide and strikes NNW (Fig. 4.35). The foliation is vertical and a mineral lineation plunges gently SSE. At the southwestern boundary, the foliation and shear zone margin are parallel. On the opposite side of the zone the foliation curves in the manner described by Ramsay and Graham (1970). The zone of well defined foliation adjoins the wall rock in which a faint elongation is discernible in a modified subophitic texture. This very weak fabric, which is at a high angle to the zone, gradually fades away in the space of a metre. The rock here is highly amphibolized although it does not have a mesoscopic tectonic fabric.

The least deformed sample (WR) is taken from 2 metres from the shear zone (Fig. 4.35) from the mesoscopically undeformed, amphibolized wall rock in which subophitic texture is preserved. The second sample (SZM) is from the edge of the shear zone where the gneissic foliation is for the first time clearly discernible. The third sample (SZ) is from the zone where the foliation is subparallel to the shear zone margin. SZ differs mesoscopically from SZM in its high degree of planarity.

There are no major gains or losses of major or minor elements across the zone (Table 30, Appendix I), the transition is largely isochemical. It must be noted however

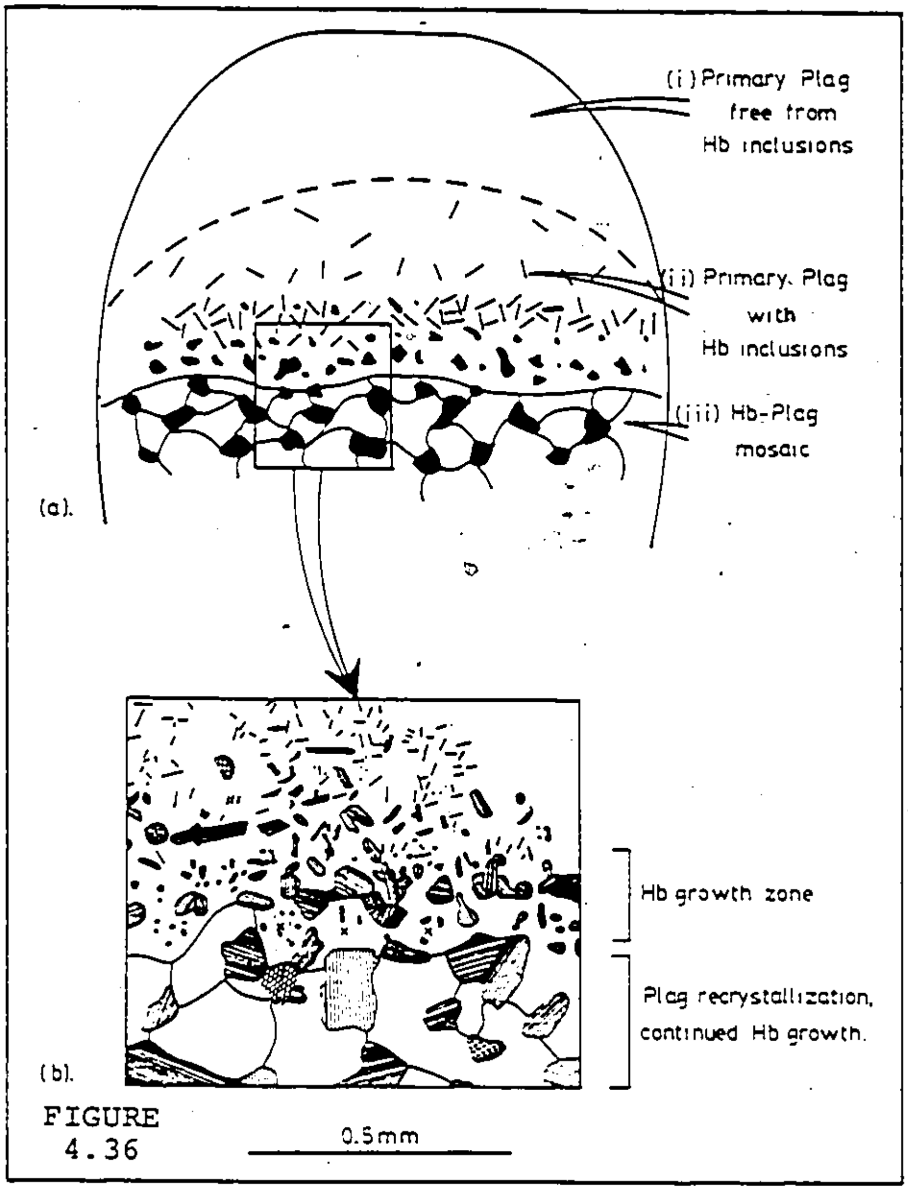

FIGURE 4.36

Microstructure of hornblende and plagioclase from near margin of partially recrystallized primary plagioclase in metagabbro from weakly deformed shear zone wall (sample WR). (a) diagram of partially recrystallized primary plagioclase. The part of the grain which is free from hornblende inclusions abuts other primary plagioclase grains. Inclusion-filled plagioclase abuts a mosaic of hornblende and recrystallized plagioclase. Density and size of hornblende inclusions increases towards recrystallization boundary. (b) drawing from photomicrograph of boundary of hornblende-filled plagioclase. Hornblende inclusions are larger and often touching near boundary fencing off small volumes relatively free of hornblendes (marked with x), possible future recrystallized plagioclase grains.

that the gabbros are hydrated and the presence of scapolite implies addition of Cl and CO_2.

4.4.3. Microstructure

Wall Rock: In the unstrained wall rock (WR) sample two microdomains abut and represent two stages of recrystallisation (Plate 3b). In the first a subophitic texture is clearly visible under the microscope. Clinopyroxene and hornblende form a delicate intergrowth resembling a mesoperthite. Primary plagioclase has clean uncorroded margins, is free from inclusions and is unzoned. The plagioclase has multiple wedge shaped deformation twins.

In the second microdomain the subophitic texture is obscured. The microstructure is complex (Plate 3b). The clinopyroxene hornblende intergrowth is replaced by a decussate aggregate composed solely of hornblende. The primary lath-like plagioclase has irregular corroded margins, is zoned and surrounded by small equant plagioclase grains. The modification of the primary plagioclase takes place in three locations: (1) at the interface of the primary plagioclase and the hornblende aggregates; (2) at mutual boundaries of plagioclase grains; (3) at sub-boundaries within the plagioclase grains (Plate 4a,c).

(1) The interface area between primary plagioclase and the hornblende aggregates may themselves be split into three domains (Fig. 4.36): (i) the primary plagioclase free from inclusions; (ii) primary plagioclase with hornblende

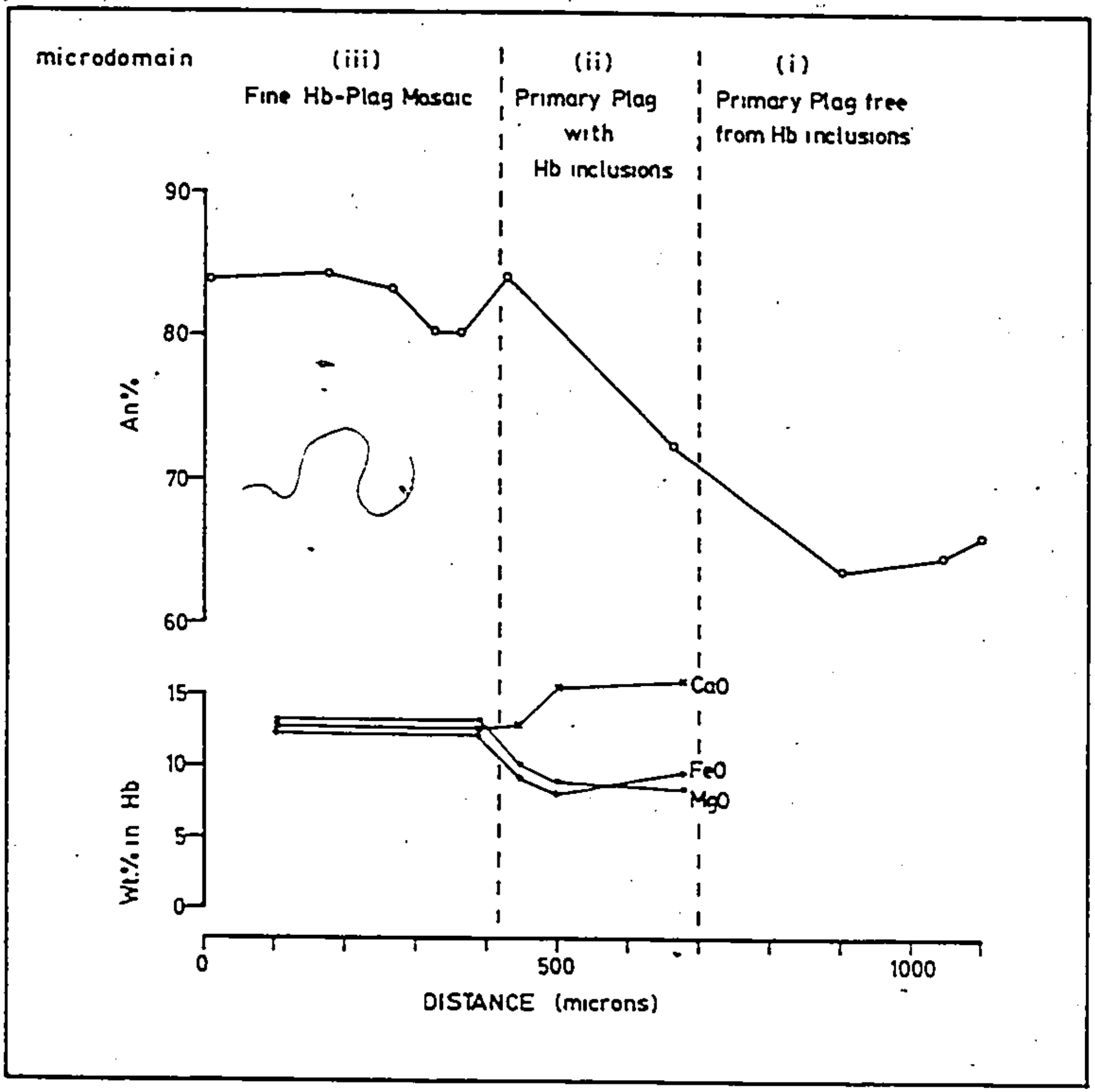

FIGURE
4.37

Chemical variation in hornblende and plagioclase from near margin of partially recrystallized primary plagioclase in metagabbro from weakly deformed shear zone wall. Zones named as in Fig. 4.36a.

inclusions (Plate 5a) which abuts (iii), a fine mosaic of hornblende and plagioclase, largely free from inclusions (Plate 5c), which adjoins the hornblende aggregate.

(i) The primary plagioclase farthest from the interface is free from hornblende inclusions, and retains the primary composition (An_{66}). (ii) The primary plagioclase close to the interface is strongly zoned to more calcic compositions (Fig. 4.37), displays bright lamellae interpreted as the huttenlocher intergrowth lying at 18-20° to (010) (Plate 5b) and is crowded with hornblende inclusions (Plate 5a-c). This domain of the plagioclase is itself zoned compositionally being more anorthite rich the more hornblende inclusions are present (Fig. 4.37). The number and size of hornblende inclusions increases in a direction toward the fine hornblende-plagioclase mosaic Domain (iii) until a point where there appears to be a sudden decrease in the number of hornblende grains present. At this point, close to the boundary with Domain (iii) there are a number of relatively large hornblendes many of which impinge on one another and fence off an area of plagioclase which is almost inclusion free (Fig. 4.36). The hornblende inclusions have slight changes in composition, becoming generally less calcic and more ferromagnesian as the boundary with Domain (iii) is approached (Fig. 4.37).

In Domain (iii), the fine hornblende-plagioclase mosaic, the hornblendes are rarely included with the plagioclase but are located on the boundaries of the feldspar.

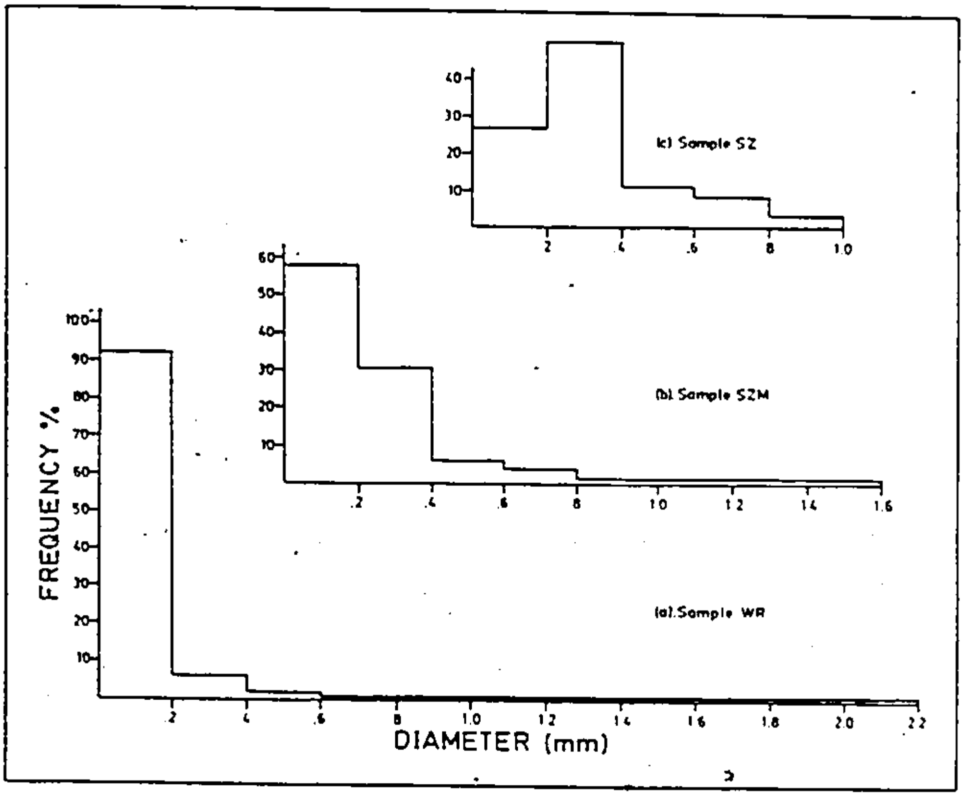

FIGURE 4.38

Grain size distribution of plagioclase from shear zone in metagabbro, south Farquhar Lake. (a) Sample WR from weakly deformed shear zone wall; note very small population of grains with large grain size, these are the unrecrystallized primary grains; N 259. (b) Sample SZM, foliated metagabbro from moderately deformed shear zone edge, where recrystallization is advanced; N 263. (c) Sample SZ, from centre of shear zone where foliation is subparallel to shear zone margins and no relict primary grains remain; N 254. Grain size distribution measured by the Spektor method (Underwood 1970).

They are considerably larger than those in Domain (ii), but smaller than those in the hornblende aggregates. There is a variety of isolated and mutually impinging grains. Plagioclase in this Domain is considerably more An rich than the primary grains (Fig. 4.37).

(2) At the mutual boundaries of primary plagioclase grains there are fine equant, evidently new grains. There is no hint, however, of subgrain development in the primary grains.

(3) Along kink boundaries within the primary grains there are strings of new plagioclase grains and ~~occasional~~ hornblende grains (Plate 4c,d). The kink boundary is discontinously zoned towards more calcic compositions with bright lamellae sparsely developed. The kink is flecked with very fine scapolite. There are two dominant orientations of new grains, both having bifringence suggesting lattice orientations close to those of the twins in the host grain. The number of twins and the twin lamellae thickness varies across the kinks (Plate 4c).

A consequence of the variety of the varied microstructural character of this rock is the extremely wide range of grain size of plagioclase (Fig. 4.38a). Noteworthy is the very large number of very small grains.

There is evidently also a very wide grain size range for hornblende (Plate 3b), corresponding to its variety of microstructural environments. Non-impinging hornblendes,

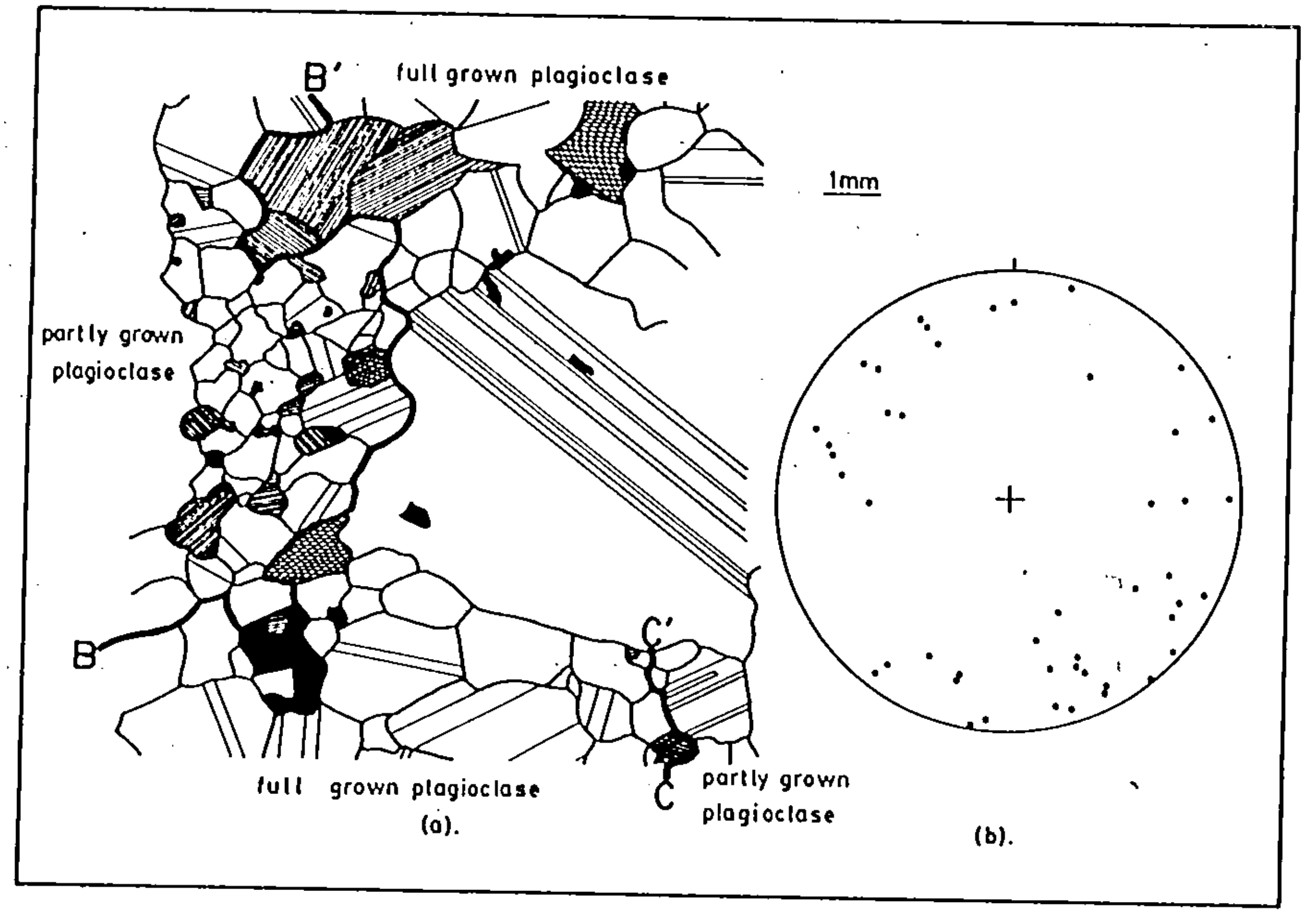

FIGURE 4.39 Microstructure in recrystallized plagioclase in metagabbro from edge of shear zone (sample SZM). (a) partly grown plagioclase and hornblende to left of B-B' and to right of C-C', elsewhere relict primary plagioclase is surrounded by full grown recrystallized plagioclase. Bright lamellae and hornblende inclusions are restricted to partly grown grains in which twin morphology is varied and grain boundaries more curved than in fully grown grains. (b) poles to bright lamellae for partly grown grains.

especially those included within plagioclase, are smaller than those which are mutually impinging.

Shear Zone Margin: In the moderately strained gneissic metagabbro (SZM) no primary textures are visible. Relict primary minerals are rare. However, most of the microstructural domains of the least deformed sample (WR) are present in an advanced stage of development.

The decussate hornblende aggregates which have replaced the clinopyroxene (Plate 3c) are considerably coarser than in the least deformed sample.

There are a few large plagioclase grains interpreted as primary grains. They are relatively irregular in outline. They have multiple twins which are thicker and fewer than those in primary grains in less deformed rocks. Microdomains composed of hornblende-free aggregates of subequant plagioclase are correlated with microdomains (2) and (3) of the least deformed sample. These grains are free of compositional zoning and have simple, continuous twins (Fig. 4.39). Grain boundaries are straight to gently curved. Well formed scapolite is found within this microdomain.

The microdomains with the finest grain size are composed of aggregates of plagioclase and hornblende (Fig. 4.39). These microdomains, which abut both mafic aggregates and, where present, relict primary plagioclase, are interpreted as a further evolved form of the fine hornblende-plagioclase mosaic and inclusion-filled primary

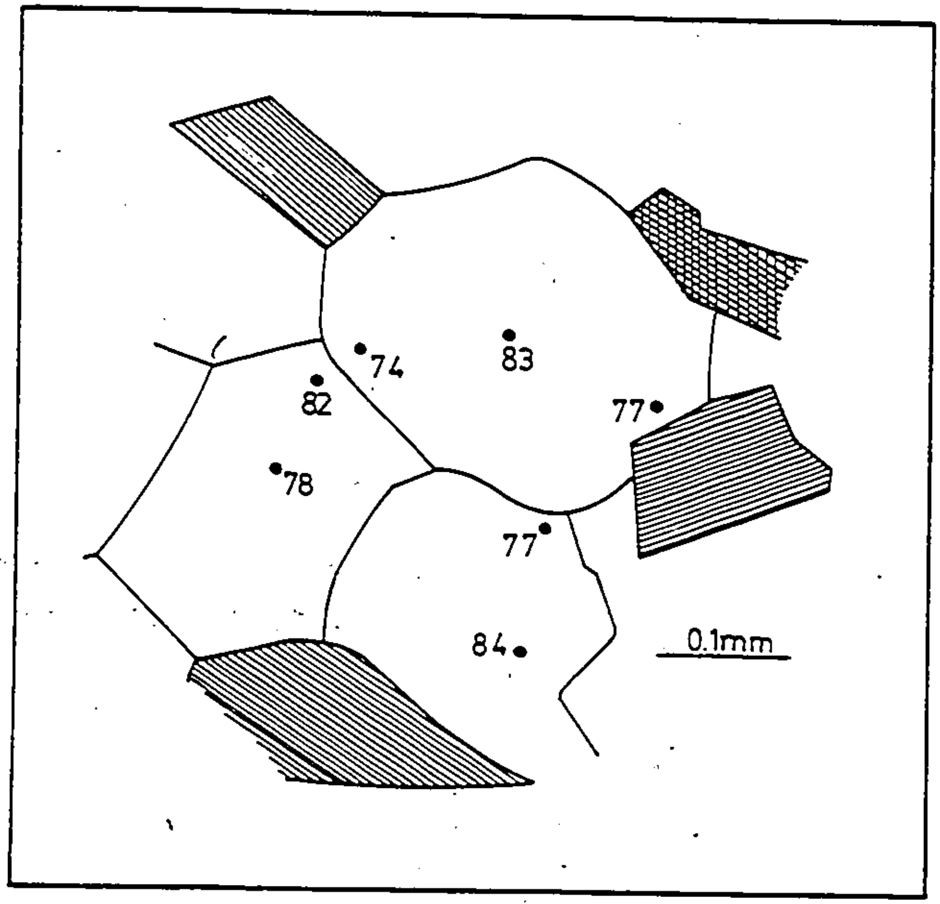

FIGURE
4.40
Variation in anorthite content in partly grown recrystallized plagioclase in meta-gabbro from edge of shear zone (sample SZM). Hornblende ornamented.

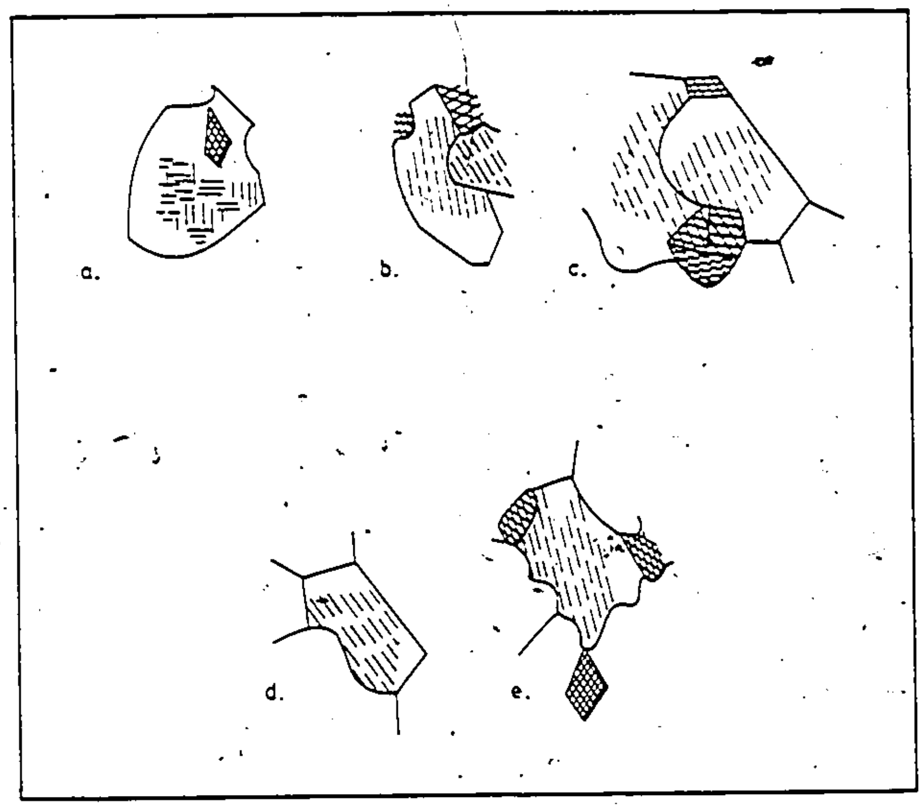

FIGURE
4.41
Grain morphology in partly grown plagioclase with bright lamellae (dashed lines) in metagabbro from edge of shear zone (sample SZM). Curved boundaries as well as relatively straight boundaries occur. Hornblende cross-hatched.

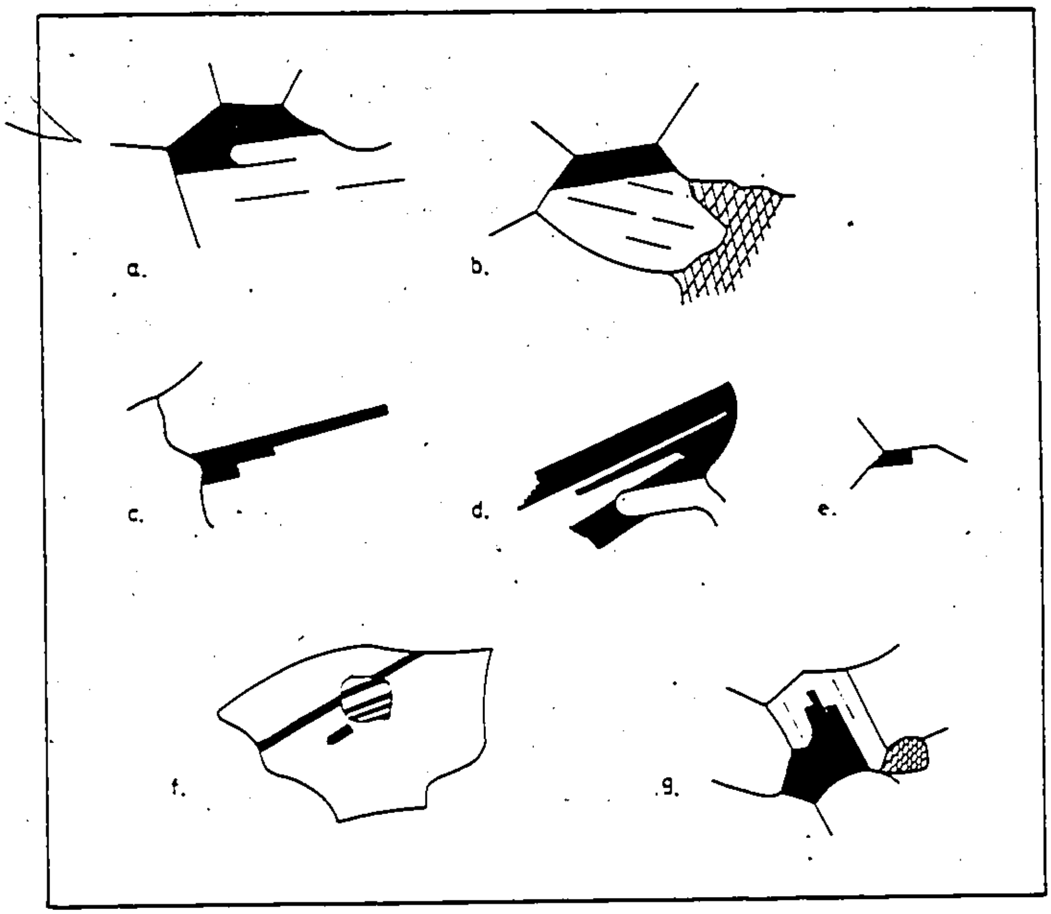

FIGURE
4.42

Twin morphology in partly grown recrystallized plagioclase from edge of shear zone (sample SZM). Edge twins (a),(b),(d),(e) and (g);partial twins (c),(d),(e) and (g);enclosed and continuous twins (f).Twinning associated with curved grain boundaries in (a),(c),(d),(f) and (g).Many twins have stepped and abrupt terminations.

plagioclase of the least strained sample (microdomain (1) subdomains (ii) and (iii)).

Plagioclase in this microdomain are compositionally zoned (Fig. 4.40) and all display the bright lamellae (Plate 5d). There is evidence that their lattice orientation is related to the postulated parent grain since both the bright lamellae in the new grains and the albite twins in the relict grain lie at a high angle to the section (Fig. 4.39b). Twins have distinctive morphologies attributed to formation during growth (Vernon 1965, Spry 1969) (Fig. 4.42). Grain boundary morphology in this domain is also unique, straight and strongly curved boundaries are present (Fig. 4.41). Hornblende grains are mostly located on the boundaries of plagioclase grains or protrude into them (Figs. 4.40 and 4.41).

The range of plagioclase grain size is still wide (Fig. 4.38b) but somewhat more restricted than the least deformed sample (Fig. 4.38a). The number of fine grains has increased relative to the very fine grains and the mean size is larger.

Hornblende also still has a wide grain size range (Plate 3c), reflecting the varied microstructural environments.

<u>Shear Zone</u>: The microstructure of the highly strained gneissic metagabbro (SZ) is relatively simple. None of the microstructural domains found in the less deformed samples are present (Plate 3d).

Plagioclase is more sodic (An_{58}) than the primary plagioclase. It is free from zoning except for very minor thin normally zoned rims. Bright lamellae are absent. Simple continuous twins are dominant. Discontinuous and enclosed twins are not present. Grain boundaries are gently curved to planar. Scapolite is very common. Plagioclase grain size range is restricted (Fig. 4.38c). Fine grains now dominate over very fine grains and the mean grain size is larger than in the moderately strained rock.

Hornblende forms elongate decussate clusters, which are one or two grains thick (Plate 3d). There are few grains not in contact with another. Grain size range is very restricted (Plate 3d) and appears somewhat finer than the coarsest grains in less strained samples.

4.4.4. Deformation Mechanisms

The petrographic and crystal-chemical data suggest that deformation of the gabbro involved: (i) hydration; (ii) recrystallisation, grain-growth and attainment of a chemical and microstructural equilibrium. These interrelated processes are completed in the most highly strained part of the shear-zone. There are problems determining whether these processes are wholly or partly syntectonic (dynamic or metadynamic). The postulated mechanisms and relevant evidence are outlined below.

The addition of water obviously accompanied deformation of the gabbro with amphibolitization simply described by the equation:

$$\text{clinopyroxene} + \text{plagioclase } (An_{66}) + H_2O = \text{hornblende} + \text{plagioclase } (An_{60}).$$

Scapolite may be ignored since, although it increases in amount within the shear-zone, it is a late addition, replacing recrystallised plagioclase.

In addition to the reaction being in part the driving force of nucleation and grain growth, it may be important in providing a specific softening process. White and Knipe (1978) describe "reaction-softening" as occurring when reactants and products are present together in an aggregate undergoing a phase transformation. The volume difference between reactants and products generates an internal stress which allows the aggregate to flow at relatively low stress. This mechanism may have been significant in the less deformed samples where reactants and products are present (WR and SZM).

The microstructural history of amphibole in the shear zone is complicated. Nucleation is not always simply followed by growth but may be followed by growth then dissolution.

The location of the finest amphibole, and therefore the probable sites of nucleation are: (i) within clinopyroxene. (ii) within primary plagioclase (WR microdomain (i) and (ii)), where it occurs as tiny rod-like inclusions (Plate

5a-c); and (iii) at the plagioclase-clinopyroxene interface. Subsequently there is no optical evidence for intracrystalline-strain, such as deformation twins, undulatory extinction or subgrains.

There is evidence for grain-growth and shrinkage of amphibole in all microstructural environments. Within the pure hornblende aggregates grain-size at first increases with increasing strain (WR- SZM) then diminishes somewhat in the shear-zone centre (SZ). This is illustrated by increase in grain size in pure mafic aggregates within WR from left to right of Plate 3b, and subsequent further growth in SZM, centre Plate 3c; in contrast grains in SZ, Plate 3d are smaller than those in SZM. A more complex evolution is observed in the recrystallisation of amphibole inclusions in primary plagioclase (microdomains (ii) and (iii) of WR, Fig. 4.36). In this location there is an initial nucleation of a large number of amphibole crystals within the plagioclase (micro-domain (ii)), subsequent growth of some and shrinkage of others implied by the decrease in number but increase in size observed as the boundary with microdomain (iii) is approached, where relatively few impinge on one another. In microdomain (iii) the increase in size and decrease in number of amphibole grains implies growth of some individuals at the expense of others. In the development of similar microdomains in the moderately strained sample (SZM) the amphibole, which still occurs primarily as isolated individuals (Plate 3c), has grown further.

Nucleation within plagioclase and clinopyroxene and growth and shrinkage of these amphibole grains and those which are surrounded by grains of fine plagioclase implies cation mobility on the grain scale both through host lattices and along grain boundaries. The mobility requirement for growth of mutually impinging amphibole is much less drastic.

In plagioclase strong intracrystalline deformation is limited to primary grains. These are replete with multiple wedge-shaped twins, which change thickness across kinks (Plate 4c) and were thus formed at the same time as the kinks. These twin morphologies are characteristic of deformation twins (Vance 1961, Seifert 1964, Vernon 1965, Lawrence 1970). Comparable kinking has been demonstrated to be accommodated by (010) slip (Borg and Heard 1969, Vernon 1975).

The lack of optical signs of recovery is unexpected in plagioclase deformed in the amphibolite facies, according to White (1975). Although this may be an effect of the scale of observation, the apparent absence of recovery rules out nucleation by grain-boundary migration or subgrain rotation. The same author points out that nucleation may be enhanced in plagioclase grain-boundaries by the multiplication of dislocations which are aided by the availability of water (rehbinder effect). The presence of water is demonstrated along kinks and near the boundary of primary plagioclase and mafic aggregates by the presence of amphibole. The rehbinder effect may have aided nucleation at these points.

It was suggested earlier that hornblende growing within primary plagioclase near the boundary of the fine hornblende-plagioclase mosaic (WR microdomain (i),(ii) and (iii), Fig. 4.36, Plate 5a-c) plays a role in plagioclase recrystallization. The amphibole inclusions will elastically strain the host lattice (Van Vlack 1965). Furthermore, mutually impinging amphiboles may effectively separate domains of plagioclase from the host effectively forming a new grain boundary (Fig. 4.36).

The evidence for control of new grain orientation by that of the host grain has been noted (especially Fig. 4.39). This effect has been noted in andesine (Vernon 1975), quartz (Hobbs 1968) and olivine (Ave'Lallemant and Carter 1970).

There is an overall difference between the composition of the primary grains (An_{66}) and the fully-grown recrystallised grains of the most deformed rock (An_{58} in SZ), comparable effects are found in anorthosites of the complex. Moreover newly recrystallised grains near the hornblende aggregate-plagioclase boundary are more calcic than primary grains (Fig. 4.37). Similar compositional differences have been observed in recrystallised andesine (Vernon 1975) and biotite (Etheridge and Hobbs 1974). These are considered to reflect a decrease in free energy between old and new grains which aided in promoting recrystallisation. In the present case there are compositional differences not only between the primary grain and the fully-grown grains of the most highly strained sample but also between these and the finest new grains (Fig. 4.37). This suggests the possible rôle of free-energy differences enhancing growth as well as recrystallisation.

The evidence for grain-growth in the plagioclase is several fold: (i) the new grains increase in size from least to most strained part of zone (Fig. 4.38); (ii) relatively highly curved boundaries are found in the finer new grains, indicating mobility (Fig. 4.41); (iii) the same grains show exclusively growth twins (Fig. 4.42); (iv) bright lamellae (huttenlocher intergrowth) are confined to these same grains, but are absent from the grains of the most deformed specimen. This type of intergrowth has been found in recrystallised plagioclase from shear zones (Brodie 1981, Borges and White 1980, Brown et.al. 1980) where its disappearance has been specifically linked with grain growth. Peristerite intergrowth, an analagous features from sodic plagioclase, has been shown to be associated only with grain boundary migration in sheared pegmatite (Marshall and Wilson 1976).

4.4.5. Chemical and Textural Equilibrium

The most strongly deformed sample from the centre of the shear zone has attained a chemical and textural equilibrium. The evidence for this is: (i) the elimination of hornblende inclusions within plagioclase. The expulsion of hornblende to plagioclase grain boundaries implies a lowering of interphase grain boundary energy (Van Vlack 1965). (ii) the elimination of strongly curved plagioclase-plagioclase grain-boundaries and the overall increase of grain size of new plagioclase implies a minimization of grain-boundary energy. (iii) the bright lamellae and microscopically-visible zoning of plagioclase are absent in the most sheared rock.

4.4.6. Timing of Microstructural Development

There can be little doubt that the microstructure is in part syntectonic. This interpretation is favoured by: (i) the fact that initial microstructural development and amphibolization are simultaneous and that, throughout the complex, amphibolization and development of a foliation are uniquely related. Amphibolization is often accompanied by development of a linear amphibole fabric. (ii) in the less deformed rocks evidence of textural disequilibrium (see above) is not annealed out. (iii) it is known in metals that annealing results in a grain-size which varies inversely with strain (Cahn 1965, Sellars 1978). The reverse is the case in the sheared gabbro. Although this rules out annealing sensu-stricto (all grain-growth <u>and</u> nucleation post-tectonic) it is still compatible with some measure of post-tectonic grain-growth, if the metallurgical analogy is applicable to these rocks. (iv) Metadynamic recrystallisation may be viewed as dynamic recrystallisation followed by a static chemical and textural equilibration that is controlled in its amount by strain. The case that it took place is supported by comparison with some metals.

Materials with similar microstructures to the meta-gabbro are hot-worked low stacking-fault energy metals, e.g. Cu, Ni, Pb, γ-Fe. These are metals in which, because of their lattice geometry, climb and polygonisation rates are very slow. Softening is accomplished by rapid re-crystallisation. There is a period of rapid work-hardening before the onset of steady-state dynamic recrystallisation. The microstructure changes with the achievement of a steady state deformation from a mixture of new and old grains to an aggregate consisting only of equant new grains (Hardwick and Tegart 1961a&b). Growth twins are common and grain growth occurs prior to the achievement of steady-state flow (Hardwick, Sellars and Tegart 1961).

The similarity of the microstructure of these metals with that of the plagioclase which consists of an aggregate of new grains is clear. Moreover there is evidence for achievement of a steady-state flow in the macroscopic morphology of the shear-zone. This is, as previously mentioned, that on one side of the shear zone the foliation and margin are concordant, indicating that the zone was not spreading sideways during deformation. Beach (1980) noted that many high-grade shear zones had a comparable morphology which he attributed to the achievement of steady-state flow.

However, if the microstructure is developed purely dynamically a change of deformation mechanism may have occurred, since none of the signs of grain size change evident in the less strained rocks are visible at the shear zone centre. A change of deformation mechanism within a shear zone has been proposed for anorthosite by Borges and White (1980) and discussed for retrogressed Lewisian rocks by Beach (1980). Such a new mechanism would be grain boundary sliding, since there is little visible evidence (such as grain elongation, sub-grains, deformation twins) for dislocation dominated mechanisms. One objection to grain boundary sliding is that in metals, where this is probably the dominant mechanism in 'superplastic' materials, a very fine grain size is the rule. There are however exceptions. Superplastic Ti-Mn alloy has a 500 μm grain-size (Griffiths and Hammond 1972) which is very coarse for superplastic metals. In geological materials, however, superplasticity has only been suggested for very fine grained rocks (Boullier and Guegen 1975).

4.4.7. Conclusions

A textural and chemical equilibrium was attained in the most deformed rock of the shear zone. Deformation and microstructural development in the two least deformed samples can be accounted for by the processes accompanying amphibolization although microstructural evolution outlasted this process. These processes are: (i) nucleation, by a method other than grain-boundary migration or sub-grain rotation; (ii) growth of hornblende in pure hornblende aggregates and of all plagioclase by migration of high angle grain-boundaries; (iii) the growth and shrinkage of hornblendes which are surrounded by plagioclase, by diffusion both along the grain boundaries and through the lattice of plagioclase. The migration of high angle boundaries and the growth and shrinkage of hornblende continued after the completion of amphibolization and must have been wholly syntectonic (dynamic) or partly (meta-dynamic). Steady-state flow was achieved in the centre of the shear zone and was probably accomplished by similar processes. Such processes probably account for deformation of other metagabbroic gneisses within the study area which have similar microstructure.

In conclusion it must be noted that the slowest process in the deformation of the gabbro is the recrystallisation of the mafic minerals. This process is governed by the long range influx of water to initiate the nucleation of amphibole and the diffusion of several chemical species over greater than single grain scale distances during growth and shrinkage of the non-impinging grains. In contrast grain growth of plagioclase must be much faster since consumption of one grain by its neighbour simply requires movement of material across a grain boundary and, if grain boundary sliding is an important process, components may have to move from one part of a boundary to another a short distance away. In this way, the relative ductility of anorthosite, gabbro and pyroxene (Section 2.4.1) may be in part explained and the relative hardness of these rocks compared to the quartz-feldspathic and carbonate rocks of their envelope. Thus, the gabbroic rocks may persist as resistant masses during considerable periods of deformation.

5. SUMMARY OF TECTONICS AND STRUCTURAL PROCESSES IN RELATION TO REGIONAL TECTONICS AND CONSEQUENT HYPOTHESES

5.1. Introduction

In this section the tectonics in the study area and the structural processes described from it are summarized. Also, hypotheses relating events within the area to those in the larger western Grenville Province are presented as guidelines for future study.

5.1.1. Tectonics in the Study Area

Rocks in the amphibolite facies, predominantly calcareous metasediments situated near the border of the Central Metasedimentary Belt with its basement, are interlayed with probable basement and a variety of orthogneiss. Granites form two large subcircular tilted complexes. The probable basement, which is mostly tonalitic orthogneiss, has near or at its structural top a discontinuous horizon of interlayered pelitic, semi-pelitic and Ca and K poor (orthoamphibole bearing) intermediate to mafic gneiss, possibly a metamorphosed weathering product marking the unconformity. The grey gneiss forms stratiform slabs lying within the supracrustal rocks, and if the basement hypothesis is correct, they are allochthonous.

The oldest orthogneisses which are undoubtably not basement are gabbroic rocks (ranging from pyroxenite through gabbro to anorthosite) which were followed by syenitic rocks. Both were probably emplaced as sheets, implying emplacement into a stratiform pile, possibly syntectonically (with respect to the main lineation-forming or an earlier event). The Farquhar Lake Mafic complex may have been emplaced during thrusting after differentiation. Major syntectonically and diapirically emplaced granitoid complexes form the northern tip of a regional magmatic and migmatitic arch. Gravity tectonics and ductile shearing appear to have played important roles both in the emplacement of the granites and in modification of structures around the Allen Lake pyroxenite. Requirements of density contrast and ductility contrast appear to be satisfied.

Evidence for low angle tectonic transport includes the syn-metamorphically imposed SE plunging regional lineation, the asymmetric structure of the major granitoid bodies, and the quartz C-axis microfabrics and microstructures. Such transport is assumed to be responsible for the purported basement thrusting and the dismemberment of the Farquhar Lake Mafic complex. This lineation is imposed on the Harvey-Cardiff Arch which tilted a major tight F2 fold, correlated with a set of folds present regionally and is particularly strongly developed in a zone of high strain which traverses the northern part of the map area. The low angle transport event thus postdated a folding event of considerable importance and is most likely an episode of the Ottawan orogeny (ca. 1100-1050 Ma., Moore and Thompson 1980).

5.1.2. Structural Processes

On the large scale the most important processes displayed by the rocks are penetrative regional ductile flow which accompanied the thrusting and shearing and the interplay of this with gravity driven tectonics. The softness of the rock during the main deformation is witnessed by the ubiquity of the stretching lineation and the chaotic inclusion-fabrics of the voluminous marbles. The lineation also imposes an important control on the geometry of many of the structures, for example, the zones of folding coaxial with it and the NW tilt of the granitoid complexes.

On the small scale the importance of oriented grain growth subsequent to dynamic recrystallisation has been demonstrated in the formation of the common quartz ribbons in granitic gneisses. The oriented grain growth in the granites represents an arrested stage of metadynamic microstructural adjustment, which results in exaggerated grain growth in high grade quartz-rich rocks if the density of other minerals is sufficiently low. A result of this cessation of grain growth is that C-axis microfabrics in the granitic gneisses are determined by the strain history.

Local kink-like recrystallisation of the early quartz microstructure results in the production of asymmetric microfabrics whose linear element (L2) lies in the XZ plane of the earlier fabric and which can be used as kinematic indicators. Tectonites with these microfabrics occur in narrow zones which may represent zones of antithetic shear related to the main deformation.

The production of foliation in the gabbro is accompanied by quite different processes. Intracrystalline dislocation dominated plasticity appears to be negligible. Instead intra- and intercrystalline diffusional processes which rely on the presence of introduced water dominate. The relative slowness of this process explains both the preservation of primary fabrics in the gabbros and the relative hardness of these bodies during regional ductile deformation.

It is hoped that the processes described above contribute something to our understanding of the modes of deformation at various scales of deep seated crustal rocks.

5.1.3 Hypothetical Relations to Grenville Tectonics and suggestions for further work

(a) It has been stated previously that the map area is part of a larger zone of high strain where there is a southeast plunging lineation which, in turn, is one of several such zones in the western Grenville Province, that include the Grenville Front.

Although not known in detail, the similarity of fabric type and orientation in these zones suggests a similar significance and age for all of them. If, as argued for the map area, they all are zones of northwest directed ductile

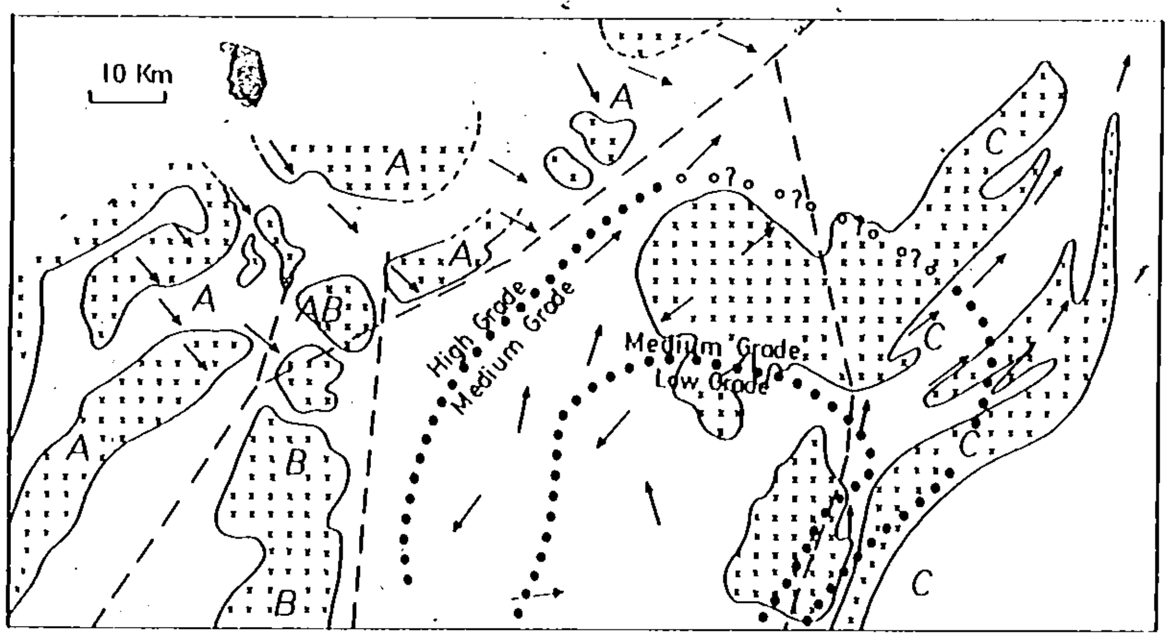

FIGURE
5.1

Schematic map of aspects of geology of the Haliburton-Bancroft-Sharbot Lake region of the Central Metasedimentary Belt. The area of high grade metamorphism can be divided into zones of three contrasting but possibly synchronous tectonic modes. In Zone A low angle tectonic transport is dominant, as shown by the shallow lineation. In Zone B subvertical gravity driven tectonics are present. In Zone AB both the foregoing styles are present. In Zone C another mode is evidenced by the sinuous pattern of the plutons.

shearing and/or thrusting, then a Tibetan-type model of crustal thickening is favored (Davidson et.al. 1981).

(b) The map area is part of the edge of an extensive high grade zone which almost encircles the lower grade rocks of the Hastings Lowlands (Fig. 1.1 and 5.1). There is evidence that this high grade margin has a distinctive tectonic style and its boundary zone with the low grade area is marked in places by a fabric transition: (i) In the region including the east side of the map area extending east of Bancroft, there is a switch from northeast to southeast trending lineations (Fig. 1.1) and a shallowing of dip with increasing grade . (ii) In the region including the south and southwest side of the map area extending to the south of the Harvey-Cardiff Arch upright structures give way to shallow away from the low grade zones, here there is some evidence for a fabric transition (Fig. 1.1). (iii) East of the bulbous Weslemkoon and Elzevir plutons (Fig. 1.1 and 5.1), batholiths of the sodic and potassic group have a different style, forming sinuous, elongate bodies (Abinger, Cross Lake and Northbrook plutons) and lineations have shallow plunges at higher grade (Rivers 1976). A tectonic model for the Grenvillian orogen as a whole should take these facts into account. Full cognizance should be given to the possibility of simultaneous gravitational adjustment (sinking of Hastings lowland and complementary rising of marginal gneiss and plutonic complexes) and, at the margins, low angle transport tectonics.

(c) Large tight folds are found in the Hastings Lowlands (Divi 1972, Carmichael 1968), on the margin of the Lowlands (the Burleigh fold), where they appear to predate the diapirism, and the Flinton-Ompah area, east of the Elzevir and Weslemkoon Batholiths (Rivers 1976, Moore and Thompson 1980). A regional correlation of these folds would imply a widespread folding episode, postdating the deposition of the Flinton Group and predating the formation of the Harvey-Cardiff arch. Early thrusting has been suggested adjacent to the east flank of the arch (Heamon et.al. 1982). Such thickening of cover rocks and subsequent elevation of metamorphic grade would help explain the diapiric uplift of the arch. Similar sequences are reported from the Norwegian Caledonides (Cooper and Bradshaw 1980) and the Australian Archean (Bickle et.al. 1980).

(d) The Drag Lake Complex and the Glamorgan Complex of migmatitic tonalitic gneisses both extend considerable distances beyond the map area (Fig. 1.1). Structures within and adjacent to the map area suggest these bodies are very large low dipping slabs. If they are indeed basement gneisses, a very widespread thrusting episode is implied, since they overlie rocks of the Central Metasedimentary Belt.

(e) Recently published dates of rocks within and near the map area fall into two groupings similar to those named the Elziviran ca. 1300-1100 Ma. and the Ottawan, ca. 1100-1050 Ma. (Moore and Thompson 1980). The earlier dates are:

Emplacement of the Tallan Lake Sill (gabbro) which lies to the east of the Harvey-Cardiff arch, 1246±24 m.y. (Heamon 1982, Rb-Sr).

Crystallisation of the mafic nepheline bearing gneiss,

1225±3 m.y. (Miller and Gittins 1982, U-Pb).

Emplacement of igneous textured nepheline syenites,

1187±20 (Miller and Gittins 1982, Rb-Sr).

A date of unspecified significance for the Cheddar Granite,

1200 m.y. (Fowler and Doig 1979, Rb-Sr).

the later dates are:

the emplacement, at the metamorphic peak, of the Silent Lake Pluton,

1118±12 m.y. (Heamon 1982, Rb-Sr).

The emplacement of nepheline bearing pegmatites, shortly after the metamorphic peak.

In the range of 1040-1075 m.y. (Miller and Gittins, 1982, U-Pb).

The emplacement of uraniferous pegmatites,

970 m.y. (Fowler and Doig, 1979, Rb-Sr).

It will be noted that many of the rocks in the early group correlate with the orthogneiss in the study area which are sill-like (gabbros and syenites). Indeed the Tallan Lake sill has this form, suggesting emplacement into stratiform rocks.

(f) Considering the suggestion that the line of alkaline rocks lying near the base of the Central Metasedimentary belt marks the site of a rift (Miller and Gittins 1982) we may reasonably speculate that such a rift at depth would be the site of low angle ductile normal faulting (Ramsay 1980) and that the plutons emplaced into it would be sill-like and that in many respects the geometry and fabric of rocks marking such ductile rifting would be barely distinguishable from the planar-linear tectonites now exposed. This site of Elziviran low angle ductile rifting would become the preferred site of ductile thrusting during the Ottawan orogeny, leading to strong deformation of the Farquhar Lake complex.

This hypothesis may be checked during mapping of the boundary of the Central Metasedimentary Belt and its basement by ascertaining: (i) if the thrust tectonics die out along the boundary; (ii) if at the point where they die out thrust tectonics are replaced by earlier ductile rifting. Perhaps early orthogneiss in such a terrain would be less deformed.

(g) There are several petrological problems whose solution would shed light on the tectonics of this part of the Grenville Province, these have been mentioned in the section on lithologies. Briefly they are: i) the possibility that there is a relationship between gabbroic rocks of the map area, those similar locations in the high grade terrain and those in the low grade Hastings Lowlands. If they are of the same age, their use as a marker of tectonic style is obvious; ii)the possibility of consanguinity between any or all of the plutonic suites. For example, bearing in mind the nepheline normative nature of the gabbroic rocks, a possible link between these rocks and the syenitic suite should be investigated. Similar possible links have been postulated between the grey tonalites and the potassic granites (Chesworth et.al. 1975) and between mafic and sodic plutons of the Hastings Lowlands (Lumbers 1967).

(h) An essential feature of the structural map is the presence of disharmonic but apparently synchronous northeast and northwest striking foliations and associated folds. These structures are seen as forming during deformation that was locally polyphase but regionally continuous and progressive (Fig. 3.19), the northwest structures in many cases forming between plutons. There are also mesoscopic and even microscopic structures which have progressively formed elements which are mutually orthogonal.

On the mesoscopic scale coeval structures trending both northeast and northwest include minor folds with SE plunging axes which appear on account of their relatively open profile to have formed with their axes initially parallel to the stretching lineation.

On the regional scale, there are several features with possibly simultaneous northeast and northwest trending structures. For example, two hundred and fifty kilometres to the northwest of the map area, between Sudbury and the northern shores of Lake Nipissing, the Grenville Front Tectonic Zone is exposed (Lumbers 1975). Within the Tectonic Zone foliations striking northeast dip southeast with a down dip lineation. This is overlain to the southeast by northwest striking foliations with a lineation of similar orientation. To the southwest of this area the northwest structures are picked out by large folds of distinctive granitoids with axes plunging shallowly southeast parallel to a stretching lineation (Davidson et.al. 1982). In this area the northwest oriented structures are in turn overlain by a southeast dipping shear zone with a down dip lineation. Regional mapping, continuing at the time of writing, shows that between this latter area and the study area the southeast trending lineation and associated shear zones are important structural elements (Davidson and Mawer, personal communications, 1982).

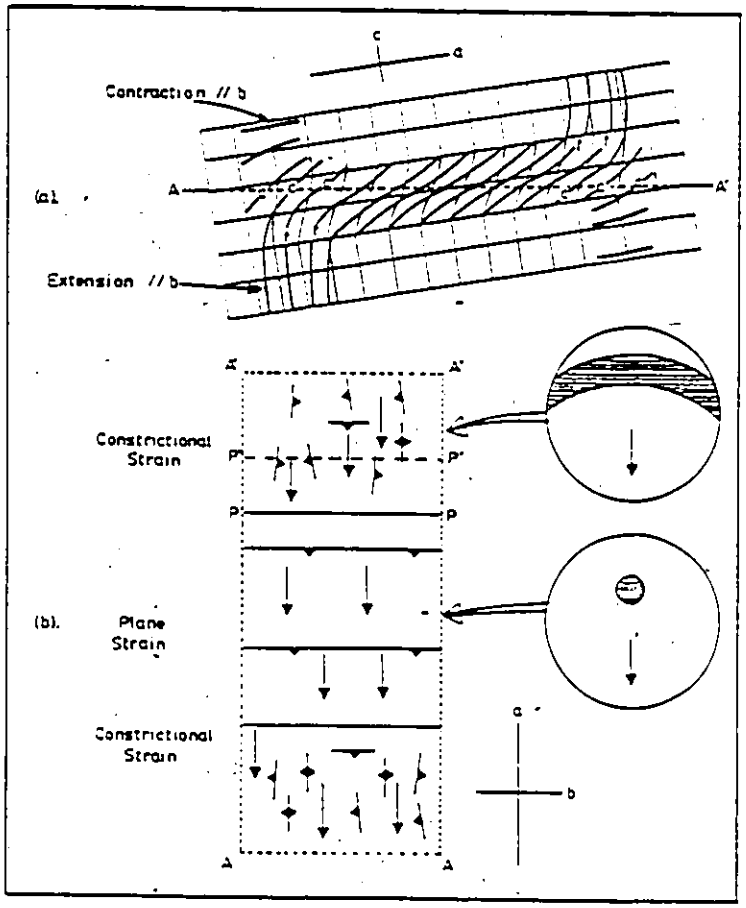

FIGURE
5.2

Structural relations of a propagating shear zone. (a)distribution of strain in a cross-section of a propagating shear zone;heavy lines,trace of foliation;c,constrictional strain;f,flattening strain,elsewhere,plane strain;in this model accomodations of departures from plane strain are only permitted perpendicular to the movement direction,within the shear plane (parallel to 'b').Adapted from Ramsay and Allison 1979. (b)Plane along A - A';attitudes shown of passive layering,the trace of which lies parallel to 'a' in (a).Foliations in zone of constrictional strain are folded cylindrically around stretching lineation.The expected distribution of lineations and poles to foliations is shown on nets.If boundary of plane strain zone (P) propagated into zone of constrictional strain to P' the folds formed by constriction would be refolded.

To explain these major and minor structures a model, proposed by Ramsay and Allison (1979) is adopted that shows the strain distribution at the termination of propagating ductile shear zones. The model, in which the plane strain condition of simple shear is relaxed so that strains at the shear zone tips are accommodated by displacements perpendicular to the movement plane (i.e. in 'y' or 'b'), may be used to predict the behaviour of passive planar elements during propagation of a shear zone (Fig. 5.2). In the model there are areas near the tips of the shear zone where there is contraction in the shear direction leading to extension perpendicular to the shear direction (in 'b') and local flattening where this strain is superimposed on the plane strain of the shear zone. On the opposite side of the shear zone there is contraction in the shear plane perpendicular to the shear direction (in 'b') and locally constrictional strains where this strain and the plane strain of the shear zone are superimposed.

It follows that folds may form with their axes in 'a' parallel to the shear zone lineation in layers lying subparallel to the shear zone margin in the area where contraction is perpendicular to the shear direction (Fig. 5.2). Propagation of the shear zone may further deform these folds progressively tightening the profiles.

On the regional scale, structures where a zone with a down-dip lineation is overlain or underlain by rocks where the foliation is gently folded around the stretching lineation, as with the Grenville Front tectonic zone and overlying rocks, may thus represent subhorizontal sections through moderately dipping propagating shear zones in layered rocks (Fig. 5.2). In this case the section passes from the area where constriction forming the folds was perpendicular to the shear direction into the shear zone where there was plane strain, with planar foliation, and the lineation down-dip. An important feature of this arrangement is that the folds formed by constriction or contraction would be transposed as the shear zone propagates; northwest striking structures (fold limbs) would be crossed by northeast structures.

Careful mapping of areas where these mutually orthogonal structures are well exposed may show if some have in fact been formed by the mechanism proposed.

(i) In future petrofabric work aimed at obtaining kinematic information, granite gneiss with quartz ribbons should be sampled since their C-axis microfabric retains a memory of the major episode of dynamic recrystallisation (LS1). Coarse grained quartzites should be avoided since their C-axis microfabrics retain no memory of the LS1 kinematics.

(j) Fine grained tectonites and any suspected of showing the effects of destruction of LS1 microstructure should be cut in the XZ plane and inspected for asymmetric microfoliations which indicate shear sense.

(k) The regional extent of the LS2 shear-sense reversal should be mapped and more fully investigated.

Plates

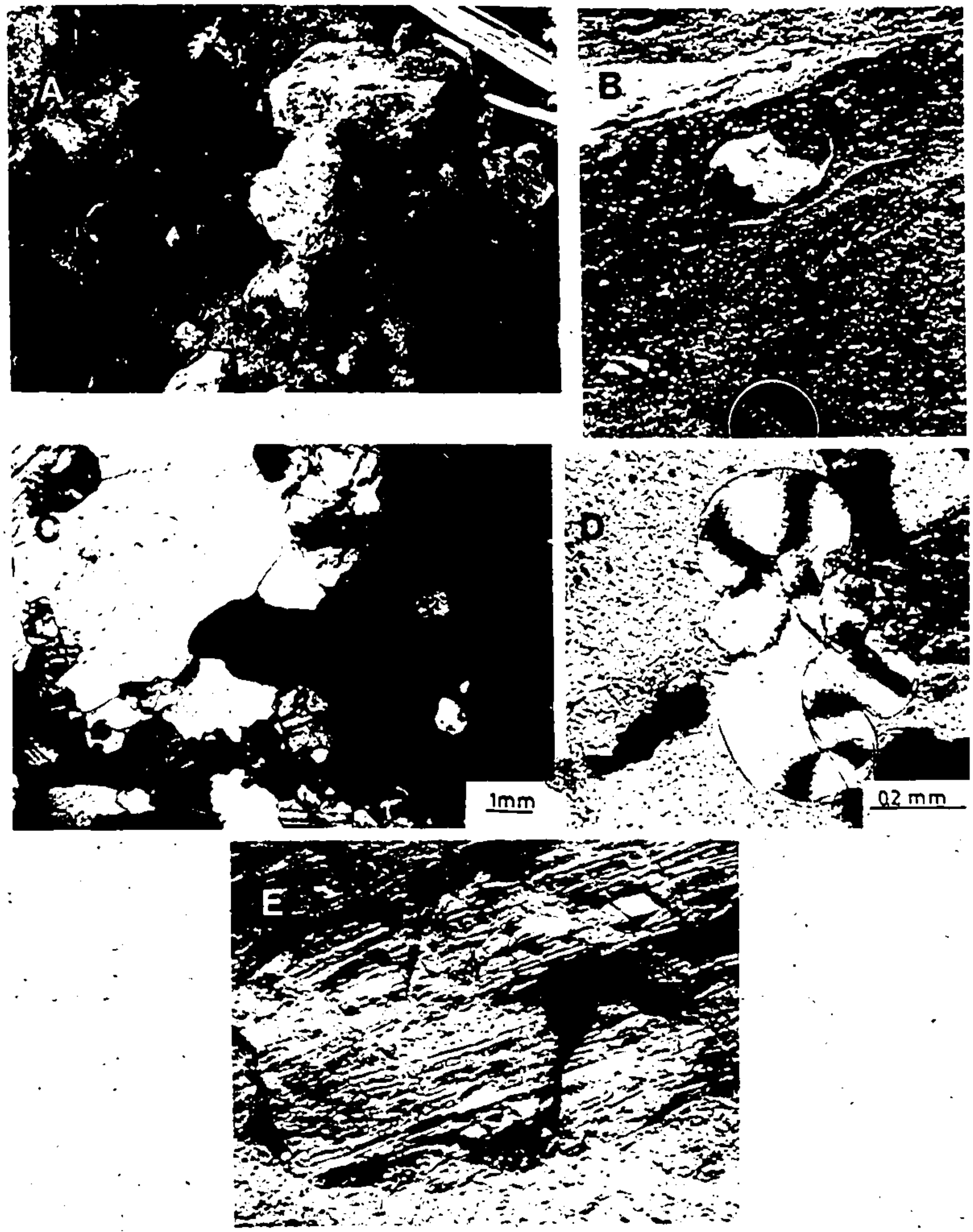
A
B
C
D
E
1mm
0.2 mm

PLATE 1

Tectonic Fabrics of Marbles (Unit 1A)

(A) Tectonic breccia displays angular syenitic blocks in a medium grained matrix. Northeast shore of Farquhar Lake.

(B) Sense of rotation of a disrupted pegmatite in tectonic breccia indicates dextral shear (upper layers to northwest, towards right side of photo). Southwest shore of Baptiste Lake.

(C) Coarse carbonate grains in tectonic breccia. Diopside is situated both within these grains and on their boundaries (compare with quartzite microstructures, Plate 15). From Highway 21, 5 km west of Dudmon Lake. Polarized light.

(D) Folded quartz ribbon in tectonic breccia indicates high strain undergone by the rock before carbonate grain growth. From north shore of small lake to east of Esson Lake.

(E) Very straight, high strain fabric of a migmatitic calc-silicate gneiss which is interlayerd with marble tectonic breccia (illustrated in B). Southwest shore of Baptiste Lake.

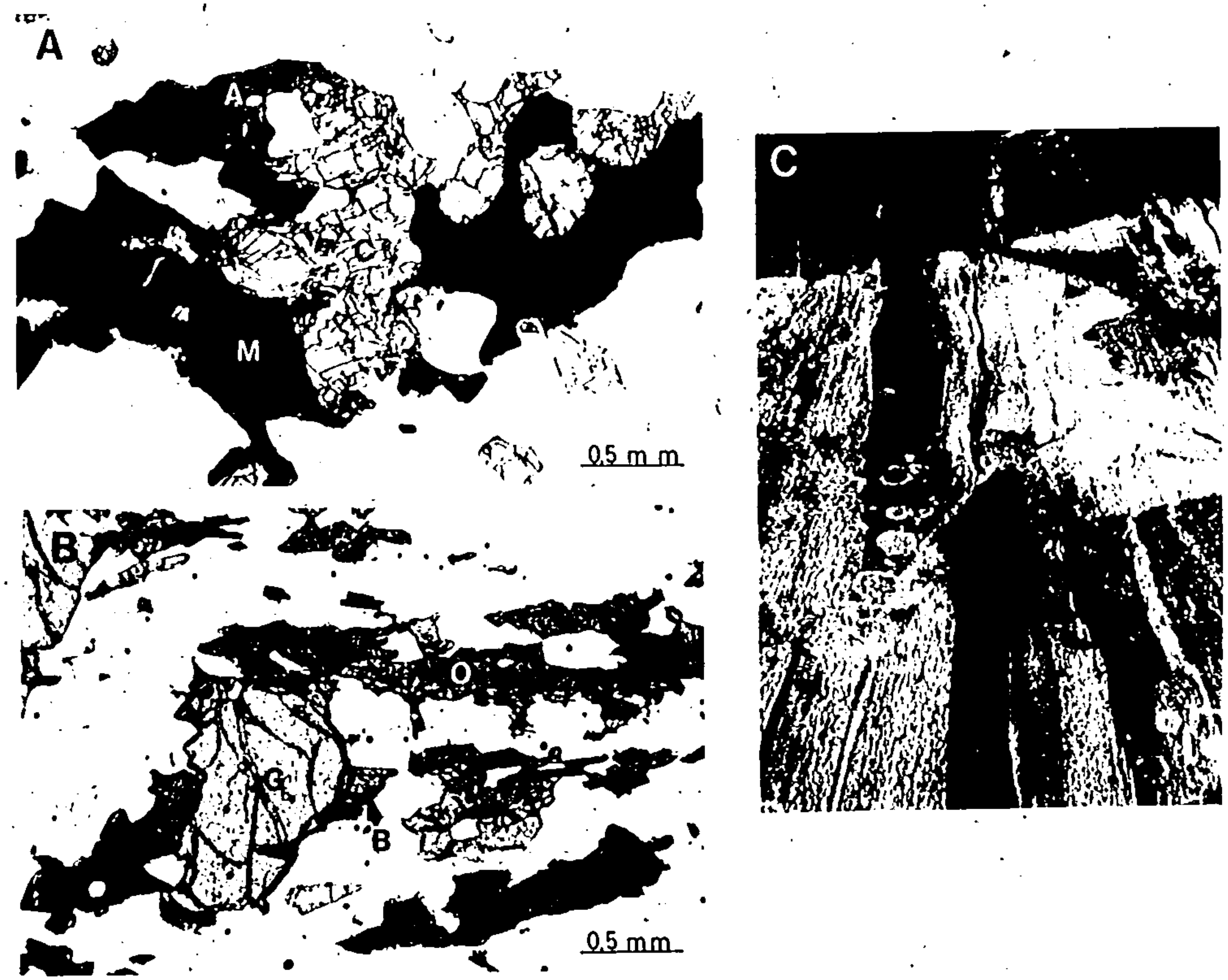
A
A
C
M
0.5 mm
B
O
G
B
0.5 mm
C

PLATE 2

Features of the Grey Gneiss Complexes (Unit 3)

(A) Replacement of clinopyroxene (C) by amphibole (A), juxtaposed with magnetite (M). In a trondhjemite horizon from layered gneiss from northeast of Drag Lake (Unit 3A). Plain light.

(B) Garnet (G), orthoamphibole (O) and biotite (B) in quartz and plagioclase in garnet gneiss (Unit 3C) from north of Drag Lake. Plain light.

(C) Typical aspect of tonalitic grey gneiss (Unit 3A); two phases of grey gneiss, amphibolite layer and granitic leucosome are visible. East shore of Drag Lake. The width of the photograph is approximately 1 m.

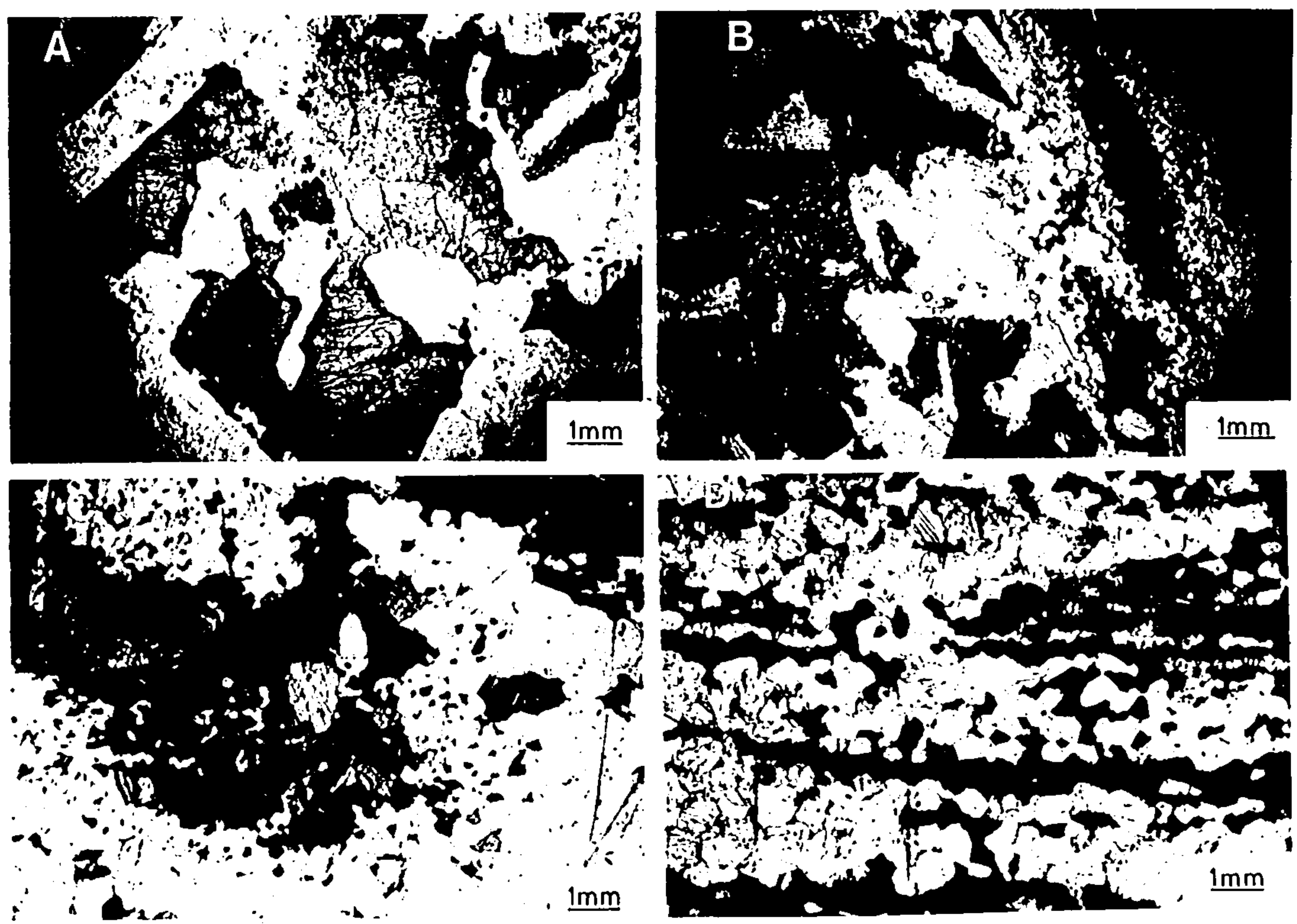
A
B
1mm
1mm
1mm
1mm

PLATE 3

Variation of Microstructure with Strain in Metagabbro (Unit 4A)

All from metagabbro, south shore of Farquhar Lake (illustrated in Fig. 3.14). (B), (C) and (D) from shear zone illustrated in Fig. 4.35.

(A) In undeformed gabbro with sub-ophitic texture clinopyroxene is rimmed by a narrow amphibole corona.

(B) In weakly deformed wall rock of shear zone (WR, Fig. 4.35) two microstructural domains are visible: left, hornblende and clinopyroxene are finely intergrown with subophitic texture present and plagioclase interiors are free from inclusions; right, clinopyroxene is entirely replaced by hornblende (dark aggregates) and neighboring plagioclase is filled with hornblende inclusions and locally recrystallised (see Fig. 4.36).

(C) Moderately deformed gneissic metagabbro from the edge of the shear zone (SZM, Fig. 4.35) is microstructurally very similar to the second microstructural domain in (B), except that grain size range is greater and there are not hornblende inclusions in the plagioclase (see Fig. 4.39). Foliation trace runs from U. left to L. right corner.

(D) In the highly deformed gneissic metagabbro from the shear zone centre (SZM, Fig. 4.35) the foliation is well defined by elongate amphibole aggregates only one or two grains thick. Grain size range is restricted.

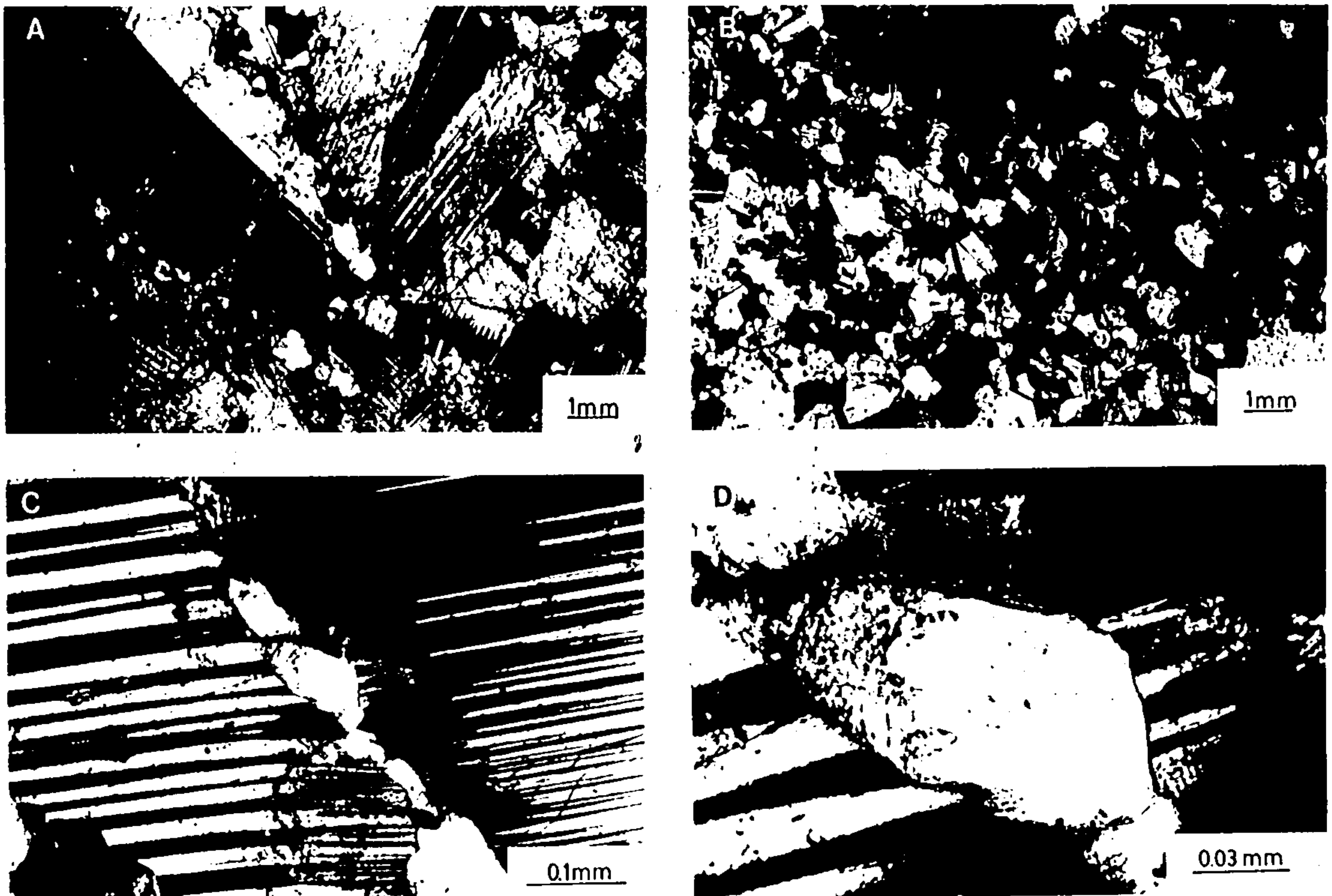
A
1mm
B
1mm
C
0.1mm
D
0.03 mm

PLATE 4

Microstructure of Plagioclase
In Anorthositic and Gabbroic Rocks (Unit 4B,A)

(A) New grains located along boundaries of large primary grains. Gabbroic-anorthosite, northwest of Grace Lake.

(B) Gneissic anorthosite, from Kennibik Lake, composed of an aggregate of fine equant grains. Relict primary plagioclase, top centre, has irregular grain boundaries, undulatory extinction and enclosed twins.

(C) Weakly deformed wall rock of shear zone in metagabbro (S. shore of Farquhar Lake, Fig. 4.35), recrystallized small grains occur along a kink in primary plagioclase. Local zoning to more An rich composition (lighter tones in dark areas) is evident along the kink across which the number and width of deformation twins varies.

(D) Detail from (C). New grain is traversed by fine lamellae, interpreted as huttenlocher intergrowths.

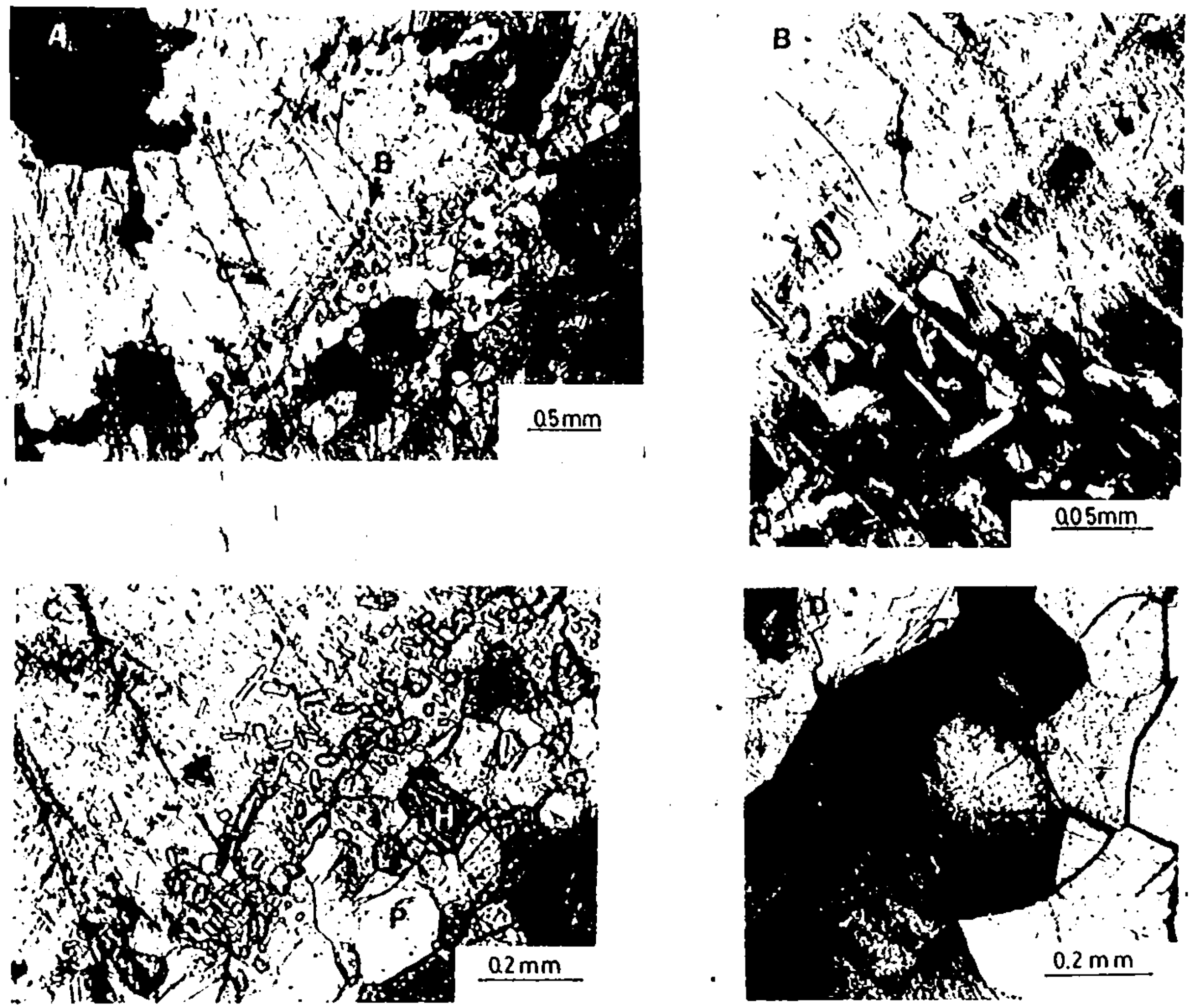
A
B
0.5mm
B
0.05mm
C
0.2mm
D
0.2 mm

PLATE 5

Microstructure at the Interface of Primary Plagioclase With a Hornblende Aggregate in Metagabbro (Unit 4A)

In metagabbro from shear zone, south shore of Farquhar Lake (Fig. 3.14). (A), (B) and (C) from weakly deformed wall rock (Fig. 4.35); (D) from moderately deformed edge of shear zone (SZM, Fig. 4.35).

(A) Primary plagioclase is crowded with amphibole inclusions near boundary with hornblende aggregate (see Fig. 4.36). Location of (B) and (C) indicated.

(B) Inclusion filled primary plagioclase. Fine bright lamellae lie oblique to the trace of the albite twins (U. left to L. right). The lamellae may be huttenlocher intergrowth.

(C) Narrow zone of recrystallized hornblende (H) and plagioclase (P) (microdomain iii of Fig. 4.36) separates inclusion filled primary plagioclase (U. left, microdomain ii of Fig. 4.36) from hornblende aggregate (L. right). Hornblende grains coarsen towards zone of recrystallized hornblende and plagioclase (microdomain iii). Within microdomain iii the plagioclase interiors are almost completely free of hornblende.

(D) Partly grown plagioclase grains from a zone of recrystallised hornblende and plagioclase (see Fig. 4.39). These grains are zoned to more An rich compositions and display bright lamellae, interpreted as huttonlocher intergrowth.


A
0.1 mm
B
0.1 mm
C
0.1 mm
D
0.1 mm

PLATE 6

Feldspar Microstructures in Granites (Units 6C,D)

(A) and (B) Albite from Upper Faraday granite, west of Albion Lake (Unit 6C), medium grained to pegmatitic leucogranite).

(A) Grain is divided into subdomains by irregular kink-like boundaries.

(B) Some subdomains have relatively high misorientations; in these both the simple twinning and the grain size are comparable to that of plagioclase in more thoroughly recrystallised granite gneiss.

(C) and (D) Perthite from the Cheddar granite, from west of N. EEls Lake (Unit 6D, biotite-hornblende granite).

(C) Albite braids from neighboring grains of microcline perthite merge along the grain boundary, forming individual grains; a precursor of the production from a perthite granite of a two feldspar, perthite free granite gneiss.

(D) Microcline perthite; most exsolved albite is restricted to braids. Coalescence on grain boundaries visible at bottom right.

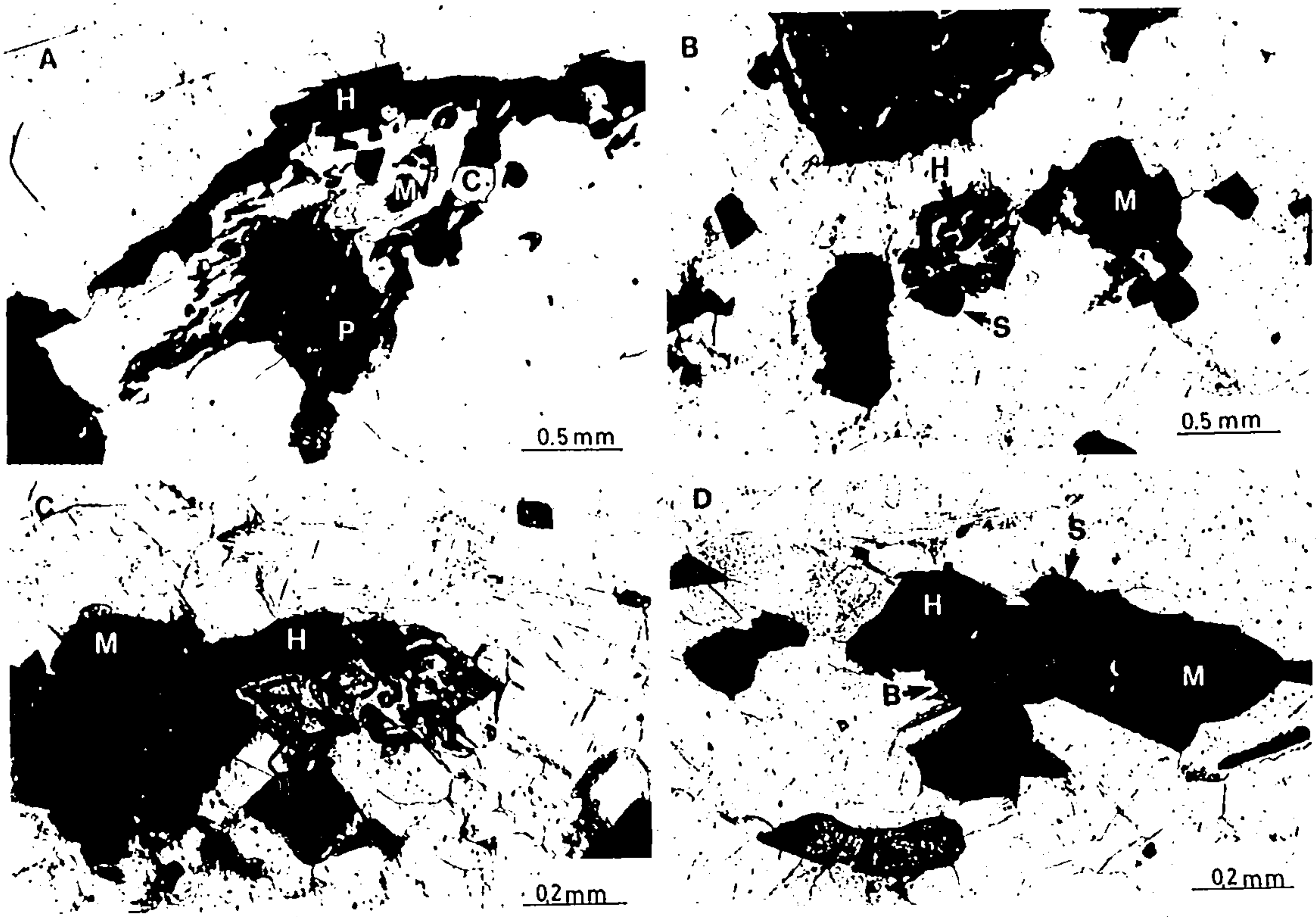
A
H
M
C
P
0.5 mm
B
H
M
S
0.5 mm
C
M
H
0.2 mm
D
S
H
M
B
0.2 mm

PLATE 7

Amphibole Development in Biotite-Hornblende Granite (Unit 6D)

(A) Skeletal hornblende (H) replacing clinopyroxene (P), intergrown with colourless quartz, carbonate (C) and magnetite (M). In poorly foliated granite, southeast corner of Cheddar granite.

(B) Skeletal and well formed hornblende (H) with sphene (S) and magnetite (M). From well foliated granite, Cheddar granite, south shore of Hook Lake.

(C) Skeletal hornblende (H) in Lower Faraday granite.

(D) Well formed amphibole in contact with magnetite (M), sphene (S) and biotite (B). Lower Faraday granite.

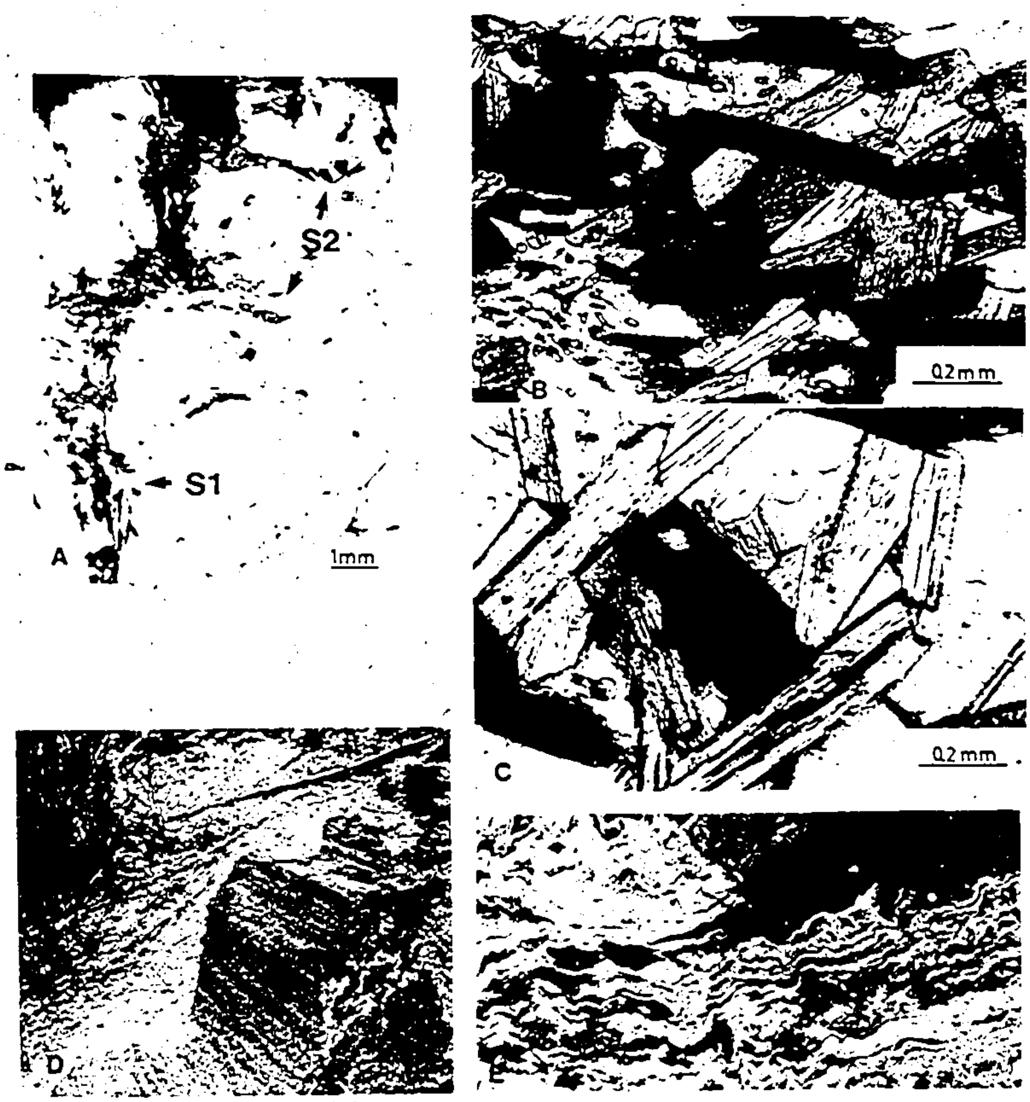
S2
S1
A
1mm
B
0.2mm
C
0.2mm
D
E

PLATE 8

Lineation in Supracrustal Rocks

(A) In garnet gneiss (Unit 3C) from north of Drag Lake an intersection lineation is formed on a vertical northwest striking S1//S0 by shallowly southeast dipping S2. Biotite and orthoamphibole lie in both foliations. S2 lies in axial planes of minor reclined open folds with southeast plunging axes. View perpendicular to L1.

(B) View perpendicular to lineation in paragneiss (Unit 2B) with decussate texture of biotite; from south shore of Eels Lake. Grains with the highest aspect ratio lie parallel to moderately southeast dipping foliation (horizontal). The intersection of micas on the foliation gives Type I mica edge lineation (see Fig. 3.2a). View perpendicular to L1.

(C) Similar view and texture as in (B), in calc-silicate gneiss (Unit 2A); from Highway 121, southeast of Colbourn Lake. Steeply dipping, southeast striking S0//S1 is subvertical. Mica cleavage trace is uniformly oriented and all grains have similar aspect ratios. Type II mica edge lineation (see Fig. 3.2c). View perpendicular to L1.

(D) Axial lineation formed by upright folding in southeast dipping layering from belt of generally steeply dipping northwest striking foliations between Cheddar batholith and Cardiff complex. Calc- silicate gneiss (Unit 2A), Highway 648, south, near intersection with Highway 121.

(E) Similar view and location as (D). Isoclinal folds refolded. Biotite gneiss (Unit 2B).

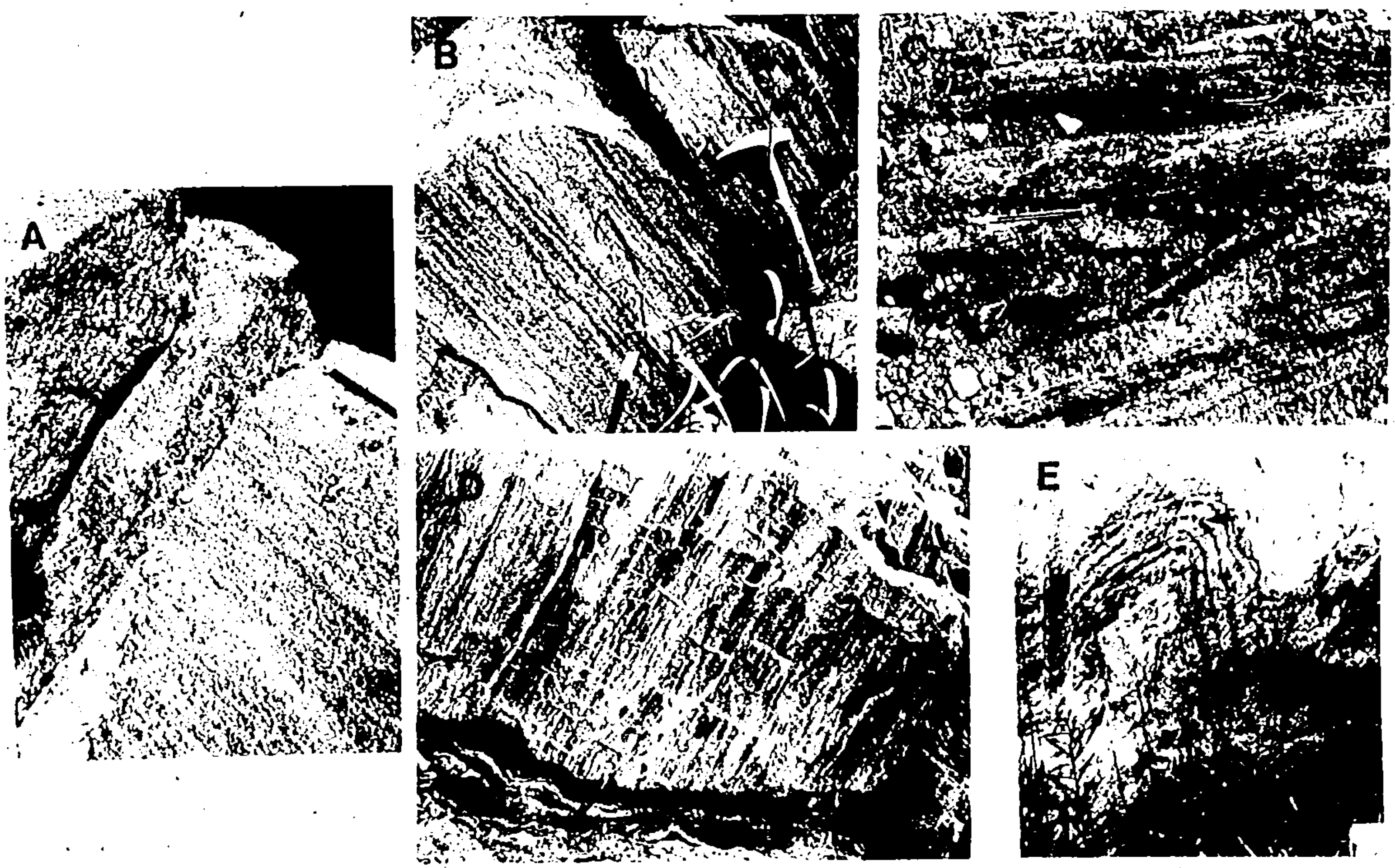
A
B
D
E

PLATE 9

Lineation in Orthogneiss and Supracrustal Rocks

(A) Linear shape fabric in alkali granite (Unit 6B), Cheddar granite, north of Hook Lake. Erosion surfaces approximately parallel and perpendicular to lineation.

(B) Ridge-like intersection lineation in calc-silicate gneiss (Unit 2A); Highway 121, southeast of Colbourn Lake. The lineation is formed by intersection of S1 and isoclinally folded layering (S0).

(C) View near perpendicular to lineation in (B), showing isoclinal folding of S0; a slightly oblique S1 visible at bottom right.

(D) Streaky intersection lineation of S2 on S1//S0 in marble (Unit 1A), Highway 28, south of Paudash Lake; extension fractures (arrow) lie sub-perpendicular to lineation.

(E) View perpendicular to lineation of (D); asymmetric fold of S1//S0 and formation of axial S2 (arrow). Photograph is approximately 1 m wide.

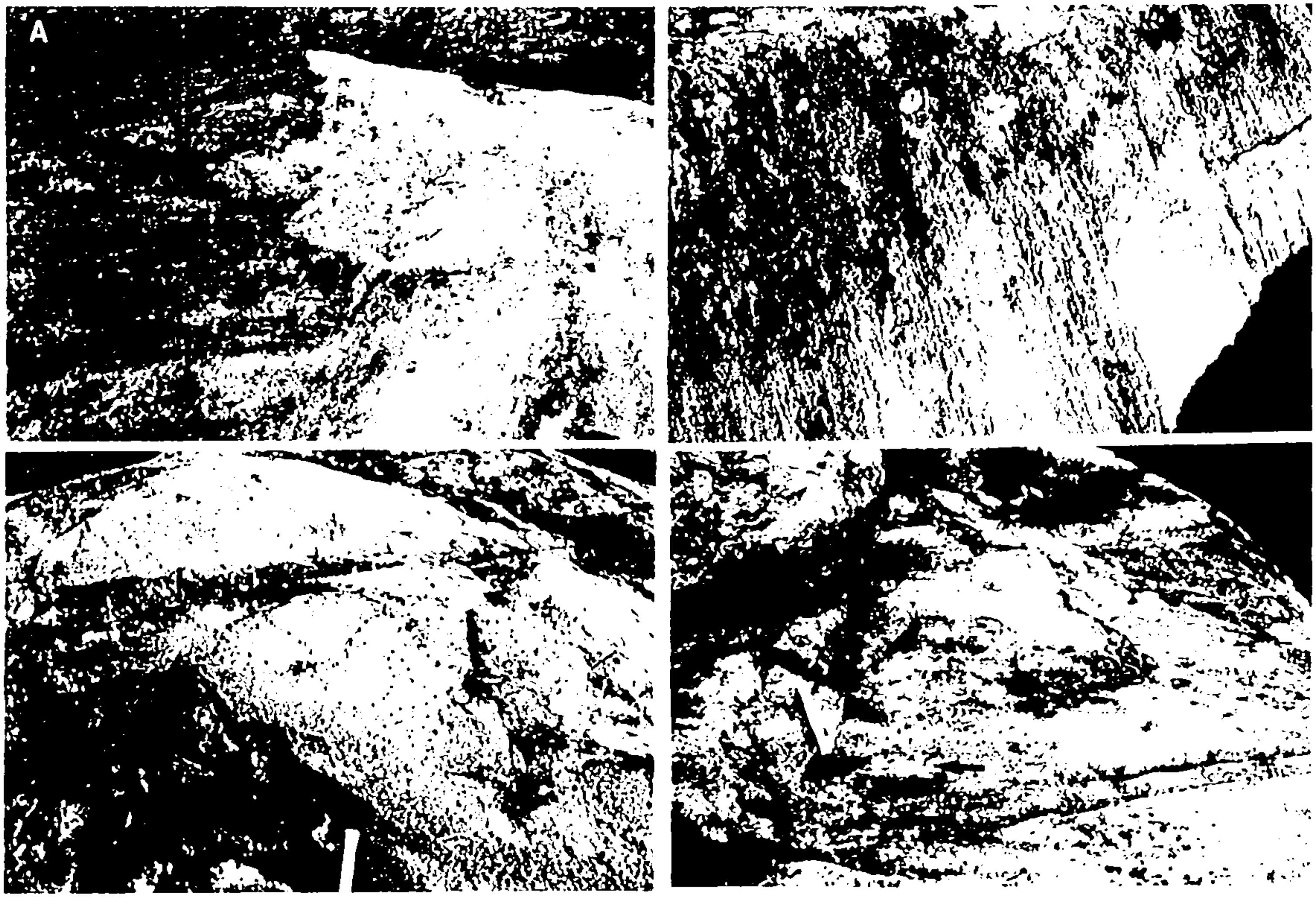
A

PLATE 10

Mesoscopic Fabric of Granitoid Veins

(A) In nose of Burleigh Fold (Fig. 1.1, area 4b) leucogranite both cross cuts and lies parallel to foliation in paragneiss. Erosion surface at high angle to lineation.

(B) Nearby, on a surface in zone with lineation, the margin of a granite vein and lineation are parallel. Photograph is approximately 2 m wide.

(C) Folds in granite veins displayed on surface subperpendicular to lineation; grey tonalitic gneiss (Unit 3A), northeast shore of Drag Lake.

(D) At same outcrop on surface in zone with lineation the trace of granite veins and lineations (arrow) are parallel.

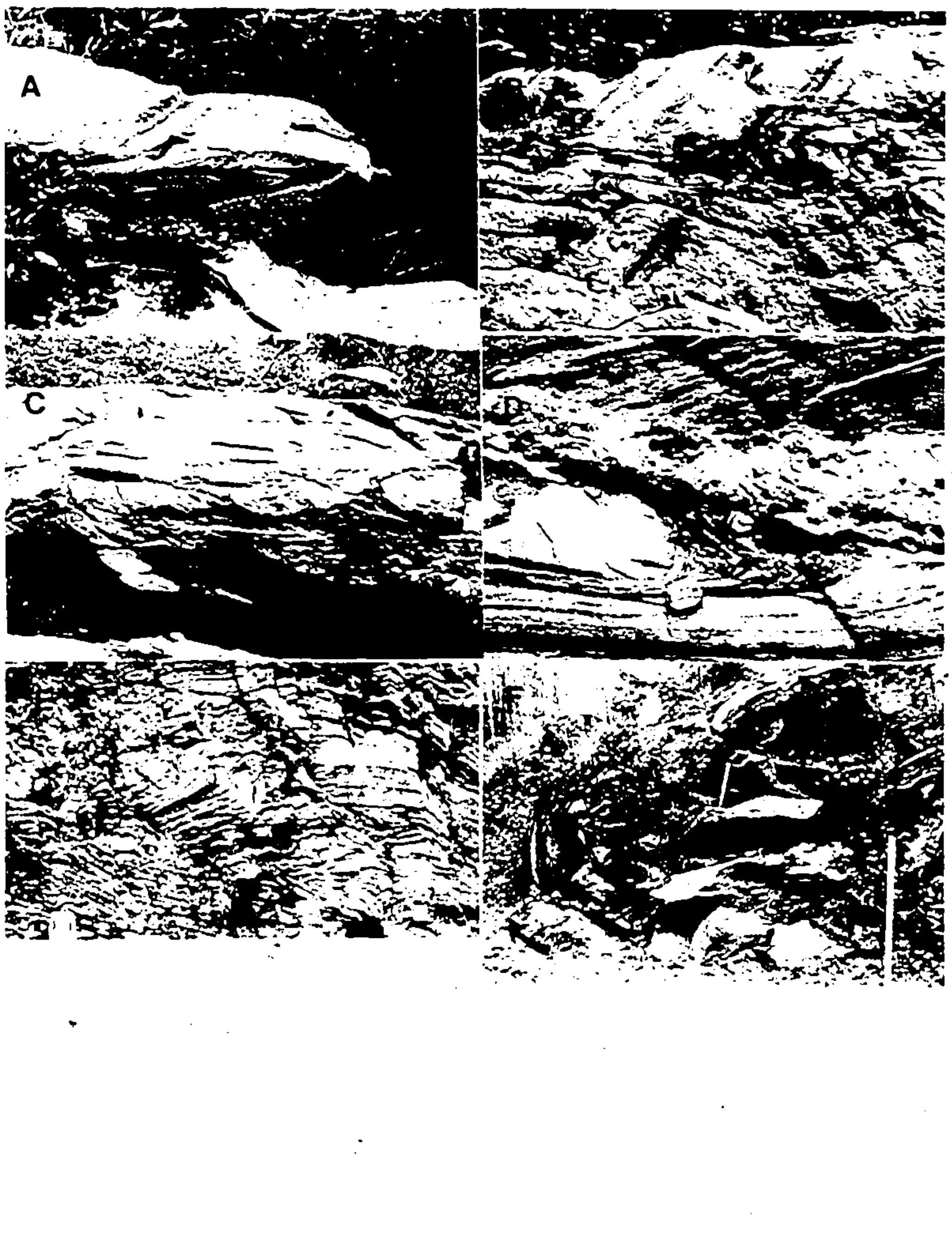

PLATE 11

Minor Folds

(A) Isoclinal fold with axial surface parallel to S0//S1, folding syenitic vein. Biotite-plagioclase gneiss (Unit 2B), 1 km west of Harcourt on Highway 648. Northwest margin of Cardiff complex.

(B) Asymmetric NE verging fold of boudinaged migmatitic layering (Unit 2B). Andrews gravel pit, Highway 648, 1 km south of Highland Grove. Crest of Cardiff complex.

(C) Asymmetric NE verging fold of boudinaged granitic layer and S0//S1 in biotite-plagioclase gneiss (Unit 2B). South shore of Diamond Lake.

(D) Asymmetric NE verging fold in calc-silicate gneiss (Unit 2A). Syenitic pegmatite lies along axial surface. 1.5 km west of southwest corner of Baptiste Lake.

(E) Asymmetric NE verging folds in biotite-plagioclase gneiss (Unit 2C), Elephant Lake Road, near southwest corner of Elephant Lake. These folds underlie horizon of marble tectonic breccia. Note variation of tightness and flaggy aspect in lower left.

(F) Fold with curved hinge in biotite plagioclase gneiss (Unit 2C). Elephant Lake Road, west shore of Elephant Lake, view toward southwest. Curvature of hinge indicated by arrows.

All except (F), near profile views.

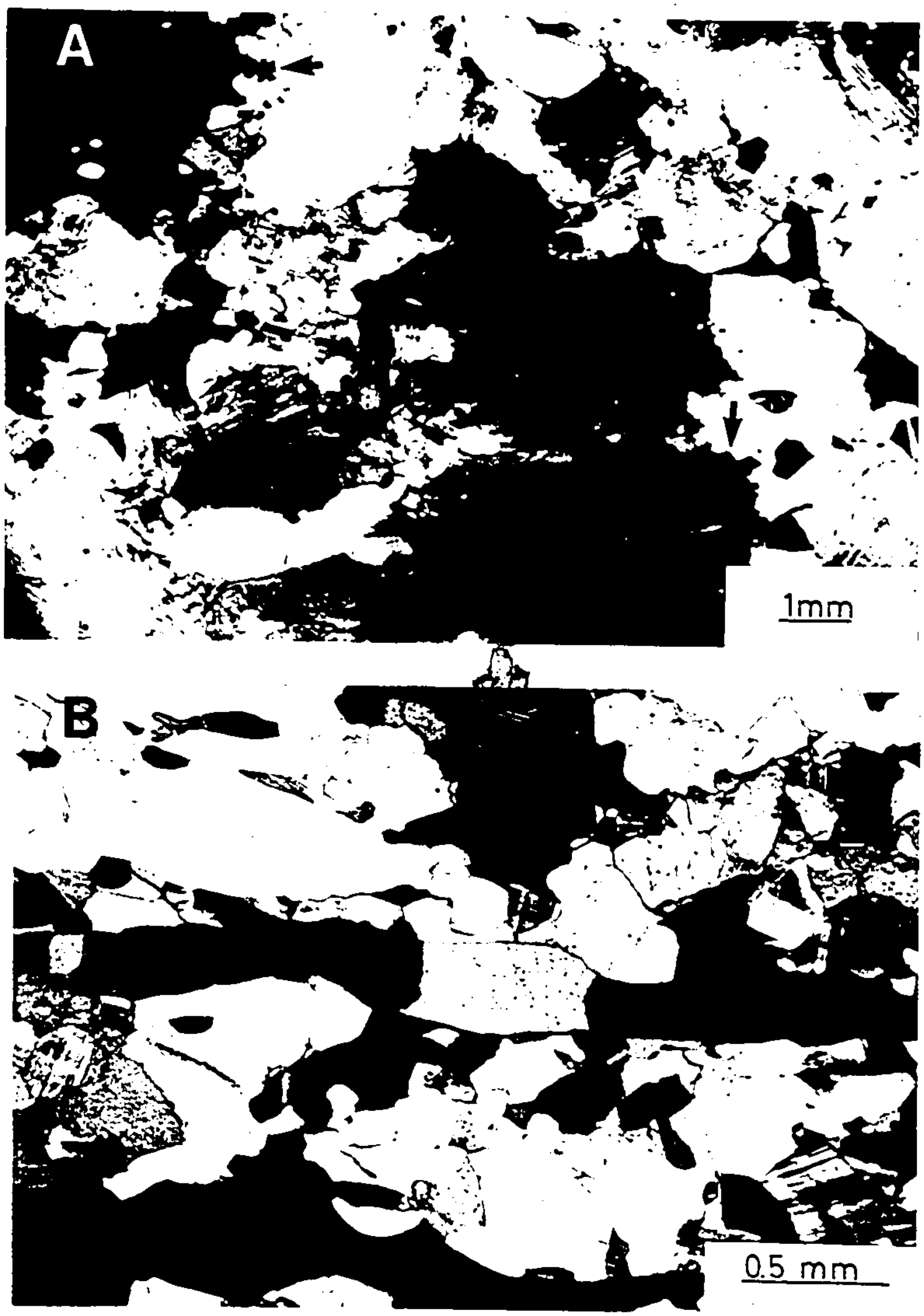
A
1mm
B
0.5 mm

PLATE 12

Variation of LS1 Quartz Ribbon Microstructure with Strain In Granite Gneiss

See Fig. 1.2b for location. All XZ sections of LS1, X horizontal.

(A) Low strain, immature microstructure (ALT) (1491C, Unit 6C, Upper Faraday Granite, west of Albion Lake). Quartz has low aspect ratio, the few quartz/quartz boundaries are indentate (arrows) and unoriented with respect to horizontal foliation trace; relatively high intragranular distortion.

(B) High strain, mature microstructure (MCT) (1092B, Unit 6D, Lower Faraday granite). Quartz is elongate, with numerous quartz/quartz boundaries which are smooth and sub-perpendicular to foliation trace; intragranular distortion is low.

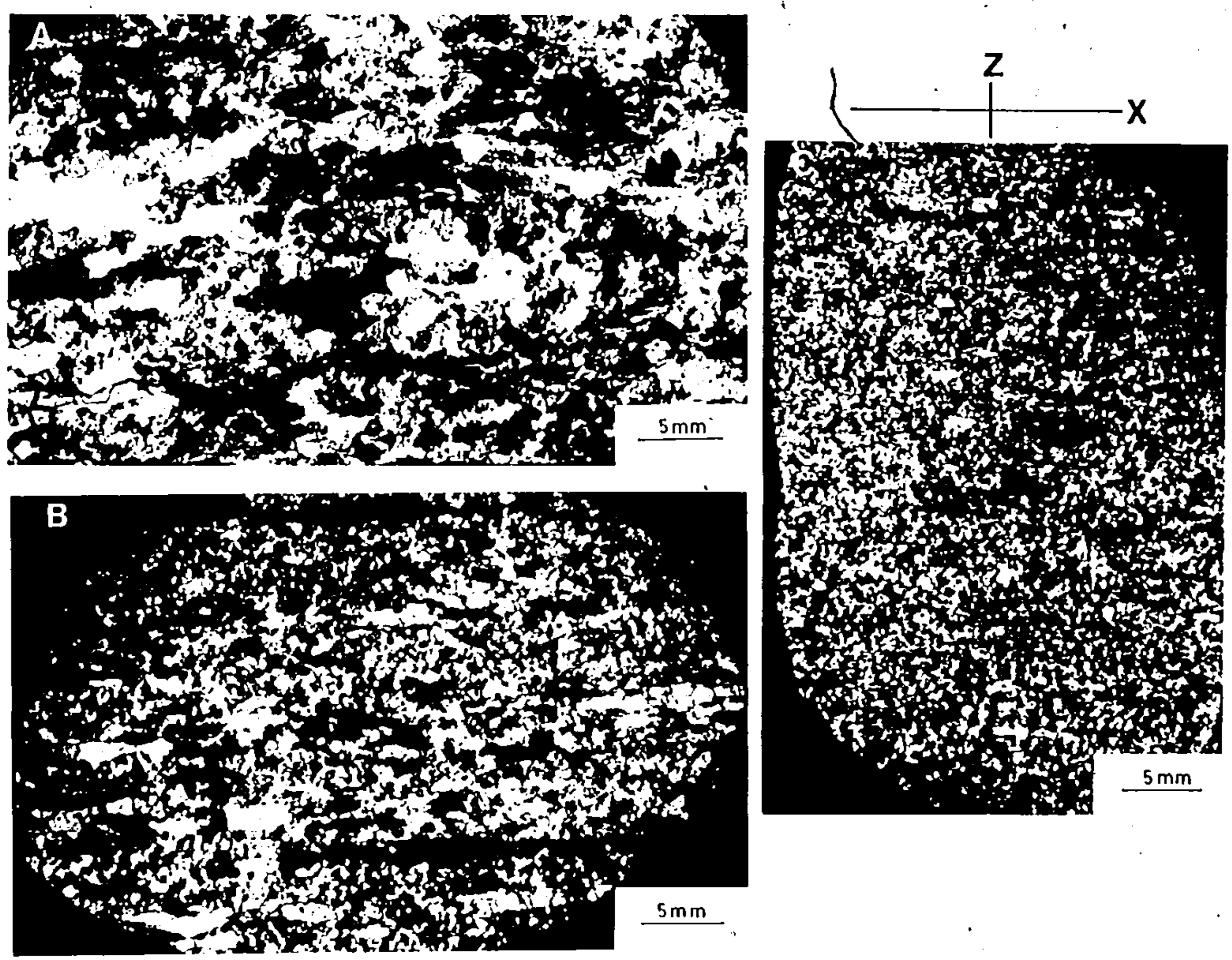
A
5mm
B
5mm
Z
X
5mm

PLATE 13

LS1 Microstructure in Granite Gneiss, Faraday Granite

See Fig. 1.2b for location.

(A) Upper Faraday granite, west of Albion Lake (1395C, Unit 6C).

(B) Lower Faraday granite, southern end (22103B, Unit 6D).

(C) Lower Faraday granite, northern end (1691B, Unit 6D).

Increase in strain from (A) to (C) is indicated by progressive attenuation of quartz ribbons and reduction of feldspar grain size.

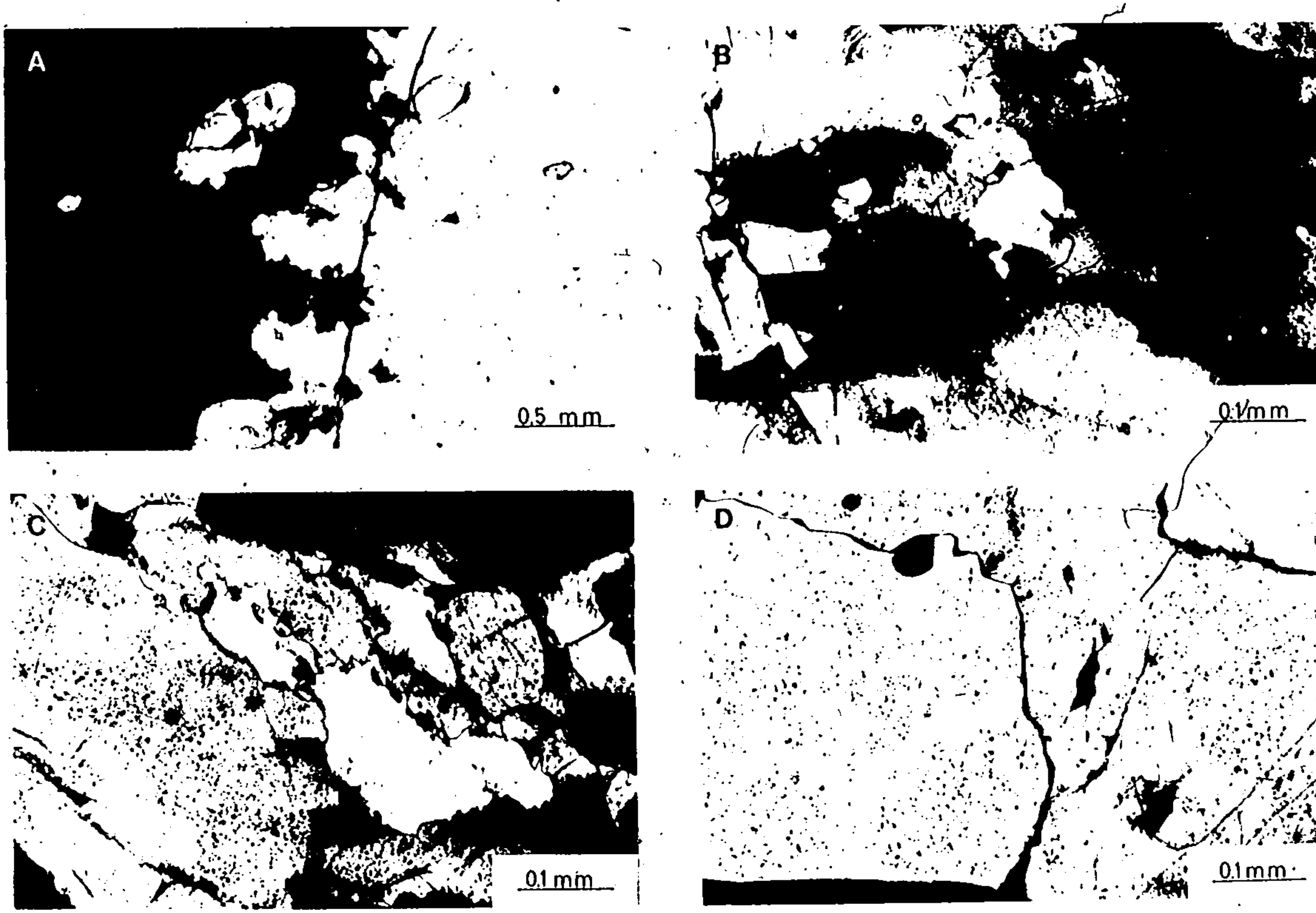
A
0.5 mm
B
0.1 mm
C
0.1 mm
D
0.1 mm

PLATE 14

Immature LS1 Quartz Microstructure in Weakly Deformed Granite Gneiss, Upper Faraday Granite (Unit 6C)

See Fig. 1.2b for location. All XZ sections of LS1, X horizontal.

(A) Very irregular interlobate quartz-quartz boundary (1941C).

(B) New grains in quartz with high intragranular distortion (1395C).

(C) A new grain with a very irregular boundary. The grain has grown somewhat but is yet to impinge on the feldspathic matrix (1395C).

(D) Quartz-quartz boundary, free from small scale irregularities. This type of boundary co-exists with the very irregular type (1395C).

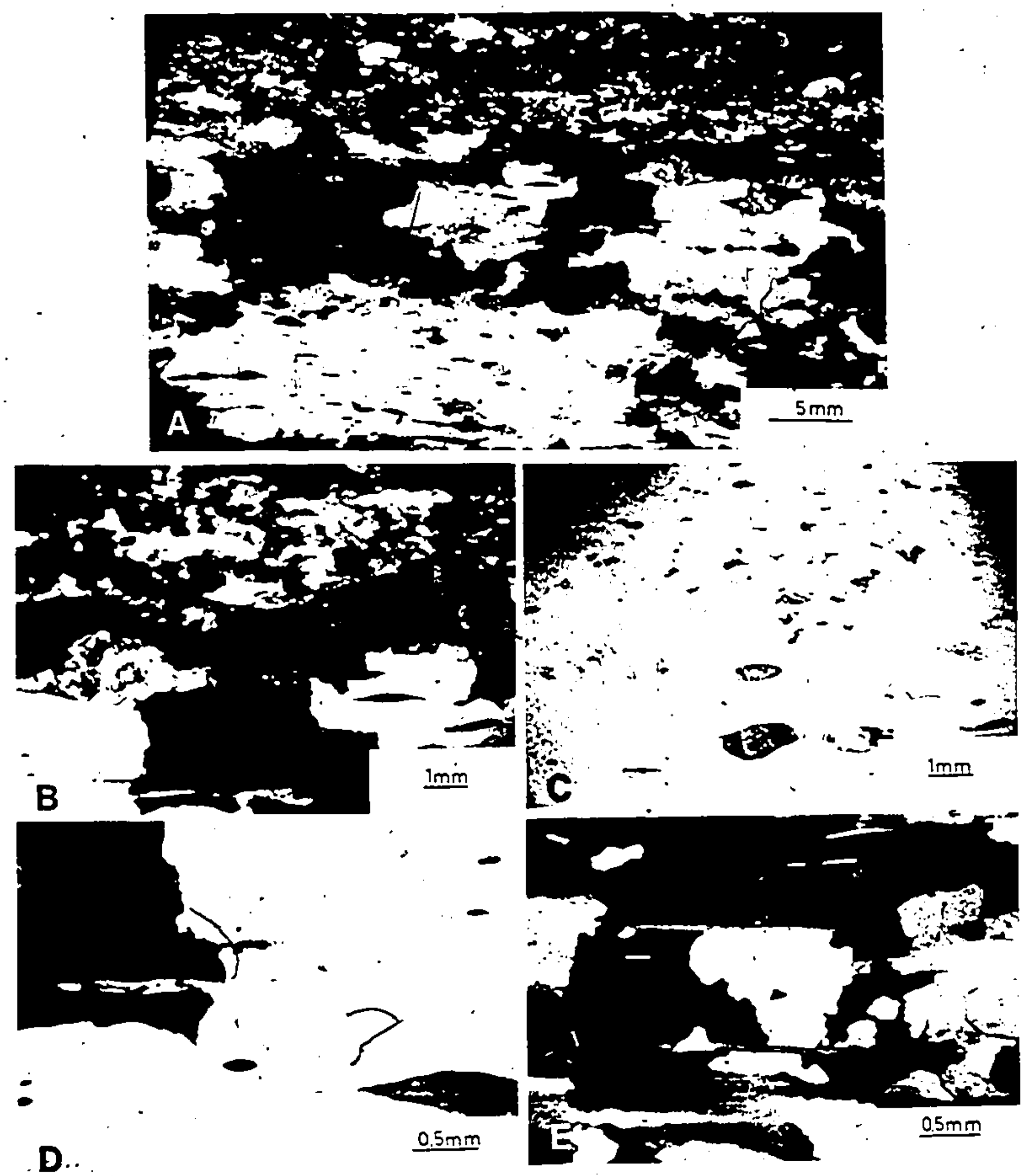

A
5mm
B
1mm
C
1mm
D
0.5mm
E
0.5mm

PLATE 15

Exaggerated Grain Growth Microstructure in Quartzite. (LS1)

See Fig. 1.2b for location. All XZ sections of LS1, X horizontal.

(A) Quartzite from north of Farquhar Lake (2465C) displays large grain size, irregular grain shape and location of non-quartz inclusions (on boundaries and within grains) which are characteristic of exaggerated grain growth microstructure.

(A) and (B) Decrease of quartz grain-size with increasing number of non-quartz minerals. View from upper part of (A). (B) polarized, (C) plain light.

(D) Feldspar and clinopyroxene inclusions whose lensoid shapes and tails of boudinaged fragments indicate the high strain undergone by the rock before grain growth (2465C).

(E) In quartzite from west of Grace Lake (1391C) biotite is well aligned and pins quartz boundary.

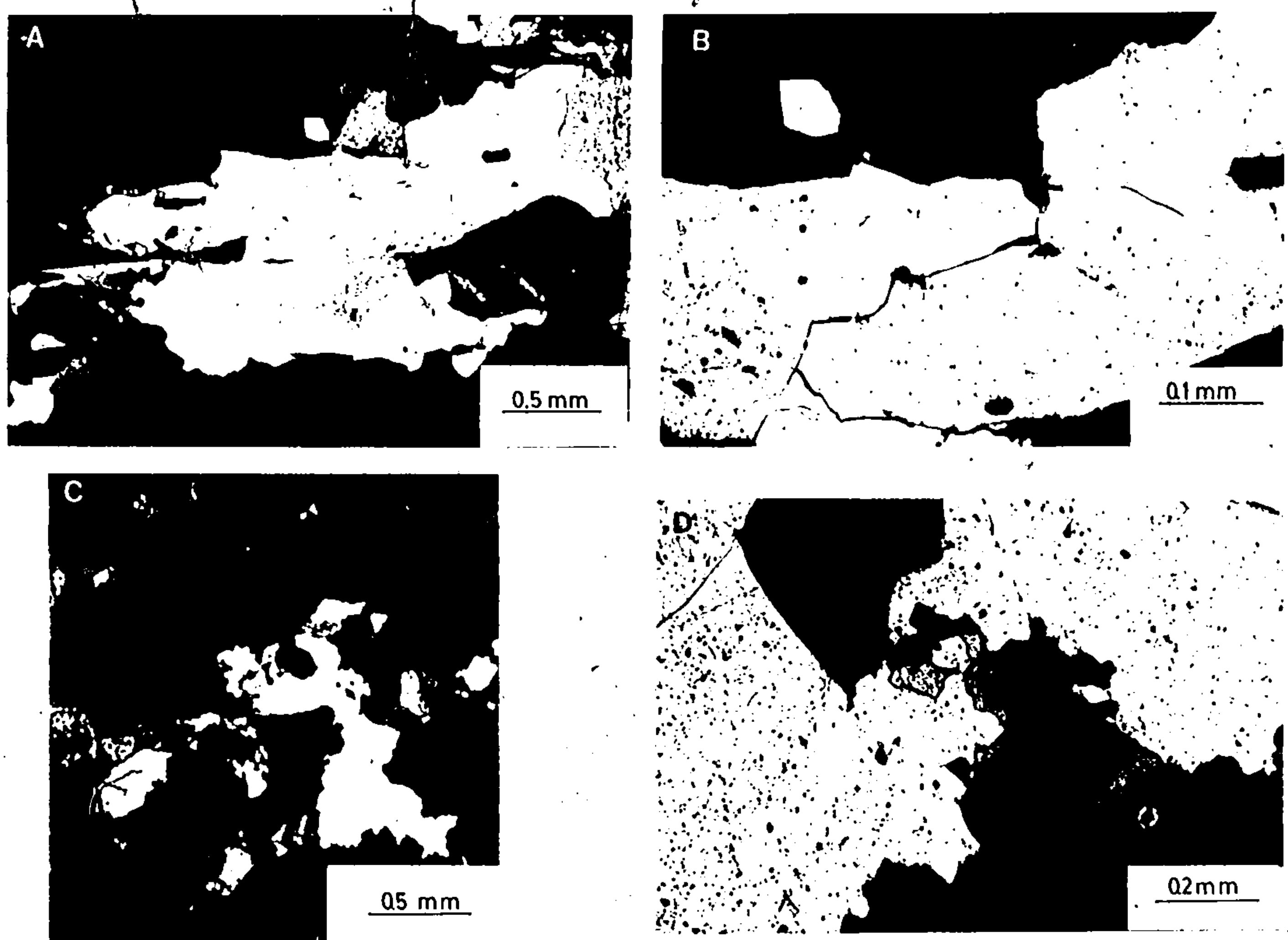
A
0.5 mm
B
0.1 mm
C
0.5 mm
D
0.2 mm

PLATE 16

Modification of Exaggerated Grain Growth Microstructure in Quartzite (LS1) by Later Grain Growth

See Fig. 1.2b for location, Sample 12101D. All XZ sections of LS1, X horizontal.

(A) In sample farthest from overlying syenite gneiss the coarse grain-size and regular grain boundaries of exaggerated grain growth are displayed.

(B) Detail of regular grain boundary of (A).

(C) In sample close to overlying syenite the large grains are transected by irregularly shaped grains which have grown into distorted quartz.

(D) Detail of irregular boundary of (C).

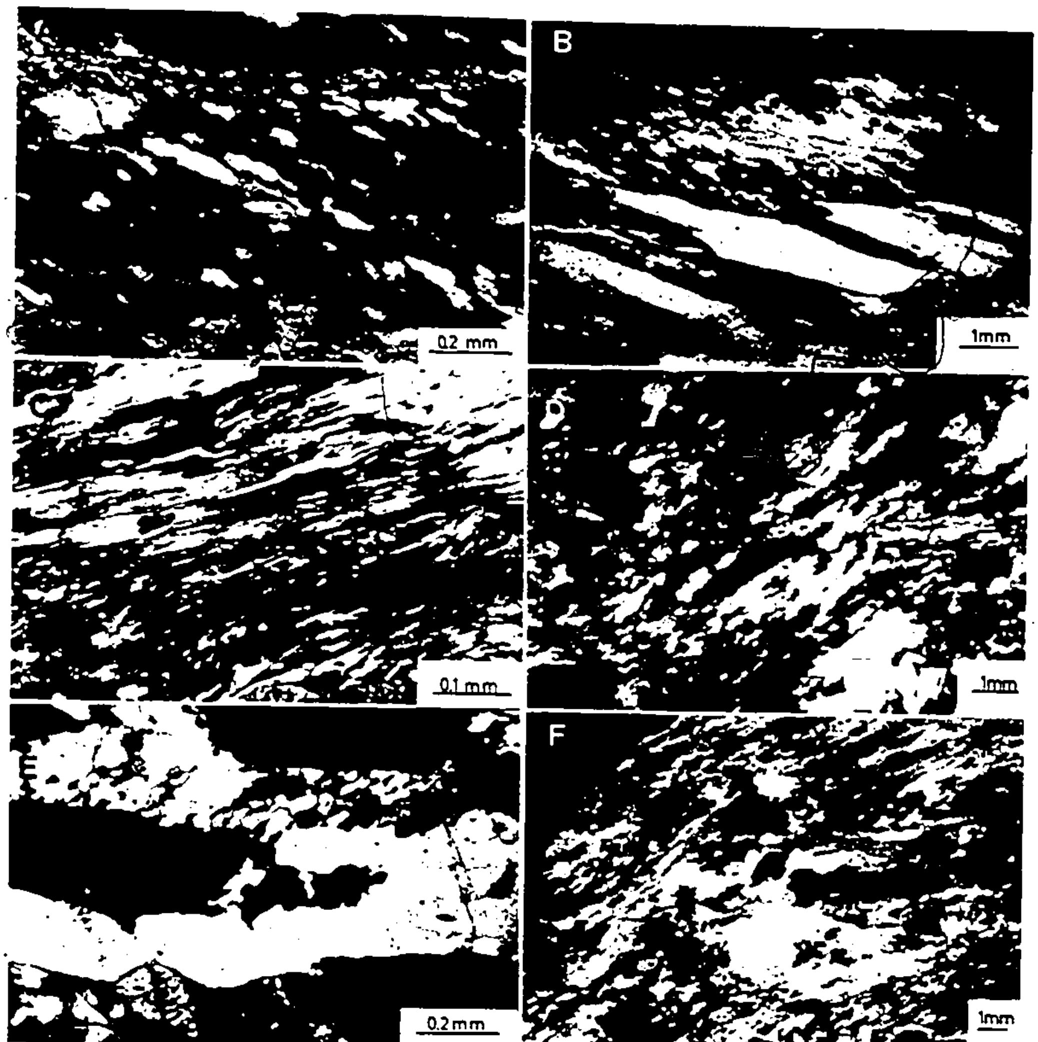

B
0.2 mm
1mm
D
0.1 mm
1mm
F
0.2 mm
1mm

PLATE 17

Quartz Microfoliations (LS2) Oblique to LS1 in LS2 Tectonites

See Fig. 1.2b for location; Fig. 4.26 for C-axis microfabrics. All XZ sections of LS1, X horizontal. All indicate shear of upper layers to SE (opposite to dip direction of LS2).

(A) Quartzite from near Tory Hill (THQ). Horizontal foliation of fine biotite with aligned feldspar and pyroxene porphyroclasts is parallel to S1.

(B) Quartz vein in granite gneiss from northern margin of Cardiff complex, Jordan Lake (24101B). View of fringe of unrecrystallised quartz at vein edge abutting new quartz grains, aligned along LS2.

(C) Granite gneiss from western margin of Cardiff complex (30103B). A detail of a recrystallized LS1 quartz blade consisting of numerous LS2 ribbons and deformation bands.

(D) Quartzite from south shore of Elephant Lake (695C). Feldspar and clinopyroxene lying within LS1 are slightly rotated.

(E) Granite gneiss from south shore of Farquhar Lake (194C). LS1 ribbon is partially recrystallised.

(F) Quartz vein in granite gneiss from west-central part of Cardiff complex (26102B). LS2 curves around unrecrystallised area (featured in Fig. 4.27).

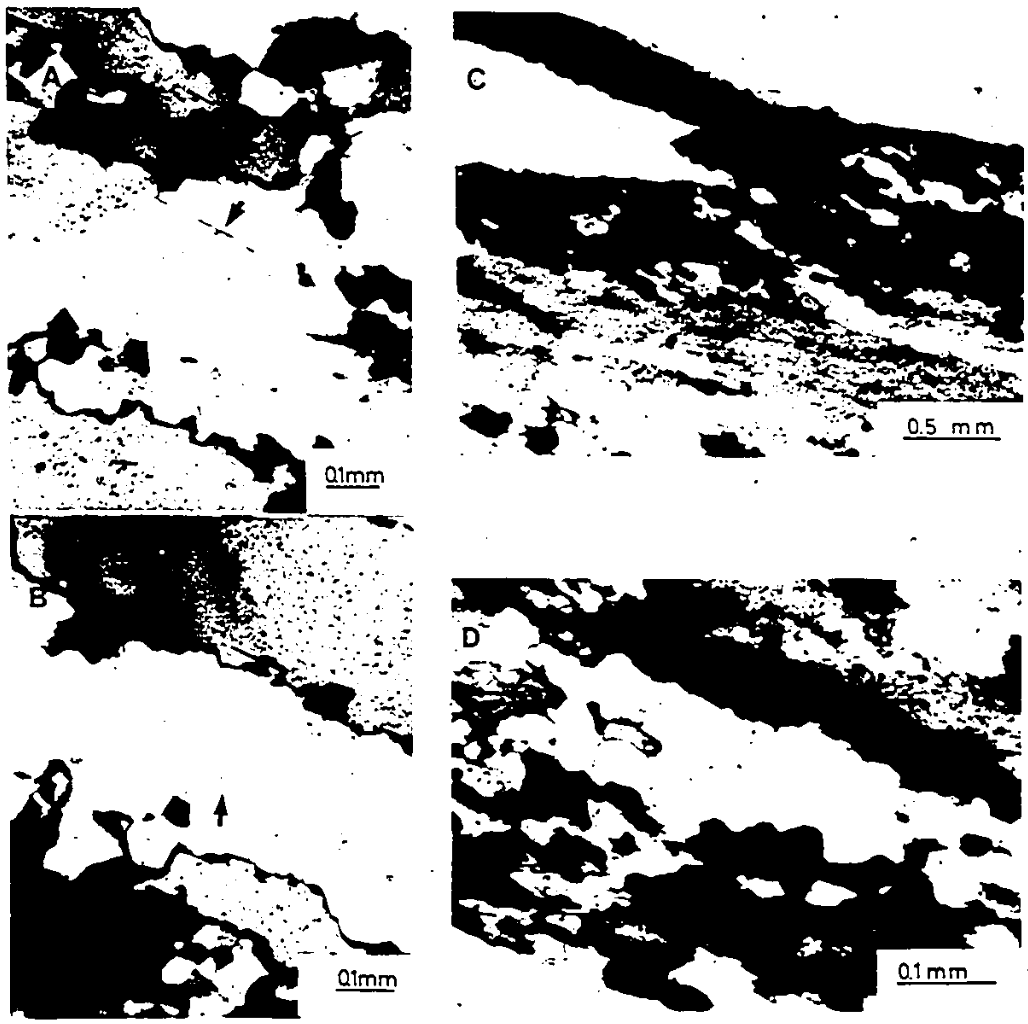
A
0.1mm
B
0.1mm
C
0.5 mm
D
0.1 mm

PLATE 18

Rutile Fabrics and LS2 Quartz Microstructures

All in XZ section of LS1, X horizontal. See Fig. 1.2b for location.

(A) and (B) Quartz vein in granite gneiss from west central part of Cardiff complex (26102B). (A) Rutile needles with long axes subparallel LS2 (dipping to right) are boudinaged (see arrow); or (B) those at a high angle to LS2 are folded (see also Fig. 4.27). Note evidence for bulge nucleation along LS2 boundary.

(C) and (D) Quartz vein from granite gneiss at northern margin of Cardiff complex, Jordan Lake (24101B). (C) is in boundary zone between unrecrystallised and recrystallised quartz; rutile needles, in lower half of photo, lie subparallel to trace of lower deformation band boundary which lies closer to trace of X1 than does LS2, which dips more steeply to the right; the margin of this deformation band is mobile, forming protrusions parallel to LS2. (D) Detail from area comparable to (C). LS2 dipping to right is interpreted as lying closer to the axis of instantaneous stretching than subhorizontal rutile needles, which reflect finite strain (see also Fig. 4.34).

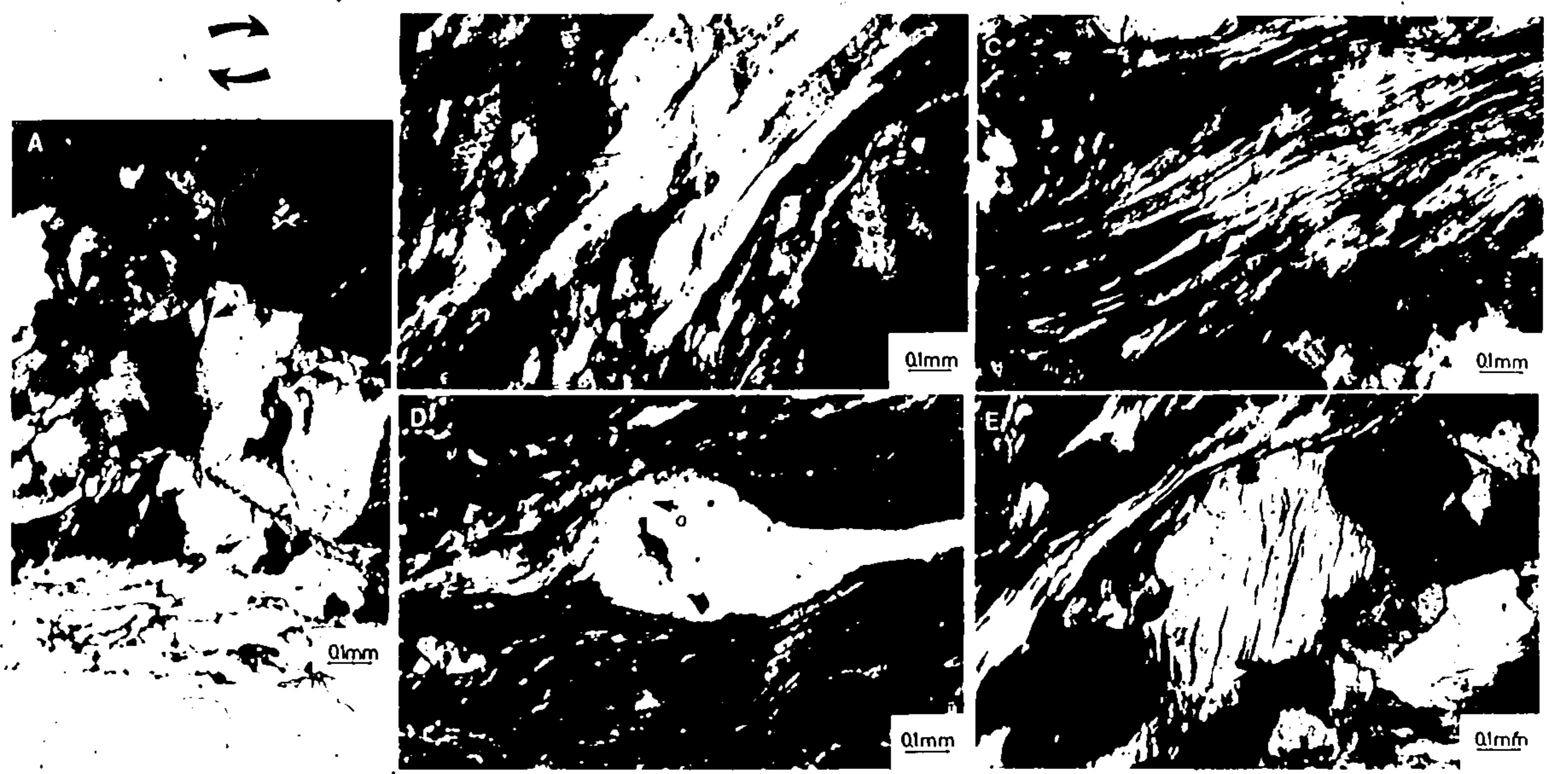
A
0.1mm
0.1mm
C
0.1mm
D
0.1mm
E
0.1mm

PLATE 19

Formation of LS2 Ribbons in Granite Gneiss

30103B, western margin of Cardiff complex. See Fig. 1.2b for location. (A) YZ section of LS1; (B), (C), (D) and (E) XZ sections, X of LS1 horizontal, arrows show sense of shear.

(A) In a section perpendicular to the lineation a kink band boundary (arrow), sub-basal deformation lamellae (fine, subhorizontal lines) and kink axis lie at a high angle to the section; (this grain illustrated in Fig. 4.29).

(B) A kinked grain similar to that in (A) forms embryonic ribbons with long axes dipping left at a high angle to X of LS1; misorientation between ribbons is low and deformation lamellae dipping gently to left are perpendicular to the section.

(C) A family of LS2 ribbons merges with unrecrystallised quartz across a narrow zone of kink-like deformation bands (arrow).

(D) Kink-like deformation bands form at edge (arrow) of a globular augen of unrecrystallised quartz.

(E) Ribbons, abutting an area of unrecrystallised quartz, curve round a K feldspar grain which is untwinned and has lunate albite intergrowths.

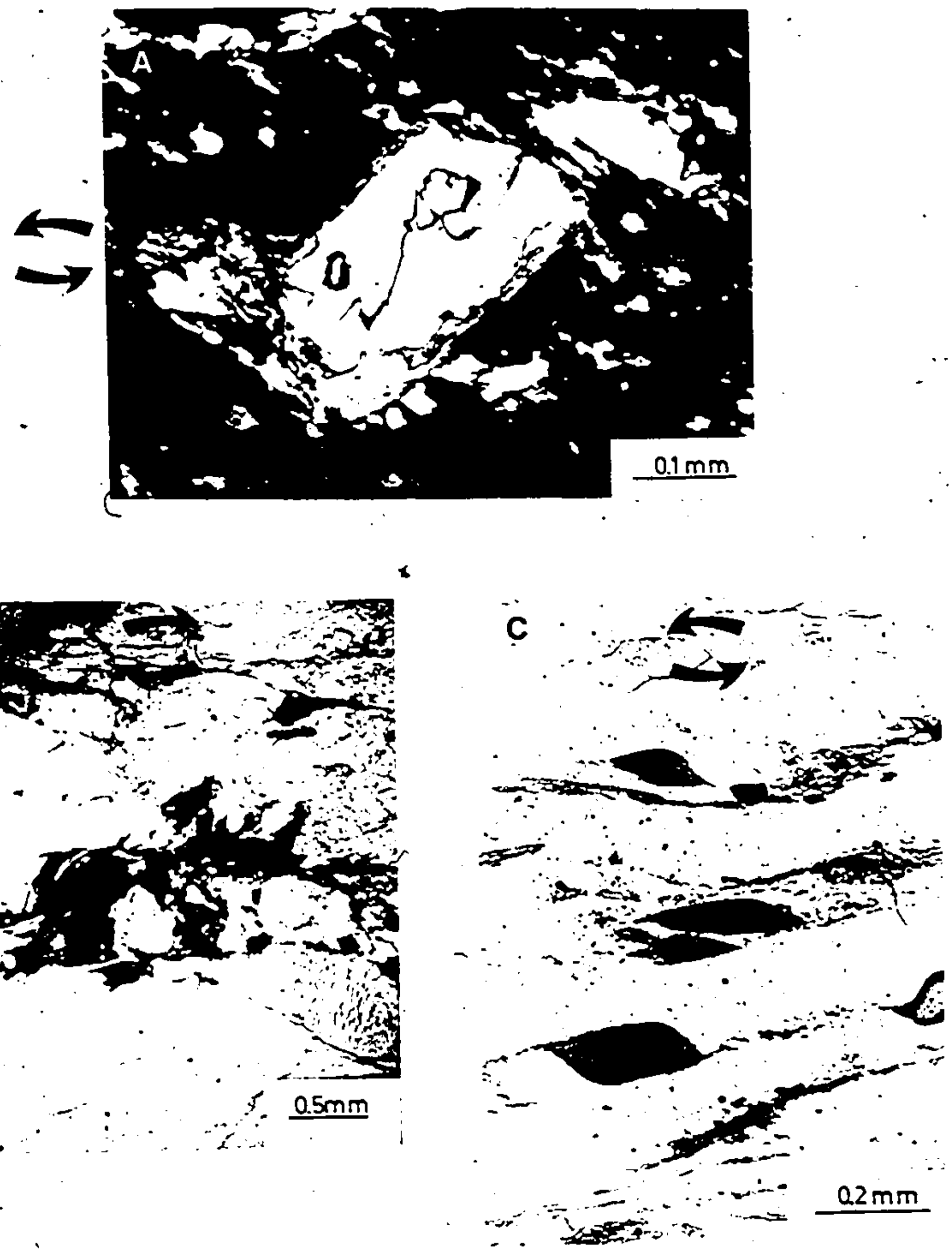
A
0.1 mm
B
0.5mm
C
0.2mm

PLATE 20

Indicators of Shear Sense in LS2 Tectonites

All XZ section of LS1, X horizontal; shear sense indicated by arrows (top to southeast); see Fig. 1.2b for location.

(A) Rotated feldspar porphyroclast entrains biotite foliation; quartzite from near Tory Hill (THQ).

(B) Biotite curves into and lies along narrow planes lying parallel to X; granite gneiss from western Cardiff complex (30103B).

(C) Asymmetric shape of clinopyroxene in quartzite from near Tory Hill (THQ).

Appendix I

Tables

Table 1. Estimated Lithological Proportions of map-area.

Rocks not grouped in time order.

Plutonic Orthogneiss	Pink Granite Gneiss	20	
	Grey Tonalitic Gneiss	25	
	Syenitic Gneiss	15	66%
	Mafic Plutonic Rocks	5	
Supracrustal Rocks	Marble and Quartzite	18	
	Paragneiss	7.5	
	Calcareous Gneiss (Amphibolite to Pyroxene Gneiss)	7.5	33%

Table 2 Mutual Time Relations of Plutonic Gneisses and Supracrustal Rocks According to Various Authors in Area[illegible]t to and Overlapping with Area of Present Study

	A	B	C	D
Post Tectonic	8	7	7,8	
	7	---		
Late Tectonic		5,3		
Mid Tectonic	6 5			4 --- 6
Early Tectonic	3			5 --- 3
Pre Tectonic	2(=4)[1] unconformity 1	4,1 --- 2	1[2] 5 3 --- 2	2

A: Eels Lake Area, Bright (1980)
B: Glamorgan and Monmouth Townships, Armstrong and Gittins (1968)
C: Glamorgan Township, Chesworth (1967)
D: Cardiff and Faraday Townships, Haliburton Highlands, Hewitt (1957 a)

Dotted line is an igneous contact stated in the published tables of formations.

[1] The Cheddar Batholith is purportedly a feldspathic arenite which has been remobilized by in situ anatexis (Bright 1980)

[2] Chesworth (1966) cites evidence that 1 intrudes 3 and 2.

[3] Corresponds generally to Chesworth 1975.

Lithostratigraphic Units

1. Tonalitic gneiss and migmatite of Glamorgan gneiss complex
2. Supracrustal rocks, predominantly calcareous metasediments, of the Grenville Supergroup
3. (Meta-) gabbro, diorite, minor anorthosite and pyroxenite
4. Granitoids of the large plutonic complexes eg. Cheddar Granite
5. Nepheline bearing gneisses
6. Syenitic gneisses eg. Deer Lake Syenite
7. Smaller sills, dykes and irregular bodies of granite, syenite and pegmatite
8. Mafic Dykes

Table 3. Summary of Known Relationships Between Major Rock Types

INTRUDED		INTRUDER B	C	D	E
Supracrustal Rocks	A	very large conformable bodies, including sheets. No cross-cutting relations known	large conformable sheets	mostly conformable sheets of all scales. Some smaller bodies cross-cutting	large conformable sheets and plugs. Foliated sheets and dykes, all scales
Tonalitic Grey Gneiss and Associate Rocks	B		no unequivocal cross-cutting relations known*	Isolated small dyke west of Fishtail Lake	foliated granitic sheets and dykes of all sizes are part of complex
Mafic Plutonic Rocks	C	no unequivocal cross-cutting relations known		some foliated pink syenite veins cut c. larger bodies rarely carry xenoliths of c.	small foliated pink granite veins cut meta-gabbro (c)
Syenitic Gneiss	D	N.A.	N.A.		small foliated granite veins cut larger Buff syenites and are interlayed with pink syenite.
Granitic Gneiss	E	N.A	N.A	in northern domains pink syenite and granite is interlayed in ambiguous relationship	

*some equivocal contacts between foliated grey gneiss and unfoliated gabbro occur. See text.

Table 4. Minerals present in supracrustal rocks.

Rock Type	Marble and related supracrustal rocks: Marble (Map Unit 1a)															Quarzite (1b)		Diopside rock (1a)
Quartz							5									1	1	
Plagioclase							3									2		
Microcline														2	2	2		
Scapolite																		
Amphibole							4	3	2	2								
Clinopyroxene		3	2	3			2		3							2		1
Biotite															3		2	
Phlogopite	2	2						2	4	3								
Garnet																		
Calcite	1	1	1	1	1	1	1	1	1	1	1	1	1	1	1			
Dolomite	1					1		1										
Sillimanite																		
Kyanite																		
Serpentine			3	2														
Forsterite								4										
Chondrodite																		
Apatite														3				
Sphene														4				
Magnetite															4			
Most common accessory mineral	Graphite																	
Other accessory minerals	Quartz, Tremolite, Pyrite, Fluorite, Sphene																	

Non-Carbonate Supracrustal rocks.	Calcareous (Map Unit 2a): Amphibolite							Calcareous (Map Unit 2a): Pyroxene rich							Non-Calcareous (Map Unit 2b): Paragneiss							
Quartz															2	2	2	2	2	2		
Plagioclase	2	2	2	2	2	2	2	3	3	2	3	5	4	3	1	1	1	1	1	1	1	1
Microcline												4	3	4				3	6			3
Scapolite		3				3																
Amphibole	1	1	1	1	1	1	1	2	2			2	1	2			4					
Clinopyroxene					3		4	1	1	1	1	1	1	1								2
Biotite				3		4	3		4		2	3	2		3	3	3	4	3	3	2	4
Phlogopite																						
Garnet			3													5		5	4	4		
Calcite																						
Dolomite																						
Sillimanite																						
Kyanite																4			5			
Serpentine																6						
Forsterite																						
Chondrodite																						
Apatite																						
Sphene																						
Magnetite																						
Most common accessory mineral	Sphene							Sphene, Calcite							Magnetite							
Other accessory minerals	Quartz, Garnet, Calcite, Magnetite, Epidote.							Plagioclase, Tourmaline, Magnetite, Epidote.							Graphite, Amphibole, Calcite, Tourmaline, Apatite, Sphene, Zircon.							

Minerals are numbered in order of decreasing importance.

Table 5. Minerals present in Grey Gneiss Complexes.

Map Unit	Grey Tonalitic Gneiss (3a)							Garnet Gneiss (3c)								
Quartz	2	2	2	2	2	2	2	2	2	1	2	2	2	2	2	2
Plagioclase	1	1	1	1	1	1	1	1	1		1	1	1	1	1	1
Microcline	3		5													
Hornblende	5	3	3		4	3	3									
Orthoamphibole									3			4	4			5
Clinopyroxene							4									
Biotite	4	3	4	3	3			3		2	3	3	3	3	3	3
Garnet								4	4	4	4		5	4	4	4
Cordierite										3		3		3	3	
Sillimanite											5		6		5	6
Magnetite								5	5	4	6	5	7	5	6	7
Accessory Minerals	Microcline, Apatite Zircon, Garnet, Magnetite.							Apatite.								

Minerals are numbered in order of decreasing importance.
Outlined assemblages in Garnet Gneiss occur in different layers in one section.
Fishtail Lake Rocks not documented (see Lal and Moorhouse 1969)
Pink Mobilizate and Amphibolite not included.

Table 6. Modes of some Grey Tonalitic Gneisses
(Unit 3a)

Gneiss Type	Hornblende-Biotite 1.	Hornblende-Biotite 2.	Hornblende 3.	Biotite 4.
Quartz	26.8	29.8	28.0	33.0
Plagioclase	57.7	52.3	51.1	56.0
An %	25	26-27	30	21-22
Microcline	7.3	0.6	2.9	0.1
Biotite	4.5	7.0	3.1	10.3
Hornblende	3.3	7.7	14.2	—
Others	0.5	3.05	0.2	0.7
Totals	100.1	100.45	100.2	100.1

Location: 1. Farquhar Lake Sheet. 2-4 Drag Lake Complex.

Table 7. Comparative Geochemistry of the Grey Tonalitic Gneisses

	1	2	3	4	5
SiO_2	67.7 (1.8)	67.16	73.05 (0.55)	72.34 (1.4)	72.2 (2.17)
Al_2O_3	15.2 (0.1)	15.20	14.0 (0.20)	14.46 (1.4)	14.0 (0.83)
Fe_2O_3	)				1.6 (0.45)
FeO	) 3.06(0.45)	2.74	2.61 (0.08)	2.8 (0.61)	1.5 (0.48)) 3.1
MgO	1.56(0.03)	0.89	0.94 (0.03)	0.73 (0.15)	0.7 (0.41)
CaO	4.09(0.24)	2.99	2.26 (0.43)	2.89 (0.44)	1.8 (0.68)
Na_2O	3.43(0.45)	4.62	4.19 (0.49)	4.91 (0.43)	4.30(0.51)
K_2O	2.23(0.31)	2.41	1.47 (0.04)	1.3 (0.06)	2.30(0.54)
TiO_2	0.26 (0.01)	0.28	0.41 (0)	0.29 (0.03)	0.40(0.14)
P_2O_5	0.12 (0.01)	0.07	0.07 (0.02)	0.05 (0.01)	
MnO	0.08 (0.01)	0.04	0.12 (0.08)	0.04 (0.01)	0.10(0.03)
K/Rb	476.9(158.12)	400.1	241.47(71.89)	315.57 (59.1)	
Rb/Sr	0.095(0.03)	0.13	0.24(0.09)	0.096(0.03)	
K/Ba	45.93(10.51)	40.01	82.46(42.89)	33.27 (5.6)	

1, 3, 4, 5, are mean values. Standard deviations, where available, in brackets.

1. Hornblende-biotite gneiss, Drag Lake Complex (N=2)
2. Hornblende-biotite gneiss Yankton Lake, Farquhar Lake Sheet
3. Biotite gneiss, Drag Lake Complex (N=2)
4. Hornblende-Biotite gneiss, Farquhar Lake Sheet and Straggle Lake Complex (N=3)
5. Grey granite of Glamorgan Complex (N=22) (Chesworth 1967)

	6	7	8	9	10
SiO_2	71.4 (0.4)	65.3	69.8	67.17	66.72
Al_2O_3	15.94(0.03)	17.1	15.9	15.79	16.04
Fe_2O_3	0.27(0.15))1.33	0.16)3.24	0.50)2.87	1.68)3.09	1.94)3.41
FeO	1.06(0.32	3.08	2.37	1.41	1.47
MgO	0.65(0.18)	1.92	1.43	1.09	1.44
CaO	3.5 (0.11)	2.53	2.59	3.54	3.18
Na_2O	5.25(0)	5.07	4.43	4.74	4.90
K_2O	1.15(0.1)	2.06	2.51	2.10	2.09
TiO_2	0.18(0.04)	0.48	0.40	0.31	0.34
P_2O_5		0.12	0.11	0.12	0.14
MnO	0.02(0.01)	0.03	0.05	0.04	0.04
K/Rb				395	234
Rb/Sr				0.08	0.13
K/Ba				16.7	24.3

6,9,10 are mean values. Standard deviations, where available, in brackets.

6. Boulter granite (N=2) (Hewitt and James 1956)
7. Trondjhemite, Weslemkoon Batholith (Lumbers 1967)
8. Granodiorite, Weslemkoon Batholith (Lumbers 1967)
9. Hornblende-Biotite gneiss, E. Greenland (N=41) (Sheraton et al 1973)
10. Hornblende-Biotite gneiss, Laxfordian, Scotland (N=39) (Sheraton et al 1973)

(See Appendix IV for analytical details)

Table 8. Correlation coefficients of selected element pairs in the Grey Tonalitic Gneiss of the Drag Lake Complex. Hornblende-, Hornblende-Biotite and Biotite-Gneisses.

	S_iO_2	T_iO_2	Al_2O_3	FeO	MnO	MgO	CaO	Na_2O	K_2O	P_2O_5	Sr	Rb	Ba
S_iO_2	-	.1734	.2842	.9142	.1141	.8855	.9362	.8143	.0713	.8552	.4451	.6927	.0959
FeO	.9142	.9811	.2262	-	.2398	.9688	.8798	.7291	.4455	.6006	.1649	.7634	.2691
CaO	.9362	.1773	.2567	.8798	.1899	.9223	-	.9336	.3887	.7713	.3185	.6533	.1455

Table 9. Comparison of Geochemistry of Minor Potassium rich Granites.

	1.	2.	3.	4.
S_iO_2	74.10	71.4(0.4)	73.73(2.20)	75.4(2.64)
Al_2O_3	13.90	14.35(0.5)	13.29(1.17)	13.8(1.47)
FeO	1.64	0.61(0.28)	0.86(0.45)	1.4
MgO	0.64	0.17(0.03)	0.01(0.07)	0.3(0.31)
CaO	1.80	0.85(0.39)	0.65(0.17)	0.8(0.62)
Na_2O	2.90	4.04(0.07)	3.88(0.37)	3.62(0.53)
K_2O	3.88	5.67(0.51)	5.51(0.35)	4.5(0.36)
T_iO_2	0.18	0.12(0.11)	0.20(0.07)	0.2(0.09)
P_2O_5	0.02	0.02(0.01)	0.00(0.01)	-
MnO	0.03	0.02(0.02)	0.01(0.00)	0.00(0.01)

1. Granite fraction of Grey Tonalite Gneiss Complex. Sample from thick sheet from North-East of Drag Lake.
2. Mean of 2, Leucogranites from heterogeneous Syenite Gneiss South of Drag Lake.
3. Mean of 5 Medium grained Granite and Pegmatitic Granite from the Cheddar, Centre Lake and Upper Faraday Granite.
4. Mean of 11 Pink Granite and Leucosome from the Glamorgan Complex (Chesworth 1967).

(See Appendix IV for analytical details)

Table 10. Comparative Geochemistry of Garnet Gneiss, Drag Lake Complex (1 of 2)

	1	2	3	4
S_1O_2	67.80	66.70	62.80	67.70
Al_2O_3	14.20	14.00	15.40	15.20
FeO	6.21	6.29	7.10	3.06
MgO	2.72	2.35	2.31	1.56
CaO	0.63	1.11	5.09	4.09
Na_2O	3.52	5.19	3.85	3.43
K_2O	1.30	0.50	0.81	2.23
T_1O_2	0.41	0.49	0.48	0.26
P_2O_5	0.10	0.14	0.06	0.12
MnO	0.14	0.19	0.16	0.08
LOI	0.77	0.62	0.85	
TOTAL	98.50	98.30	99.70	
K/Rb	1079.13	———	———	476.9
Rb/Sr	0.083	———	———	0.095
K/Ba	107.9	83.01	67.23	45.93

1. Sillimanite - Garnet - Gedrite - Cordierite - Quartz - Plagioclase. South West Shore of Drag Lake.
2. Garnet - Gedrite - Biotite - Quartz - Plagioclase. North of Drag Lake.
3. Garnet - Biotite - Quartz - Plagioclase. South Shore of Drag Lake.
4. Average of two Hornblende - Biotite Gneiss. Drag Lake.

(See Appendix IV for analytical details)

Table 11. Chemical analyses and norms of Farquhar Lake Complex.
(Standard deviation in brackets).

	Gabbro(N=4)	Anorthosite(N=2)	Pyroxenite(N=2)
SiO_2	48.87(0.48)	50.14(0.42)	49.27(0.34)
Al_2O_3	18.8 (1.5)	27.97(1.36)	4.06(0.87)
Fe_2O_3	6.87(0.30)	1.89(0.78)	8.52(0.6)
MgO	8.04(0.9)	1.25(0.68)	16.41(1.14)
CaO	13.33(0.33)	13.01(0.45)	19.92(0.16)
Na_2O	2.65(0.38)	3.95(0.08)	0.62(0.12)
K_2O	0.44(0.22)	0.55(0.14)	0.12(0.06)
TiO_2	0.31(0.08)	0.18(0.09)	0.56(0.15)
P_2O_5	0.01(0.01)	0.015(0.02)	0.01(0.01)
MnO	0.12(0.02)	0.03(0.02)	0.14(0)
S	0.03(0.01)	0.01(0)	0.02(0.01)
Ba	117 (27.9)	141.5(32.5)	78 (11)
Cr	328.8 (139.8)	50 (50)	772 (120)
Zr	18.5 (2.7)	20 (0)	6.5 (0.5)
Sr	327.3 (22.1)	641.5(42.5)	43 (16)
Rb	5 (4.8)	9.5(6.5)	3 (16)
Zn	43 (9.5)	17.5(0.5)	21 (0)
Ni	56.3 (7.2)	3 (3)	113.5 (0.5)
Q	-	-	-
Or	2.63(1.29)	3.258(0.81)	0.69(0.27)
Ab	19.97(2.6)	27.453(1.51)	1.58(0.95)
An	38.7(3.38)	57.61(3)	8.05(1.79)
Lc	-	-	-
Ne	1.432(0.63)	3.4(0.48)	1.99(1.06)
Kp	-	-	-
Ac	-	-	-
Di	14.92(6.27)	5.84(4.16)	62.02(2.39)
He	4.8(0.45)	-	10.72(0.86)
En	-	-	-
Fs	-	-	-
Fo	8.43(0.71)	0.31(0.15)	8.75(1.12)
Fa	2.94(0.28)	-	1.89(0.01)
Wo	-	-	-
Ln	-	-	-
Ru	-	0.05(0.05)	-
Mt	2.65(0.12)	0.87(0.87)	3.01(0.23)
Il	0.59(0.16)	0.25(0.27)	1.07(0.28)
Cr	0.074(0.04)	0.01(0.01)	0.18(0.03)
Hm	-	0.85(0.27)	-
Ap	0.03(0.02)	0.04(0.04)	0.02(0.02)
Po	0.089(0.02)	0.06(0.03)	0.042(0.01)

(See Appendix IV for analytical details)

Table 12. Lithological Makeup of Drag Lake Buff Syenite.

i).	Percentage of outcrops composed solely of Buff Syenite	66
ii)	" Buff Syenite and one other Rock-type.	23
iii)	Percentage of outcrops composed of Pink Syenite, Quartz Syenite or Granite	11
iv)	Percentage of outcrops comprised, in part, of non-Orthogneiss	4.4

Source of information: Culshaw, 1981.

Table 13. Nature of Heterogeneous Syenite Gneiss Unit.

Percentage of all outcrops in body in which:	1	2	3	4
	N=41	N=118	N=262	N=106
Outcrop has two or more rock types	48.8	54.5	64.9	42.5
Outcrop composed of single syenitic rock-type	19.5	16.0	28.24	34.9
Outcrop composed of two or more syenitic rock-types	28.6	27.9	34.7	9.4
Outcrop composed of one or more granitic rock-type	7.3	15.3	4.9	5.7
Outcrop composed of supracrustal rock only	24.4	19.4	2.29	3.7
Outcrop composed of syenite and other rock-type	41.5	31.4	32.1	29.24
Number of rock types in body	11	15	15	11
Number of supracrustal enclaves	5	9	10	-
Percentage of all rock types on map face which are:				
Syenitic	66	67	61.4	62
Granitic	11.9	13.1	20	19.2
Supracrustal	22	19.9	7.7	18.5
Ratio of Buff and White to Pink Syenite	1:3	1:4.2	1:19.3	1:2.5

1. North Cardiff.
2. West Cardiff.
3. North Farquhar Lake.
4. Little Dudmon - Miskwabi-Lake

Sources of information:

1,2: Hewitt 1957c.

3. Mapping by author.

4. Culshaw 1981.

Table 14. Minerals present in Syenitic Rocks.

	A	B	C	D	E
Quartz				4	3
Plagioclase	1 1 1	1	2 2 2	2	2
Microcline	1 1 1		1 1 1	1	3
Perthite	2 2		3	3	1
Amphibole	2		4		
Clinopyroxene	3		4 3		
Magnetite	3 3 4	3			
Biotite		2	3		
Accessory Minerals	Quartz, Sphene, Calcite, Apatite, Biotite, Amphibole.				

A Buff Syenite

B Albite Syenite

C Pink Syenite

D Quartz-Syenite and Granite

E Pegmatite.

Minerals are numbered in order of decreasing importance.

Table 15. Comparative Geochemistry of Syenitic rocks.

	1	2	3	4	5
SiO_2	54.03(1.88)	57.37	53.45(2.97)	65.9	60.8
Al_2O_3	16.53(0.26)	14.73	16.57(0.88)	15.7	16.8
Fe_2O_3)	8.83(0.67)	4.61)9.13	9.74(1.53)	2.59	0.87
FeO		4.52			
MgO	1.11(1.1)	0.44	2.39(0.57)	0.49	1.33
CaO	4.83(1.12)	5.15	5.46(1.81)	2.09	2.47
Na_2O	4.68(0.54)	6.70	6.01(0.64)	3.46	2.47
K_2O	5.02(1.36)	3.51	2.87(0.89)	7.04	10.4
TiO_2	0.81(0.70)	0.99	2.16(0.87)	0.40	0.05
P_2O_5	0.36(0.36)	0.01	0.78(0.31)	0.10	0.09
MnO	0.16(0.02)	0.13	0.18(0.08)	0.08	0.03

1. Mean of 3 Buff Syenites, Drag Lake.
2. Buff Syenite, Deer Lake (Hewitt 1957a)
3. Mean of 8 Mugearites. (Compiled from Carmichael et al 1974)
4. Buff Quartz Syenite, Drag Lake (Highway 121, 6km West of Dudmon Lake).
5. Pink Syenite, Drag Lake (Highway 121, 1km East of Dudmon Lake).

(See Appendix IV for analytical details.)

Table 16. Chemical analyses and norms of Cheddar, Centre and Monck Lake and Faraday Granites

	1	2	3	4	5	6	7	8	9
SiO_2	73.83(2.92)	72.12(1.22)	71.35(1.55)	75.17	75.33(0.44)	73.07(2.82)	74.12(3.47)	73.22(1.95)	73.44(2.22)
Al_2O_3	12.59(0.77)	8.81(1.33)	14.63(0.67)	12.55	12.33(0.05)	12.34(0.48)	12.82(0.84)	13.95(0.63)	11.44(0.60)
Fe_2O_3T	3.00(1.22)	10.10(0.42)	1.58(0.42)	1.55	2.3(0.09)	4.35(1.71)	2.85(0.69)	3.01(1.13)	4.47(0.44)
MgO	0.13(0.16)	0.03(0.05)	0.05(0.02)	0.02	0.19(0.01)	0.22(0.18)	0.23(0.13)	0.21(0.05)	0.26(0.01)
CaO	0.63(0.13)	1.03(0.47)	0.7(0.21)	0.8	0.57(0.01)	0.93(0.44)	0.66(0.40)	1.1(0.48)	1.44(0.64)
Na_2O	3.29(0.40)	3.76(0.93)	4.34(0.03)	3.55	3.60(0.04)	4.41(0.33)	4.33(0.61)	4.76(0.17)	4.65(0.57)
K_2O	5.72(0.31)	3.84(1.55)	5.83(0.32)	5.22	5.34(0.18)	4.03(0.94)	3.97(0.94)	4.51(0.01)	2.76(0.35)
TiO_2	0.29(0.18)	0.39(0.05)	0.12(0.07)	0.20	0.26(0.01)	0.36(0.24)	0.29(0.03)	0.27(0.10)	0.31(0.02)
P_2O_5	0.03(0.04)	0.00	0.01(0.01)	0.0	0.0	0.06(0.05)	0.03(0.03)	0.03(0.02)	0.07(0.03)
MnO	0.01(0.01)	0.38(0.21)	0.01(0.0)	0.01	0.01(0.0)	0.07(0.04)	0.03(0.03)	0.05(0.03)	0.13(0.05)
K/Rb	326.15(29.91)	351.10(101.21)	287.11(2.37)	235.78	260.93(13.40)	333.84(60.79)	400.06(63.86)	332.66(26.31)	364.49(58.69)
Rb/Sr	2.39(1.54)	4.82(2.77)	0.95(0.46)	1.29	1.73(0.39)	2.39(1.26)	1.10(0.69)	1.65(0.71)	0.87(0.23)
K/Ba	175.07(78.0)	303.15(41.74)	174.33(24.16)	83.49	118.14(9.15)	174.26(113.72)	81.15(45.73)	107.03(30.91)	209.59(111.2)
Q	31.30(6.94)	33.58(0.70)	22.76(3.0)	33.27	32.87(0.79)	28.69(5.57)	31.66(2.69)	23.93(1.90)	31.53(5.24)
C	0.02(0.03)	-	0.27(0.27)	-		0.05(0.14)	0.11(0.23)	-	
Or	34.06(1.87)	23.07(9.21)	34.94(2.0)	31.16	31.63(1.17)	25.30(3.93)	23.61(5.59)	26.93(0.27)	16.43(2.02)
Ab	28.05(3.46)	24.45(1.83)	37.39(0.8)	30.40	30.46(0.20)	37.49(2.87)	36.82(5.13)	40.70(1.06)	41.79(5.03)
An	2.60(0.02)	-	2.55(0.71)	2.86	1.71(0.25)	1.12(0.81)	3.54(1.84)	3.39(1.10)	1.17(0.47)
Ac	-	3.64(1.29)	-	-	-	0.05(0.10)	-	-	-
Di	0.06(0.03)	0.12(0.06)	0.11(0.11)	0.11	0.65(0.18)	0.56(0.52)	0.37(0.40)	0.61(0.18)	1.25(0.78)
He	0.09(0.12)	4.55(2.22)	-	-	-	1.69(1.34)	0.06(0.12)	0.71(1.00)	3.57(1.66)
En	0.29(0.37)	0.178(0.11)	0.101(0.10)	-	0.16(0.04)	0.29(0.31)	0.56(0.39)	0.25(0.18)	0.09(0.07)
Fs	0.60(0.51)	7.83(2.80)	-	-	-	1.25(1.12)	0.29(0.41)	0.35(0.54)	0.67(0.81)
Wo	0.03(0.04)	-	0.32(0.32)	0.47	-	0.24(0.48)	0.02(0.06)	0.14(0.20)	0.17(0.17)
Fu	0.04(0.05)	-	0.03(0.03)	0.19	-	0.37(0.09)	0.03(0.10)	-	-
Mt	1.83(1.30)	0.953(0.70)	0.111(0.111)	-	0.73(0.12)	2.39(1.11)	1.94(0.64)	1.71(1.00)	2.65(0.04)
Il	0.48(0.41)	0.73(0.09)	0.21(0.18)	0.07	0.50(0.002)	0.62(0.35)	0.43(0.22)	0.51(0.19)	0.60(0.04)
Cr	-	0.002(0.002)	0.005(0.005)	-	-	-	-	-	-
Hm	0.50(0.70)	-	1.37(0.2)	1.55	1.26(0.10)	0.33(0.64)	0.35(0.53)	0.60(0.61)	-
Ap	0.07(0.09)	-	0.02(0.02)	-	-	0.03(0.09)	0.04(0.03)	0.06(0.06)	0.06(0.09)
Fo	0.01(0.01)	-	0.014(0.014)	-	0.01(0.01)	0.003(0.001)	0.01(0.001)	0.01(0.01)	0.01(0.01)
Ms	-	0.92(1.30)	-	-	-	-	-	-	-

1 Alaskite, Mean of 3, North part of Cheddar Granite
2 Alkali Granite, Mean of 3, Cheddar Granite

Medium grained and Pegmatitic Granite

3 Mean of 2, Cheddar Granite
4 Centre Lake Granite
5 Mean of 2, Upper Faraday Granite

Biotite and Hornblende-Biotite Granite

6. Mean of 10, Cheddar Granite
7. Mean of 10, Centre and Monck Lake Granite
8 Mean of 3, Lower Faraday Granite
9. Pyroxene Granite, Mean of 3, Cheddar Granite

(See Appendix IV for analytical details)

Table 17. Structural State of Feldspar in Faraday Granite.

	1.		2.	
	K-Feldspar	Plagioclase	K-Feldspar	Plagioclase
T.O Site Occupancy	0.96	0.94	1.00	0.98

1. Sample 497c, Lower Faraday Granite, Highly Deformed, Fined Grained Gneiss.
2. Sample 1491c, Upper Faraday Granite, Weakly Deformed Medium Grained Gneiss.

TABLE 18 FELDSPAR GRAIN SIZE RANGE IN CHEDDAR AND CARDIFF COMPLEXES

SAMPLE NUMBER	PLUTON	GRAIN SIZE RANGE MM.	LOCATION
11103B	Cheddar	1 - 3	North ↑
11102B	—"—	1 - 5	South to North traverse
2692B	—"—	1 - 5	from Hook Lake to contact
201010B	—"—	0.4 - 3	↓ South
1171B	Centre Lake Granite	0.5 - 2	} South near Paudash Lake
1174B	—"—	0.4 - 2	
30101B	Monck Lake Granite	0.2 - 0.6	} North, West of Deer Lake
261B	—"—	0.2 - 0.6 (rare augen 6 mm.)	
24101B	—"—	0.2 - 0.4	Far North-east, Jordan Lake
1395B	Upper Faraday Granite	0.7 - 2	
1691B	Lower Faraday Granite	0.2 - 0.4	

Table 19. Metamorphic Mineral Assemblages.

Pelitic

Quartz - Biotite - Plagioclase (An_{35-42}) - Garnet - Sillimanite.*
Quartz - Biotite - Plagioclase (An_{23}) - Garnet - Microcline - Sillimanite.
Quartz - Biotite - Plagioclase (An_{28}) - Garnet - Cordierite - Sillimanite.
Quartz - Biotite - Plagioclase (An_{28}) - Gedrite - Sillimanite.
Quartz - Biotite - Cordierite
*Hewitt (1957a) Reports Minor Kyanite.

Basic (Metagabbro)

Hornblende - Plagioclase ($An_{35-45,\ 55-62}$) ± Clinopyroxene, Scapolite

Amphibolite

Hornblende - Plagioclase (An_{14-44}) ± Scapolite, Biotite, Clinopyroxene, Sphene, Magnetite, Quartz.

Calcareous

Calcite - Diopside (± Tremolite, Quartz Rim)
Calcite - Diopside (± Tremolite Rim) - Phlogopite
Calcite - Dolomite - Forsterite (± Tremolite Rim) - Phlogopite
Calcite - Phlogopite
Calcite - Tremolite - Chondrodite

Table 20. Variation of Plagioclase Composition (An%) with Rock Composition in Study Area, Compared with Areas of Different Grade in the Central Alps (Switzerland).

	Estimated Temperature °C	Amphibolites	Metapelites	Leucocratic Gneiss	Comments
1.	530	18-32	4-35	2-26	Intergrowths in sodic compositions (peristerite).
2.	588	14-22 28-35	11-40	0-22	No intergrowths. Just below diopside calcite isograd.
3.	635	29-46	29-37	16-25	Anatexis begins. Intergrowths in intermediate and calcic plagioclase.
4.	665	27-50 62-70	25-44	17-28	
5.	—	20-44 55-65	20-48	15-30	Intergrowths in sodic, intermediate and calcic plagioclase.

1 - 4. Variation of plagioclase compositions with metamorphic grade from Central Alps. Adaptation of Figure 6 of Wenk and Wenk 1977.

5. Plagioclase compositions in study area.

TABLE 21 EXAMPLES OF VEIN FABRICS

LOCATION	HOST ROCK TYPE	VEIN TYPE	ESTIMATED STRAIN TYPE
Fishtail Lake (South Shore)	Amphibolite	Granitic	plane
Farquhar Lake (South Shore)	Amphibolite	Tonalitic grey gneiss and granite	plane
Farquhar Lake (West Shore)	Tonalitic grey gneiss	Trondjhemite	plane
Drag Lake (North-East Shore)	Tonalitic grey gneiss	Pegmatite and Pegmatitic Granite	constrictional
South and East of Farquhar Lake	Meta-Gabbro	Granite and Syenite	plane
South of Drag Lake	Buff Syenite	Pink Syenite and Syenitic Pygmatite	plane
Baptiste Lake (South West Shore)	Granite	Mafic Dyke	plane
West Cardiff Complex (Domain 12)	Granite	Mafic Dyke	plane
West of Baptiste Lake	Amphibolite	Granite and Syenite	plane

Table 22. Density Contrasts Estimated for Possible Gravity Structures, Compared with Natural and Model Diapirs

Structure	Core Rock	Density	Mantle Rock	Density	Density Contrast (% of Mantle Density)
		g/cm^3		g/cm^3	
Cheddar Complex	average Bancroft gneissic granite (ABGG) (Jacoby 1978 pers. comm.)	2.64	average Bancroft suprcrustal rock (ABSR) (Jacoby 1978 pers. comm.)	2.79	5.38
		2.64	average of late Precambrian accumulation (ALPA) (Schwerdtner and Lumbers 1980)	2.82	6.38
Deer Lake Structure	buff syenite, biotite gneiss, gneissic granite (in ratio 3:2:5)	2.70	ABSR	2.79	3.15
			ALPA	2.82	4.18
Drag Lake Complex	average grey tonalitic gneiss	2.72	ABSR	2.79	2.51
			ALPA	2.82	3.55
			ALPA, buff syenite, pink syenites and granite (in ratio 2:1:1)	2.75	1.1
Allen Lake Synform	pyroxenite, gabbro (in ratio 2:1)	3.12	ALPA	2.82	10.64

Known Gneiss Dome	Source	Core Density	Mantle Density	Contrast	Scale Models	Core/Mantle Density Contrast (% of Mantle)
Middle Haddam, Conn.	Fletcher 1972	2.65	2.75	3.64	Schwerdtner et.al.1977	25.67 - 11.49
Chester and Holly, Vt.	Fletcher 1972	2.69	2.78	3.24	Dixon 1975	7.1
Rum Jungle, Australia	Stephansson and Johnson 1976	2.67	2.77	3.60	Ramberg 1973	3.6

TABLE 23. SUMMARY OF QUARTZ MICROSTRUCTURAL FEATURES IN GRANITE GNEISSES WITH QUARTZ RIBBONS

	Microstructure of weakly to moderately deformed granite, Albion Lake Type (ALT)	Microstructure of strongly deformed granites, most common type (MCT)
Location	Upper Faraday Granite, parts of Cardiff Complex	in all gneissic granitic bodies
Strain judged from ribbon aspect ratio	very low to moderate	high to very high
Deformation lamellae	occasional	absent
Intragranular distortion	misorientations 5-35° deformation bands	low, < 5°
Morphology of quartz-quartz grain boundaries	irregular, interlobate to regular and smooth	regular and smooth
Orientation of quartz-quartz grain boundaries	unrelated to shape - fabric	generally near perpendicular to ribbon length
Relation of quartz boundaries to Feldspar Matrix	may not impinge on Feldspathic Matrix	always impinges on Feldspathic Matrix
Quartz grain-size range	from very small new grains to very large old grains	extremes of grain size absent

TABLE 24. LINEAL ANALYSIS OF QUARTZ-QUARTZ GRAIN BOUNDARIES IN QUARTZ RIBBONS FROM GRANITE GNEISSES IN LOWER AND UPPER FARADAY GRANITES (LFG, UFG). SAMPLES IN LFG ARE ARRANGED FROM NORTH (1296B) TO SOUTH (893C) WITH DISTANCE IN KM FROM 1296B INDICATED IN LOCATION COLUMN. STRAIN IS JUDGED TO DECREASE IN A SOUTHERLY DIRECTION IN LFG. CALCULATIONS ASSUME THAT A REGULAR GEOMETRIC ARRANGEMENT OF THE SURFACES DOES EXIST. NEGATIVE QUANTITIES INDICATE A LARGE DEPARTURE FROM THIS CONSTRAINT.

SAMPLE NUMBER	LOCATION	MICROSTRUCTURE TYPE	PERCENTAGE OF TOTAL GRAIN BOUNDARY AREA WHICH IS PARALLEL TO THE YZ FABRIC PLANE
1296B	LFG 0	MCT	64.7 %
497B	LFG 1.75	MCT	16.8 %
22103B	LFG 2	MCT	16.9 %
895C	LFG 2.75	MCT	9.1 %
1395C	UFG	ALT	-13.9 %
1491C	UFG	ALT	1.01 %

TABLE 25. ROCK TYPE AND FIELD SETTING OF LS2 TECTONITES

SAMPLE #	ROCK TYPE	NATURE OF MODIFIED LS_1 FABRIC	APPROXIMATE WIDTH OF LS_2 ZONE	NATURE OF FABRIC OUTSIDE LS_2 ZONE	DOES LS_1 ASYMMETRY INDICATE SOUTH-EAST SHEAR?
26102B	concordant quartz vein	Feldspar shape fabric in large quartz; random rutile	10-20 cm	unmodified granite gneiss with LS_1 quartz ribbon	yes
30103B	granite gneiss	LS_1 quartz ribbon	10m - 50m	"	yes
24101B	concordant quartz vein	probably coarse quartz with random rutile	3-4 cm	"	yes
695C	quartzite	exaggerated grain growth quartz micro-structure	3m - 10m	most strongly devel-oped LS_1 in all rock types	yes
20102B	alkali-granite	LS_1 quartz ribbon	5m - 30m	unmodified granite gneiss, varying strength	yes
THQ	quartzite	exaggerated grain growth	10m - 100m	exaggerated grain growth quartzite present down strike	yes
Q	syntectonic quartz vein in THQ	coarse quartz	"	"	yes
194C	granite gneiss in migmatite	LS_1 quartz ribbon	10m - 100m	most strongly devel-oped LS_1 in all rock types	yes
192C*	tonalitic gneiss	"	"	"	yes
1131C	schist in 192C	"	"	"	yes
193C	syntectonic quartz vein in 1151C	"	"	"	yes

* Location adjacent to 194C.

TABLE 26. HAND SPECIMEN CHARACTERISTICS OF LS_2 TECTONITES

SAMPLE #	ROCK TYPE	SIGMOID VISIBLE?	FROSTED QUARTZ?	GRAIN SIZE REDUCTION COMPARED TO LS_1?	DELICATE LAMINATION AND AUGEN?
26102B	quartz vein	no	no	no	no
30103B	granite gneiss	no	no	yes	yes
24101B	quartz vein	yes	yes	yes	no
695C	quartzite	yes	yes	no	no
20102B	granitic gneiss	no	yes	no	no
THQ	quartzite	no	yes	yes	yes
194C	granitic gneiss	no	no	yes	yes
192C[1]	tonalitic gneiss	no	no	yes	yes
1131C[1]	biotite schist	yes	n/a	n/a	yes
193C[1]	quartz vein	no	no	no	no
Q[2]	quartz vein	no	no	no	no

[1]Located adjacent to 194C.

[2]Located adjacent to THQ.

TABLE 27. ANGLES BETWEEN LS_2 C-AXIS GIRDLES AND FOLIATIONS IN XZ PLANE

SAMPLE #	ANGLE BETWEEN GIRDLE AND LS_1	ANGLE BETWEEN GIRDLE AND AVERAGE LS_2	ANGLE BETWEEN LS_1 AND LS_2
26102B	35°	8°	43°
30103B	90°	65°	25°
24101B	80°	60°	20°
695C	90°	50°	40°
20102B	90°	65°	25°
THQ	78°	58°	20°
194C	90°	60°	30°

TABLE 28. QUARTZ MICROSTRUCTURE IN LS_2 TECTONITES

SAMPLE #	APPROXIMATE % UNRECRYSTALLIZED	NATURE OF UN-RECRYSTALLIZED QUARTZ	SUBSTRUCTURE OF OLD QUARTZ	SMALLEST NEW GRAIN SIZE	APPROX L/W IN XZ	MAXIMUM LS_2 LS_1	RANGE LS_2	SUBSTRUCTURE OF NEW QUARTZ	GRAIN BOUNDARY SHAPE	LOCATION OF RECRYSTALLIZATION
261028	50	mosaic of millimetric equant grains. S_2 wraps around.	blocky sub grains,(SG), basal and prism walls. Misorientation 5^o	50 μ m equant	5 : 1	55^o	20^o	elongate sub-grains (DB) - 5^o misorientations, prismatic walls	lobate	bulges on grain boundaries, on deformation band boundaries (DBB)
301038	35	1. wholly and partially preserved LS_1 ribbons; 2. tabular and globular augen surrounded by LS_2	in 1. curving deformatory bands (DB) with high distortions, deformation lamellae; often are kinks with {0001} slip; 2. 30^o distortion along length	40-200 μ m wide ribbon	>20 : 1	45^o	45^o	mild undulatory extinction and equant polygonal subgrains with low misorientations	saw-tooth	parallel to DBB at edge of old quartz or between DB; at end of DB
241018	5	restricted to margins of vein	undulatory extinction and DB ‖ to LS_2	50 μ m	5-20 : 1	30^o	35^o	equant polygonal subgrains (SG)	lobate, same shape as SG	DBB
695B	40 (?)	thicker and more blocky areas of quartz probably old.	undulatory extinction; elongate DB and blocky SG. Max 15^o misorientation	50 μ m	>3 : 1	50^o	35^o	same as for old	lobate	probably bulging and SG rotation on DBB and grain boundaries
201028	30	partly preserved LS_1 ribbons	elongate DB, blocky and polygonal SG. Up to 15^o misorientations.	50 μ m	3 : 1	50^o	25^o	equant polygonal subgrains, low misorientation	lobate, same shape as SG. May coarsen to polygons	
TTQ	0	NA	NA	50 μ m	3 : 1	44^o	30^o	equant polygonal subgrains, low misorientation	lobate, same shape as SG	NA
194C	45	partly and completely unrecrystallized LS_1 ribbons; rare tabular augen.	elongate SG (DB) misorientations locally > 10^o	50 μ m	4 : 1			50 - 100 m equant polygonal subgrains.	lobate, same shape as SG. Coarsens to polygons.	recrystallization front ‖ to LS with boundary bulges ‖ to LS

TABLE 29 NATURE OF DEFORMATION OF MINERALS OTHER THAN QUARTZ IN LS_2 TECTONITES

SAMPLE #	ROCK TYPE	BIOTITE	PLAGIOCLASE	K-FELDSPAR	OTHER
26102B	quartz vein	n/a	feldspar aggregates slightly rotated but unaltered		rutile extension fabric parallel to LS_2
30103B	granite gneiss	offset 0.5-1 mm in narrow smear and deformed into sigmoid.	kinked with (010) slip; undulatory extinction; discontinuous albite rims.	10% twinned, lunate perthitic intergrowths.	thin zones of equant very fine mylonitic material in feldspars.
24101B	quartz vein	n/a	n/a	n/a	rutile extension fabric subparallel to LS_1
695C	quartzite	n/a	rotated but unaltered	rotated but unaltered	clinopyroxene rotated but unaltered - 18% of elongate minerals lie perpendicular to L_1 in S_1. Rutile extension fabric parallel to LS_2
20102B	alkali-granite	n/a	unaltered	same as 30103B	rutile extension fabric subparallel to LS_1
THQ	quartzite	very fine, mechanically comminuted, entrained by rotating porphyroclasts.	undulatory extinction, complex intergrowths; fish and lozenge shape; many rotated.	undulatory extinction; grain boundary mosaics (50 μm diameter); rare twinning; fish and lozenge shapes; many rotated.	clinopyroxene, sphene: fish and lozenge shapes, boudinage and rotation. Thin zones of equant mylonitic material.
194C	granite gneiss	n/a	same as 30103B	same as 30103B	thin zones of equant mylonitic material
1131C	biotite schist	decussate texture of biotite and muscovite; uniform distribution of basal planes in YZ section; micas unstrained.	same as 30103B	same as 30103B	

Table 30. Geochemistry of Metagabbro from Shear-Zone at South Farquhar Lake.

	1	2	3
SiO_2	48.61	48.36	49.65
Al_2O_3	20.14	19.12	19.91
Fe_2O_3T	6.88	6.99	6.38
MgO	7.70	7.80	7.09
CaO	13.21	13.31	12.96
Na_2O	2.65	2.72	3.15
K_2O	0.23	0.40	0.33
TiO_2	0.25	0.29	0.26
P_2O_5	0.00	0.00	0.02
MnO	0.11	0.11	0.10
S	0.04	0.04	0.02
Total	99.918	99.258	99.974
Ba	82	112	114
Cr	223	277	236
Zn	15	20	22
Sr	309	319	365
Rb	0	4	3
Zn	33	53	52
Ni	60	62	44

1. Mesoscopically undeformed wall rock; Metagabbro, Subophitic Texture discernable (WR).
2. Moderately deformed Gneissic Metagabbro from zone-edge of Shear-Zone (SZM). 2 Metres from 1.
3. Most deformed Gneissic Metagabbro from centre of Shear-Zone (SZ). 10 centimetres from 2.

(See Appendix IV for analytical details)

APPENDIX II

Granitic Mylonites

A series of topographic lineaments cut the granites (Hewitt 1957b), which are poorly expressed or absent within the country rock. In most places there is no outcrop of fault rocks along them. An exception is the string of small scattered mylonite outcrops in the Cheddar batholith lying along the north shore of Hook Lake and 2 km to the northwest. The mylonitic foliation dips northwest with a down-dip lineation (Fig. 1.2a) striking roughly parallel to the lineament across which the distinctive purple aegirine-alkali granite (Unit 6B), outcropping in the environs of Hook Lake shows an apparent dextral offset of over one kilometre.

The mylonites vary within one outcrop from a delicately streaked very fine foliated rock to a black isotropic rock containing occasional pink augen of rock fragments. There are both cross cutting and concordant foliated ilmenite-apatite-biotite veins.

In the delicately streaked variety, feldspathic augen (grain-size greater than 1 mm) account for more than one third (34.6%) of the rock volume. A further quarter of the rock is composed of ribbons of finely recrystallized quartz and ribbons and augen of opaques. The remainder comprises a fine equant matrix, with grain-size in the 10 to 300 μm

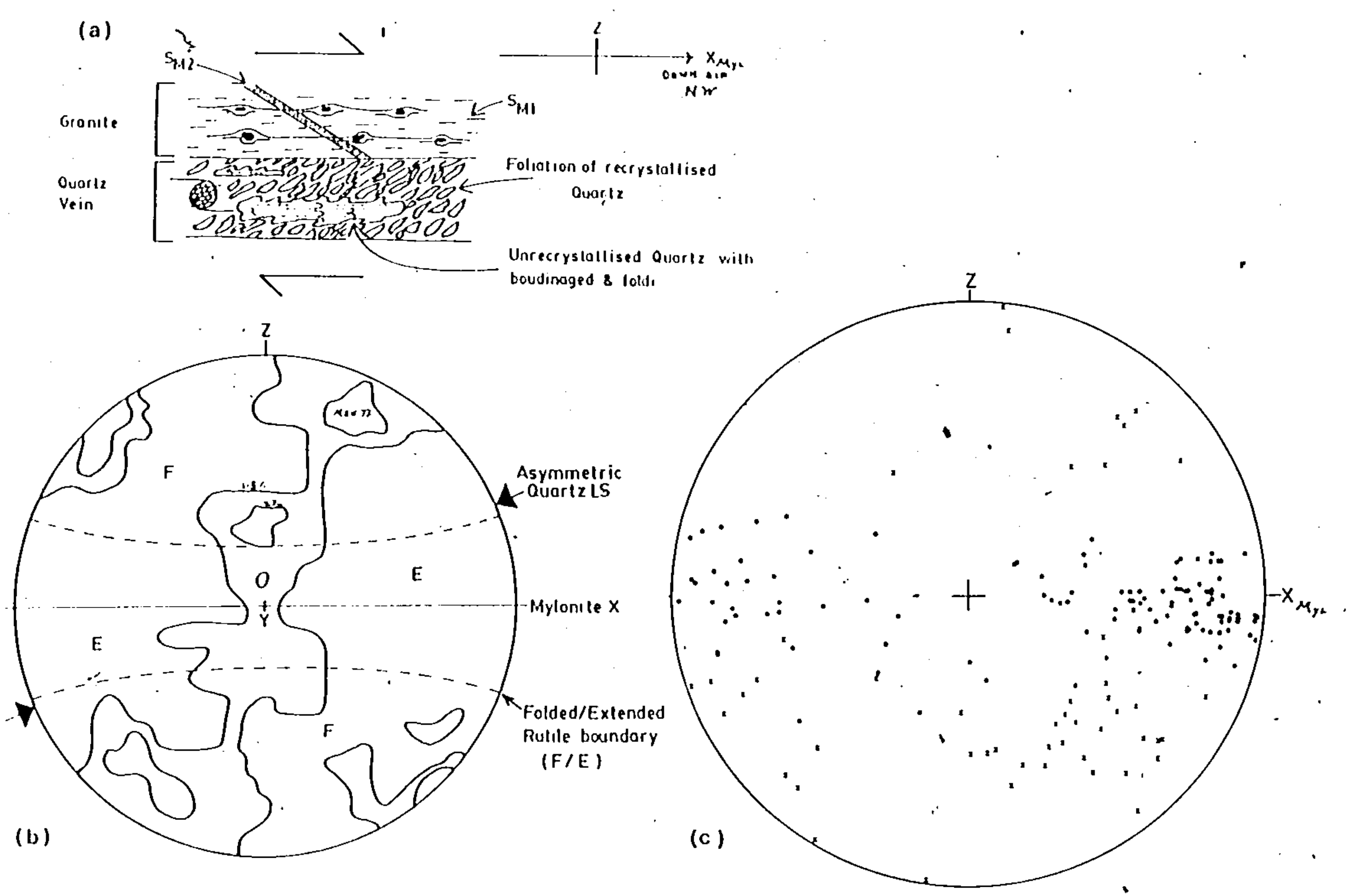
(a)
S_{M2}
S_{M1}
Z
X_{Myl}
NW
Granite
Quartz Vein
Foliation of recrystallised Quartz
Unrecrystallised Quartz with boudinaged & folds
(b)
Z
F
E
O
Y
Asymmetric Quartz LS
Mylonite X
Folded/Extended Rutile boundary (F/E)
(c)
Z
X_{Myl}

FIGURE
A.1

Fabric of mylonite from Cheddar Batholith, near Hook Lake. (a) Diagram of microstructure; (b) quartz c-axis microfabric from recrystallized grains of quartz vein (trace of asymmetric foliation of these grains indicated); (c) orientation of deformed rutile needles in unrecrystallized quartz of vein; circles, boudinaged needles; crosses, enveloping line of folded needles. In (b) the fields of extended and folded needles indicated : E, F.

the augen. The feldspar augen are traversed by planar matrix filled zones. Both microcline and albite augen have a barely visible mantle structure of very fine subgrains. The feldspars are complex perthites and antiperthites.

In the black isotropic mylonites most of the rock (88.3%) is composed of an ultrafine matrix in which an equant interlocking texture is discernible. Only feldspar augen remain. These retain the core and mantle structure, but are largely free from perthitic intergrowths.

The microstructure in quartz veins within mylonite is comparable to that of many of the LS2 tectonites (Section 4.3.4). It is the product of dynamic recrystallization and displays a microscopically visible asymmetric quartz foliation which uniquely indicates the sense of the shear, upper layers down dip, parallel to the lineation (a normal fault).

The deformed quartz veins are 2 to 6 mm wide and lie parallel to the mylonitic foliation (Fig. A.1a). Microscopically they show elongate ribbons of quartz set in a very fine recrystallized matrix (Fig. A.1a), which lie parallel to the elongation direction of rutile needles and to the mylonitic foliation. The ribbons are in places asymmetrically disposed around rigid magnetite-ilmenite inclusions suggesting a sense of shear (Fig. A.1a). Within the fine recrystallized matrix an asymmetric quartz shape foliation, visible at medium power, is inclined to the quartz ribbons (Fig. A.1a).

The quartz ribbons have aspect ratios in excess of 10 to 1 and a uniformly developed substructure of polygonal to slightly elongate subgrains (20 μm diameter). The margin of the ribbons is irregular in detail following the outline of subgrains and new grains both of which are often elongate forming the second quartz asymmetric foliation. The ribbons are crowded with deformed rutile needles. They are also present in the recrystallized matrix close to the ribbon boundary but are absent from most of the recrystallized quartz. Rutile needles are boudinaged and folded (Fig. A.1c).

New grains vary in shape from equant to elongate with a maximum elongation of approximately 3:1. The equant grains are very similar in size and shape to the subgrains (20 μm diameter). The elongate grains vary from 50 to 100 μm in length and 20 to 50 μm in width. Their long axes lie between 25 and 35° to the quartz ribbons. This new quartz foliation shows a constant orientation across the field of view. Rutile needles may rarely be observed to cross the boundary of the quartz ribbons into the recrystallized matrix. Separation of the boudinaged fragments increases noticeably across this boundary with extensions recorded in one needle varying from 47 to 140 percent, dramatically illustrating the dynamic softening caused by the recrystallization.

The crystallographic preferred orientation of the quartz is strong (Fig. A.1b). The cross-girdle has unequally developed arms and is asymmetric with respect to all the foliations, indicating the shear sense.

The microstructure is similar to that in some of the LS2 tectonites in which recrystallization is well advanced (Section 4.3.4). The similarities are the presence of two non-parallel foliations, their angular relation indicating the sense of shear, the non-parallel relation of the rutile and the shape-fabric of recrystallized quartz, the non-curving distribution of this shape-fabric, the microstructure of dynamic recrystallization and the asymmetric quartz microfabric. Like the mature LS2 microstructures, these relations may be interpreted as being part of a microstructure approaching the steady-state. The subgrain size is finer than that in the LS2 tectonites probably reflecting higher stresses. Once again the unique value of microscopically examining the XZ plane of the mesoscopic fabric is illustrated.

APPENDIX III

Measurement of Shape Fabrics in Feldspathic Orthogneiss

Twenty-eight specimens were collected (for location see Fig. 3.7). Specimens were cut parallel to the principal planes of the mesoscopic shape fabric. Measurements were made on stained slabs of these planes.

Two methods of estimation of shape fabrics were employed: (1) direct measurement of axial ratios of quartz ribbons (18 samples); 25 to 35 axial ratios per principal plane were determined. (2) The number of intercepts per unit length of equally spaced test lines laid down parallel to the principal directions were counted; from this the ratio of intercepts per unit length in the two principal directions contained in the particular plane was calculated; the inverse of this ratio was used in calculation of the Lodes Number.

Method (1) is time consuming, method (2) is relatively rapid and is an adaptation of metallographic techniques described by Underwood (1970). Two samples were measured using both methods and the resulting Lodes Numbers agree within acceptable limits.

The Lodes Number was used rather than the shape fabric parameter K since it is a simple linear expression of the relative strengths of foliation and lineation (Schwerdtner

1977). With the Lodes Number, V, purely prolate fabrics have a value of -1, purely oblate fabrics +1 and plane-strain fabrics are 0.

The Lodes Numbes determined by the two methods are as follows:

Sample Number	(1) Direct Method	(2) Intercept Method
261B	-0.45	-0.14
25101B	-0.13	
265B	-0.41	
26104B	+0.02	
266B	-0.08	
263B	-0.21	
1112B	-0.42	
25106B	-0.03	
30101B	-0.34	
26103B	-0.43	
25104B	+0.05	+0.09
30105B	+0.04	
CB2482	-0.50	
24101B	-0.22	
22103B	-0.21	
1691B	+0.57	
1293B	-0.08	
1296B	+0.12	
2510B		+0.08
30103B		+0.04
20111B		-0.55
1076D		+0.15
22104B		+0.04
1075D		+0.25
1174D		+0.17
2113D		-0.55
CB1091B		-0.74
2111D		-0.41

Appendix IV

Accuracy and precision of whole rock analyses.

Accuracy and precision of whole rock analyses performed by X ray fluorescence spectrometry by R.Hartree at the University of Ottawa quoted in:

Table	Analyses
7	4
9	3
16	1-9
11	all
30	all

may be appraised from the following results of ten replicate analyses performed at the laboratory on an international rock standard:

		Mean	S.D.	Recommended value
Wt.%	SiO_2	60.18	.168	60.09
	Al_2O_3	12.23	.103	12.15
	Fe_2O_3T	6.25	.036	6.29
	MgO	2.69	.047	2.61
	CaO	7.96	.059	8.00
	Na_2O	4.37	.067	4.35
	K_2O	4.52	.040	4.51
	TiO_2	.14	.005	.15
	P_2O_5	.43	.015	.42
	MnO	.33	.000	.32
ppm				
	Ba	467	5.17	460
	Sr	256	7.15	270
	Rb	222	3.92	220
	Zr	269	3.67	270
	Cr	9.8	8.1	10
	Ni	7.1	3.2	10

For analyses quoted in:

Table	Analyses
7	1-3
9	1-2
10	all
15	1,4,5

a synopsis of results was received from Dr.C.Riddle, Chief Analyst of the Ontario Geological Survey,77 Grenville St.,Toronto.The analyses were performed by using X ray fluorescence spectrometry by X Ray Assay Laboratories Ltd.,1885 Leslie St.,Don Mills,Ontario (under PO No.T30407G project No.80-1705).The synopsis reads:

> ...the quality of the data from XRAL is generally acceptable and within the standards expected.There are certain discrepancies which give cause for concern however...
>
> 1)Major elements:Precision is good;accuracy is generally acceptable.SiO_2 appears to be generally low by ca.2%;occasional CaO,MgO,FeO and LOI data are questionable
>
> 2)Minor elements:

Component	Precision	Accuracy
Ba	fair	bad
Sr	good	good
Rb	bad	fair
Zr	fair	fair....

An assessment copy of the XRAL report is on file at the Geoscience Laboratories of the O.G.S.

REFERENCES

Adams, F.W. and Barlow, A.F., 1910, Geology of the Haliburton and Bancroft area, Province of Ontario, accompanied by G.S.C. Map No. 708 (Haliburton Sheet): Geol. Surv. Can., Mem. 6.

Appleyard, E.C., 1974, Synorogenic igneous alkaline rocks of E. Ontario and N. Norway: Lithos 7, p. 147-169.

Armstrong, H.S. and Gittins, J., 1968, Geology of Glamorgan and Monmouth Townships, Haliburton County: Ont. Dep. Mines, Open File Rep. 5021, 210 p. Accompanied by Maps P.59 (revised) and P.60 (revised), scale 1 inch to 1/2 mile.

Armstrong, H.S. and Gittins, J., 1970, Monmouth Township, Haliburton County: Ont. Dep. Mines, Coloured Geological Map 2174, Geol. Ser., Scale 1:31,686 or 1 inch to 1/2 mile.

Ave'Lallemant, H.G. and Carter, N.L., 1970, Syntectonic recrystallization of olivine and modes of flow in the upper mantle: Geol. Soc. Am., Bull. 81, p. 2203-2220.

Bak, J., Korstgard, J. and Sorensen K., 1975, A major shear zone within the Nagsuqtoqidian of West Greenland: Tectonophysics, 27, p. 191-209.

Beach, A., 1980, Retrogressive metamorphic processes in shear zones with special reference to the Lewisian complex: J. Struct. Geol., v. 2, No. 1/2, p. 257-263.

Behr, H.J., 1961, Beitraege zur petrographischen und tektonischen Analyse des Sachsischen Granulitgebirges: Freiberg. Forschungsh, C. 119, p. 5-118.

Behr, H.J., 1965, Zur Methodik tektonischer Forschung im kristallinen Grundgebirge Ber. Geol. Ges. D.D.R. 10, H.2, p. 163-179.

Behr, H.J. 1978, Subfluenz-Prozesse im Grundgebirgs-Stockwerk Mitteleuropas: Z. dt. geol. Ges. 129, p. 283-318.

Behr, H.J., 1980, Polyphase shear zones in the granulite belts along the margins of the Bohemian Massif: J. Struct. Geol., v. 2, No. 1/2, p. 249-254.

Bell, K. and Blenkinsop, J., 1980, Whole rock Rb-Sr studies in the Grenville Province of southeastern Ontario and western Quebec; a summary report: in Curr. Res., Pt. C, Geol. Surv. Can., Pap. 80-1C, p. 152-154.

Bell, T.H. and Etheridge, M.A., 1976, The deformation and recrystallization of quartz in a mylonite zone, central Australia: Tectonophysics, 32, No. 3-4, p. 235-267.

Berthé, D., Choukroune, P. and Jegouzo, P., 1979, Orthogneiss, mylonite and non-coaxial deformation of granites: The example of the South Armorican shear zone: J. Struct. Geol., v. 1, No. 1, p. 31-42.

Best, M.G., 1966, Structural geology of Precambrian rocks south of Bancroft, Ontario: Can. J. Earth Sci., v. 3, p. 441-455.

Bickle, M.J., Bettemay, L.F., Boulter, C.A., Groves, D.I. and Morant, P., 1980, Horizontal tectonic interaction of an Archean gneiss belt and greenstones, Pilbara block, Western Australia: Geology 8, p. 525-529.

Borg, I.Y. and Heard, H.C., 1969, Mechanical twinning and slip in experimentally deformed plagioclase: Contrib. Mineral. Petrol., 23, p. 128-135.

Borges, F.S. and White, S.H., 1980, Microstructural and chemical studies of sheared anorthosites, Roneval, South Harris: J. of Struct. Geol., v. 2, No. 1/2, p. 273-280.

Bossière, G. and Vauchez, A., 1978, Deformation naturelle par cisaillement ductile d'un granite de Grande Kabylie Occidentale (Algérie): Tectonophysics, 51, p. 53-81.

Bouchez, J-L., 1977, Plastic deformation of quartzites at low T in area of natural strain gradient: Tectonophysics, 39, p. 25-49.

Bouchez, J-L., 1978, Preferred orientations of quartz a axes in some tectonites: Kinematic inferences: Tectonophysics, 49, T25-30.

Bouchez, J-L and Pêcher, A., 1981, The Himalayan main central thrust pile and its quartz-rich tectonites in central Nepal: Tectonophysics, 78, p. 23-50.

Boullier, A-M and Bouchez, J-L., 1978, Le quartz en rubans dans les mylonites: Bull. Soc. Géol. France, 1978 (7), XX, No. 3, p. 253-262.

Boullier, A-M and Gueguen, Y., 1975, S.P. mylonites; origin of some mylonites by superplastic flow: Contrib Mineral. Petrol., v. 50, No. 2, p. 93-104.

Breaks, F.W. and Shaw, D.M., 1973, The Silent Lake pluton, Ontario: A nodular sedimentary, intrusive complex: Lithos, v. 6, No. 2, p. 103-121.

Bright, E.G., 1977, Regional structure and stratigraphy of the Eels Lake area, Haliburton and Peterborough Counties: in Summary of Field Work, 1977, Ont. Geol. Surv., Geol. Br., p. 110-117, V.G. Milne, O.L. White, R.B. Barlow, eds., Misc. Pap. 75, 208 p.

Bright, E.G., 1979, The Centre Lake area, Haliburton and Hastings Counties: in Summary of Field Work, 1979, Ont. Geol. Surv., Geol. Br., p. 86-88, V.G. Milne, O.L. White, R.B. Barlow, C.R. Kustra, eds., Misc. Pap. 90, 245 p.

Bright, E.G., 1980 Eels Lake area, southern Ontario: Ont. Geol. Surv., Prelim. Map, P. 2205, Geol. Ser., scale 1:63,360 or 1 inch to 1 mile.

Brodie, K.H., 1981, Variation in amphibole and plagioclase composition with deformation, Tectonophysics, 78, p. 385-402.

Brown, R.L., Chappell, J.F. and Moore, J.M. Jr., 1975, An ensimatic island arc and ocean closure in the Grenville Province of southeastern Ontario, Canada: Geosci. Can., 2, p. 141-144.

Brown, W.L., Macaudière, J., Ohnenstetter, D. and M., 1980, Ductile shear zones in a meta-anorthosite from Harris, Scotland: Textural and compositional changes in plagioclase: J. Struct. Geol., v. 2, No. 1/2, p. 281-287.

Brunel, M., 1980, quartz fabrics in shear-zone mylonites: Evidence for a major imprint due to late strain increments: Tectonophysics, 64, T733-744.

Bryant, B. and Reed, J.C. Jr., 1969, Significance of lineation and minor folds in major thrust faults in southern Appalachians and the British and Norwegian Caledonides: Geol. Mag. 106, p. 412-419.

Buddington, A.J., 1959, Granite emplacement with particular reference to North America: Geol. Soc. Am. Bull., v. 70, p. 671-747.

Burg, J.P. and Laurent, P., 1978, Strain analysis of a shear zone in a granodiorite: Tectonophysics, 47, p. 15-42.

Byerley, G.R. and Vogel, T.A., 1973, Grain boundary processes and development of metamorphic plagioclase; Lithos 6, p. 183-202.

Cahn, R.W., 1965, Recovery and recrystallisation: in "Physical Metallurgy", R.W. Cahn (ed.), North Holland, p. 925-987.

Carmichael, D.M., 1968, Structure and progressive metamorphism in the Whetstone Lake area, Ontario, with emphasis on the mechanism of prograde reactions: Unpubl. Ph.D. thesis, Univ. of California, Berkeley, 122 p.

Carmichael, I.S.E., Turner, F.J. and Verhoogen, J., 1974, Igneous Petrology: McGraw-Hill, 739 p.

Carreras, J., Estrada, A. and White, S., 1977, The effects of folding on the c-axes fabrics of a quartz mylonite: Tectonophysics, 39, p. 3-23.

Chapman, T.J., Milton, N.J. and Williams, G.D., 1979, Shape fabric variation in deformed conglomerates at the base of the Laksefjord Nappe, Norway: Geol. Soc. Lond., J., v. 136, p. 683-691.

Chesworth, W., 1967, The origin of certain granitic rocks occurring in Glamorgan Township, southeastern Ontario; Unpubl. Ph.D. thesis, McMaster Univ.

Chesworth, W., 1971, Metamorphic conditions in a part of the Haliburton Highlands of Ontario: Lithos 4, p. 219-229.

Chesworth, W., 1972, Metamorphic facies series in the Grenville Province of Ontario: Tectonophysics, 14, p. 71-78.

Chesworth, W., Shaw, D. and Dostal, J., 1975, Granitoid rocks of the Madoc-Bancroft-Haliburton area of the Grenville Province; in GAC, MAC, GSA (North Central Section), Field Excursion Guidebook, P.G. Telford, ed., p. 1-25.

Christie, J.M., 1963, The Moine thrust zone in the Assynt Region N.W. Scotland: Univ. Calif. Publ. in Geol. Sci., v. 40, p. 345-440.

Christie, J.M., Griggs, D.T. and Carter, N.L., 1964, Experimental evidence of basal slip in quartz: J. Geol., 72, p. 734-756.

Cooper, M.A. and Bradshaw, R., 1980, The significance of basement gneiss domes in the tectonic evolution of the Salta region, Norway: J. Geol. Soc. London, v. 137, p. 231-240.

Coward, M.P., 1981, Diapirism and gravity tectonics: Report of a Tectonic Studies Group Conference held at Leeds University, March 25-26, 1980: J. Struct. Geol., v. 3, No. 1, p. 89-95.

Crampton, C.B., 1963, Quartz fabric reorientation in the Region of Benmore Assynt, North-West Highlands of Scotland: Geol. Mag., v. 100, No. 4, p. 361-370.

Culshaw, N.G., 1981, Precambrian geology of Drag Lake Area, Haliburton County, S. Ontario: Ont. Geol. Surv., Prelim. Map, P.2404, Geol. Ser., scale 1:15 840.

Dallmeyer, R.D., 1972, Compositional controls on cordierite-bearing assemblages in high-grade regional metamorphism: 24th Int. Geol. Cong., Sect. 2, p. 52-63.

Davidson, A., Britton, J.M., Bell, K. and Blenkinsop, J., 1979, Regional synthesis of the Grenville Province of Ontario and western Quebec: in Current Research, Part B, Geological Survey of Canada, Paper 79-1B, p. 153-172.

Davidson, A., Culshaw, N.G. and Nadeau, L., 1982, A tectono-metamorphic framework for part of the Grenville Province, Parry Sound region, Ontario: in Curr. Res., Pt. A, Geol. Surv. Can., Paper 82-1A, p. 175-190.

Deer, W.A., Howie, R.A. and Zussman, J., 1971, An introduction to the rock forming minerals: Longman, 528 p.

Divi, S.R.R., 1972, Structural analysis of Grenville rocks, near Bancroft, Ontario, Canada: Unpubl. Ph.D. thesis, University of Ottawa, Ottawa, Ontario.

Divi, S.R.R. and Fyson, W.K., 1973, Folds and strain in Grenville metamorphic rocks, Bancroft, Ontario, Canada: Geol. Soc. Am. Bull., v. 84, p. 1607-1618.

Dixon, J.M., 1975, Finite strain and progressive deformation in models of diapiric structures: Tectonophysics, 28, p. 89-124.

Dostal, J., 1975, the origin of the garnet-cordierite-sillimanite bearing rocks from Chandos Township, Ontario: Contrib. Mineral. Petrol., 49, p. 163-175.

Dunlop, D.J., York, D., Berger, G.S., Buchan, K.L. and Stirling, J.M., 1980, The Grenville Province: a paleomagnetic case study of Precambrian continental drift: in The Continental Crust and its Mineral Deposits, D.W. Strangway (ed.), Geol. Assoc. Can., Spec. Pap. 20, p. 488-502.

Eisbacher, G.H., 1970, Deformation mechanics of mylonitic rocks and fractured granites in Cobequid Mountains, N.S. Canada: Geol. Soc. Am., Bull. 81, p. 2009-2020.

Escher, A. and Watterson, J., 1974, Stretching fabrics, folds and crustal shortening: Tectonophysics, 22, p. 223-231.

Etchecopar, A., 1977, A plane kinematic model of progressive deformation in a polycrystalline aggregate: Tectonophysics, 39, p. 121-138.

Etheridge, M.A. and Hobbs, B.E., 1974, Chemicals and deformational controls by recrystallization of mica: Contrib. Mineral. Petrol., 43, p. 111-124.

Evans, N.N. and Bancroft, J.A., 1908, On the occurrence of gedrite in Canada: Am. J. Sci., Ser. 4, 25, p. 509-512.

Fletcher, R.C., 1972, Application of a mathematical model to the emplacement of mantled gneiss domes: Am. J. Sci., v. 272, p. 197-216

Fleuty, M.J., 1964, The description of folds: Geol. Assoc. Proc, v. 75, p. 461-492.

Flinn, D., 1962, On folding during three-dimensional progressive deformation: Geol. Soc. Lond., J. v. 118, p. 385-433.

Flinn, D., 1965, Deformation in metamorphism: in Controls of Metamorphism, Pitcher, W.S. and Flinn, G.W. (eds): Oliver and Boyd, Lond., p. 46-69.

Fowler, A.D. and Doig, R., 1979, Origin of uraniferous granitoids, Grenville Province, Quebec and Ontario: GAC/MAC Ann. Mtg., (Abstract), p. 50.

Francoeur, D., 1975, Petrographic and structural evolution of granites and gneisses of the Grenville Province, Glamorgan and Monmouth Townships, Ontario: Unpubl. M.Sc. thesis, Univ. of Ottawa.

Frodesen, S., 1968, Coronas around olivine in a small gabbro intrusion, South Norway: Nor. Geol. Tidsskr., 48, p. 201-206.

Fyson, W.K., 1970, Structural relations in metamorphic rocks, Shuswap Lake Area, British Columbia; in Wheeler, J.O., (ed.), Structure of the Southern Canadian Cordillera: Geol. Assoc. Can., Spec. Pap. 6, p. 107-122.

Ghosh, S.K. and Ramberg, H., 1976, Reorientation of inclusions by combination of pure shear and simple shear: Tectonophysics, 34, p. 1-70.

Ghosh, S.K., Roy, B.R. and Troeng, B., 1979, Superposed folding and metamorphism in the Seve Nappe around Areskutan in the Swedish Caledonides: Geol. Forens. Stockh., Forhandl. v. 101, Pt. 2, p. 85-103.

Gittins, J. and Miller, R., 1978, Alkalic rocks of the Haliburton-Bancroft region: in Toronto '78 Field Trips Guide Book, Eds. A.L. Currie and W.O. Mackasey, Jnt. Annl. Meeting, GSA-GAC-MAC, p. 213-219.

Goldsmith, J.R., 1982, Plagioclase stability at elevated temperatures and water pressures: Am. Mineral., v. 67, p. 653-675.

Green, H.V., Griggs, D.T. and Christie, J.M., 1970, Syntectonic and annealing recrystallization of fine grained quartz aggregates; in Experimental and Natural Rock Deformation, Paulitsch, J. (ed.): Springer Verlag, p. 272-335.

Grieve, R.A.F. and Gittins, J., 1975, Composition and formation of coronas in the Hadlington Gabbro, Ontario, Canada: Can. J. Earth Sci., v. 12, p. 289-299.

Griffin, W.L. and Heier, K.S., 1973, Petrologic implications of some corona structures: Lithos 6, 1973 p. 315-335.

Griffiths, P. and Hammond, C., 1972, Superplasticity in large grained materials: Acta Met., v. 20, p. 935-945.

Grocott, J., 1979, Shape, fabric and superimposed simple shear strain in a Precambrian shear belt, W. Greenland: Geol. Soc. Lond., J., v. 136, p. 471-488.

Hanmer, S. and Vigneresse, J.L., 1980, Mise en place de diapirs syntectoniques dans la chaîne Hercynienne: Exemple des massifs leucogranitiques de Locronan et de Pontivy (Bretagne Centrale): Bull. Soc. Géol. France (7), f. XXII, No. 2, p. 193-202.

Hara, I., Takeda, K., Kimura, T., 1973, Preferred lattice orientation of quartz in shear deformation: Hiroshima Univ., J. Sci., v. 7c, p. 1-10.

Hardwick, D., Tegart, W.J.McG., 1961a, Structural changes during deformation of copper, aluminium and nickel at high temperature and high strain rate: J. Inst. Metall., 1961-62, v. 90, p. 17-21.

Hardwick, D. and Tegart, W.J.McG., 1961b, La déformation des métaux et alliages par torsion à haute température: Memoires Scientifiques, Rev. Metall., LVIII, No. 11, p. 870-878.

Hardwick, D., Sellars, C.M. and Tegart, W.J.McG., 1961, The occurrence of recrystallization during high temperature creep: J. Inst. Metall., 1961-62, v. 90, p. 21-22.

Heaman, L.M., 1982, The timing of igneous and metamorphic events in the Chandos Township area, Grenville Province, Ontario: in Grenville Workshop, Ottawa-Carleton Centre for Geoscience Studies (Abstract).

Heier, K.S. and Adams, J.A.S., 1964, The geochemistry of the alkali metals: Phys. Chem. Earth, 5, p. 253-381.

Hewitt, D., 1957a, Geology of Cardiff and Faraday Townships: Ont. Dept. Mines, v. LXVI, Pt. 3.

Hewitt, D.F., 1957b, Haliburton-Bancroft area, Province of Ontario: Ont. Dept. Mines, Map No. 1957b, scale 1:126 720, or 1 inch to 2 miles.

Hewitt, D.F., 1957c, Cardiff and Faraday Townships, Counties of Haliburton and Hastings: Ont. Dept. Mines, coloured Geol. Map No. 1957-1, scale 1:31 686, or 1 inch to 1/2 mile.

Hewitt, D.F., 1962, Some tectonic features of the Grenville Province of Ontario: in "The tectonics of the Canadian Shield": Roy. Soc. of Can., Spec. Pub. No. 4, J.S. Stevenson (ed.), p. 102-117.

Hewitt, D.F. and James, W., 1956, Geology of Dungannon and Mayo Townships: Ont. Dept. Mines, v. 64, 1955, pt. 8.

Hobbs, B.E., 1968, recrystallisation of single crystals of quartz: Tectonophysics, 6, p. 353-401.

Hobbs, B.E., Means, W.D. and Williams, P.F., 1976, An outline of structural geology: John Wiley and Sons Inc., 571 p.

Hooper, P.R., 1968, The "A" lineation and the trend of the Caledonides of Northern Norway: Nor. Geol. Tidsskr., v. 48, p. 261-268.

Hossack, J.R., 1968, Pebble deformation and thrusting in the Bygdin area (southern Norway): Tectonophysics, 5, p. 315-339.

Humphreys, F.J., 1977, The nucleation of recrystallization at second phase particles in deformed aluminium: Acta Met., v. 25, p. 1323-1344.

Irwin, G.J., 1963, An investigation into the rock magnetism of the Wilberforce pyroxenite: Unpubl. M.Sc. Thesis, Univ. Western Ontario, 52 p.

Johnson, M.R.W., 1957, The structural geology of the Moine thrust Zone in Coulin Forest, Wester Ross: Geol. Soc. Lond., J. v. 113, p. 241-307.

Kehlenbeck, M.M., 1972, Deformation textures in Lac Rouvray anorthosite massif: Can. J. Earth Sci., v. 9, p. 1087-1098.

Kretz, R., 1980, Occurrence, mineral chemistry, and metamorphism of Precambrian carbonate rocks in a portion of the Grenville Province: J. Petrol., v. 21, Pt. 3, p. 573-620.

Krogh, T.E. and Davis, G.L., 1969, Old isotopic ages in the northwestern Grenville Province, Ontario: in Wynne-Edwards, H.R., (ed.), Age Relations in High-grade Metamorphic terrains: Geol. Assoc. Can., Spec. Pap. 5, p 189-193.

Lal, R.K. and Moorhouse, W.W., 1969, Cordierite-gedrite rocks and associated gneisses of Fishtail Lake, Harcourt Township, Ontario: Can. J. Earth Sci., v. 6, p. 145-165.

Lawrence, R.D., 1970, Stress analysis based on albite twinning of plagioclase feldspars: Geol. Soc. Am., Bull. 81, p. 2507-2512.

Leguet, R., Whithwam, D. and Herenguel, J., 1962, Sur la rétention de l'écrouissage après deformation à chaud: Mem. Sci. Rev. Met., 59, p. 649-664.

Lisle, Richard J., 1977, The evaluation of Laxfordian deformation in the Carloway Area, Isle of Lewis, Scotland: Tectonophysics, 42, p. 183-208.

Lister, G.S., 1974, Theory of deformation fabrics: Unpubl. Ph.D. Thesis, Australian National University.

Lister, G.S., 1979, Fabric transitions in plastically deformed quartzites: Competition between basal, prism and rhomb systems: Bull. Minéral., 102, p. 232-241.

Lister, G.S., 1981, The effect of the basal-prism mechanism switch on fabric development during plastic deformation of quartzite: J. Struct. Geol., v. 3, No. 1, p. 67-75.

Lister, G.S., Paterson, M.S. and Hobbs, B.E., 1978, The simulation of fabric development in plastic deformation and its application to quartzite: The Model. Tectonophysics, 45, p. 107-158.

Lister, G.S. and Price, G.B., 1978, Fabric development in a quartz feldspar mylonite: Tectonophysics, 49, p. 37-78.

Lister, G.S. and Paterson, M.S., 1979, The simulation of fabric development during plastic deformation and its application to quartzite: Fabric transitions: J. Struct. Geol., v. 1, No. 2, p. 99-115.

Lister, G.S. and Williams, P.F., 1979, Fabric development in shear zones: Theoretical controls and observed phenomena: J. Struct. Geol., v. 1, No. 4, p. 283-297.

Lister, G.S. and Hobbs, B.E., 1980, The simulation of fabric development and its application to quartzite: The influence of deformation history: J. Struct. Geol., v. 2, No. 3, p. 355-370.

Lumbers, S.B., 1967, Stratigraphy, plutonism, and metamorphism in the Ottawa River remnant in the Bancroft-Madoc area of the Grenville Province of southeastern Ontario, Canada: Unpubl. Ph.D. thesis, Princeton University, 331 p.

Lumbers, S.B., 1975, Geology of the Burwash area, District of Nipissing, Parry Sound and Sudbury: Ont. Div. Mines, Geol. Rept. 116.

Lunardi, L.F. and Baker, D.W., 1975, Determination of movement direction and shear sense in deep-seated thrust zones from mylonites: Am. Geophys. Union, Trans. 56(9), p. 602.

Marshall, D.G. and Wilson, C.J.L., 1976, Recrystallization and peristerite formation in albite: Contrib. Mineral. Petrol. 57, p. 55-69.

MacClaren, A.C. and Hobbs, B.E., 1970, Transmission electron microscope investigation of some naturally deformed quartzites: in "Flow and Fracture of Rocks", Griggs Volume, Am. Geophys. Union, Geophys. Mon. 16, p. 55-66.

Mason, C.S., 1959, Geophysical investigations of inversely magnetized rocks near Wilberforce, Ontario: Unpubl. M.Sc. Thesis, Univ. Western Ontario, London, Ontario, 79 p.

Means, W.D., 1981, The concept of steady-state foliation: Tectonophysics, 78, p. 179-199.

Miller, D.M. and Christie, J.M., 1981, Comparison of quartz microfabric with strain in recrystallised quartzite: J. Struct. Geol., v. 3, No. 2, p. 129-141.

Miller, R.R. and Gittins, J., 1982, Geochronology and petrology of the Grenville nepheline-bearing suites: A metamorphosed rift environment: in Grenville Workshop, Ottawa-Carleton Centre for Geoscience Studies (Abstract), p. 7.

Miyashiro, A., 1973, Metamorphism and metamorphic belts: Allen and Unwin, 492 p.

Mitra, S., 1976, A quantitative study of deformation mechanisms and finite strain in quartzites: Contrib. Mineral. Petrol., 59, p. 203-226.

Mitra, S. and Tullis, J., 1979, A comparison of intracrystalline deformation in naturally and experimentally deformed quartzites: Tectonophysics, 53, T21-27.

Moore, J.M. Jr., 1982, Stratigraphy and tectonics of the Grenvillian Orogeny in eastern Ontario: in Grenville Workshop, Ottawa-Carleton Centre for Geoscience Studies (Abstract), p. 7.

Moore, J.M. Jr. and Thompson, P.H., 1980, The Flinton Group: A late Precambrian metasedimentary succession in the Grenville Province of eastern Ontario: Can. J. Earth Sci., v. 17, p. 1685-1707.

Murthy, M.K., 1958, Coronites from India and their bearing on the origin of coronas: Geol. Soc. Am., Bull. 69, p. 23-38.

Nicolas, A. and Boudier, F., 1975, Kinematic interpretation of folds in Alpine-type peridotites: Tectonophysics, 25, p. 233-260.

Nicolas, A., Bouchez, J.L., Blaise, J. and Poirier, J.P., 1977, Geological aspects of deformation in continental shear zones: Tectonophysics, 42, p. 55-73.

Nicolas, A. and Poirier, J.P., 1976, Crystalline plasticity and solid state flow in metamorphic rocks: John Wiley and Sons Ltd., 444 p.

Nissen, H.U., 1968, A study of bytownites in amphibolites of Ivrea Zone (Italian Alps) and in anorthosites: A new unmixing gap in the low plagioclases: Schweiz. Mineral. Petrogr. Mitt., 48, p. 67-83.

Palmer, H.C. and Carmichael, C.M., 1973, Paleomagnetism of some Grenville Province rocks: Can. J. Earth Sci., v. 10, p. 1175-1190.

Pitcher, W.S., 1979, The nature, ascent and emplacement of granitic magmas: Geol. Soc. Lond., v. 136, p. 627-662.

Pride, C., 1982, Origin of granitic rocks of the Glamorgan Migmatite Complex, Ontario: in Grenville Workshop, Ottawa-Carleton Centre for Geoscience Studies (Abstract), p. 8.

Ramberg, H., 1967a, Scandinavian Caledonides as studied by centrifuged models: Bull. of Geol. Inst., Univ. Uppsala, v. XLIII, No. 4-5.

Ramberg, H., 1967b, Gravity, deformation and the earth's crust as studied by centrifuged models: Academic Press, New York, 241 p.

Ramberg, H., 1973, Model studies of gravity in controlled tectonics by centrifuged techniques: in K.A. de Jong and R. Scholten (eds.), Gravity and Tectonics: Wiley, New York, p. 49-66.

Ramsay, J.G., 1967, Folding and fracturing of rocks: McGraw-Hill Inc., 568 p.

Ramsay, J.G., 1980, Shear zone geometry: A review: J. Struct. Geol., v. 2, No. 1/2, p. 83-99.

Ramsay, J.G. and Allison, I., 1979, Structural analysis of shear zones in Alpinised Hercynian granite: Schweiz. Mineral. Petrogr. Mitt., 59, p. 251-279.

Ramsay, J.G. and Graham, R.H., 1970, Strain variations in shear belts: Can. J. Earth Sci., v. 7, p. 786-813.

Rivers, T., 1976, Structures and textures of metamorphic rocks, Ompah area, Grenville Province, Ontario: Unpubl. Ph.D. Thesis, University of Ottawa, Ottawa, Ontario.

Sanderson, D.J., 1973, The development of fold axes oblique to the regular trend: Tectonophysics, 16, p. 55-70.

Sapountzis, E.S., 1975, Coronas from Thessaloniki gabbros (N. Greece): Contrib. Mineral. Petrol., 51, p. 197-203.

Schwerdtner, W.M., Bennett, F.J. and Janes, T.W., 1977, Application of L-S fabric scheme to structural mapping and paleostrain analysis: Can. J. Earth Sci., v. 14, p. 1022-1031.

Schwerdtner, W.M., Sutcliffe, R.H. and Troeng, B., 1978, Patterns of total strain diapirism in the crestal region of immature diapirs: Can. J. Earth Sci., v. 15, p. 1437-1447.

Seifert, K.E., 1964, The genesis of plagioclase twinning in the Nonewang Granite: Am. Mineral., 49, p. 297-320.

Sellars, C.M., 1978, Recrystallisation of metals during hot deformation: R. Soc. Lond., Philos. Trans., Ser. A, 288, p. 147-158.

Shaw, D.M., 1962, Geology of Chandos Township: Ont. Dept. Mines, Geol. Rept. 11, p. 1-28.

Shaw, D.M., 1968, A review of K-Rb fractionation trends by co-variance analysis: Geochim. Cosmochim. Acta, 32, p. 573-601.

Shelley, D., 1980, Quartz (0001)-axes preferred orientation, Bluff, New Zealand: Origin elucidated by grain-size measurements: Tectonophysics, 62, p. 321-337.

Sheraton, J.W., Skinner, A.C. and Tarney, J., 1973, The geochemistry of Scourian gneisses of the Assynt District: in "The Early Precambrian of Scotland and Related Rocks of Greenland", R.G. Park and J. Tarney (eds.), Univ. of Keele, 1973, p. 13-30, 193 p.

Silver, L.T. and Lumbers, S.B., 1965, Geochronological studies in the Bancroft-Madoc area of the Grenville Province, Ontario, Canada: Geol. Soc. Am., Spec. Publ. 87, p. 156.

Skjernaa, L., 1980, Rotation and deformation of randomly oriented planar and linear structures in progressive sample shear: J. Struct. Geol., v. 2, No. 1/2, p. 101-109.

Smith, J.V., 1974, Feldspar minerals, v. 2, Springer Verlag.

Spry, A., 1969, Metamorphic textures: Pergamon Press Ltd., 350 p.

Starkey, J., 1977, The contouring of orientation data represented in spherical projection: Can. J. Earth Sci., v. 14, p. 268-277.

Starkey, J., 1979, Petrofabric analysis of Saxony granulites by optical and X-ray diffraction methods: Tectonophysics, 58, p. 201-219.

Starmer, I.C., 1969, Basic plutonic intrusions of the Risor-Sondeled area, South Norway: The original lithologies and their metamorphism: Nor. Geol. Tidsskr., 49, p. 403-431.

Stephansson, O. and Johnson, K., 1976, Granite diapirism in the Rum Jungle area, Northern Australia: Prec. Res., v 3, No. 2, p. 159-185.

Strand, T., 1945, Structural petrology of the Bygdin Conglomerate: Nor. Geol. Tidsskr., 24, p. 14-31.

Streckeisen, A., 1976, To each plutonic rock its proper name: Earth Sci. Rev., 12 p. 1-33.

Sylvester, A.G. and Christie, J.M., 1968, The origin of crossed-girdle orientations of optic axes in deformed quartzites: J. Geol., v. 76, p. 571-580.

Talbot, C.J., 1970, The minimum strain ellipsoid using deformed quartz veins: Tectonophysics, 9, p. 47-76.

Thompson, P.H., 1972, Stratigraphy, structure and metamorphism of the Flinton Group in the Bishops Corner area, Grenville Province, eastern Ontario: Unpubl. Ph.D. Thesis, Carleton Univ., Ottawa, Ontario.

Tullis, J., Christie, J.M. and Griggs, D.T., 1973, Microstructure and preferred orientation of experimentally deformed quartzite: Geol. Soc. Am. Bull., v. 84, p. 297-314.

Turner, F.J., 1981, Metamorphic petrology: Mineralogical, field, and tectonic aspects: 2nd Ed., McGraw-Hill, 524 p.

Underwood, E.E., 1970, Quantitative Stereology: Addison-Wesley, Reading, Massachusetts.

Urai, J.L. and Humphreys, F.J., 1981, The development of shear zones in polycrystalline camphor: Tectonophysics, 78, p. 677-685.

Van Roermund, H., Lister, G.S. and Williams, P.F., 1979, Progressive development of quartz fabrics in a shear zone from Monte Mucrone, Sesia-Lanzo Zone, Italian Alps: J. Struct. Geol., v. 1, No. 1, p. 43-52.

Van Vlack, L.H., 1965, Microstructures: in "Physical Metallurgy", R.W. Cahn (ed.), North Holland, p. 589-614.

Vance, J.A., 1961, Polysynthetic twinning in plagioclase: Am. Mineral., 46, p. 1097-1119.

Vernon, R.H., 1965, Plagioclase twins in some mafic gneisses from Broken Hill, Australia: Mineral. Mag., 35, p. 488-507.

Vernon, R.H., 1975, Deformation and recrystallisation of a plagioclase grain: Am. Mineral., 9 and 10, v. 60, p. 884-887.

Vernon, R.H., 1976, Metamorphic processes, reactions and microstructural development: Alley and Unwin, London, 247 p.

Warren, R.G., 1979, Sapphirine bearing rocks with sedimentary and volcanogenic protoliths from the Arunta Block: Nature, 278, p. 159-161.

Watterson, J., 1968, Homogeneous deformation of the gneisses of Vesterland, Southwest Greenland: Groenlands Geol. Unders., Bull. 78, p. 1-75.

Wenk, H.R., 1973, The structure of Bergell Alp: Eclogae Geol. Helv., v. 66, p. 255-291.

Wenk, E. and Wenk, H-R, 1977, An variation and intergrowths of plagioclase in banded metamorphic rocks from Val Carecchio (Central Alps): Schweiz. Mineral. Petrogr. Mitt., 57, p. 41-57.

White, A.J.R., 1966., Petrology and structure of the Rathjen granitic gneiss of the Palmer Region, S. Australia: Geol. Soc. Aust. J., v. 13, Pt. 2, p. 471-489.

White, S., 1973, The dislocation structures responsible for the optical effects in some naturally-deformed quartzites: J. Mtls. Sci., 8, p. 490-499.

White, S., 1975, Tectonic deformation and recrystallisation of oligoclase: Contrib. Mineral. Petrol., v. 50, No. 4, p. 287-304.

White, S., 1976, The effects of strain on the microstructures, fabrics, and deformation mechanisms in quartzites: R. Soc. Lond. Philos. Trans., Ser. A, 283, p. 69-86.

White, S., 1977, Geological significance of recovery and recrystallization in quartz: Tectonophysics, 39, p. 143-170.

White, S., Carreras, J., Shaw, M.D. and Humphreys, F.J., 1980, On mylonites in ductile shear zones: J. Struct. Geol., v. 2, No. 1/2, p. 175-187.

White, S. and Knipe, R.J., 1978, Transformation and reaction enhanced ductility in rocks: Geol. Soc. Lond. J., 135, p. 513-516.

Whitney, P.R. and McLelland, J.M., 1973, Origin of coronas in metagabbros of Adirondack Mountains, N.Y.: Contrib. Mineral. Petrol., 39, p. 81-98.

Williams, G.D., 1978, Rotation of contemporary folds into the X direction during overthrust processes in Laksefjord, Finnmark: Tectonophysics, 48, p. 29-40.

Wilson, C.J.L., 1973, The prograde microfabric in a deformed quartzite sequence, Mount Isa, Australia: Tectonophysics, 19, p. 39-81.

Wilson, C.J.L., 1975, Preferred orientation in quartz ribbon mylonites: Geol. Soc. Am. Bull., 86, p. 968-974.

Winkler, H.G., 1976, Petrogenesis of metamorphic rocks: Springer Verlag, N.Y., 334 p.

Wright, A.E., Tarney, J., Palmer, K.F., Moorlock, B.S.P. and Skinner, A.C., 1973, Stratigraphic, structural and metamorphic features of the Archaean (pre-Ketilidian) rocks in the Frederinshab district, South-West Greenland: in The Early Precambrian of Scotland and Related Rocks of Greenland, R.G. Park and J. Tarney (eds.): Univ. Keele, p. 157-178.

Wynne-Edwards, H.R., 1972, The Grenville Province: in Variations in Tectonic Styles in Canada, R.A. Price and R.J.W. Douglas (eds.): Geol. Assoc. Can., Spec. Pap. 11, p. 263-334.

Yund, R.A. and Ackermand, D., 1979, Development of Perthites in the Storm King granite, N.Y.: Contrib. Mineral. Petrol. 70, p. 273-280.

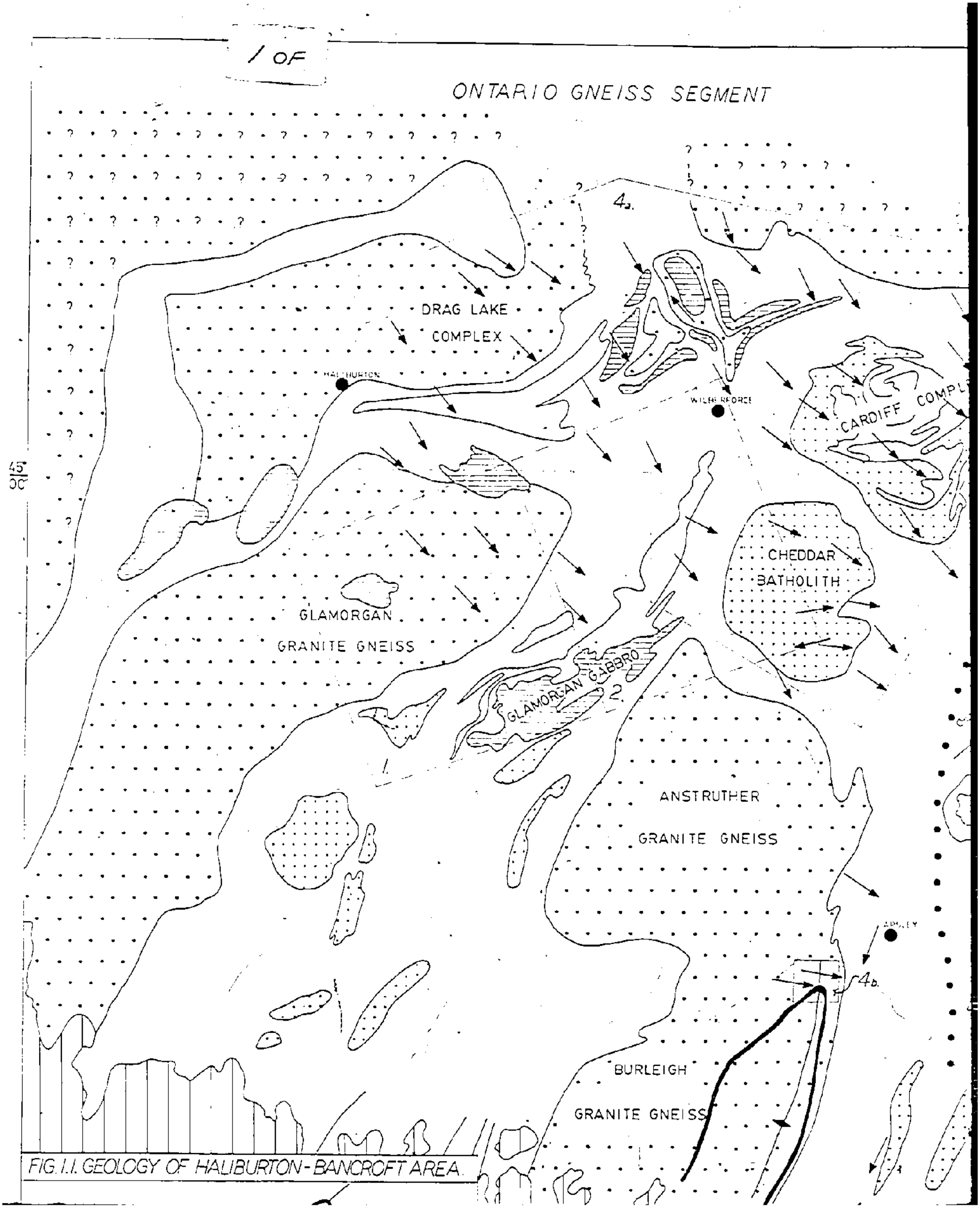

FIG. 1.1. GEOLOGY OF HALIBURTON - BANCROFT AREA.

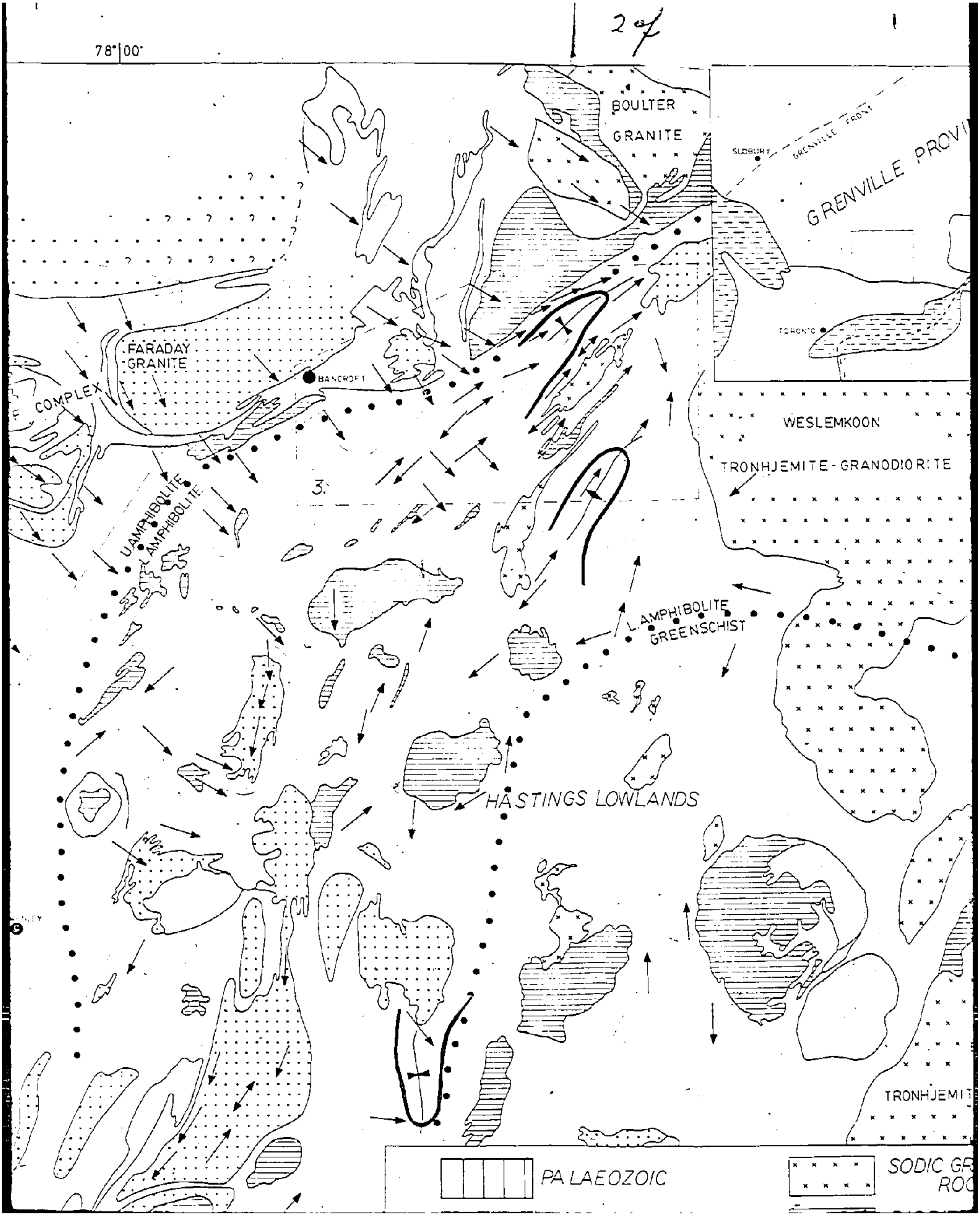
2 of
78°|00'
BOULTER
GRANITE
GRENVILLE FRONT
SUDBURY
TORONTO
FARADAY
GRANITE
BANCROFT
COMPLEX
U.AMPHIBOLITE
L.AMPHIBOLITE
WESLEMKOON
TRONHJEMITE-GRANODIORITE
L.AMPHIBOLITE
GREENSCHIST
HASTINGS LOWLANDS
PALAEOZOIC

1. 3 of

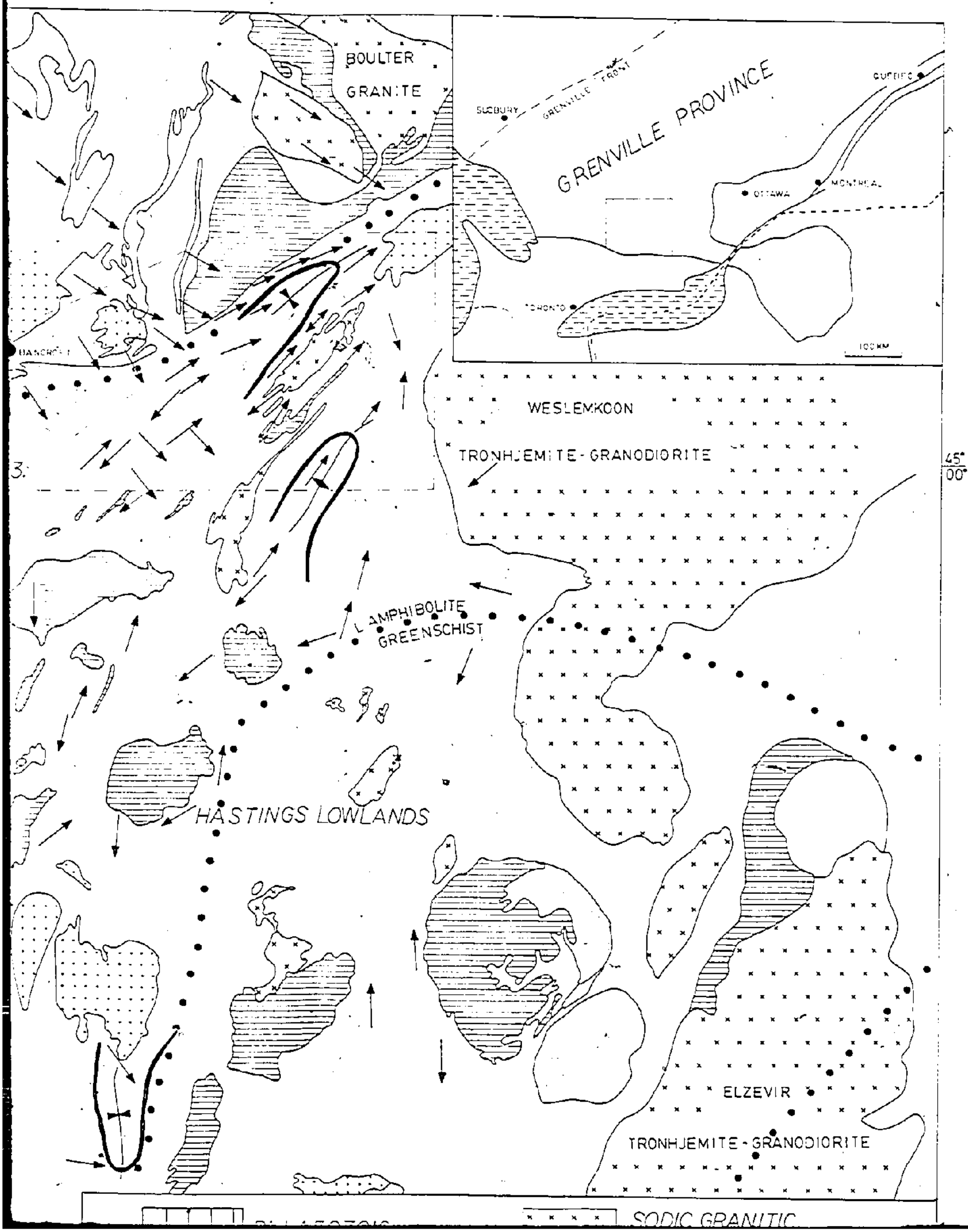

BOULTER
GRANITE
GRENVILLE PROVINCE
GRENVILLE FRONT
SUDBURY
QUEBEC
OTTAWA
MONTREAL
TORONTO
100 KM
BANCROFT
WESLEMKOON
TRONHJEMITE-GRANODIORITE
45°
00'
AMPHIBOLITE
GREENSCHIST
HASTINGS LOWLANDS
ELZEVIR
TRONHJEMITE-GRANODIORITE
SODIC GRANITIC

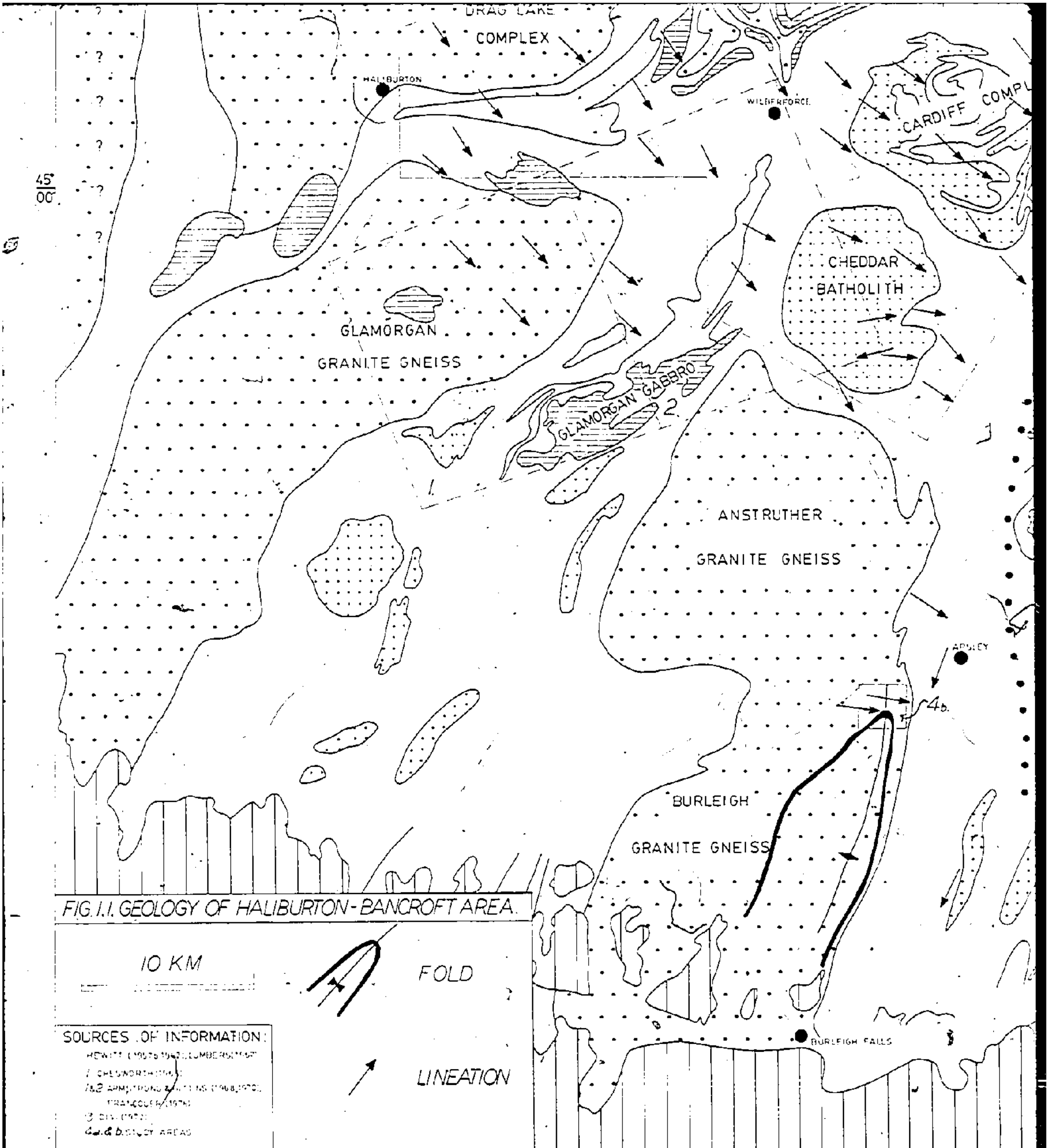

FIG. 1.1. GEOLOGY OF HALIBURTON-BANCROFT AREA.

4 of

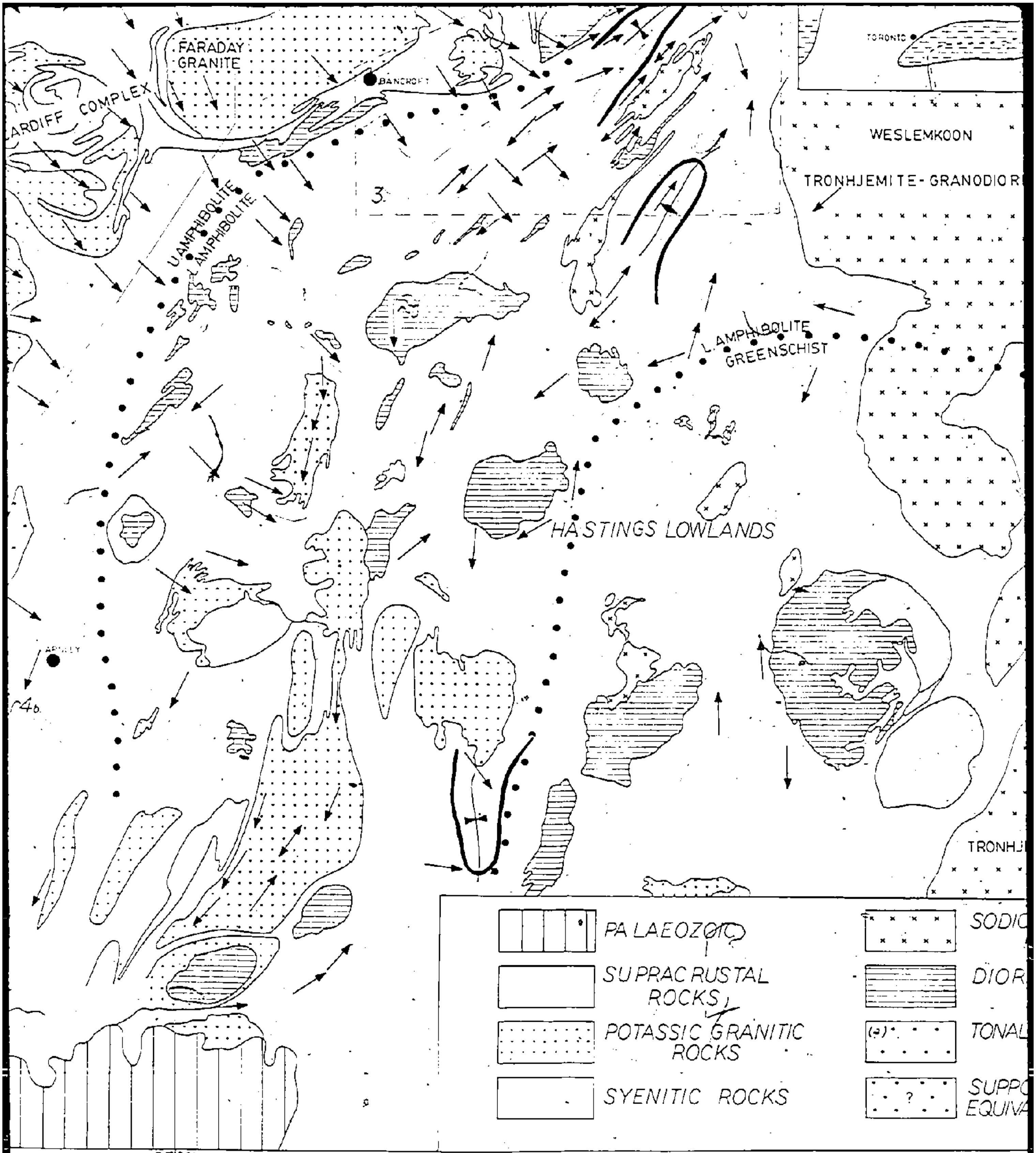

FARADAY GRANITE
BANCROFT
CARDIFF COMPLEX
U. AMPHIBOLITE
L. AMPHIBOLITE
3
TORONTO
WESLEMKOON
TRONHJEMITE-GRANODIOR
L. AMPHIBOLITE
GREENSCHIST
HASTINGS LOWLANDS
APSLEY
4b
TRONHJ
PALAEOZOIC
SUPRACRUSTAL ROCKS
POTASSIC GRANITIC ROCKS
SYENITIC ROCKS
SODIC
DIOR
TONAL
SUPPO
EQUIVA
78°00'

5 of.

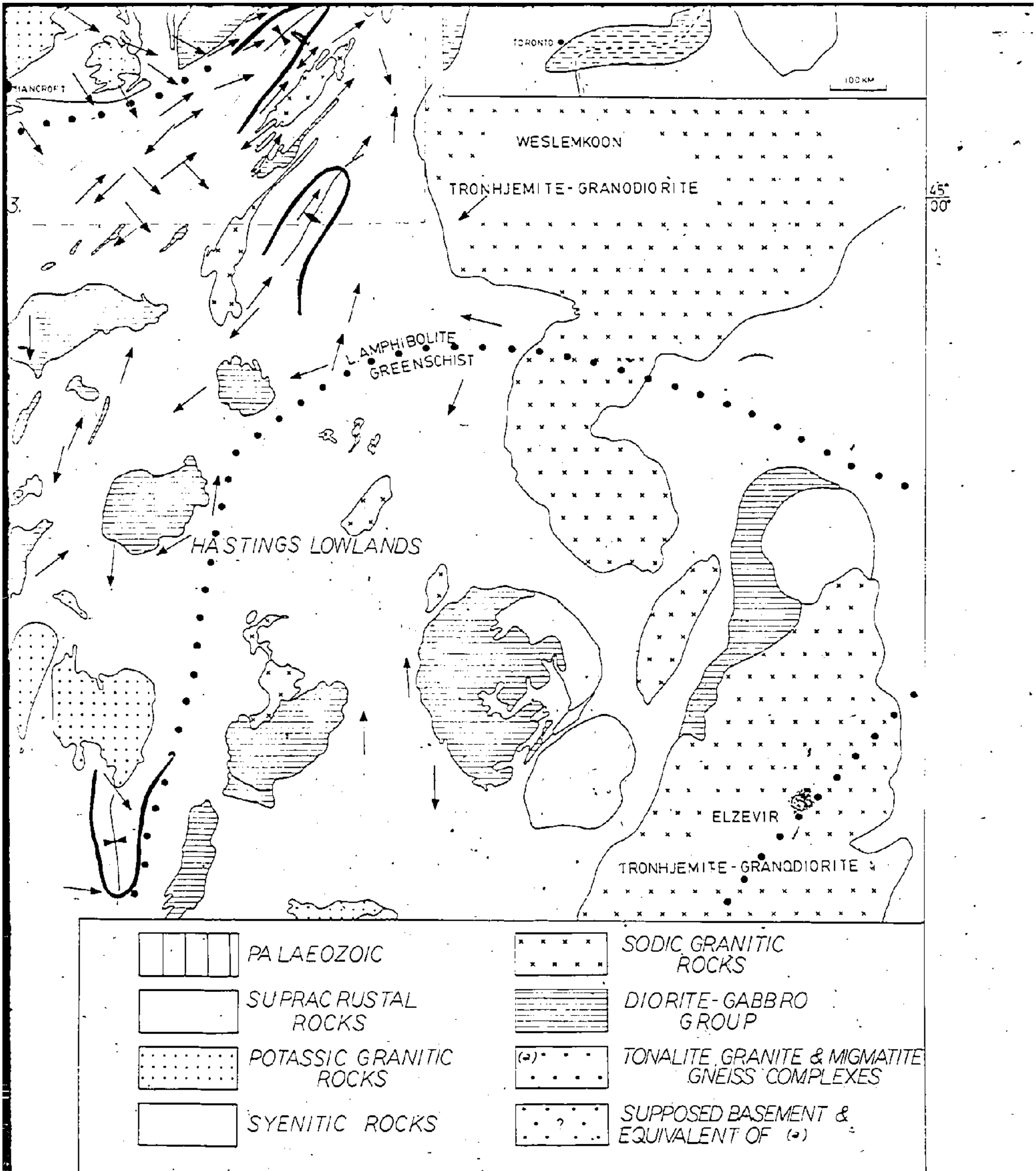

TORONTO
100 KM
BANCROFT
WESLEMKOON
TRONHJEMITE - GRANODIORITE
45°
00'
L. AMPHIBOLITE
GREENSCHIST
HASTINGS LOWLANDS
ELZEVIR
TRONHJEMITE - GRANODIORITE
PALAEOZOIC
SUPRACRUSTAL ROCKS
POTASSIC GRANITIC ROCKS
SYENITIC ROCKS
SODIC GRANITIC ROCKS
DIORITE-GABBRO GROUP
TONALITE, GRANITE & MIGMATITE GNEISS COMPLEXES
SUPPOSED BASEMENT & EQUIVALENT OF (a)

6 of 6

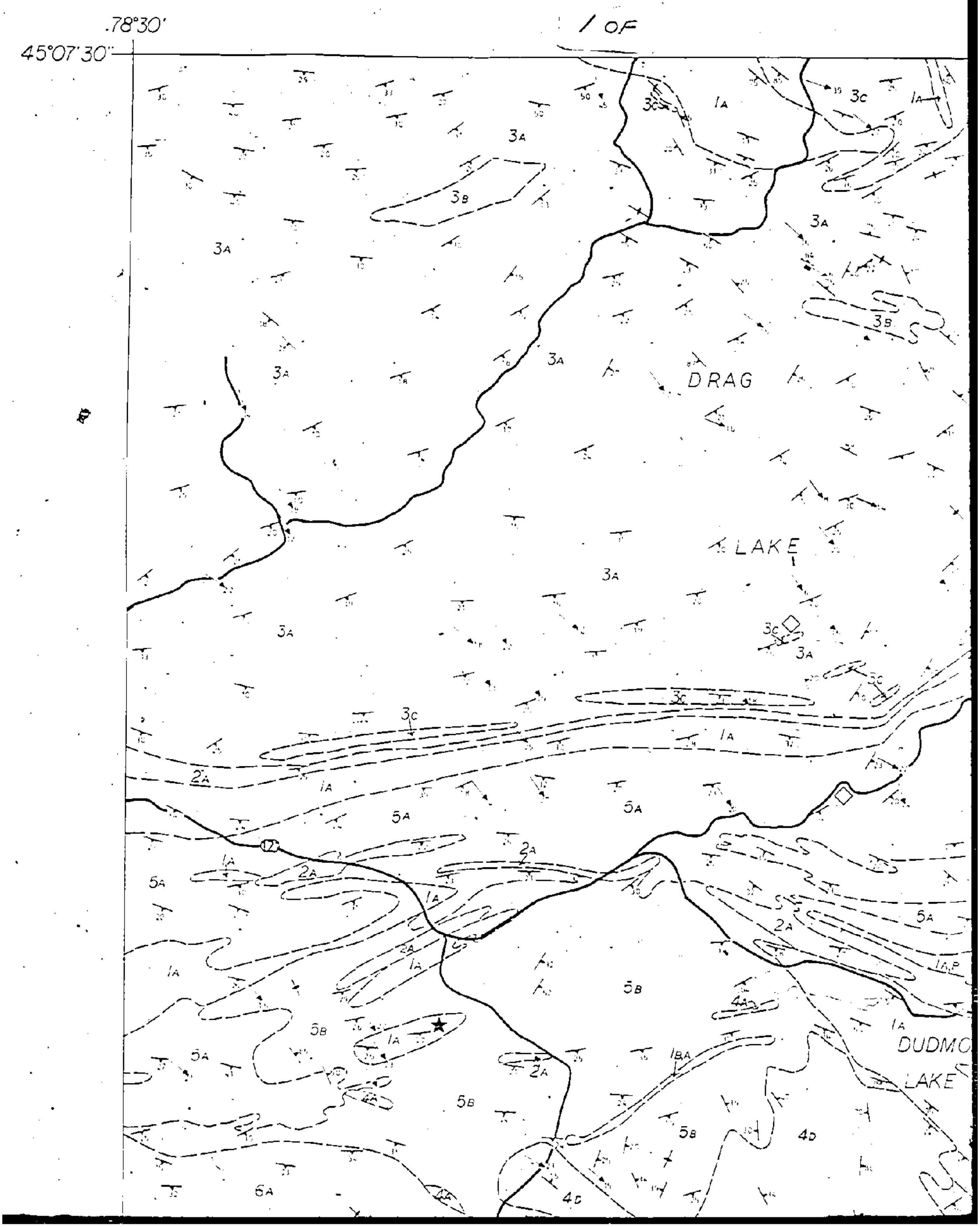

1 OF
78°30'
45°07'30"
DRAG
LAKE
DUDMO
LAKE
3A
3B
3C
1A
2A
5A
5B
4A
4D
1BA
1AP
6A
127

2 of

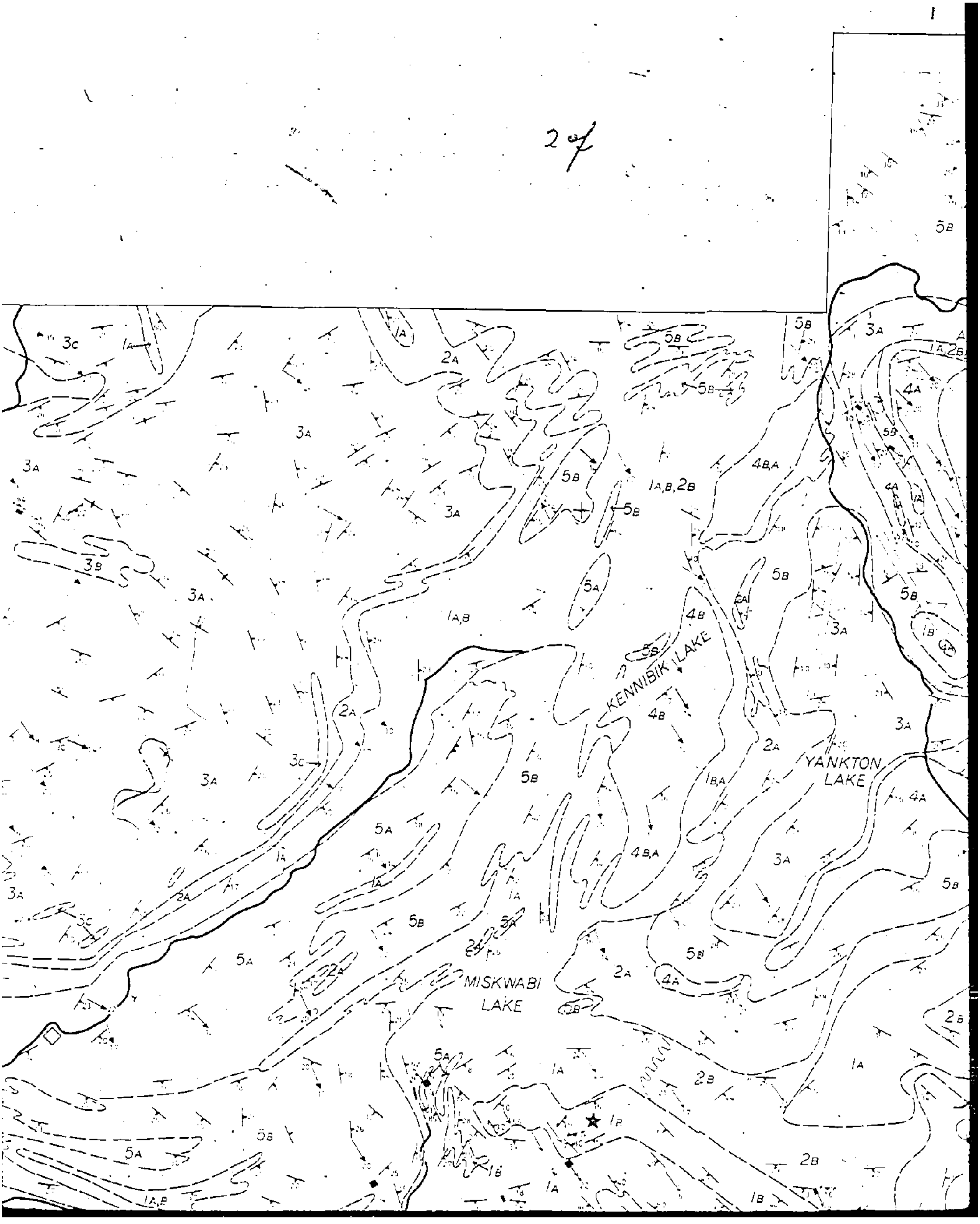

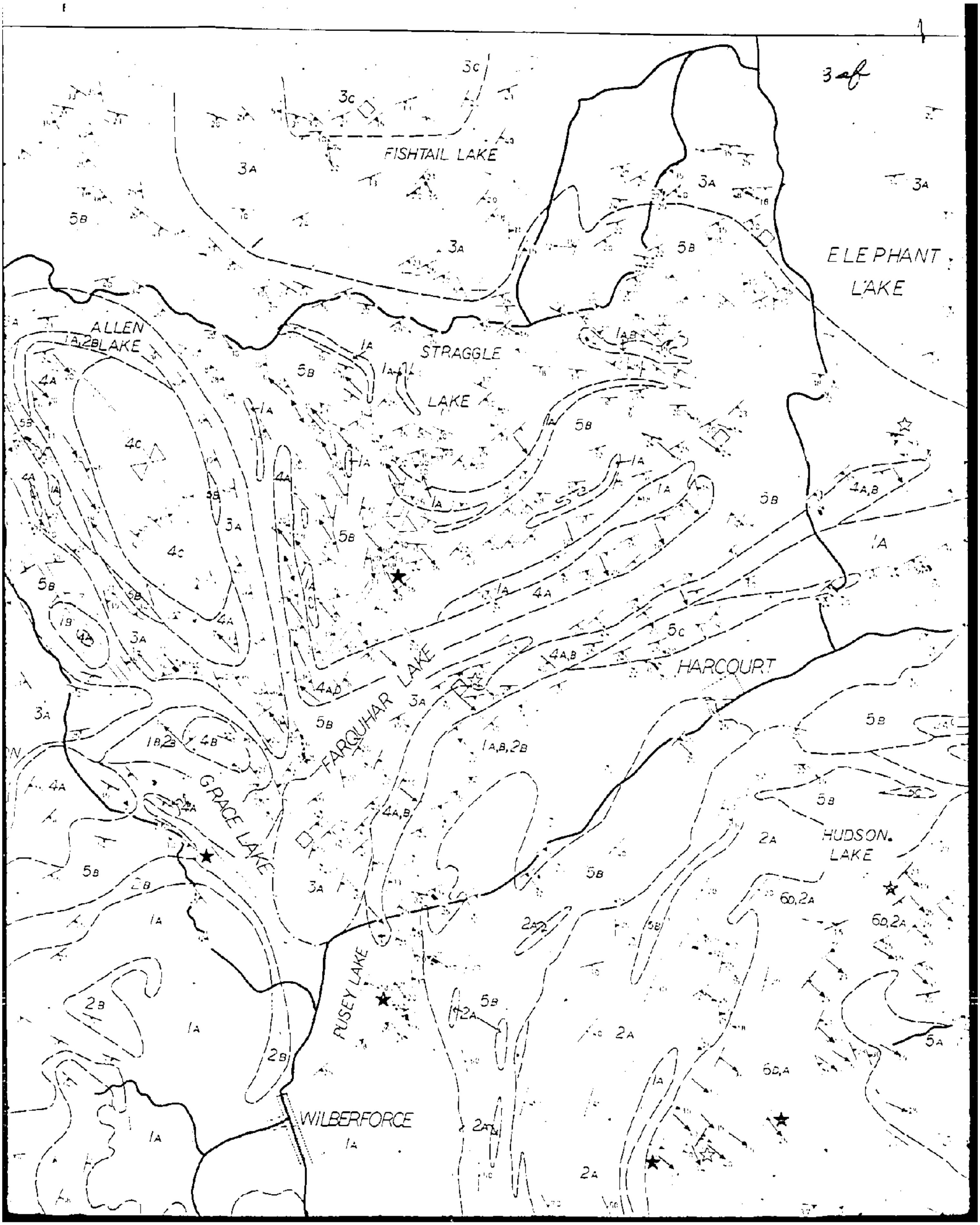

3 of
FISHTAIL LAKE
ELEPHANT LAKE
ALLEN LAKE
STRAGGLE LAKE
FARQUHAR LAKE
HARCOURT
GRACE LAKE
HUDSON LAKE
PUSEY LAKE
WILBERFORCE

4 of

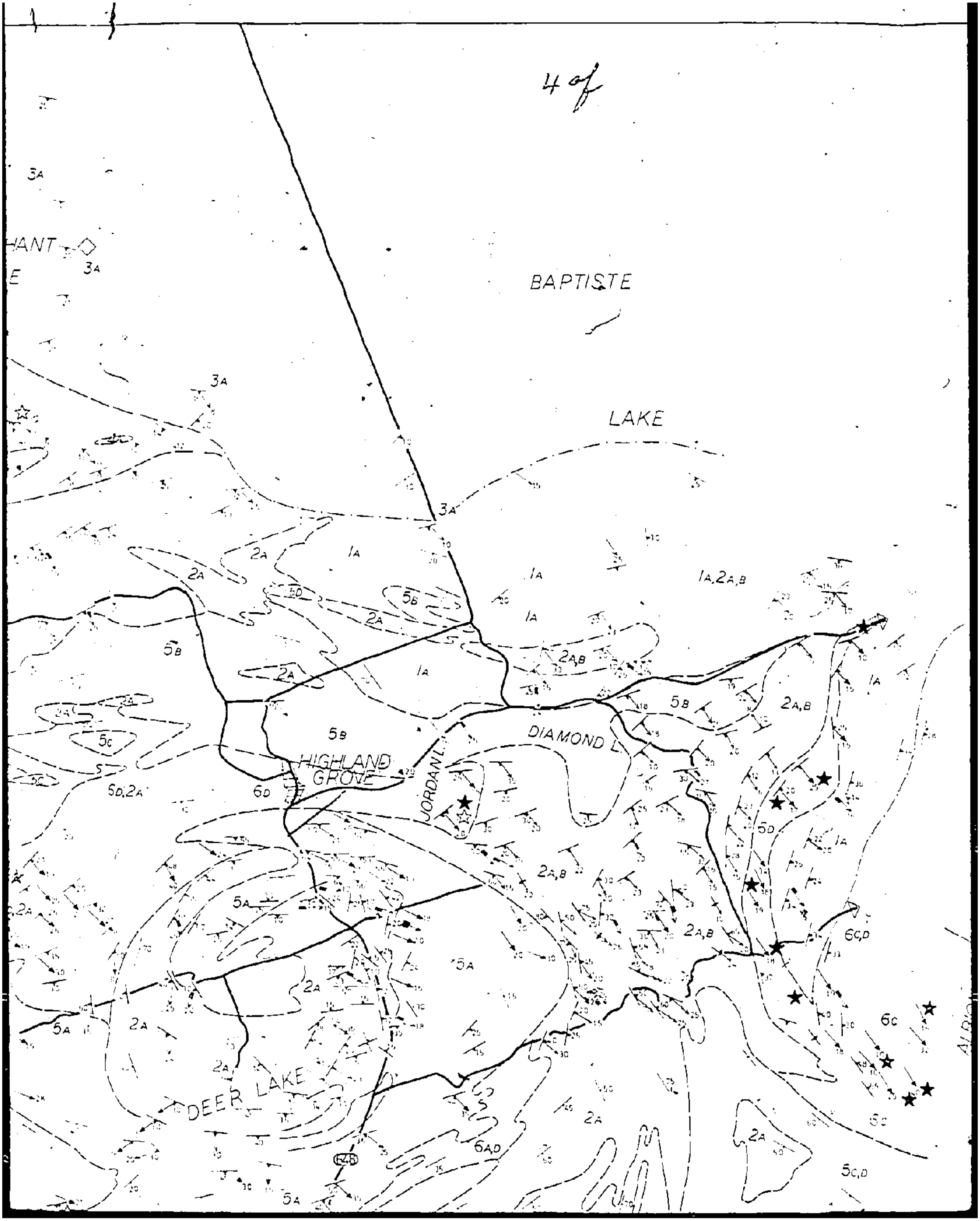
BAPTISTE
LAKE
HIGHLAND
GROVE
JORDAN L
DIAMOND L
DEER LAKE
1A
1A,2A,B
2A
2A,B
3A
5A
5B
5C
5D
5D,2A
6D
6A,D
6C
6C,D
5C,D
648

5 of.

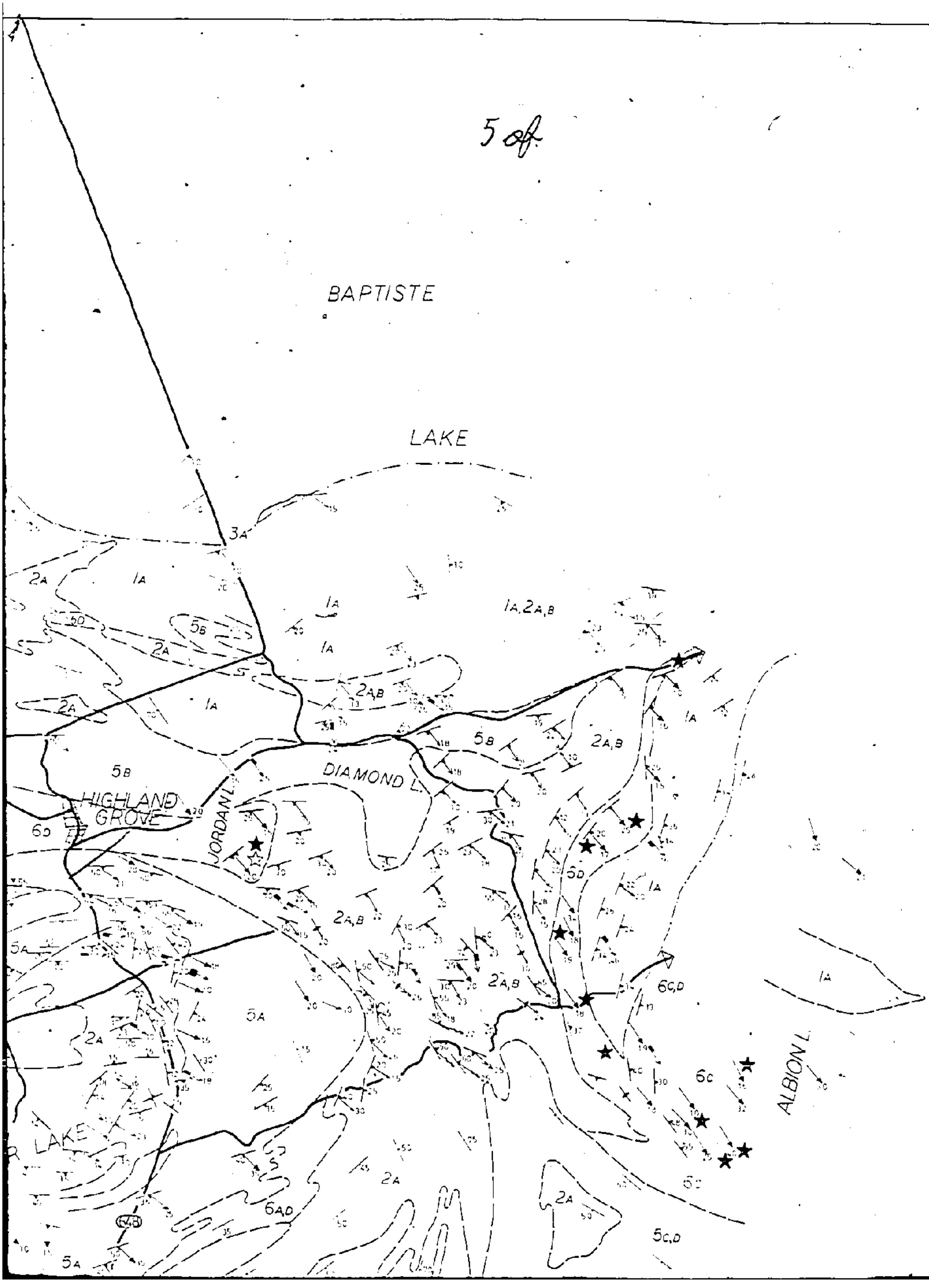

BAPTISTE
LAKE
DIAMOND L.
HIGHLAND GROVE
JORDAN L.
ALBION L.
R LAKE

45°00'

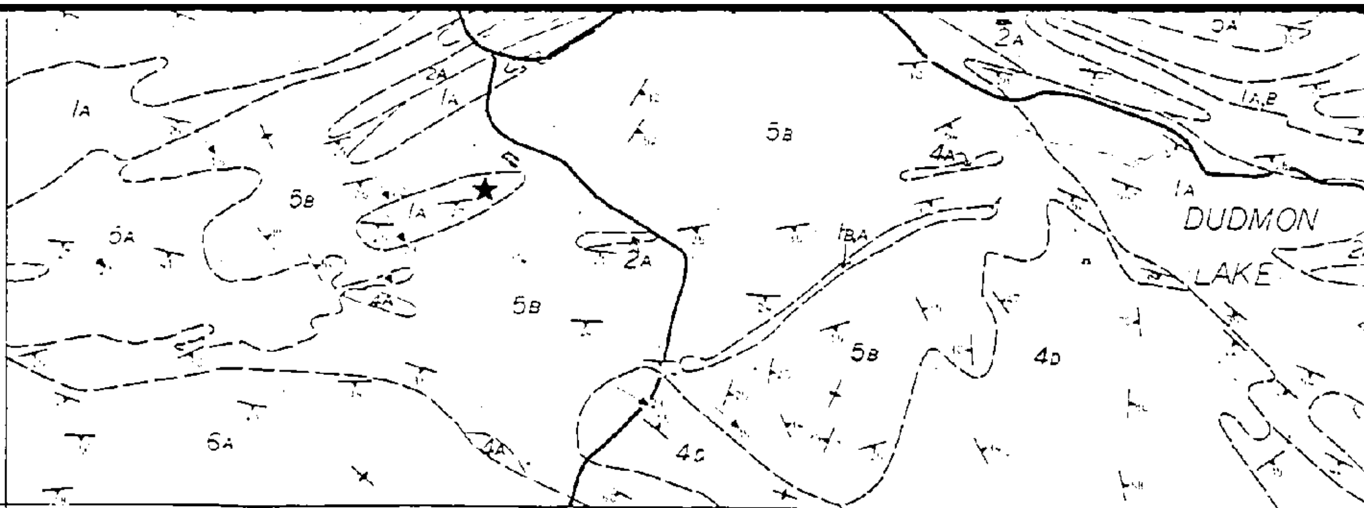

FIG. 1.2A. COMPILATION OF LITHOLOGY & STRUCTURE OF BAPTISTE L., EELS L. & DRAG L. AREA OF PRECAMBRIAN OF S. ONTARIO.

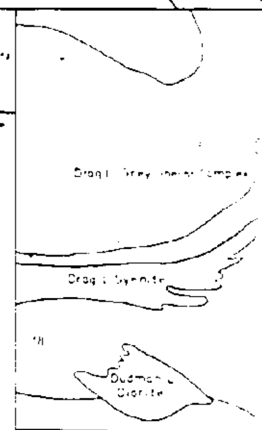

Fig.1.2b Location of petrofa[...] & main gneiss bodies LS1[...]

SUPRACRUSTAL ROCKS

1
- 1A Impure calcitic and dolomitic marble, skarn and metamorphic pyroxenite.
- 1B Quartzite.

2
- 2A Amphibolite, amphibole and pyroxene bearing calcareous schist and gneiss.
- 2B Biotitic and feldspathic schist and gneiss, rare pelite.

GREY GNEISS COMPLEXES

3
- 3A Tonalite gneiss [bi-hb-cz-pl; bi-qz-pl].
- 3B Granite.
- 3C Garnet gneiss, includes pelitic and gedrite and/or cordierite bearing varieties.

PLUTONIC GNEISS

4
- 4A Gabbro, primary textures present, locally.
- 4B Anorthosite and anorthositic gabbro.
- 4C Pyroxenite and hornblendite.
- 4D Diorite

5
- 5A Buff syenite.
- 5B Heterogeneous syenite [interlayered pink syenite, granite, pegmatite and supracrustal rocks; locally, granite fraction dominates].
- 5C Unsubdivided syenite.
- 5D Nepheline syenite.

6
- 6A Alaskite [equigranular, no quartz LS fabric].
- 6B Alkali granite.
- 6C Medium grained to pegmatitic leucogranite.
- 6D Biotite and biotite-hornblende granite.
- 6E Layered granite gneiss [± clinopyroxene].

NOTE: Units not numbered in stratigraphic order.

SYMBOLS

FOLIATIONS
- S0//S1.[1]
- S2.
- LS2 Microfabric, shear-plane.
- Mylonite foliation.
- Axial surface
- Foliation, from Hewitt (1957c) & Francoeur (1975)

LINEATIONS[1]
- Linear element of shape-fabric (LS1).
- Mineral & intersection lineation.
- Intersection on foliation of mica with axially symmetric fabric.

[1] (maybe combined)

FOLD AXES
- Axis of 'M' fold.
- Axis of 'S' fold.
- Axis of 'Z' fold.

GEOLOGICAL BOUNDARIES
- Approximate.
- Assumed.
- Fault.
- Tectonic schist.

- Road & highway (numbered).
- ★ LS1 Petrofabric sample.
- ☆ LS2 Petrofabric sample.

0 1 2 3 4 5 KILOMETRES

Quartz microstructure type [...] samples (sample number[...]

LS1 Granite (MCT)
1 (1691b)
2 (1295b)
3 (1092b)
4 (497c)
5 (22103b)
6 (895c)
7 (24101b)
8 (25101b)
9 (30105b)
10 (30101b)

(ALT)
11 (1113d)
12 (2111d)
13 (1491c)
14 (1395c)

LS1 [...]

LS2 [...]

See text for details.

Shear-sense of up[...]

LS1 [Trace on XZ o[...] Synoptic c-axis[...]

LS2 [Asymmetric [...] C-axis girdle & [...]

6 of

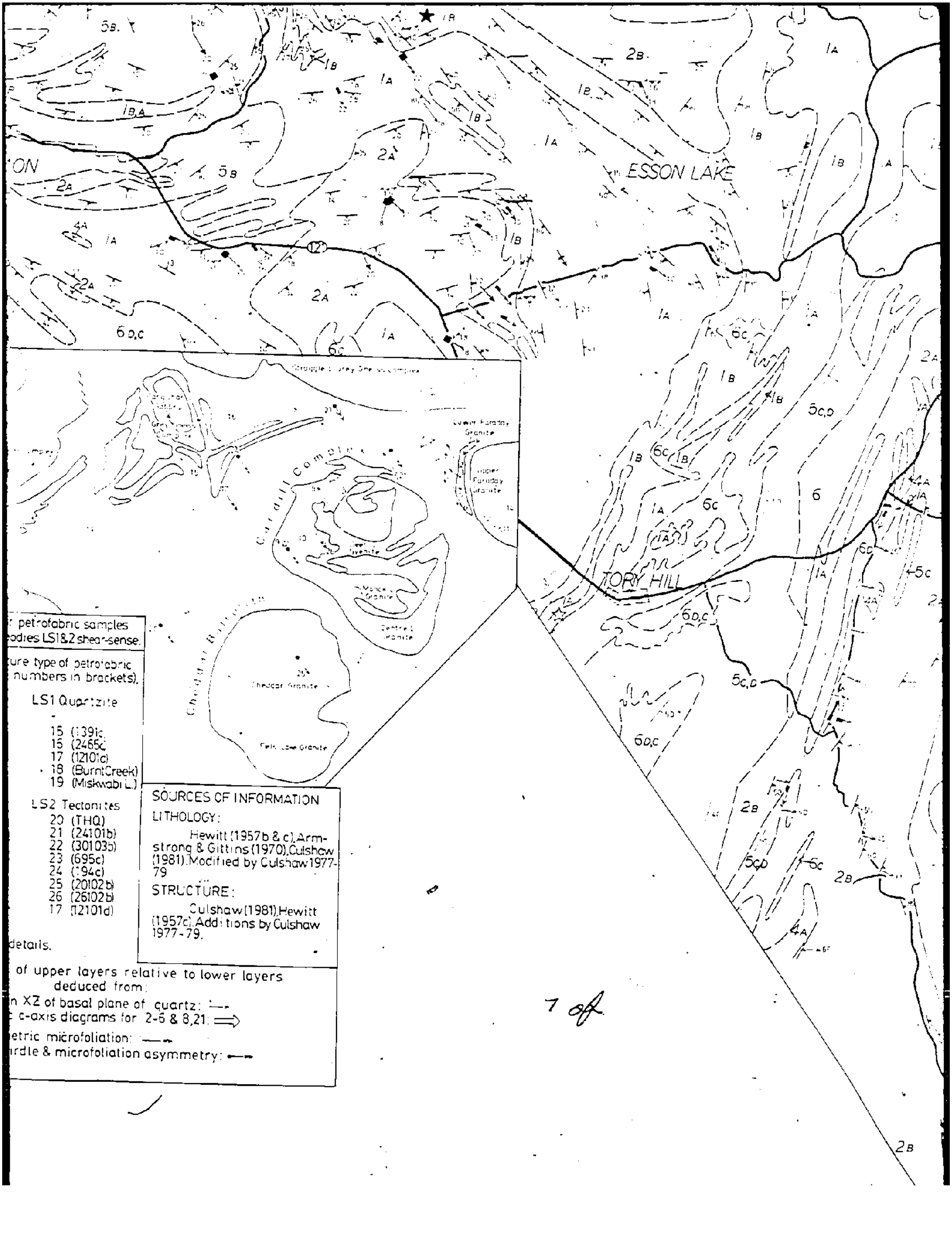
ESSON LAKE
TORY HILL
ON
121
Cardiff Complex
Cheddar Batholith
Lower Faraday Granite
Upper Faraday Granite
Centre Granite
Cheddar Granite
Glamorgan Granite
Monck Granite
r petrofabric samples
odres LS1&2 shear-sense.
ture type of petrofabric
numbers in brackets).
LS1 Quartzite
15 (1391c)
15 (2465c)
17 (12101c)
18 (BurntCreek)
19 (Miskwabi L.)
LS2 Tectonites
20 (THQ)
21 (24101b)
22 (30103b)
23 (695c)
24 (194c)
25 (20102b)
26 (26102b)
17 (12101d)
details.
of upper layers relative to lower layers deduced from:
n XZ of basal plane of quartz:
c-axis diagrams for 2-6 & 8,21:
etric microfoliation:
irdle & microfoliation asymmetry:
SOURCES OF INFORMATION
LITHOLOGY:
Hewitt (1957b & c), Armstrong & Gittins (1970), Culshaw (1981). Modified by Culshaw 1977-79
STRUCTURE:
Culshaw (1981), Hewitt (1957c). Additions by Culshaw 1977-79.
7 of

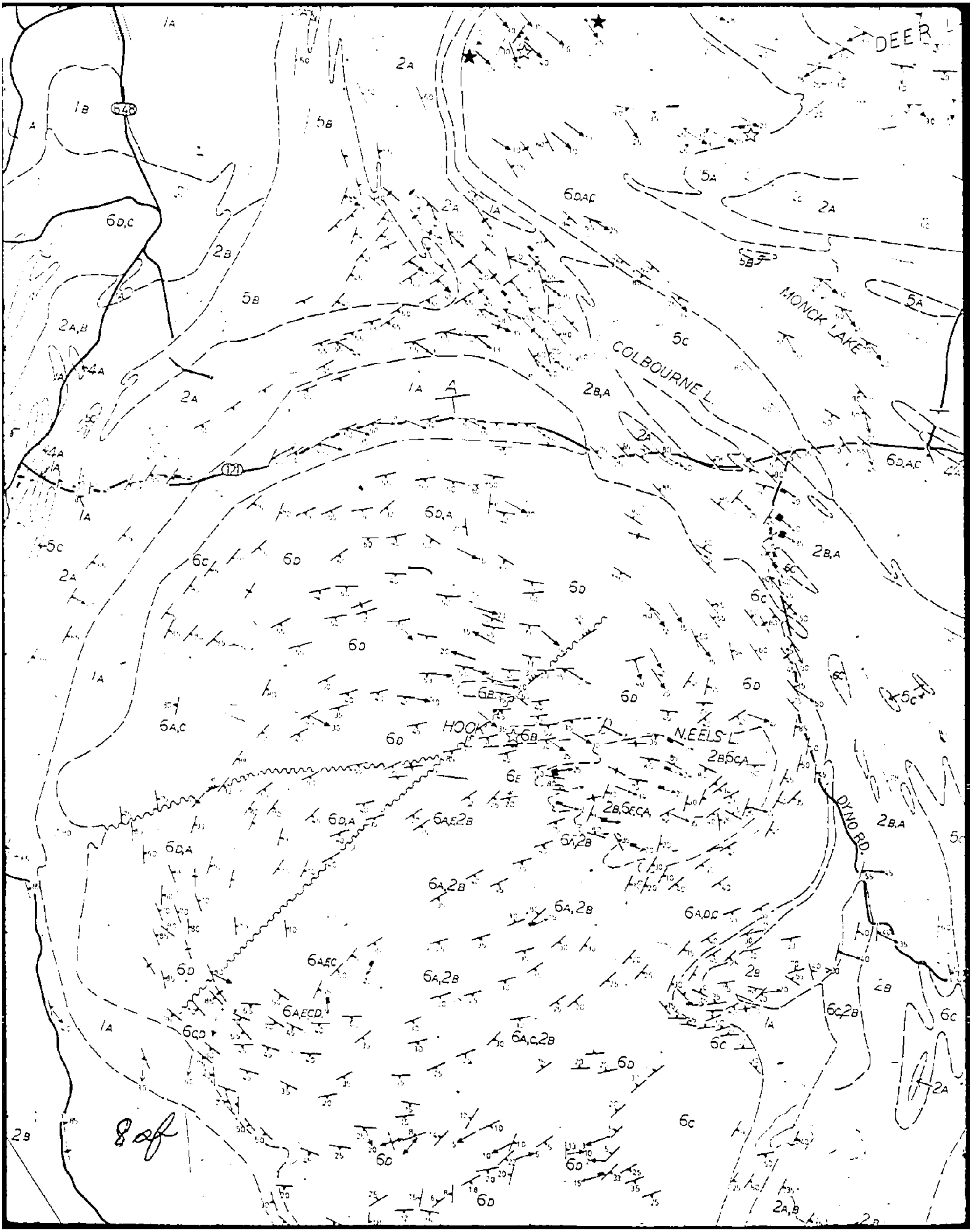
DEER L
MONCK LAKE
COLBOURNE L.
HOOK
N. EELS L.
DYNO RD.
8 of

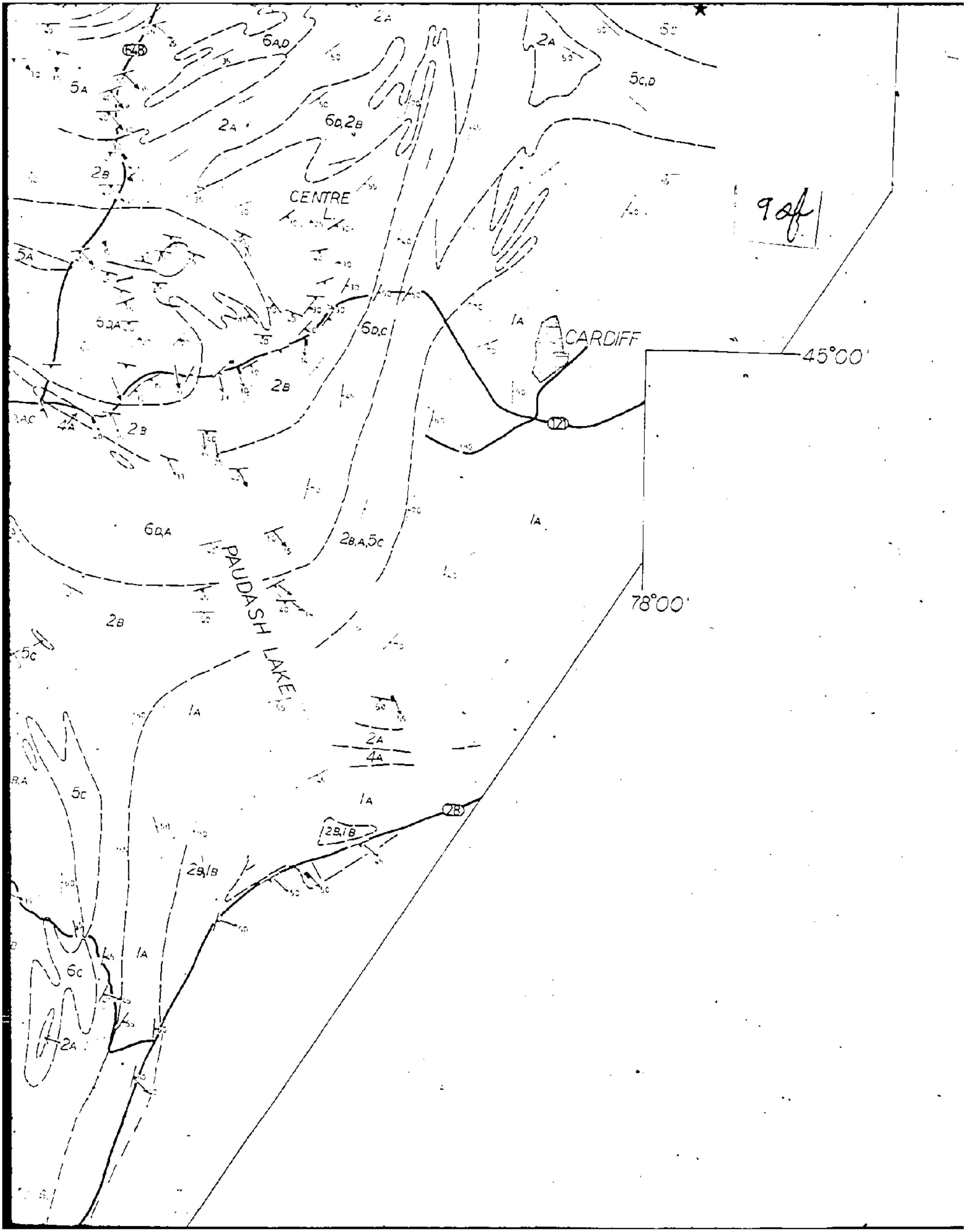
CENTRE
CARDIFF
PAUDASH LAKE
45°00'
78°00'
9 of
6A,D
5C,D
6D,2B
6D,A
6D,C
2B,A,5C
2B,1B
2A
4A
1A
5A
2B
5C
6C

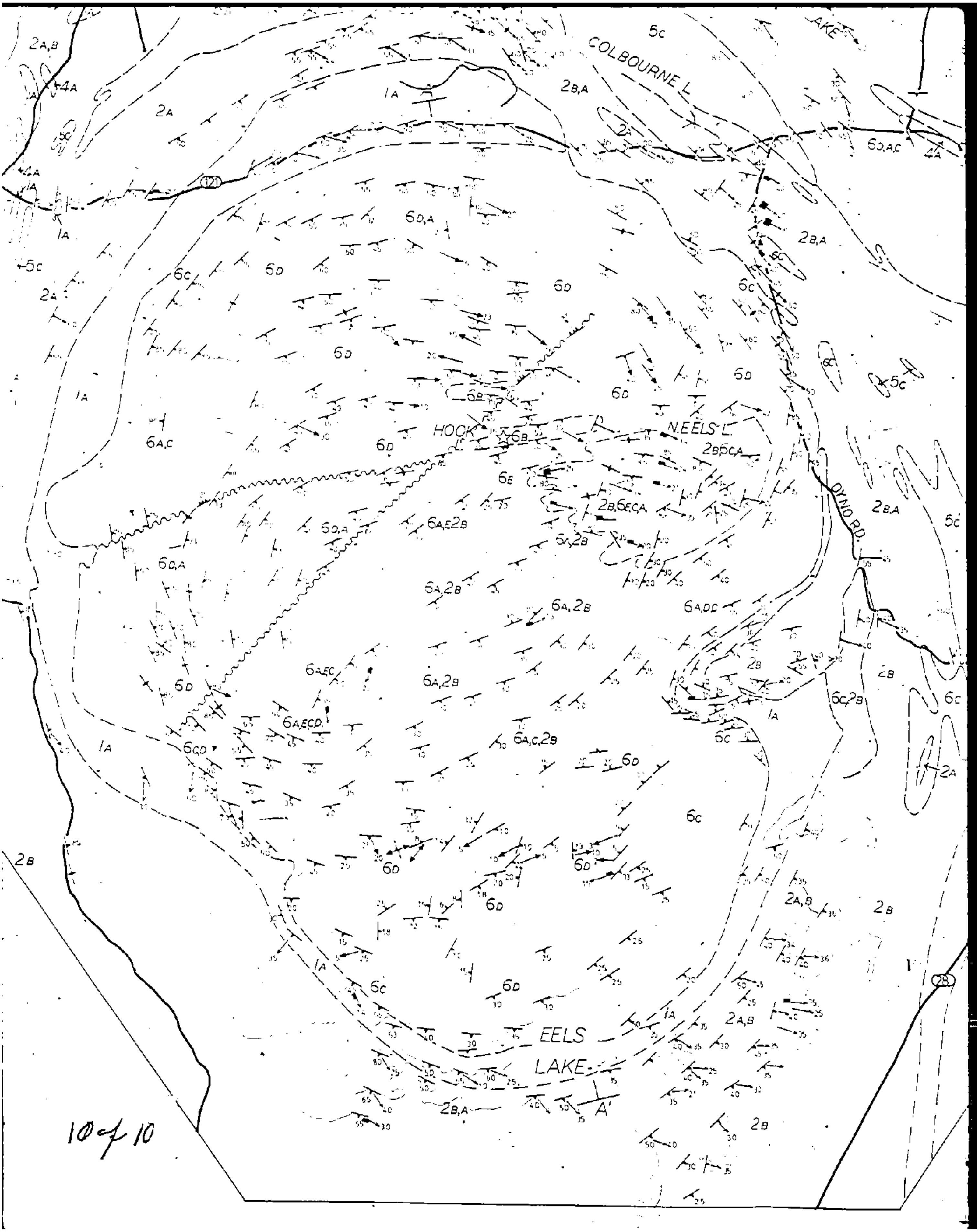

COLBOURNE L.
5C
2B,A
1A
2A,B
4A
2A
121
6D,A
6D
6C
6A,C
HOOK
6B
N.EELS L.
2B,6EC,A
6A,E,2B
6A,2B
6A,D,C
6A,E,C,D
6A,C,2B
6C,D
6C,2B
2A,B
2B
EELS
LAKE
A'
DYNO RD.
28

10 of 10

1 OF

FIG. 1.3

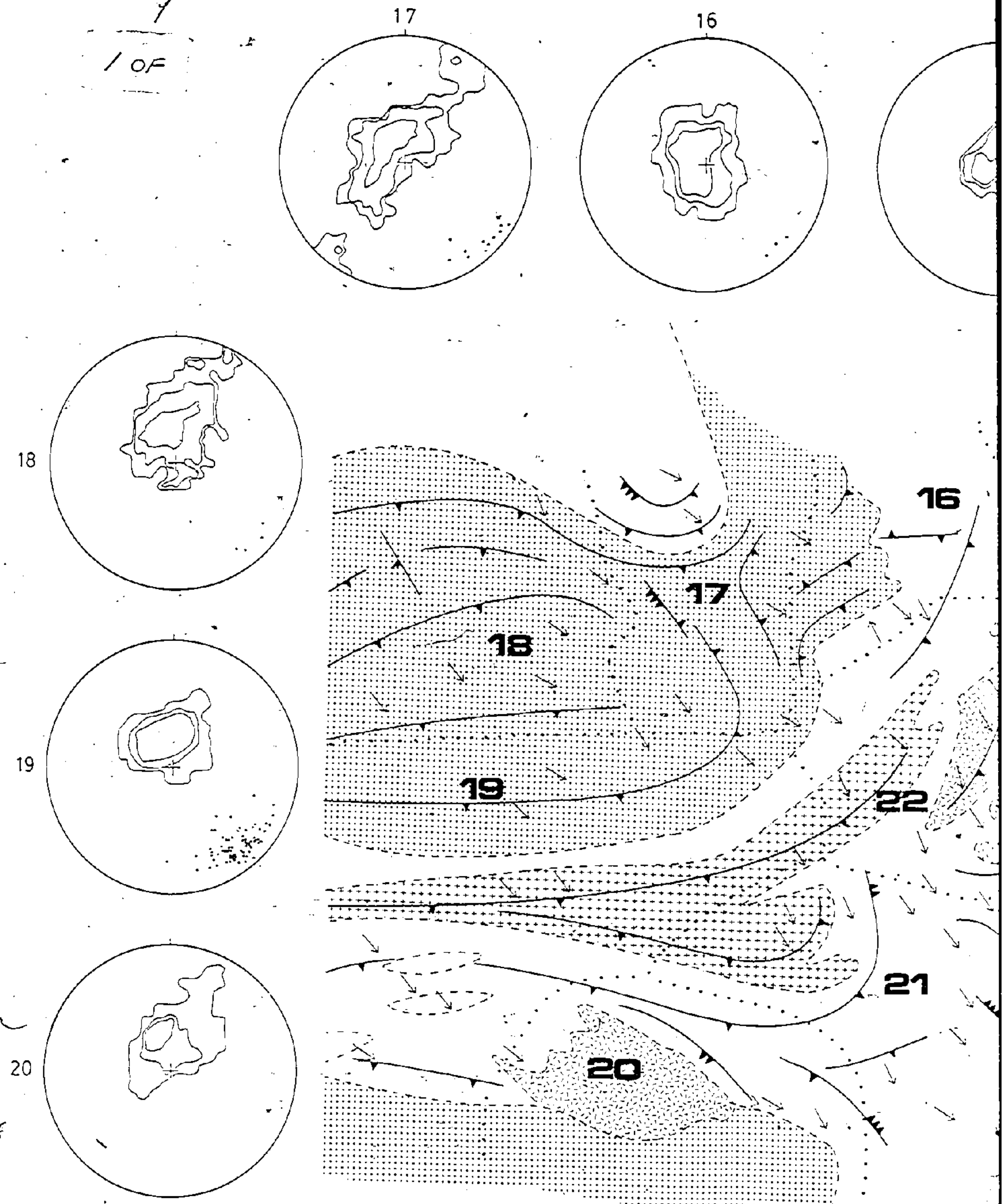

G. 1.3. SUMMARY OF STRUCTURAL GEOLOGY.

2 of

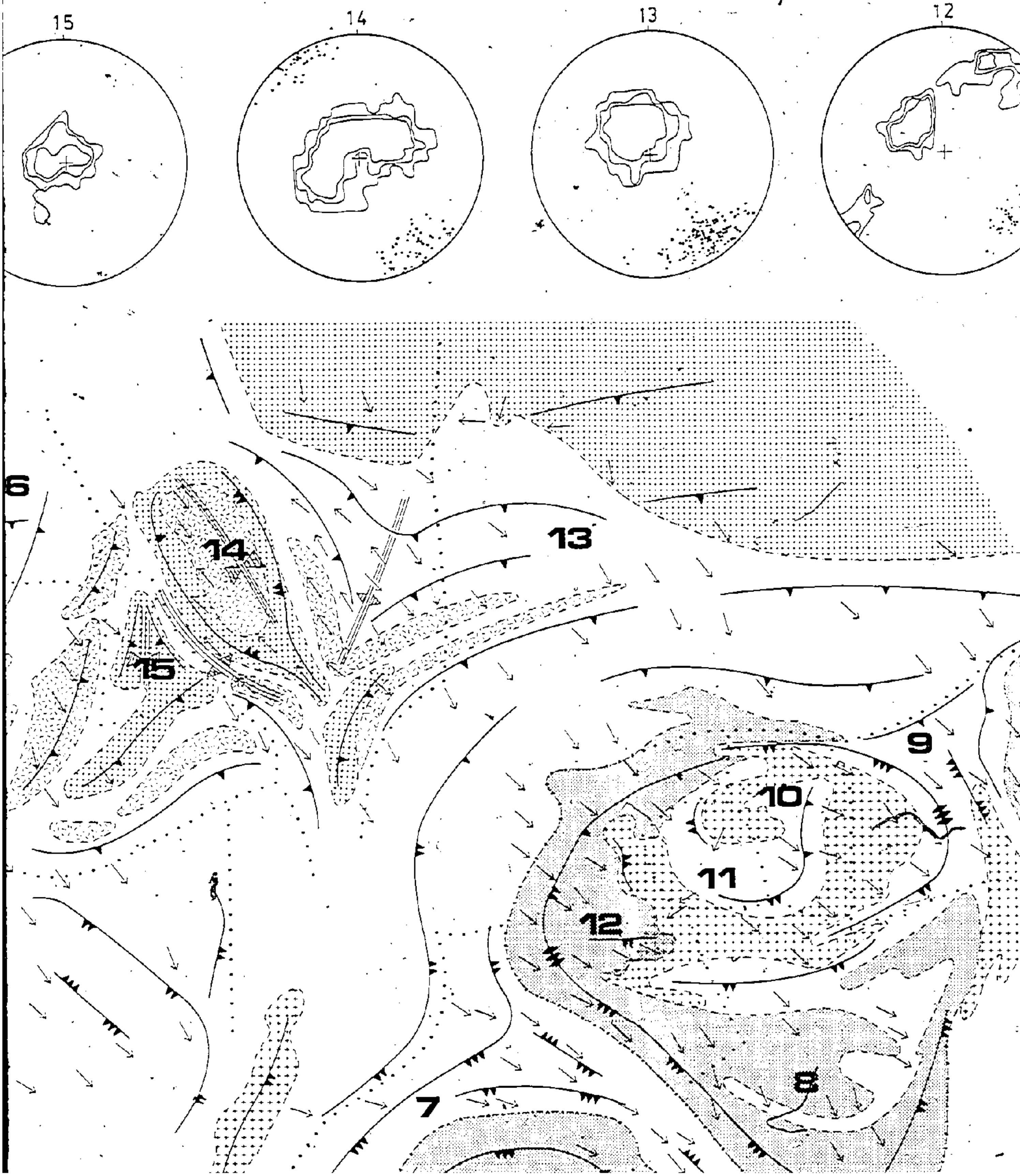

3 of

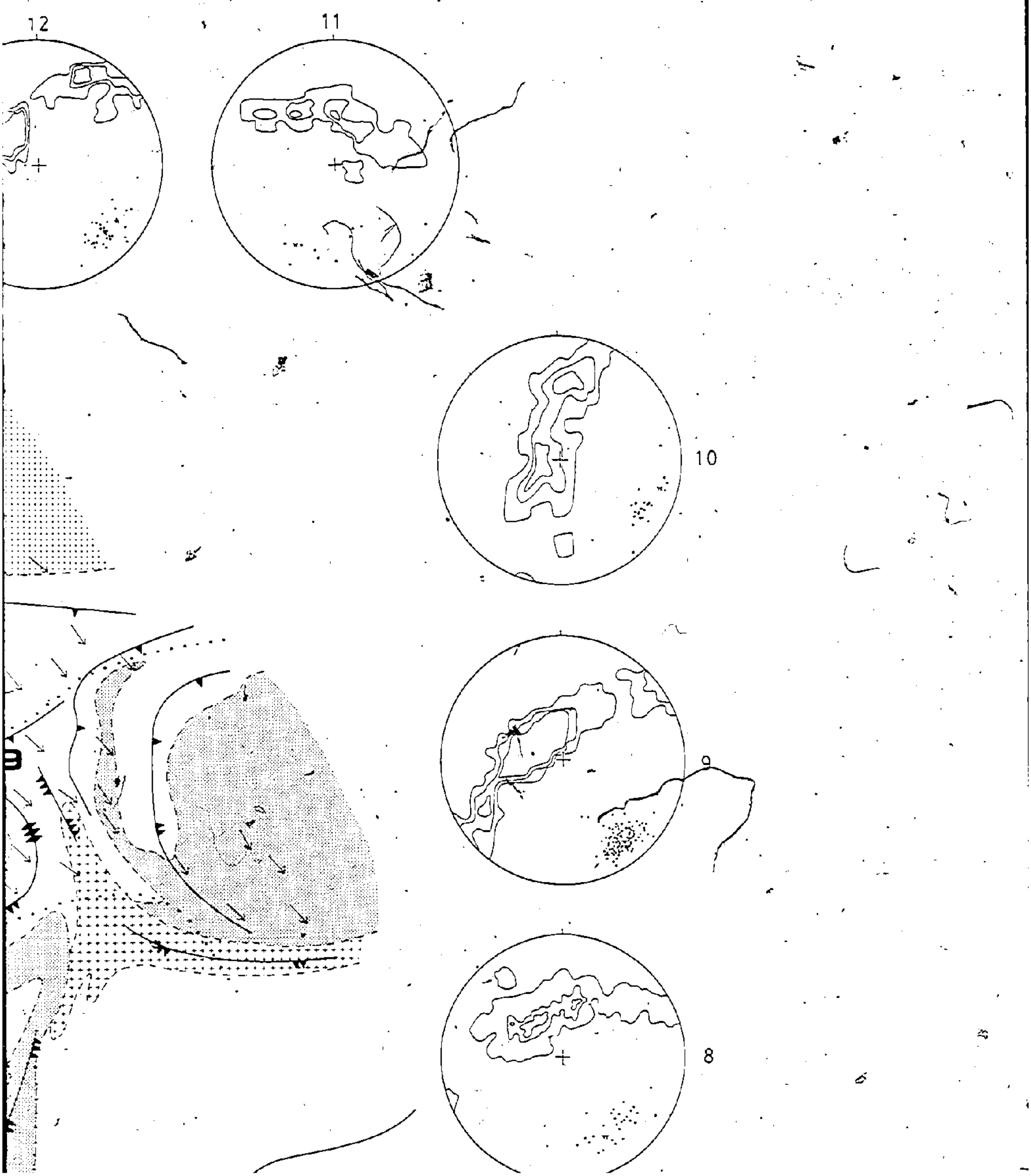

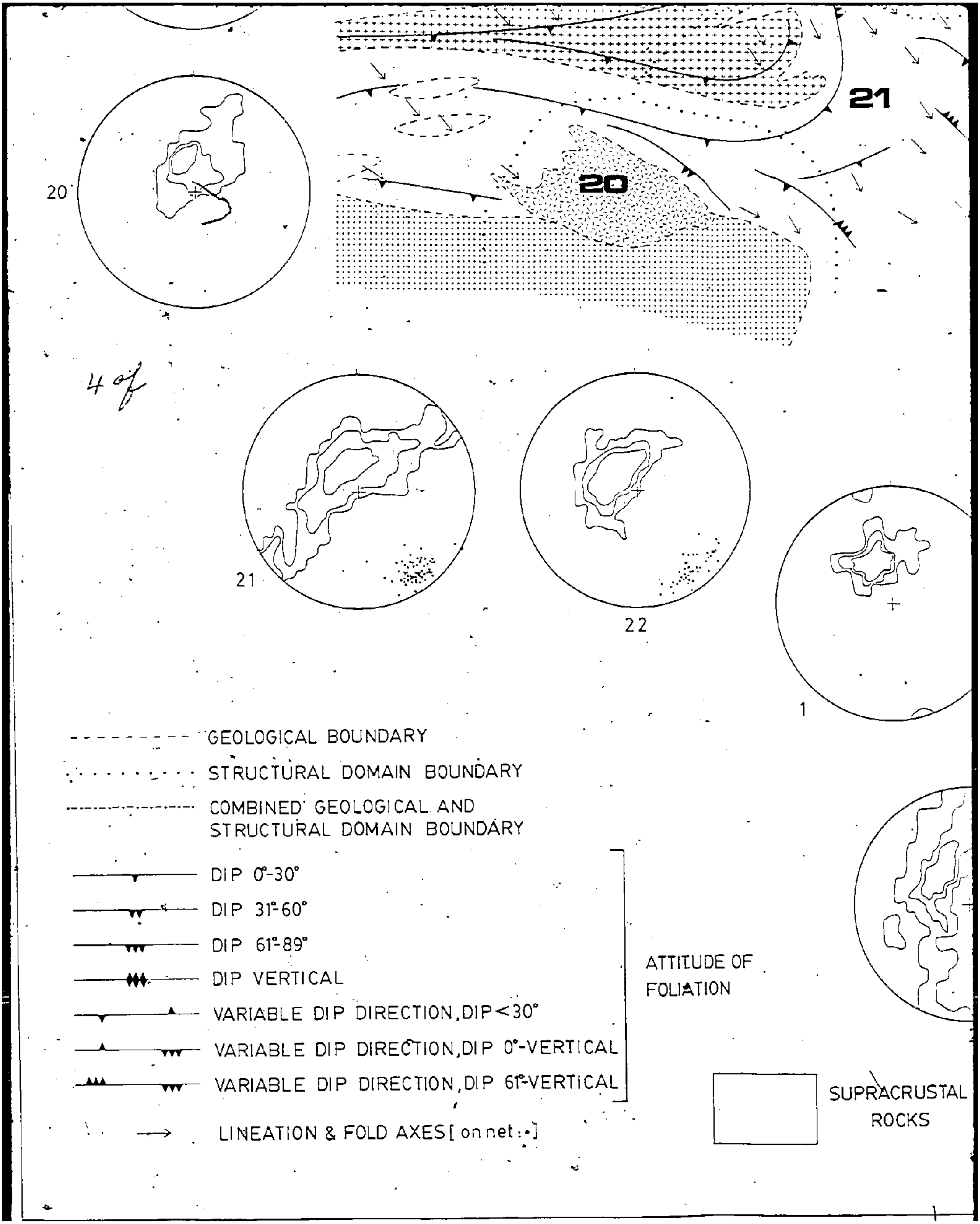
21
20
20
4 of
21
22
1
GEOLOGICAL BOUNDARY
STRUCTURAL DOMAIN BOUNDARY
COMBINED GEOLOGICAL AND STRUCTURAL DOMAIN BOUNDARY
DIP 0°-30°
DIP 31°-60°
DIP 61°-89°
DIP VERTICAL
VARIABLE DIP DIRECTION, DIP <30°
VARIABLE DIP DIRECTION, DIP 0°-VERTICAL
VARIABLE DIP DIRECTION, DIP 61°-VERTICAL
ATTITUDE OF FOLIATION
LINEATION & FOLD AXES [on net : •]
SUPRACRUSTAL ROCKS

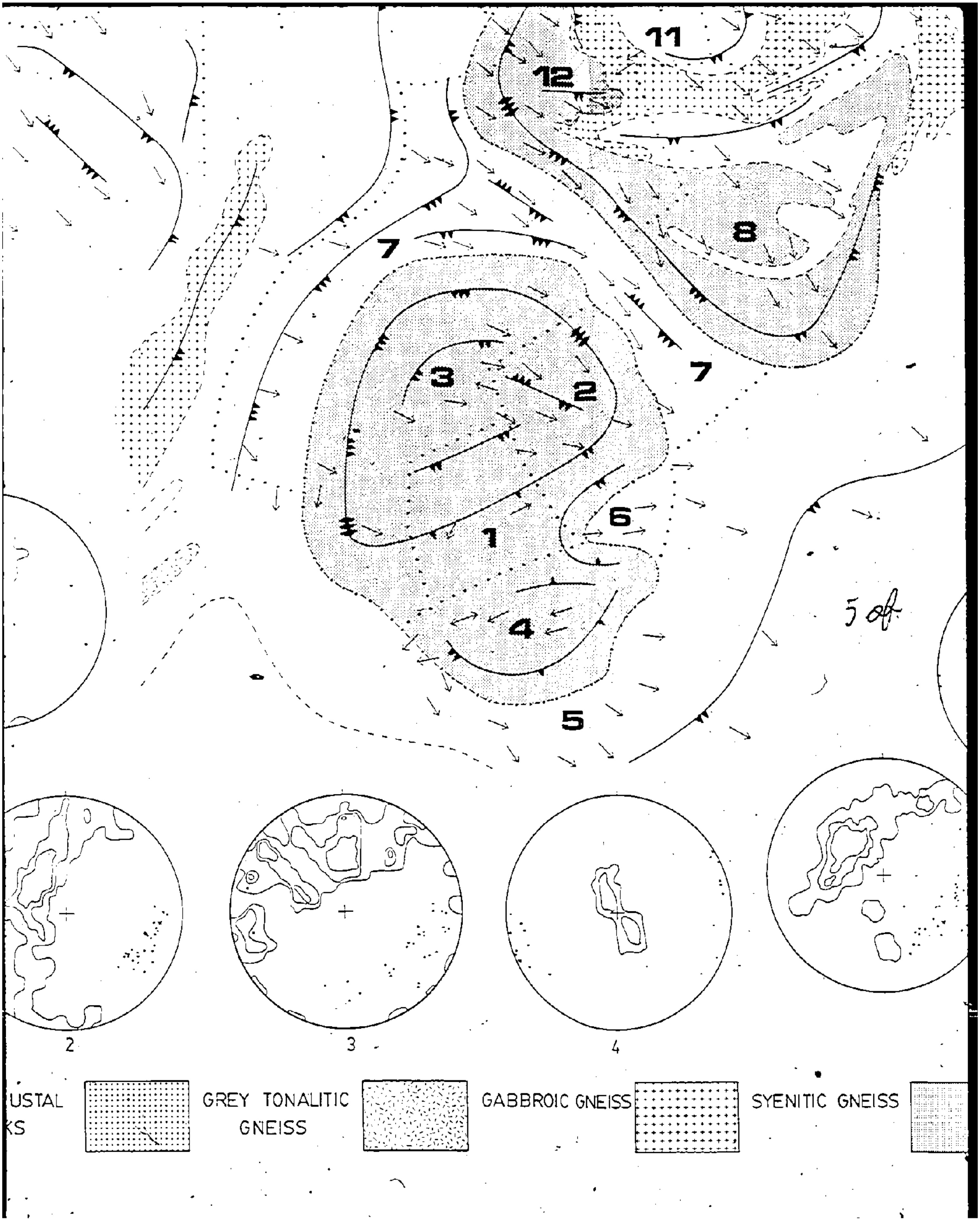
11
12
8
7
3
2
1
6
4
5
7
2
3
4
USTAL
KS
GREY TONALITIC
GNEISS
GABBROIC GNEISS
SYENITIC GNEISS

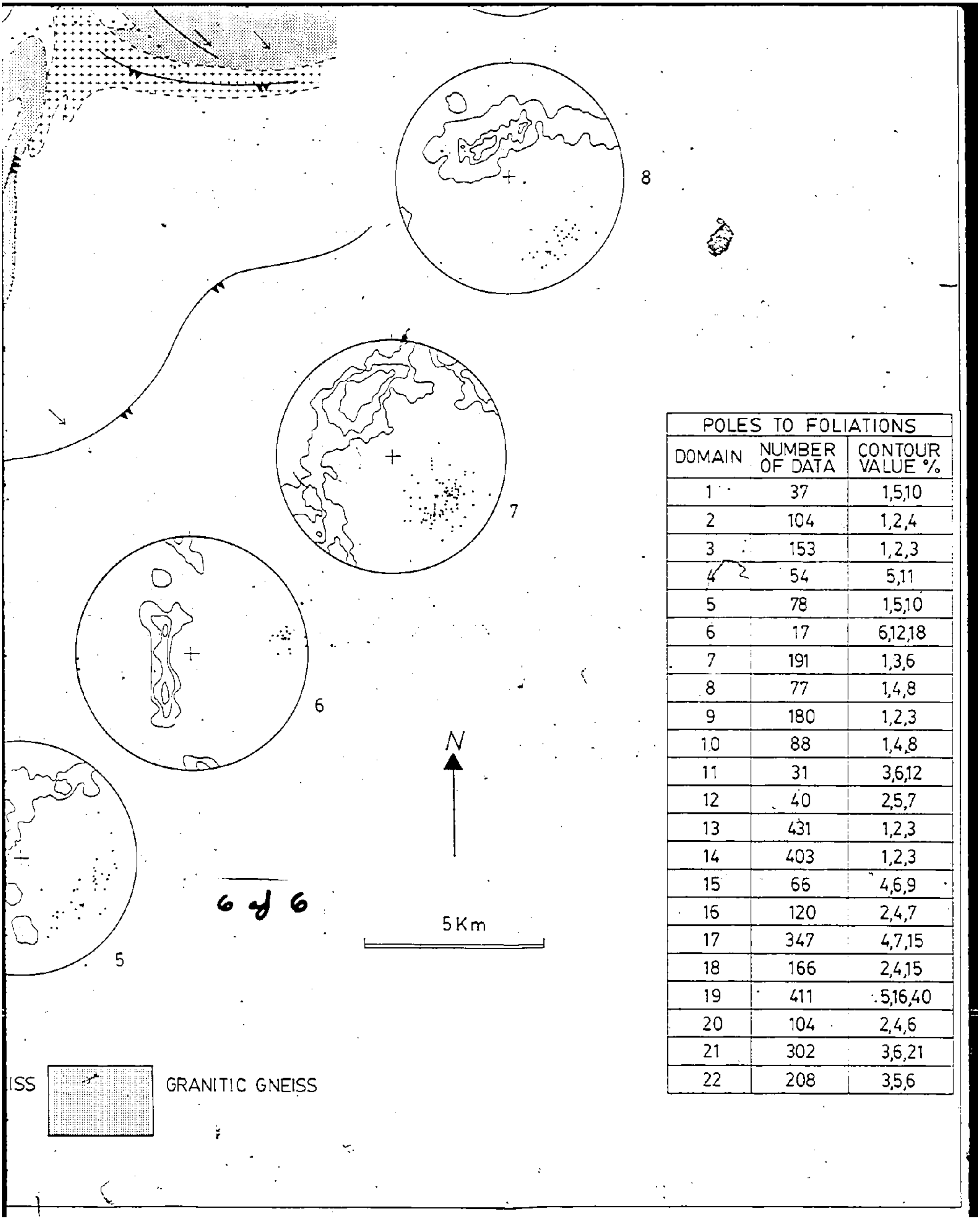

POLES TO FOLIATIONS		
DOMAIN	NUMBER OF DATA	CONTOUR VALUE %
1	37	1,5,10
2	104	1,2,4
3	153	1,2,3
4	54	5,11
5	78	1,5,10
6	17	6,12,18
7	191	1,3,6
8	77	1,4,8
9	180	1,2,3
10	88	1,4,8
11	31	3,6,12
12	40	2,5,7
13	431	1,2,3
14	403	1,2,3
15	66	4,6,9
16	120	2,4,7
17	347	4,7,15
18	166	2,4,15
19	411	5,16,40
20	104	2,4,6
21	302	3,6,21
22	208	3,5,6